

*Volume 19, Number 1*

---

*July, 1965*

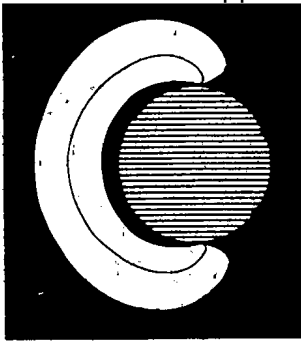
# **SOVIET ATOMIC ENERGY**

**АТОМНАЯ ЭНЕРГИЯ  
(АТОМНАЯ ЭНЕРГИЯ)**

**TRANSLATED FROM RUSSIAN**



**CONSULTANTS BUREAU**



# NEW BOOKS ON PLASMA PHYSICS

## REVIEWS OF PLASMA PHYSICS

A systematic, multi-volume review of the present status of plasma theory, serving both as an introduction for students and for researchers entering the field, and as a convenient, authoritative, up-to-date presentation of current knowledge for workers in plasma physics. This continuing series, prepared by internationally known Soviet experts in specific fields, is under the editorship of Academician M. A. Leontovich, of the Kurchatov Institute of Atomic Energy. Each volume contains a number of integrated tutorial reviews, covering in depth and in breadth specific aspects of the theory of the given field of plasma physics. In many cases, new material is presented. Translated by Herbert Lashinsky, University of Maryland.

**Volume 1:** A comprehensive introduction to "classical" plasma physics, contains authoritative papers on: Motion of Charged Particles in Electromagnetic Fields in the Drift Approximation, **D. V. Sivukhin** • Particle Interactions in a Fully Ionized Plasma, **B. A. Trubnikov** • Transport Processes in a Plasma, **S. I. Braginskii** • Thermodynamics of a Plasma, **A. A. Vedneov**. Much of the material in the first two papers is presented here for the first time. Although the theoretical analyses are quite advanced, the experimental aspects of the subject are kept firmly in view throughout. This is especially true of the article on transport phenomena, in which the kinetic approach is developed in parallel with qualitative physical descriptions of transport phenomena, including some of the less familiar "transverse" thermal transport effects in plasmas

in magnetic fields. Many physical examples and applications of the theory are given.  
326 pages \$12.50

**Volume 2:** Contains four review papers concerned primarily with the problem of plasma confinement: Magnetic field geometries, **A. I. Morozov** and **L. S. Solov'ev** • Plasma equilibrium in magnetic fields, **V. D. Shafranov** • Hydromagnetic plasma stability, **B. B. Kadomtsev** • Motion of charged particles in electromagnetic fields, **A. I. Morozov**.  
Approx. 280 pages 1966 \$12.50

**Volume 3:** Devoted to plasma waves, includes: Electromagnetic waves in a plasma, **V. D. Shafranov** • Oscillations of an inhomogeneous plasma, **A. B. Mikhailovskii** • Introduction to the theory of a weakly turbulent plasma, **A. A. Vedneov** • Symmetric magnetohydrodynamic flow and helical waves in a circular plasma cylinder, **L. S. Solov'ev**.  
Approx. 300 pages 1966 \$12.50

**Volume 4:** To be published out of sequence, contains three papers: Hydrodynamic description of a collisionless plasma, **T. F. Volkov** • Cooperative phenomena and shock waves in collisionless plasmas, **R. Z. Sagdeev** • Coulomb collisions in a fully ionized plasma, **D. V. Sivukhin**. The latter paper contains new material on the relevance of this topic to mirror machines, provided by the author for the English edition.  
241 pages 1966 \$12.50

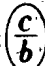
**Volume 5:** In preparation

## SPACE PHYSICS WITH ARTIFICIAL SATELLITES

By Ya. L. Al'pert, A. V. Gurevich, and L. P. Pitaevskii

The first study of its kind, this monograph is devoted to a theoretical investigation of phenomena attending the movement of satellites through a highly rarefied plasma. In approaching his problem, the author employs the kinetic approach in place of usual hydrodynamic and aerodynamic principles. Two cases are considered: a body with velocity greater than the thermal motion of neutral particles and ions and with dimension larger than the Debye radius; and a body with dimension comparable to or smaller than the Debye radius and velocity comparable to that of the particles. The results of calculations of the disturbances in the concentration of neutral particles, ions, and electrons and the consequent disturbances of the electric and

magnetic fields in the satellite's vicinity are presented in Chapters II through VI. Chapter VII is devoted to an investigation of the scattering of radiowaves in the satellite's wake. Disturbances in the plasma in the vicinity of a body at rest are calculated in Chapters VIII and IX, enabling the development of a more rigorous theory of a probe in a rarefied plasma. Also considered is the question of the influence of an alternating electric field (field of the transmitting antennas) on the plasma. This work represents the first investigation and generalization of an extremely complex and manifold problem urgently being posed by contemporary physics and technology. Translated from Russian.  
250 pages \$25.00

 **CONSULTANTS BUREAU** 227 West 17th Street, New York, New York 10011

EDITORIAL BOARD

A. I. Alikhanov	M. G. Meshcheryakov
A. A. Bochvar	M. D. Millionshchikov
N. A. Dollezhal'	( <i>Editor-in-Chief</i> )
V. S. Fursov	P. N. Palei
I. N. Golovin	V. B. Shevchenko
V. F. Kalinin	D. L. Simonenko
N. A. Kolokol'tsov	V. I. Smirnov
( <i>Assistant Editor</i> )	A. P. Vinogradov
A. K. Krasin	N. A. Vlasov
A. I. Leipunskii	( <i>Assistant Editor</i> )
V. V. Matveev	

# SOVIET ATOMIC ENERGY

A translation of *ATOMNAYA ÉNERGIYA*,  
a publication of the Academy of Sciences of the USSR

© 1966 CONSULTANTS BUREAU, A DIVISION OF PLENUM PUBLISHING CORPORATION, 227 West 17th Street, New York, N. Y. 10011

Volume 19, Number 1

July, 1965

## CONTENTS

	PAGE	RUSS. PAGE
Igor' Evgen'evich Tamm . . . . .	855	2A
<b>ARTICLES</b>		
Absolute Measurement of the Absorption Cross Sections of Neutrons of 24 keV Energy —T. S. Belanova, A. A. Van'kov, F. F. Mikhailus, and Yu. Ya. Stavisskii . . . . .	858	3
Study of the Interaction of Resonance Neutrons with Nuclei on the Linear Accelerator in Saclay—F. Netter . . . . .	863	8
Effectiveness of Heterogeneous Absorbers in Homogeneous Uranium-Water Reactions —G. M. Vladykov, B. G. Dubovskii, A. V. Kamaev, V. Ya. Sviridenko, F. M. Kuznetsov, G. A. Popov, and Yu. D. Palamarchuk . . . . .	871	14
Relative Vapor Pressure Differences of $B^{11}F_3$ — $B^{10}F_3$ —I. B. Amirkhanova, A. V. Borisov, I. G. Gverdsiteli, and A. T. Karamyan . . . . .	877	20
A Method of Determining the Concentrations of Short-Lived Daughter Products of Radon in Air by the $\alpha$ - and $\beta$ -Radiations—V. G. Labushkin and L. S. Ruzer . . . . .	882	24
Radioactive Fallout on the Territory of the USSR in 1963—S. G. Malakhov, G. A. Sereda, V. F. Brendakov, T. V. Polyakova, R. I. Pervunina, V. I. Svishcheva, and V. N. Churkin. . . . .	887	28
<b>NOTES ON ARTICLES RECEIVED</b>		
Shaping of the Thermal Neutron Flux in Heterogeneous Nuclear Reactors by Profiling the Fuel Charge—E. I. Inyutin . . . . .	895	36
Equalization of the Volume Energy Release in Heterogeneous Thermal Reactors by Profiling the Fuel Charge—E. I. Inyutin . . . . .	897	37
Equalized Thermal Neutron Flux in Aqueous Uranium Reactors—E. I. Inyutin, V. P. Kochergin, and I. P. Markelov . . . . .	899	38
Determining the Self-Absorption of $\alpha$ -Radiation in a Sample During Air Filtration —V. G. Labushkin, N. M. Polev, and L. S. Ruzer . . . . .	900	39
Scattering of $\beta$ -Radiation from Thin Specimens by Material Equivalent to Tissue —M. A. Malevich and Yu. M. Shtukkenberg . . . . .	902	40
<b>LETTERS TO THE EDITOR</b>		
Measurement of the Mean Number of Fission Neutrons Emitted by $U^{235}$ and $Pu^{239}$ on the Capture of a Single 24 keV Neutron—A. A. Van'kov and Yu. Ya. Stavisskii . . . . .	903	41
Fast Neutron Capture Cross Section for Rhenium—Yu. Ya. Stavisskii, A. V. Shapar', and R. N. Krasnokutskii . . . . .	905	42
Fission Cross Section of $U^{235}$ for Resonance Energy Neutrons—Wan Shih-Ti, Wang Yung-Ch'ang, E. Dermendzhiev, and Yu. V. Ryabov . . . . .	907	43

Annual Subscription: \$95

Single Issue: \$30

Single Article: \$15

All rights reserved. No article contained herein may be reproduced for any purpose whatsoever without permission of the publisher. Permission may be obtained from Consultants Bureau, A Division of Plenum Publishing Corporation, 227 West 17th Street, New York, N. Y. 10011, U.S.A.

## CONTENTS (continued)

	PAGE	RUSS. PAGE
Relative Yields of Delayed Neutrons in the Fission of $U^{235}$ and $U^{238}$ —B. P. Maksyutenko. . . .	910	46
Distribution of Neutrons in a Straight Cylindrical Channel—E. A. Kramer-Ageev, V. N. Markov, V. P. Mashkovich, V. K. Sakharov, and V. M. Sakharov . . . . .	911	46
Variation of the Yield of the ( $\alpha$ , n) Reaction with the Energy of the $\alpha$ Particles —E. M. Tsenter and A. B. Silin . . . . .	914	48
Matrix Analysis of Data Obtained by Means of a Single-Crystal Fast-Neutron Scintillation Spectrometer—G. G. Doroshenko, V. G. Zolotukhin, and B. A. Efimenko. . . . .	917	51
Analysis of Systematic Error in Differentiating Apparatus Spectra Measured by Means of a Single-Crystal Fast-Neutron Spectrometer—V. G. Zolotukhin, G. G. Doroshenko, and B. A. Efimenko . . . . .	924	56
Analysis of the Spectra of Instantaneous Neutrons from the Spontaneous Fission of $Cf^{252}$ —A. E. Savel'ev . . . . .	928	59
Production of $Az^{26}$ on Irradiating Magnesium with 20 MeV Deuterons—N. N. Krasnov, P. P. Dmitriev, Yu. G. Sevast'yanov, and A. S. Bezmaternykh . . . . .	931	62
Separation of $Na^{22}$ from a Magnesium Target Irradiated by Deuterons—Yu. G. Sevast'yanov and A. S. Bezmaternykh . . . . .	933	63
International Comparisons of the Specific Activities of $P^{32}$ , $Co^{60}$ , and $Ti^{204}$ Solutions and of the Activity of "Solid" $Co^{60}$ Sources—A. A. Konstantinov, V. V. Perepelkin, and A. E. Kochin . . . . .	936	65
Asymptotic Form of the Scattering Law for Slow Neutrons—L. V. Maiorov. . . . .	940	67
Physical Characteristics of a Critical Assembly with Beryllium Oxide Moderator —S. S. Lomakin. . . . .	944	69
The Problem of $\gamma$ -Ray Penetration through Shields—S. M. Ermakov and É. E. Petrov. . . . .	947	71
Calorimetric Determination of Absorption of a Dose of Ionizing Radiation from a Reactor by Compensation of the Heat Evolved in the Specimen—V. S. Karasev and V. M. Kolyada . . . . .	950	74
The UKP-30 000 Isotope Apparatus for $\gamma$ -Irradiation—G. N. P'yankov, M. A. Barashkin, and N. V. Kulyupina. . . . .	952	75
The UK-70 000 High-Power Isotope Apparatus for $\gamma$ -Irradiation—G. N. P'yankov and N. V. Kulyupina. . . . .	954	77
Advantages of Radiometric Enrichment of Uranium Ores and the Choice of Optimum Separation Level—I. A. Andryushin, Yu. V. Roshchin, L. D. Chebotareva, and Yu. A. Érivanskii . . . . .	957	79
Optimal Indices of Radiometric Enrichment and Suitable Conditions for its Use on an Ore with Log-Normal Distribution of Uranium Content in its Volume Elements —Yu. V. Roshchin. . . . .	960	80
Isotope Shift Between $U^{234}$ and $U^{238}$ in Secondary Uranium Minerals of Some Hydrothermal Deposits—P. I. Chalov, Ya. A. Musin, T. V. Tuzova, and K. I. Merkulova . . . . .	964	82
Measuring Low Radium Activities by Means of a Scintillation Chamber with an Electrostatic Field—L. V. Gorbushina, G. S. Semenov, and V. G. Tyminskii . . . . .	967	84
Radiation Conditions Near a VVR-M Nuclear Reactor—P. V. Ramzaev, I. A. Belyaeva, V. N. Gus'kova, M. S. Ibatullin, Yu. O. Konstantinov, S. P. Nikolaev, and A. F. Oreshina . . . . .	970	86
SCIENCE AND ENGINEERING NEWS		
Collaboration of the Socialist Countries in Nuclear Power Development. . . . .	974	90
A Meeting of IAEA Experts on Nuclear Water Desalinization—A. Loginov. . . . .	975	90
International Symposium on Chemical Effects Caused by Nuclear Reactions and Radioactive Transformations—B. G. Dzantiev. . . . .	979	94

# CONTENTS (continued)

	PAGE	RUSS. PAGE
Atoms for Peace at the Leipzig Fair—Yu. Mityaev. . . . .	982	95
The Warsaw Exhibit . . . . .	984	96
Applications for Radioactive Isotopes in Meteorology—M. T. Dmitriev. . . . .	986	97
Brief Communications. . . . .	988	99
New Books—M. V. Filippov . . . . .	989	100

The Russian press date (podpisano k pečati) of this issue was 7/10/1965. .  
Publication therefore did not occur prior to this date, but must be assumed  
to have taken place reasonably soon thereafter.

## IGOR' EVGEN'EVICH TAMM.

Translated from *Atomnaya Énergiya*, Vol. 19, No. 1,  
pp. 2A-2B, July, 1965

July 8 was the seventieth birthday of Academician Igor' Evgen'evich Tamm, one of the greatest Soviet theoretical physicists.

I. E. Tamm was born in 1895 in Vladivostok. His childhood was spent in Elisavetgrad (now Kirovograd), where he completed preparatory schooling. For a year he studied in Edinburgh University (Scotland), but when the first World War began he transferred to the Physicomathematical Faculty of Moscow University. On finishing University (1918) he taught physics, first at the Crimean University and later at Odessa Polytechnic Institute. Since 1922 Tamm has lived and worked in Moscow. For many years he occupied the Chair of Theoretical Physics in the Physics Faculty of Moscow State University. After the Academy of Sciences, USSR, moved to Moscow in 1934, Igor' Evgen'evich became Director of the Theoretical Department of the P. N. Lebedev Physical Institute, Academy of Sciences, USSR. Here he still works, heading the large group of theoreticians trained by himself.

I. E. Tamm's immense scientific and socio-scientific services have been acknowledged both in the Soviet Union and abroad: He has been elected an active member of the Academy of Sciences, USSR, and a number of foreign Academies, has received the title of Hero of Socialist Labor, and has been awarded two State prizes and the Nobel prize.

The nature of I. E. Tamm's scientific works is so diverse that in a brief article it is hard to list or characterize them fully. Let us confine ourselves to mentioning merely the most outstanding.

Tamm began his first scientific investigations under the influence of L. I. Mandel'shtam. These were devoted to the electrodynamics of an anisotropic medium and to crystal optics in the theory of relativity. In 1930 he published a paper containing the complete theory of light scattering in crystals. The quantization of elastic (sound) waves in solids was carried out and the concept of sound quanta (phonons) introduced in this paper. Here, not only the Rayleigh scattering of light but also Raman scattering in crystals, was considered.

In the same year there appeared a number of papers by Igor' Evgen'evich on the recently-established Dirac relativistic quantum mechanics of the electron. The Dirac theory, though constituting a major step in a leading field of physics (the creation of relativistic quantum mechanics), was at that time undergoing considerable difficulties owing to its fostering of the concept of states of negative energies. Igor' Evgen'evich carried out the first systematic quantum-electrodynamic calculations of relativistic effects, after developing the necessary method of calculation and gave a strict and systematic derivation of the famous Klein-Nishina formula; simultaneously with P. Dirac and R. Oppenheimer he indicated the inevitability of a free electron passing to a negative level, and calculated the annihilation probability of an electron. With his characteristic eye for the essence of things, Igor' Evgen'evich showed the important part played by negative-energy states even in obtaining the low-frequency limit in the scattering of light at electrons. In view of this the many attempts to eliminate negative-energy states became pointless.

At the beginning of the thirties, Tamm was engaged in studying one of the then most urgent fields of quantum mechanics, the quantum theory of metals. Here Igor' Evgen'evich and his students carried out a number of investigations which are firmly entrenched in the modern understanding of metals. Tamm set out the groundwork of the theory of the photoeffect in metals, and discovered the existence of levels of a special type, "Tamm levels", which play a great part in the development of the theory of surface and contact properties in solids.

From 1934 up to the present time Igor' Evgen'evich has been working enthusiastically on the most difficult central problem of contemporary physics, the construction of a theory of elementary particles. Tamm's papers have played an outstanding part in the development of the theory of elementary particles and especially in the physics of strong interactions.



In 1934 I. E. Tamm first pointed out that for all types of interaction, including nuclear, there must exist definite quanta of field, which, just as photons in the case of electromagnetic interactions, can be emitted and absorbed by interacting particles. In the same paper he showed that the only then-known particles, the electron and the neutrino, could not bear responsibility for the forces acting between the proton and the neutron. Yukawa's famous paper setting out the fundamentals of meson theory begins with a reference to this paper of Tamm's.

In subsequent years Tamm published a whole series of papers on the properties of elementary particles. His papers on vector particles, particles with higher spins, and the true order of magnitude and sign of the magnetic moment of the neutron are widely known. (The latter appeared very revolutionary and at first was doubted by many physicists).

Tamm's greatest achievement in the post-war period in the physics of elementary particles is without doubt his idea of using an approximation based on cutting off the equations of the quantum theory of field according to the number of particles in the theory of strong interactions. This idea found its simplest expression in the so-called Tamm-Dancoff method, later used in hundreds of papers. The Tamm-Dancoff method met with great difficulties in the quantum theory of field. Tamm's idea of constructing an approximation method according to the num-

ber of particles, however, had a colossal influence on the development of new ideas in the quantum theory of field in the physics of strong interactions (in particular, on attempts to construct the equations on the basis of dispersion relations).

Of later papers by I. E. Tamm we must mention the semiphenomenological theory in which the isobaric states of nucleons were considered as particles with spin  $3/2$ . This concept, developed by Tamm and his students, met strong opposition. Even to many leading physicists it seemed completely unacceptable to consider the wide maximum, in the energy relation for the scattering cross section of mesons, as a particle, and a formulation involving only the lower approximations of the theory of perturbations seemed entirely foreign. The result of this opposition is that now more than ten years later, these papers have been forgotten and are rarely quoted. The many calculations now being carried out on the interaction of elementary particles in the so-called resonance approximation nevertheless often do no more than repeat the work of Tamm and his students. The resonance approximation and the consideration of resonances as particles now play an important part in the physics of elementary particles.

The characteristics which have always distinguished Igor' Evgen'evich and doubtless bear witness to his truly great talent are his vast intuition, the ability to perceive what others working intensively on physical problems were unable to see, and his ability to separate out the most fundamental questions.

The fundamental basis of theory was always the main object in Tamm's investigations. When, as a result of circumstances, he was occupied with problems having a more particular character, then there appeared papers containing the complete solution of the fundamental aspect of the problems and the beginning of new concepts in physics. Among work of this kind we must above all mention papers on the theory of radiation from an electron moving in a medium above the velocity of light. For these papers Tamm was first awarded the State prize and then the Nobel prize "for discovering and explaining the Cerenkov effect" (together with P. A. Cerenkov and I. M. Frank). The discovery and theoretical explanation of this effect is undoubtedly one of the most outstanding achievements of Soviet physics.

I. E. Tamm also carried out important work of an applied character in connection with the requirements of popular economy at the time of the Great Fatherland (Second World) War and after. In particular, together with A. D. Skharov, he laid the foundations of Soviet studies in controlled thermonuclear reactions.

Igor' Evgen'evich has always given great attention to the teaching profession and the solution of practical and scientific-organization problems. Widely known both in the Soviet Union and abroad is his course on "The Fundamentals of the Theory of Electricity." Much work was done by Tamm in developing courses of theoretical physics at Moscow State University and Moscow Institute of Physics and Engineering when he was professor in these institutions.

Igor' Evgen'evich has devoted much time and effort to his fellow-workers and students, among whom we may name such well-known scientists as S. A. Al'tshuler, S. Z. Belen'kii, D. I. Blokhintsev, A. D. Galanin, V. L. Ginzburg, A. S. Davydov, A. D. Sakharov, E. L. Feinberg, V. S. Fursov, S. P. Shubin, and many others.

I. E. Tamm frequently comes forward with articles and reports devoted to the popularization of science, to scientific-organization questions, and to the education of youth. In one of such articles he developed the thesis: "The student is not a vessel that must be filled but a torch that must be lit." Igor' Evgen'evich is a shining example of such a burning torch and knows how to inflame others with his enthusiasm. Very typical of his genius is a sparkling mastery of the apparatus of theoretical physics, yet the apparatus always plays a subsidiary part in his work. Tamm has an amazing ability to create a qualitative picture of a phenomenon before applying complex apparatus, and most clearly to see the purpose of an investigation.

In recent years, with unaltered enthusiasm and vast ability, Igor' Evgen'evich has been studying the possibilities of overcoming the fundamental difficulties in the quantum theory of field on the basis of the quantization of space-time. As always, the concepts which he is developing lie off the beaten track, which leads physicists not having his intuition, energy and ability, to assert his point of view.



## ARTICLES

ABSOLUTE MEASUREMENT OF THE ABSORPTION CROSS SECTIONS  
OF NEUTRONS OF 24 keV ENERGY

(UDC 539.17.02.:539.172.4)

T. S. Belanova, A. A. Van'kov, F. F. Mikhailus,  
and Yu. Ya. StavisskiiTranslated from Atomnaya Énergiya, Vol. 19, No. 1,  
pp. 3-7, July, 1965

Original article submitted November 9, 1964

The absolute absorption cross sections of neutrons from an Sb-Be source were measured for a number of elements by the transmission method in spherical geometry. As all-wave detector, a long counter and a water tank with a system of fission chambers were used independently. The effect of resonance blocking on the value of the cross sections was studied. The results obtained were analyzed on the basis of transmission calculations by the Monte Carlo method.

The improvement of the system of nuclear-physical constants is a pressing problem both for the further development of industrial reactor construction and for the formulation and perfection of various model representations of the nucleus. Among constants difficult to measure is the absorption cross section  $\sigma_a(E)$  of fast neutrons, since the absorption takes place against a very large background scattering process. Measurements of  $\sigma_a(E)$  are therefore usually made by comparison with known reference absorption cross sections of certain "standard" elements. The absorption cross sections of these elements must be measured with great accuracy.

Reasonably precise values of the reference absorption cross sections of fast neutrons may be obtained by the method of the transmission of neutrons in spherical geometry, i.e., from the relative variation in the count rate on surrounding an isotropic neutron source by a spherical sample. For such measurements one must use an all-wave detector, the efficiency of which does not depend on the energy of the neutrons in the region studied. In this case the softening of the neutron spectrum as a result of repeated scattering in the sample does not affect the value of the transmission. The published data available [1, 2] had been obtained by means of a long counter for 24 keV neutrons. In [1] measurements were also made with high-energy neutron sources, but the difficulties (connected with the severe reduction in absorption effects and the effect of inelastic scattering) here encountered prevented sufficiently exact results from being obtained. In the presence of the several sources of error, the over-all error in the absorption cross section obtained by the spherical-transmission method may substantially exceed that resulting from the mean square scatter of the measurements.\* This fact was allowed for in carrying out the experiments in question.

Method of Measurement

Neutron Source. Measurements of the transmission of neutrons in spherical geometry were made with an Sb-Be neutron source; the external diameter of the source was 30 mm and the thickness of the beryllium can 2, 4, and 6 mm. Owing to elastic scattering of neutrons at beryllium nuclei, there was a certain softening of the neutron spectrum (Fig. 1), which could be taken into account by introducing a correction into the results of the measurements. It was also necessary to allow for an accompanying group of  $\sim 380$  keV neutrons with a relative yield 4.6% [2]. The intensity of the sources used was roughly  $10^8$  neutrons/sec. Owing to the high level of  $\gamma$ -radiation, an automatic remote control system was used in carrying out the experiments [3].

\*It should be noted that the error in  $\sigma_a$  given in [1] did not take account of the approximations which were made in analyzing the results.

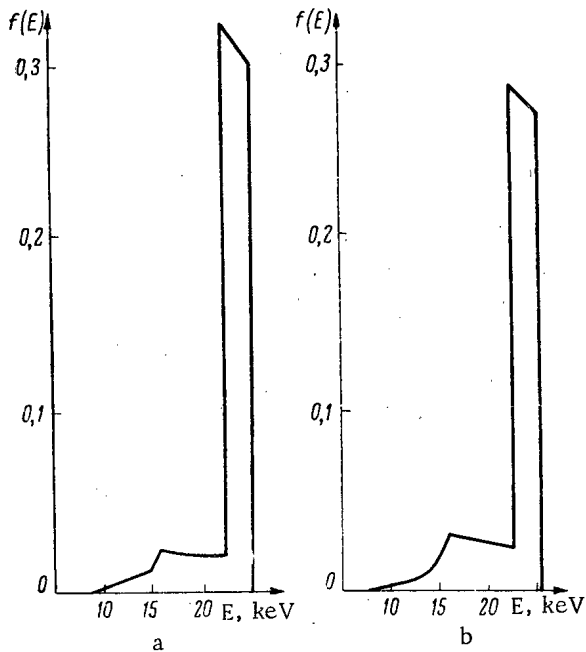


Fig. 1. Calculated neutron spectrum of Sb-Be source for beryllium-can thickness 3 and 5 mm (Fig. 1a and b respectively).

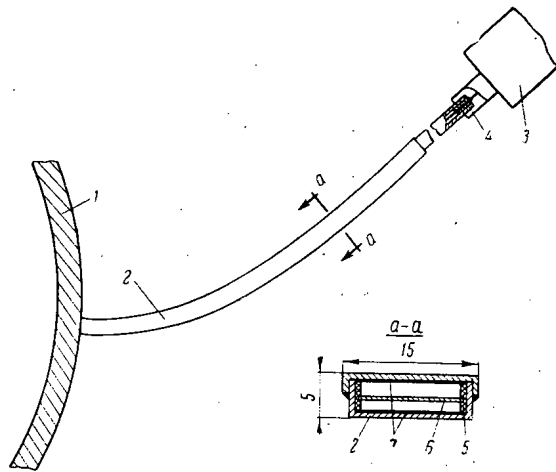


Fig. 3. Integrating fission chamber. 1) Shell of hollow sphere of tank; 2) Body of chamber; 3) Housing of cathode follower; 4) Glass insulator; Teflon insulator; 6) Collecting electrode; 7) Layers of  $U^{235}$ .

from spherical symmetry in the geometry of the experiment. A failing of this detector is the need to correct for the depression of the thermal neutron flux resulting from absorption in the sample. This correction, however, was negligible thanks to the provision of a spherical cavity 1 m in diameter in the tank. Figure 2 gives an idea of the measuring system. The main elements of the detector are two systems of fission chambers sensitive to thermal neutrons. The radial distributions of the neutron flux  $N(r)$  from the source in the water were measured by means of a movable system of plane fission chambers. Measurements were made with and without the sample.

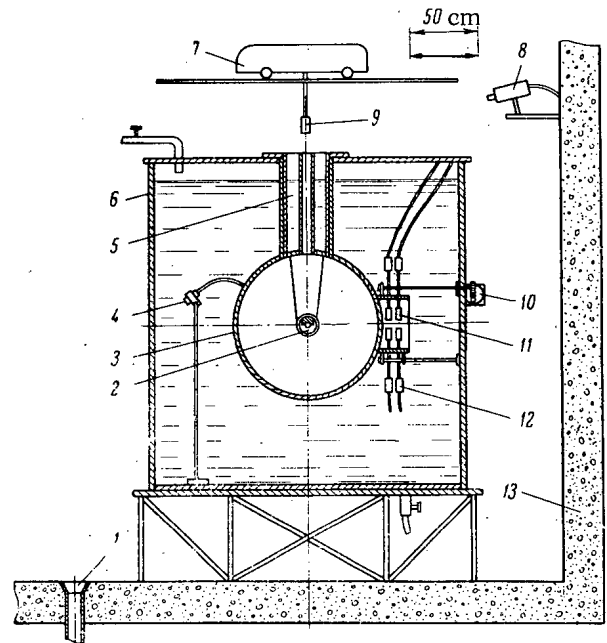


Fig. 2. Arrangement of measuring system (water tank). 1) Well (storage for source); 2) Sample; 3) Aluminum sphere, wall thickness 7 mm; 4) Integrating fission chamber; 5) Neck of sphere with water "stopper"; 6) Body of tank; 7) Transporter for loading source; 8) Television camera; 9) Magnetic clutch for extracting source; 10) Drive for movable system of plane fission chambers; 11) Plane fission chamber; 12) Housing of cathode follower; 13) Concrete shield.

**Neutron Detector.** As all-wave neutron detector, a long counter and a water tank with a system of integrating fission chambers were used independently. A long-counter system and measurements made with it are described in [1, 2, 4]. In the present measurements four long counters set at distances of 1.5 to 2 mm from the source were used. The all-wave properties were checked by means of a graphite scatterer. As shown by control measurements with a bismuth scatterer, under these conditions the correction to the angular dependence of efficiency did not exceed measuring error.

The advantage of the water tank is as follows: The region of all-wave properties is extended in the direction of lower energies, and better conditions are created from the point of view of lower sensitivity to small departures/

TABLE 1. Absorption Cross Sections of Neutrons with  $E_n = 24$  keV for Various Experimental Conditions

Characteristics of samples					Results of experiment			
Element, Z	$R_1$ , cm	$R_2$ , cm	$\sigma_{tr}$ , b	$nZ$	long counter		water tank	
					$\delta$ %, %	$\sigma_a$ , mb	$\delta$ %, %	$\sigma_a$ , mb
Cr	2,0	4,2	$2,7 \pm 0,5$	0,8	$0,27 \pm 0,16$	$9 \pm 5$	$0,39 \pm 0,17$	$13 \pm 6$
Cu	5,0	8,0	$9,0 \pm 1$	8,0	$6,45 \pm 0,22$	$74 \pm 13$	$5,92 \pm 0,45$	$62 \pm 13$
Cu (b)	3,0	11,0	$8,0 \pm 1$	6,2	$4,26 \pm 0,35$	$66 \pm 7$	$3,77 \pm 0,32$	$59 \pm 7$
Cu (b)	3,0	13,0	$10,0 \pm 1$	12,3	$6,58 \pm 0,24$	$60 \pm 6$	$6,97 \pm 0,38$	$64 \pm 6$
Zn	3,0	11,0	$12,0 \pm 1,0$	6,6	$3,49 \pm 0,25$	$66 \pm 7$	$4,22 \pm 0,25$	$79 \pm 7$
Zn (b)	3,0	13,0	$12,0 \pm 1,0$	9,6	$4,94 \pm 0,28$	$67 \pm 8$	$5,49 \pm 0,41$	$74 \pm 8$
Sr	1,5	9,7	$9,5 \pm 1,0$	2,2	$2,50 \pm 0,25$	$105 \pm 13$	—	—
Zr	2,05	5,05	$9,5 \pm 1,0$	2,3	$0,52 \pm 0,18$	$22 \pm 8$	$0,44 \pm 0,12$	$18 \pm 5$
Nb (b)	3,0	11,0	$7,2 \pm 0,4$	2,4	$9,63 \pm 0,26$	$294 \pm 12$	$10,39 \pm 0,22$	$316 \pm 10$
Nb (b)	3,0	13,0	$7,2 \pm 0,4$	3,3	$12,49 \pm 0,45$	$280 \pm 15$	$14,41 \pm 0,43$	$320 \pm 15$
Mo	2,0	4,5	$6,9 \pm 0,5$	1,8	$5,03 \pm 0,20$	$191 \pm 19$	$4,76 \pm 0,45$	$178 \pm 23$
Mo (b)	3,0	11,0	$6,9 \pm 0,5$	2,7	$8,68 \pm 0,23$	$220 \pm 9$	$8,36 \pm 0,38$	$212 \pm 12$
Mo (b)	3,0	13,0	$6,9 \pm 0,5$	3,9	$11,46 \pm 0,39$	$204 \pm 12$	$10,66 \pm 0,41$	$190 \pm 12$
Ag	2,05	2,55	$7,6 \pm 0,3$	0,3	$3,63 \pm 0,17$	$1065 \pm 60$	—	—
Ag	2,05	3,05	$7,6 \pm 0,3$	0,6	$7,78 \pm 0,25$	$1005 \pm 66$	—	—
Ag	2,05	5,05	$7,6 \pm 0,3$	1,9	$27,23 \pm 0,45$	$1017 \pm 55$	$28,54 \pm 0,50$	$1140 \pm 55$
Cd (b)	2,5	5,0	$6,4 \pm 0,4$	1,2	—	—	$7,22 \pm 0,20$	$398 \pm 28$
Cd (b)	3,0	9,0	$6,4 \pm 0,4$	1,1	$7,28 \pm 0,25$	$434 \pm 18$	$6,88 \pm 0,30$	$411 \pm 20$
Cd	3,0	11,0	$6,4 \pm 0,4$	1,7	$11,85 \pm 0,35$	$450 \pm 20$	$11,05 \pm 0,35$	$423 \pm 20$
In	2,5	3,5	$6,1 \pm 0,2$	0,3	$3,75 \pm 0,32$	$820 \pm 77$	$3,82 \pm 0,38$	$836 \pm 90$
Sn (b)	3,0	13,0	$5,5 \pm 0,1$	1,6	$3,59 \pm 0,40$	$125 \pm 16$	$4,03 \pm 0,28$	$140 \pm 11$
Sn (b)	3,0	15,0	$5,5 \pm 0,1$	2,2	$6,57 \pm 0,43$	$166 \pm 10$	$5,01 \pm 0,30$	$127 \pm 8$
Sb	1,5	2,5	$6,0 \pm 0,2$	0,2	—	—	$2,37 \pm 0,42$	$610 \pm 72$
W (b)	3,0	9,0	$10,2 \pm 1,0$	2,8	$8,23 \pm 0,22$	$298 \pm 18$	$8,30 \pm 0,52$	$300 \pm 25$
W (b)	3,0	13,0	$10,2 \pm 1,0$	5,8	$17,37 \pm 0,60$	$308 \pm 28$	$18,60 \pm 0,50$	$330 \pm 27$
Au	2,05	3,55	$13,5 \pm 0,3$	2,3	$10,45 \pm 0,23$	$610 \pm 28$	$11,13 \pm 0,27$	$640 \pm 30$
Hg	5,0	7,5	$12,0 \pm 1,0$	2,8	$6,35 \pm 0,30$	$271 \pm 32$	$5,54 \pm 0,24$	$236 \pm 30$
Pb (b)	3,0	11,0	$10,3 \pm 0,4$	2,8	—	—	$1,25 \pm 0,17$	$45 \pm 6$
Pb (b)	3,0	13,0	$10,3 \pm 0,4$	4,0	$1,79 \pm 0,37$	$50 \pm 9$	$1,60 \pm 0,27$	$45 \pm 8$
Pb (b)	3,0	15,0	$10,3 \pm 0,4$	6,0	—	—	$2,86 \pm 0,20$	$53 \pm 5$
Bi	2,05	10,50	$11,5 \pm 0,3$	6,3	—	—	$0,24 \pm 0,30$	$3 \pm 3$
Th	2,05	5,05	$14,0 \pm 0,3$	2,1	$9,89 \pm 0,38$	$658 \pm 29$	$9,26 \pm 0,25$	$610 \pm 24$
U	3,5	5,5	$13,5 \pm 0,3$	2,9	$8,38 \pm 0,23$	$390 \pm 16$	$7,83 \pm 0,24$	$365 \pm 16$
U	3,5	8,5	$13,5 \pm 0,3$	9,4	$26,09 \pm 0,30$	$372 \pm 15$	$26,77 \pm 0,30$	$383 \pm 15$
U (b)	3,0	9,0	$13,5 \pm 0,3$	3,0	$8,18 \pm 0,33$	$430 \pm 18$	$6,84 \pm 0,46$	$360 \pm 27$
U (b)	3,0	13,0	$13,5 \pm 0,3$	5,8	$17,90 \pm 0,52$	$427 \pm 20$	$16,30 \pm 0,25$	$395 \pm 17$

The relative change in the integral on surrounding the source with the sample characterizes the absorbed proportion of neutrons. At the same time the relationship  $N(r)$  gives additional information on the energy variations of the neutron spectrum in the sample, and also on the value of the depression at the cavity boundary. Another stationary-system of chambers ensured a higher count efficiency and enabled integration to be effected automatically in the course of the measurements, thanks to a special construction of the chambers, which had the form of a bent, slot-like cavity. The shape of the bend corresponded to a curve constituting the solution of the equation for arc S as a function of radical coordinate:  $dS = \text{const} \cdot r^2 dr$ . For a constant linear efficiency and sufficient length, the count of the curved chamber, duly set up in the tank as in Fig. 3, was proportional to the intensity of the source.

Samples. The samples comprised spherical layers inside which the neutron source was placed. For some of the elements studied, samples of both pure absorbent and samples containing scattering material, were prepared. As scattering diluent a lead-bismuth alloy was used, since lead and bismuth are characterized by small absorption cross sections, weak resonance structure of the cross sections, and negligible energy losses for elastic collisions of the neutrons. Measurements of the absorption cross sections for the full-strength and diluted absorbent and for equal thicknesses of the samples increased the reliability of the results (in particular enabling the effect of resonance blocking to be estimated). The purity of the samples was verified by spectrochemical analysis.

Calculation of Spherical Transmission. The calculation of transmission as a function of absorption cross section was made in the one-velocity transport approximation for a point source of neutrons, by the method of statistical tests (Monte Carlo method). In this a statistical accuracy of 0.1 to 0.5% was achieved with respect to the absorbed proportion of neutrons  $\delta[\Sigma_a; R_1/R_2; \Sigma_t(R_2 - R_1)]$ , depending on the ratio between the internal and

TABLE 2. Averaged Absorption Cross Sections for Neutrons with Energy 24 keV

Element	$\sigma_a$ , mb	Element	$\sigma_a$ , mb
Cr	10 $\pm$ 4	Sn	128 $\pm$ 9
Cu	59 $\pm$ 8	Sb	580 $\pm$ 73
Zn	64 $\pm$ 7	W	300 $\pm$ 25
Zr	19 $\pm$ 5	Au	570 $\pm$ 30
Nb	270 $\pm$ 15	Hg	233 $\pm$ 30
Mo	192 $\pm$ 12	Pb	43 $\pm$ 7
Ag	980 $\pm$ 60	Bi	3 $\pm$ 3
Cd	384 $\pm$ 20	Th	615 $\pm$ 25
In	776 $\pm$ 66	U <sup>238</sup>	412 $\pm$ 18

external radii of the sample,  $R_1/R_2$ , and its optical thickness  $\Sigma_t (R_2 - R_1)$ . For neutron energy 24 keV the anisotropy of the angular distributions of scattered neutrons was small, so that the error associated with application of the transport approximation could be neglected [5].

#### Analysis of Experimental Results

The mean values of the transmissions and the mean square errors were found from the results of 20 to 30 measurements with each sample. The results obtained by means of the long counter and water tank were analyzed independently by the same method (Table 1).

Corrections. The results of the measurements with the diluted absorbent were corrected for absorption in the

lead-bismuth alloy; the correction was  $\sim 10\%$  of the value of  $\delta$  and was calculated from experimental data to  $\sim 10\%$  accuracy. Small corrections were also calculated for the departure of the neutron source from a strict point and for its absorbing properties, for the presence of a group of  $\sim 380$  keV neutrons, and for the softening of the spectrum in the samples (copper, zinc) and the beryllium can of the source. For samples of natural uranium, the fission of nuclei belonging to isotope U<sup>235</sup> was taken into account.

In the case of the water tank, a correction was introduced for absorption of thermal neutrons in the sample, this forming on average 10% of the relative absorption  $\delta$ . The correction was determined to an accuracy of 5 to 10% on the basis of experimental results and calculations of the probability of the absorption of neutrons incident from outside on the spherical sample. Corresponding calculated data were obtained by Vakhromeeva and G. I. Marchuk on solving the kinetic equation by a finite-difference method.

Errors. The values and errors of the cross sections were found on the basis of calculated curves of  $\delta [\Sigma_a; R_1/R_2; \Sigma_t (R_2 - R_1)]$ . In the present experiment we may distinguish two groups of errors:

1. Error in  $\sigma_a$ , connected with the indeterminacy of  $\delta$ : This contains the mean square error of the transmission measurements and the error resulting mainly from the introduction of a correction for the effects of the absorption of thermal neutrons in measurements with the water tank, and absorption in the lead-bismuth scattering material. This group of errors  $\Delta\sigma_a(\delta)$  is determined mainly by the accuracy of measurements and predominates over the computing errors.
2. The other group of errors  $\Delta\sigma_a(\sigma_t)$  depends on the thickness of the sample and concentration of absorbent, and arises as a result of inaccuracy in the over-all cross sections, constituting a computing parameter. The latter were taken mainly from the atlas of neutron cross sections [6]. The total error  $\sigma_a$  was determined as the mean square of the partial errors mentioned.

A source of possible distortion in the results is the effect of resonance blocking, arising when there are irregularities in the neutron cross sections within the limits of the spectrum of neutrons acting in the sample. It follows from qualitative considerations that, with increasing sample thickness, the experimental absorption cross sections should fall, and on diluting the absorbent with scattering material should rise. It may be shown that, for the effect to appear, the average number  $n$  of collisions in the sample must substantially exceed unity:  $n = \delta / \Sigma_a / \Sigma_t > 1$ .

The results of measurements for a number of elements with considerable variations in sample thickness (and hence mean number of collisions  $n$ ) and also absorbent concentration showed that, within experimental error, the absorption cross sections did not depend on the conditions in question; this indicates the smallness of the effect. The final values of absorption cross sections and their errors, allowing for measurements on different samples, were found by averaging the results obtained by means of the long counter and the water tank. For individual samples there were slight discrepancies between the data obtained from the long counter and the water tank, apparently due to the scattering of fast neutrons. In these cases the over-all error increased accordingly.

Results. Table 1 gives the results of the experiments and data obtained by analysis. The cases of diluted absorbent are indicated by the symbol (b);  $R_1$  and  $R_2$  are the internal and external radii of the samples respectively.

The samples are characterized by the total microscopic transport absorption cross section  $\sigma_{tr}$ , and also by the average number of collisions  $n_Z$  with absorbent nuclei. The results of the measurements are the values of the absorbed proportion of neutrons expressed in percent ( $\delta^*$  after introducing the corrections), and the corresponding absorption cross section expressed in millibarns (mb).

Table 1 takes account of all the corrections mentioned above, except an insignificant correction for the softening of the neutron spectrum in the beryllium can of the source. The latter correction is introduced in the final averaged results for the absorption cross sections given in Table 2.

### CONCLUSIONS

The results of our investigations (see Table 2) agree closely with those of Schmitt and Cook obtained by an analogous method [2], if we disregard their computed correction for the effect of resonance blocking, except for the value of  $\sigma_a$  for lead. Satisfactory agreement is found with the results of experiments in which, for absolute calibration of the relative  $\sigma_a(E)$  relation, parameters of isolated resonances, thermal absorption cross sections [7-10], or data of spherical geometry [11] were used. In this connection it is interesting to elucidate the causes of the discrepancy between the results of the investigations mentioned and the data of methods using the fission cross section of  $U^{235}$  for calibration [12, 13].

In conclusion the authors express thanks to A. I. Leipunskii and O. D. Kazachkovskii for constant interest in the work, and also N. A. Artemov, V. V. Piskunova, Yu. M. Nikitin, and L. E. Fedorov for help in adjusting the apparatus, in the measurements, and in analyzing the results.

### LITERATURE CITED

1. T. S. Belanova, ZhÉTF, 34, 574 (1958).
2. H. Schmitt and C. Cook, Nucl. Phys., 20, 202 (1960).
3. Yu. Ya. Stavisskii et al., "Atomnaya Énergiya," 15, 489 (1963).
4. O. Hanson and J. McKibben, Phys. Rev., 72, 673 (1947).
5. H. Bethe, J. Beyster, and R. Carter, J. Nucl. Energy, 3, 207 (1956).
6. D. Hughes and J. Hazvey, Neutron Cross Sections, BNR-325 (1958).
7. V. A. Konks, Yu. P. Popov, and F. L. Shapiro, ZhÉTF, 46, 80 (1964).
8. Yu. P. Popov and F. L. Shapiro, ZhÉTF, 42, 988 (1962).
9. A. A. Bergmann et al., In the book "Material of the International Conference on the Peaceful Use of Atomic Energy (Geneva, 1955)." Vol. 4, [in Russian] (1956), p. 166.
10. M. Moxon and E. Rae, Nucl. Instrum. and Methods, 24, 445 (1963).
11. J. Gibbons et al. Phys. Rev., 122, 182 (1961).
12. B. Diven et al. Phys. Rev., 120, 556 (1960).
13. S. Cox, Phys. Rev., 133, B378 (1964).

---

All abbreviations of periodicals in the above bibliography are letter-by-letter transliterations of the abbreviations as given in the original Russian journal. Some or all of this periodical literature may well be available in English translation. A complete list of the cover-to-cover English translations appears at the back of this issue.

STUDY OF THE INTERACTION OF RESONANCE NEUTRONS WITH NUCLEI  
ON THE LINEAR ACCELERATOR IN SACLAY\*

UDC 539.172.4)

F. Netter

(Center for Nuclear Studies, Department of Low-Energy Nuclear Physics, Saclay, France)

Translated from Atomnaya Énergiya, Vol. 19, No. 1,

pp. 8-14, July, 1965

Original article submitted January 13, 1965

Work on the interaction between resonance neutrons and nuclei now being carried out on the linear accelerator in Saclay is described. Objects for study are nuclei of the following elements: Al, V, Mn, Co, Cu, Zn, Ga, As, Se, Br, Y, Z, Nb, Mo, Ag, Ba, La, Pr, Nd, Tm, W, Pt, Au, Hg,  $U^{238}$ . The main aim of the work is to study the statistical properties of resonance parameters.

We describe an apparatus for measuring total cross sections, capture cross sections, and partial radiative transitions. At the present time a resolution of 0.3 nsec/m is achieved for a flight distance of 103 m, enabling experiments to be made for neutrons up to 80 keV energy. The analysis of the results is briefly described and methods of identifying resonances with spins are considered.

From the results obtained, the statistical properties of the scattering widths are analyzed and the statistical properties of the radiative widths considered.

The linear electron accelerator in Saclay [1, 2] is used by the Tzar group for studies on fundamental nuclear physics in the field of photonuclear reactions. The rest of the time it is used for producing neutrons for time-of-flight analysis. Two groups operating in the field of neutron physics simultaneously employ the five beams available. The group headed by Jolie is associated with nuclear reactors and in the main carries out research on heavy (especially fissile) nuclei. In this article we consider studies on nuclear physics carried out since 1958 by the other group, associated with the Department of Low-Energy Nuclear Physics. This group contains Julien, Huynh, Morgenstern, Samur, Netter, and also Corge and Bianchi, specialists in the analysis of experimental data on electronic computers. Also taking part in the work of the group are the foreign students Simik and de Barros and Colmaine University lecturers le Poittevin and Vastel.

#### Direction of Research

For studying interactions with resonance neutrons, nuclei were chosen mainly from the neighborhood of the force function maximum with mass numbers close to 60, 140, and 190, and also with mass numbers close to 75 for the neutron s-wave and 100 for the neutron p-wave. Nuclei were also chosen near the force-function minimum (mass number 100 for the s-wave). We also studied nuclei close to those with filled shells of 50, 82, and 126 neutrons. We studied nuclei of the elements Al, V, Mn, Co, Cu, Zn, Ga, As, Se, Br, Y, Zr, Nb, Mo, Ag, Ba, La, Pr, Nd, Tm, W, Pt, Au, Hg,  $U^{238}$ . In some cases (Al, Zn) we were able to observe new resonances [3], determine the spins of known resonances (Ag) [4], or examine the statistical distribution of levels ( $U^{238}$ ) [5]. In general, however, we systematically studied the statistical properties of the resonance parameters.

The main direction of the experiments was to measure simultaneously the total effective cross section (by transmission) and capture cross section, and to study the relative intensities of the radiative transitions observed in the resonances, with simultaneous use of three time-of-flight bases. In each case everything possible was done to

\*Translation from French.

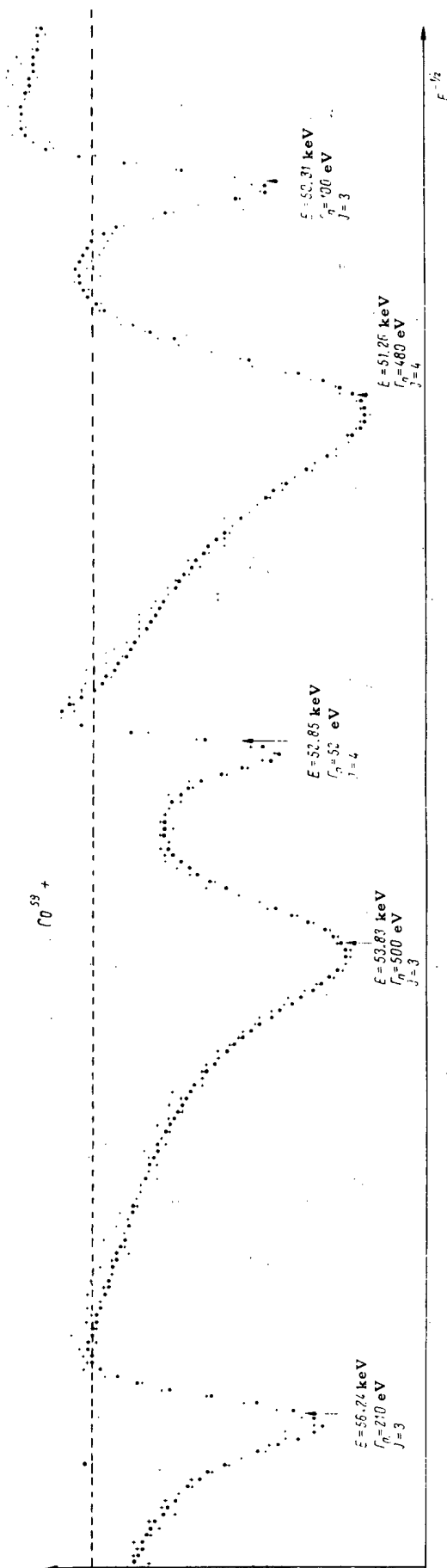


Fig. 1. Transmission of cobalt sample ( $7 \cdot 10^{-26}$  atom/cm<sup>2</sup>), resolution 0.3 nsec/m; (+) experimental points; (●) computed points.

determine the spin of the resonance in question. Statistical effects cannot be interpreted correctly unless they relate to a family of resonances having the same spin. For example, for s-neutrons and target nuclei with spin  $I$  there are two different families of resonances with spins  $J_+ = I + 1/2$  and  $J_- = I - 1/2$ .

Furthermore, in order to obtain the essential statistics, one must study a fair number of resonances. Earlier, such investigations were carried out only for certain heavy nuclei, for example, platinum [6]. At the present time experiments on transmission are being made with a resolution better than 1 nsec/m, which offers the possibility of studying resonance levels of medium nuclei, such as cobalt [7], in the energy range up to 30 keV; not long after reaching the limiting resolution of 0.3 nsec/m this range was broadened to 80 keV [8].

## APPARATUS

### Measurement of Total Cross Sections

Transmission measurements with maximum resolution are made on a flight distance of 103 m. The neutrons are taken out through a vacuum tube closed by pure aluminum plates. For studying the energy range around 35 keV, in which aluminum has resonances, magnesium plates are used. The detector is a compartment  $29 \times 15 \times 3$  cm in size filled with  $B^{10}$  and surrounded by six NaI(Tl) crystals 12.5 cm in diameter and 5 cm thick. The crystals record the  $\gamma$ -radiation emitted by the excited  $Li^7$  nucleus formed in the reaction  $B^{10}(n, \alpha)Li^7$ . The sample being studied is one third of the flight distance away from the neutron source.

Pulses from the photomultipliers are amplified, fed to a single-channel amplitude analyzer passing only pulses corresponding to the photopeak of  $\gamma$ -radiation (energy 478 keV), and then taken to a time analyzer (the so-called accordion [9]) with  $2^n - 1$  channels ( $n = 9, 10, \dots, 16$ ), the breadth of which may be varied in each experiment between 0.05 and 3.2  $\mu$ sec. The number of possible values of channel breadth, equal to 16, is determined by a ferrite memory unit having 4096 channels.

In 1963 the best resolution obtained for a 0.06- $\mu$ sec neutron pulse width in the accelerator, allowing for the accuracy of the detection time, was 0.8 nsec/m. After inserting new electronic detection systems, an effective resolution of 0.3 nsec/m was obtained for a neutron pulse width of 20 nsec and time-analyzer channel width 10 nsec. This makes it possible to study neutron energies above 30 keV. This resolution was ensured by a suitable delay time of the neutrons in a polyethylene block 2 cm thick situated around the target. Shortly the resolution will again be improved by increasing the flight distance to 200 m.

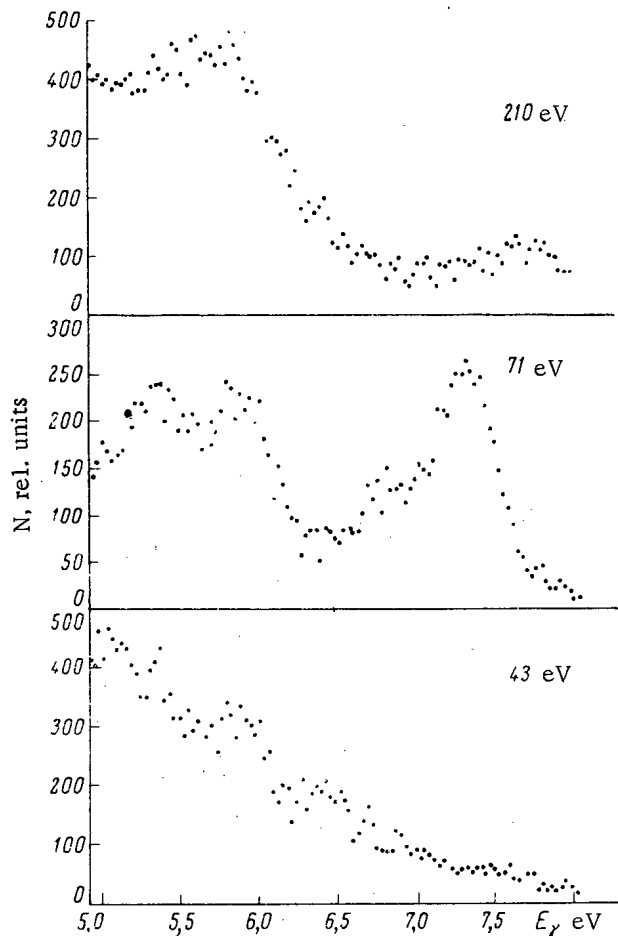


Fig. 2. Spectrum of  $\gamma$ -rays emitted by  $\text{Hg}^{202}$  formed in the reaction  $\text{Hg}^{201} + n$  in resonances 43, 71, and 210 eV.

neutron exciting it to be simultaneously recorded on a magnetic tape within the limits of the total number of channels,  $2^{16}$ ; usually 128 amplitude and 512 time channels are used.

#### Measurement of Capture Cross Section

In these measurements a large liquid scintillation detector is used.† This has  $4\pi$ -geometry and constitutes a reservoir of diameter 1 m with a through channel directed along the diameter for passing the beam. In the center of the channel is the sample in which the radiative capture of neutrons takes place. The reservoir contains 500 liter of liquid scintillator (xylene with the addition of POPOP and 15 liter methylborate, introduced for capturing scattered neutrons and weakening 2.2 MeV  $\gamma$ -radiation arising on capture of the neutrons in hydrogen). The volume is surveyed by eight photomultipliers of diameter 12.5 cm mounted in immediate contact with the liquid scintillator. Use of an internal reflector (dye) raised the light collection by 17%. Sometimes the detector was used with a multidimensional analyzer, but usually a single-channel amplitude analyzer set for an amplitude corresponding to the total energy released by the compound nucleus under study was employed. The single-channel analyzer was connected to a time analyzer (accordeon) and memory unit of 4096 channels.

In order to facilitate analysis, the data obtained were considered together with the results of measuring the transmission of a sample placed in the center of the  $4\pi$ -detector. The transmission was determined by means of a  $\text{B}^{10}$  detector set at the exit from the diametral channel of the  $4\pi$ -detector.

\*Manufactured by "Harshow," USA.

†Manufactured by "Nuclear Enterprise," England.

At the present time, simultaneous recording of two spectra (corresponding to measurement with and without the sample) is frequently carried out by means of the ferrite unit; each of the spectra is disposed in 2048 channels. Two units with 4096 channels each may also be used. The sample being studied is placed in the beam for 30 sec every minute and then taken away. In order to avoid the overlapping of neutrons from neighboring cycles (repetition frequency 500 cps), a  $\text{B}^{10}$  filter is placed in the beam. For measuring the background, filters made up of elements giving "black" resonances in the energy range under examination were constantly situated in the beam. Filter materials included La, Co, Zn, Cu, Bi, Al.

#### Measurements of Partial Radiative Transitions

Measurements were made for flight distances of 14 and 28 m. The first results were obtained with NaI (Tl) crystals of diameter 12.5 and height 12.5 and 15 cm. At the present time a system\* in which the first annihilation peak is separated out by coincidences is used for the measurements. This system is analogous to that used in the Yale laboratory [10]. It consists of a central crystal of NaI (Tl), of diameter 10 and height 15 cm, connected with a photomultiplier, and surrounding this an annular NaI (Tl) crystal with internal aperture 11, external diameter 29, and height 30 cm, connected to nine photomultipliers. The  $\gamma$ -rays recorded in the central crystal are studied in coincidence with the  $\gamma$ -rays (511 keV) recorded in the annular crystal. A multidimensional analyzer [11] enables the pulse amplitude of each  $\gamma$ -quantum being studied and the flight time of the



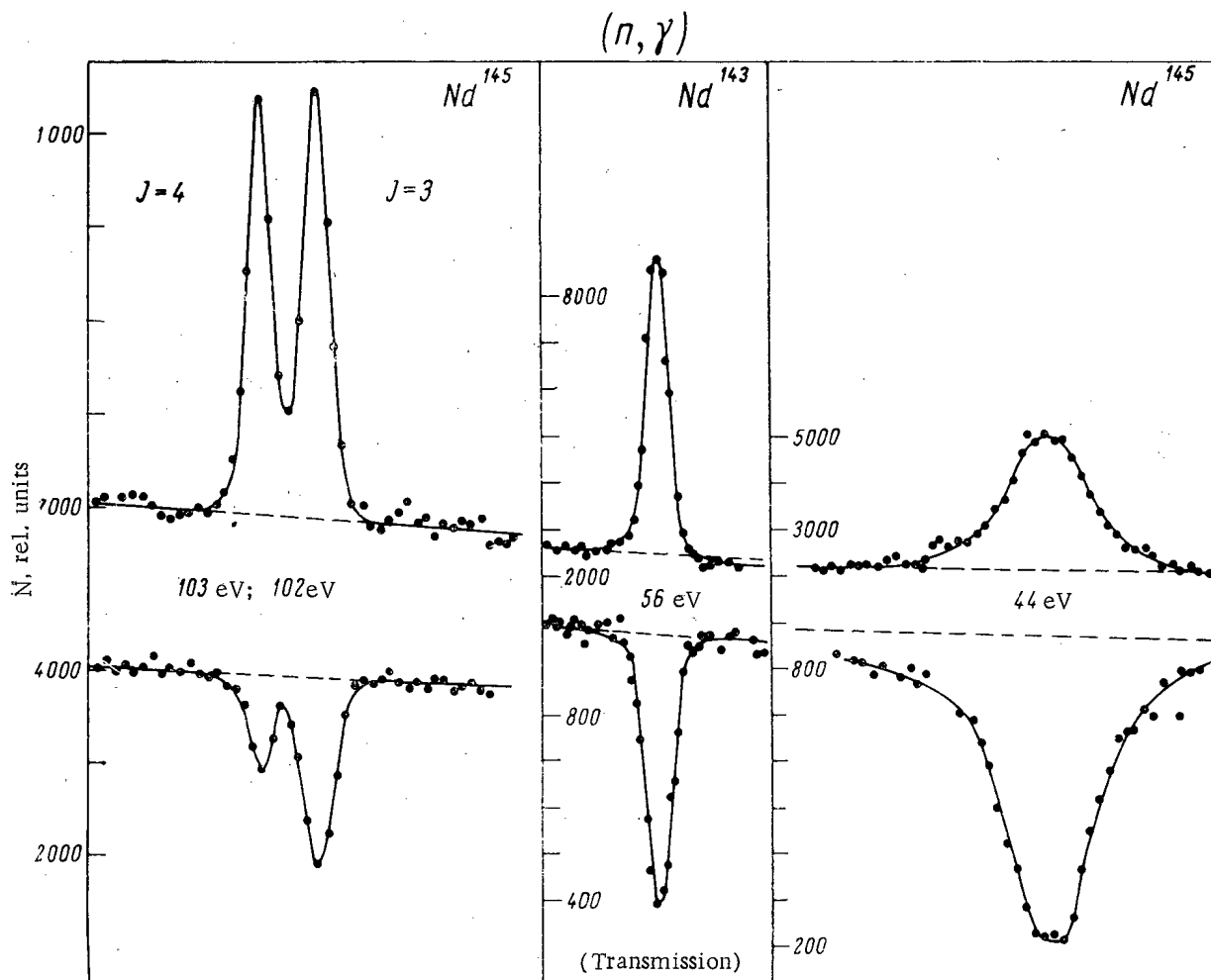


Fig. 3. Simultaneous measurement of capture and transmission in a sample of natural neodymium.

#### Methods of Analyzing the Results

The transmission results were systematically analyzed by various methods [12] on an IBM-7094 computer, mainly using a program which enabled calculations to be made with due allowance for the Doppler effect, and solutions to be obtained simultaneously for some tens of resonances over a wider energy range. Figure 1 shows the results obtained.

The  $\gamma$ -ray spectra obtained on the coincidence system were analyzed on the computer with respect to various components by means of a specific program (Fig. 2).

#### Methods of Identifying Resonances

In a number of cases the need arises to identify the isotope responsible for a given resonance, but a more frequent problem is the choice, for an  $s$ -resonance, of the  $J_+$  or  $J_-$  spin of the compound nucleus, and sometimes one has to determine whether certain resonances belong to the  $p$ -type.

The experiments carried out give certain information for the solution of these problems.

Multidimensional Analysis. The multidimensional analysis of radiative transitions [11] arising on absorption of a neutron in resonance sometimes enables us to identify the isotope responsible for the resonance. For example, from the low-energy ( $< 1$  MeV)  $\gamma$ -ray spectrum measured with one crystal it was established that the resonance doublet at 102.2 and 103.6 eV observed in the cross section of natural neodymium was connected with  $Nd^{145}$ . In other cases identification was made from the total energy of a cascade of  $\gamma$ -transitions as measured by a large liquid scintillation detector. Knowledge of the total energy of the cascade and the binding energy of the neutron enables us to identify the isotope.

In some cases a study of the high-energy radiative transitions offers the possibility of deciding whether certain resonances belong to the p-type: The exceptionally high intensity of the corresponding direct transitions to the ground level, showing that they are dipolar electric, enables us to determine the parity of the original level. In this way p-resonances in target nucleus  $Zr^{91}$  were identified for neutron energies of 1933, 1991, and 4320 eV [4, 11].

The most classical case is the choice between the values of  $J_+$  and  $J_-$  when the target nucleus has spin  $1/2$  and negative parity, and the ground state of the compound nucleus is  $O^+$ . Then an intense radiative transition to the ground state will indicate that the excited state of the compound nucleus has spin  $J_+ = 1$  (parity negative [13]). Such measurements were made in our experiments for target nuclei  $W^{183}$  [14, 15],  $Pt^{195}$  [15, 16], and others (for example, thulium [17]). Considerations connected with high-energy transitions also enable us to choose between  $J_+$  and  $J_-$  for other types of nucleus. For example, in the already-mentioned doublet for  $Nd^{145}$ , spin  $J_- = 3$  was ascribed to resonance 102.2 eV [18].

Measurement of Total Width  $\Gamma$  and Total Radiative Width  $\Gamma_\gamma$ . This also enables us to determine the spin of an s-resonance when the neutron width  $\Gamma_n$  is not too close to  $\Gamma$ . This related mainly to resonances for which we can measure  $\Gamma$  exactly (the value of  $\Gamma_n$  is small) and make relative measurements of  $\Gamma_\gamma/\Gamma$  for other resonances of the same nucleus by means of a liquid scintillation detector. Figure 3 shows curves obtained for simultaneous measurements of transmission and radiative capture made for neodymium [19]. This method was used for many nuclei, and in particular for praseodymium [20] and iron [21].

Measurement of one Transmission. This sometimes enables us to solve certain problems directly. Identification of certain p-resonances may be effected from the symmetry of the transmission curve, indicating the absence of interference between potential and resonance scattering. In studying very thick samples of niobium [22] it was also shown that certain resonances with not-very-small values of  $\Gamma_n$  are nevertheless p-resonances, although it was earlier usually considered that this was simply the case of extremely small values of  $\Gamma_n$ . On the other hand, asymmetry indicates that the nonforce resonance of  $Pr^{141}$  at 85 eV belongs to the s-type.

If the ratio  $\Gamma_n/\Gamma$  is fairly large, then for s-resonances it is sufficient to measure one transmission. Interference between two resonances on the transmission curve indicates that both of these have the same spin (and relate to the same isotope). After checking these ideas for praseodymium [23], the method was used for iron, neodymium (the absence of interference between the two already-mentioned resonances of the  $Nd^{145}$  doublet at 102 to 103 eV showed that they corresponded to different spins), arsenic [24], and isotopes of bromine [25], and for studying medium nuclei (Co [7], Mn [8], V [8]) in the energy range above a few keV.

When  $\Gamma_n$  is very close to  $\Gamma$ , for determining the statistical factor  $g$  or spin  $J$  of the resonance it is sufficient to determine the minimum transmission of an isolated, fairly strong resonance, examined for a thin sample and high resolution. Finally, measurement of the intensity of the interference effect between potential and resonance scattering on a fairly thick sample enables us to estimate the cross section at the resonance maximum and hence the  $J$ , on the assumption that the value of the potential cross section is known; and, conversely, we may determine the value of the potential cross section if the parameters of the resonance are known from other sources (as, for example, in the case of the resonance at 1120 eV for  $Pr^{141}$ ). This method is simply a particular case of the method of form analysis for a thick sample, enabling us to determine  $\Gamma$  by fixing the upper limit for  $\Gamma_n$ .

## STATISTICAL PROPERTIES OF SCATTERING WIDTHS

### Force Function

The force function  $S_0$  for the s-neutron wave is determined from measurements of the reduced neutron widths  $\Gamma_n^0$ . It is usually assumed that for the two families of spins  $J_+$  and  $J_-$  the force functions are identical. We confirmed this supposition for the case of  $Pt^{195}$ . It was noted in [6, 24, 25], however, that for many other nuclei this condition is not observed. We should note the dependence of  $S_0$  on  $J$ , which may be explained by the fact that certain combinations of the states of the original nucleus and the particle favor one of the values of spin  $J$  [26].

The results of our investigations are partly given in the table, from which we see that resonances with certain spins are strongest and hence form the main contribution to  $S_0$ . Assuming that for the quantity  $\Gamma_n^0$  the Porter-Thomas distribution is valid [27], and supposing that  $S_0$  does not depend on  $J$ , we calculated the probability that the ratio of  $S_0$  for  $J_+$  to  $S_0$  for  $J_-$  ( $> 1$ ) was larger than or equal to the value found by experiment. This probability is given in the last column of the table.

## Properties of Neutron Resonances of Certain Elements

Target nucleus	Total number of observed resonances	Neutron energy range, eV	Number of resonances for which spin determined	Spin	Number of resonances having given spin	Force function $S_0 \times 10^{-4} \text{ eV}^{-1/2}$	Experimental ratio	Probability, %*
Ga <sup>69</sup>	12	200—2500	7	$J_+ = 2$ $J_- = 1$	7 0	$1,8 \pm 0,9$ $< 0,4$	—	—
As <sup>75</sup>	55	40—4000	27	$J_+ = 2$ $J_- = 1$	15 12	$2,5 \pm 0,6$ $1 \pm 0,3$	2,5	1
Se <sup>77</sup>	10	100—1500	9	$J^- = 0$ $J_+ = 1$	3 6	—	7	1
Br <sup>79, 81</sup>	82	30—2000	23	$J_+ = 2$ $J_- = 1$	16 7	—	2	7†
Pt <sup>195</sup>	19	10—310	19	$J_- = 0$ $J_+ = 1$	6 13	$2,3 \pm 1,3$ $1,9 \pm 0,7$	—	—
Au <sup>197</sup>	64	50—1000	43	$J_+ = 2$ $J_- = 1$	28 15	$2,5 \pm 0,5$ $1,2 \pm 0,35$	2	1

\*The probability given in the table is that of finding a value of the ratio equal to or exceeding the experimental value, on the assumption that  $S_0$  does not depend on J.  
†For each isotope.

Nuclei with Spin  $I = 1/2$ . Whereas Pt<sup>195</sup> is the classical example of a weak dependence of  $S_0$  on J, for selenium [7] this dependence shows up strongly; however, the number of observed resonances is small and the main contribution to  $S_0$  ( $J = 0$ ) comes from levels disposed below 1000 eV. For cadmium [28] and thulium [29] the dependence shows up weakly. Experiments for yttrium are continuing, since the number of resonances so far studied is not great.

Nuclei with Spin  $I = 3/2$ . At the moment we can consider six nuclei of this type: two single isotopes (arsenic and iron) and two elements each with two isotopes (gallium and bromine). The relationship  $S_0(J)$  is in order of magnitude roughly the same for the six cases and suggests the value  $J = 2$ . For other nuclei (Cu<sup>63</sup>, Cu<sup>65</sup>, Hg<sup>201</sup>, Ba<sup>135</sup>) the statistics are insufficient to allow conclusions.

Nuclei with Spin  $I > 3/2$ . Our results for nuclei Mn<sup>55</sup> [8] and Pr<sup>141</sup> [20], which have spin  $5/2$ , are still being analyzed. Examination of Co<sup>59</sup>, having a spin of  $7/2$ , up to 80 keV has yielded no definite conclusion. For Nd<sup>143</sup> and Nd<sup>145</sup> [18] not enough resonances have yet been studied. The case of the p-wave may be studied, for example, in Nb<sup>93</sup> + n, for which the force functions  $S_1$  may be directly determined from the parameters of 33 resonances [22] disposed below 2200 eV. The value obtained,  $S_1 = (5.05 \pm 1.0) \cdot 10^{-4}$ , agrees closely with that determined from measurements of the mean effective cross section [30].

## STATISTICAL PROPERTIES OF RADIATIVE WIDTHS

Total Radiative Widths

The excellent apparatus resolution, in combination with the method of form analysis, enables us to study the total radiative widths  $\Gamma_\gamma$  as a function of mass number. We may assume that the total radiative width never exceeds 0.5 eV, its fluctuations from resonance to resonance are smallish, except for certain nuclei (Pt<sup>195</sup> + n, Hg<sup>201</sup> + n), and its variations are connected with the character of the s- or p-resonance.

Case of s-Neutron Wave. We studied the target nuclei Fe<sup>56</sup>, Cu<sup>63</sup>, Cu<sup>65</sup>, Zn, Ga<sup>69</sup>, Ga<sup>71</sup>, As<sup>75</sup>, Se<sup>77</sup>, Br<sup>79</sup>, Br<sup>81</sup>, Zr<sup>91</sup>, Zr<sup>96</sup>, Nb<sup>93</sup>, La<sup>139</sup>, Pr<sup>141</sup>, Nd<sup>143</sup>, Nd<sup>145</sup>, Tm<sup>169</sup>, W<sup>183</sup>, Pt<sup>195</sup>, Au<sup>197</sup>, Hg<sup>199</sup>, Hg<sup>201</sup>. The values of  $\Gamma_\gamma$  obtained were close to 0.3 eV for nuclei with mass numbers A between 56 and 90 and fell to 0.1 eV for nuclei with A around 145. The tendency for  $\Gamma_\gamma$  to fall also occurs in the region of deformed nuclei, but for nuclei close to those with a filled shell,  $\Gamma_\gamma$  begins to rise and reaches values exceeding the value of  $\Gamma_\gamma$  for Hg<sup>201</sup>. We should also note the considerable fluctuations of  $\Gamma_\gamma$  from resonance to resonance for Hg<sup>199</sup> and Hg<sup>201</sup> (for the same value of spin).

Extremely refined analysis shows that for the transition from Nd<sup>143</sup> + n to Nd<sup>145</sup> + n [19] there is a considerable fall in  $\Gamma_\gamma$ , as predicted by Cameron's formula [31].

Case of p-Neutron Wave. Study of the  $\text{Nb}^{93} + n$  reaction showed that in resonances of the p-type,  $\Gamma_\gamma$  equalled  $230 \pm 50$  meV and in resonances of the s-type,  $140 \pm 30$  meV. Study of the  $\gamma$ -ray spectra of capture in resonances revealed great differences in the spectra, but these could not serve as sufficient criterion to prove that these resonances belonged to the p-wave. The nature of these resonances, having elevated values of  $\Gamma_\gamma$ , was elucidated from the symmetry of the transmission curve in measurements with thick samples.

#### Partial Radiative Widths

At the present time systematic work is going on with the help of the crystal ring detector in order to repeat and continue the previous measurements concerning  $\text{Pt}^{195}$  [16] and  $\text{U}^{238}$  [32], and also to study the fluctuations from resonance to resonance of the widths relating to the high-energy transitions. For  $\text{Hg}^{199}$  and  $\text{Hg}^{201}$  the fluctuations of the total widths  $\Gamma_\gamma$  must be explained as a function of spin.

A study was made of iron, where the transition with energy around 6 MeV is connected with a partial width, fluctuating in accordance with the strength of the resonances, enabling us to determine the possible contribution of direct radiative capture to the wings of the resonance at 4.8 keV. The resonances of copper at 648 and 990 eV and of zinc at 281 and 322 eV, for which  $\Gamma_\gamma \approx \Gamma$ , were also objects for investigation.

#### CONCLUSIONS

We expect that when the third section of the accelerator is set up, increasing the energy of the electrons to 45 MeV, and experiments with more intense neutron beams begin, a great deal of data will be obtained on the relation between the statistical properties of resonances for medium nuclei situated in the range 5 to 100 keV and the spin. In this region, where a resolution of 0.1 nsec/m can be attained, the system used in Saclay may successfully compete with the Van der Graaf accelerator. On the other hand, the intensive development of studies on the partial radiative widths at higher intensity or resolution should lead to the improvement of existing results.

#### LITERATURE CITED

1. R. Bergere, Neutron time-of-flight methods, Publie par Euratom. Bruxelles (1961), p. 329.
2. H. Leboutet et al., *Onde electrique*, 37, 358, 28 (1957).
3. *Rapports interieurs EANDC (1963-1964)*.
4. J. Julien, Neutron time-of-flight methods, Publie par Euratom. Bruxelles (1961), p. 139; C. Corge et al., *J. Phys.*, 22, 724 (1961).
5. C. Corge et al., *C. R. Acad. Sci.*, 253, 859 (1961).
6. J. Julien et al., *Phys. Letters*, 3, 2, 67 (1962).
7. J. Morgenstern et al., *Nucl. Phys.* (in press).
8. J. Morgenstern et al., (in press).
9. J. Thenard and G. Victor, *Nucl. Instrum. and Methods*, 26, 45 (1964).
10. C. Bostrom and J. Draper, *Rev. Sci. Instrum.*, 32, 1024 (1961).
11. J. Julien et al., *C. R. Acad. Sci.*, 254, 4162 (1962).
12. G. Bianchi and C. Corge, *Rapport C. E. A.* 2346 (1963); *Rapport C. E. A.* (in press).
13. H. Landon and E. Rae, *Phys. Rev.*, 107, 1333 (1957).
14. V. Huynh et al., *C. R. Acad. Sci.*, 248, 2330 (1959).
15. C. Corge et al., *C. R. Acad. Sci.*, 249, 413 (1959).
16. J. Julien et al., *J. Phys.*, 21, 423 (1960).
17. G. Bianchi et al., *J. Phys.*, 24, 994 (1963).
18. G. Bianchi et al., *J. Phys.*, 24, 997 (1963).
19. G. Bianchi et al., *J. Phys.*, 24, 999 (1963).
20. M. Vastel, *These de 3e cycle*. Orsay (1963).
21. J. Julien et al., *Nucl. Phys.* (in press).
22. J. Julien et al., *Congrès International de Physique Nucleaire*, Paris, Juillet (1964).
23. J. Julien, *C. R. Acad. Sci.*, 252, 3233 (1961).
24. J. Julien, *Phys. Letters*, 10, 86 (1964).
25. J. Julien, *Nucl. Phys.* (in press).
26. F. Firk et al., *Proc. Phys. Soc.*, 82, 477 (1963).
27. C. Porter and R. Thomas, *Phys. Rev.*, 104, 483 (1956).

28. L. Bollinger et al., *Congres International de Physique Nucleaire, Paris, Juillet* (1964).
29. P. Singh, (Private Communication).
30. K. Seth et al., *Phys. Letters*, 13, 70 (1964).
31. A. G. W. Cameron, *Canad. J. Phys.*, 37, 322 (1959).
32. C. Corge et al., *J. Phys.*, 22, 722 (1961).

EFFECTIVENESS OF HETEROGENEOUS ABSORBERS IN HOMOGENEOUS  
URANIUM - WATER REACTORS

(UDC 621.039.520.22)

G. M. Vladykov, B. G. Dubovskii, A. V. Kamaev, V. Ya. Sviridenko,  
F. M. Kuznetsov, G. A. Popov, and Yu. D. Palamarchuk

Translated from *Atomnaya Énergiya*, Vol. 19, No. 1,  
pp. 14-19, July, 1965  
Original article submitted July 20, 1964

Experiments on the effectiveness of absorbers in homogeneous uranium-water reactors are described and the results are reported. A study was made of the effectiveness of one (absorber) and of a group of cylindrical rods made of cadmium and boron carbide, as a function of their dimensions and uranium concentration in the active zone. The influence of steel cladding on the effectiveness of the rods is demonstrated.

The results of a two-group calculation of the effectiveness of a boron carbide central rod are compared with experimental data.

Heterogeneous neutron absorbers have been widely used to reduce nuclear hazards during the processing of fissile materials. In this paper an analysis is made of the effect of absorbers on the critical mass of homogeneous uranium reactors. The experiments were performed on reactors without reflectors, and also on reactors with lateral and bottom reflectors 25 cm thick. The active zone of the reactors was a water solution of  $\text{UO}_2(\text{NO}_3)_2$  which was poured into the cylindrical stainless steel tank (1Kh18N9T steel, wall thickness 1.5 mm).

In experiments with bare reactors the minimum distance of the active zone from the walls, the floor, and the surrounding objects was not less than 2 m. The experiments were performed with uranium solutions (90% enriched). The absorbing rods consisted of boron carbide powder with free density of  $1.25 \text{ g/cm}^3$ , placed in cylindrical stainless steel containers, or water filled cadmium tubes with wall thickness of 0.5 mm, also placed in stainless steel containers.

#### Method of Measurement

From the point of view of nuclear safety, the effectiveness of absorbers can conveniently be estimated from the change in the critical volume (critical mass, or critical height) when the absorbers are introduced into the active zone of the reactor. In this paper the effectiveness of the absorbers is expressed as a difference in the critical volumes and critical heights of reactors with and without absorbers.

The effectiveness of the absorbing rods and inserts was determined in a reactor with an active zone having a diameter of 400 mm. The absorbing rod was introduced into the active zone of the critical reactor of height  $H$ . The level of the solution rose as a result of the displacement of the liquid by the absorber. By adding a further amount of the solution, the reactor was again brought to the critical state with the new height of the active zone  $H^f$  ( $H$  and  $H^f$  are the critical heights of the reactor without and with absorbing rod, respectively). The critical height could be determined to within  $\pm 1.5\%$ . Chemical analysis of the uranium solution was performed by precipitating ammonium diuranate [1]. The concentration of uranium in the solution was determined to within  $\pm 1\%$ . Solutions with uranium concentrations  $C = 38, 72, \text{ and } 286 \text{ g/liter}$  were used in the experiments.

The rate of change of reactivity with varying critical height of the active zone was measured to determine the effectiveness of the absorbers. Different values of the critical height were achieved by varying the diameter of the active zone. These experiments were performed with a solution having a uranium concentration of  $72 \text{ g/liter}$ . The critical volume of the solution was achieved in the active-zone tank. In order to induce the supercritical state in the critical reactor, small portions of the uranium solution were added, and this was followed by measurement of the settling periods for the supercritical reactors. Next, for each height of the active zone, the reactivity  $\Delta\rho$  was calculated from the inhour formula, with allowance for delayed neutrons, as a function of the increase  $\Delta h$  in the

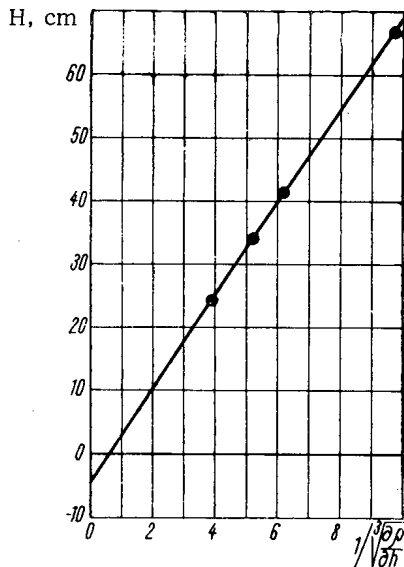


Fig. 1. Experimental dependence of  $(\partial\rho/\partial h)$  on the critical height  $H$  of the reactor.

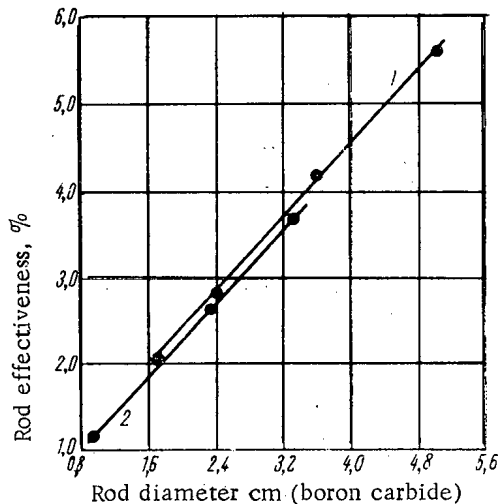


Fig. 2. Dependence of the effectiveness of a boron carbide absorbing rod on its diameter in a bare cylindrical reactors (active zone diameter  $d=400$  mm, concentration of uranium in solution  $C=72$  g/liter): 1, 2 steel clad rods (4 and 0.3 mm of steel respectively).

sions of the reactor with and without a rod were determined by solving the system of two-group reactor equations. The radical problem was solved for a cylindrical reactor with equivalent heights  $H_e = H + 2\lambda$  (reactor without rod) and  $H_e^r = H^r + 2\lambda$  (reactor with rod). It was assumed that the extrapolation length  $\lambda$  was unaffected when the absorbing rod was inserted and consequently  $\Delta H = H_e^r - H_e = 2\lambda$ . The steel tank of the reactors and the steel cladding of the rods were not taken into account in the calculations. The boundary conditions on the surface of the rod were written down in accordance with [3]. The neutron scattering in the rod was taken into account within the framework of the one-collision theory. The capture and fission cross sections, and also the diffusion coefficient and the quantity  $1/\gamma(u)$ , which characterises the "greyness" of the rod for a lethargy  $u$  of the epithermal neutrons, were averaged over the spectrum on the 10-group diffusion approximation for a bare spherical reactor [4]. In order to estimate the

height of the active zone. The delayed neutrons were represented by coefficients expressing for each group of such neutrons the ratio of escaping, delayed, and prompt neutrons. From the one-group diffusion theory we have according to [2]

$$\frac{\partial\rho}{\partial h} = \frac{2\pi^2 M^2}{k_\infty} \cdot \frac{1}{(H+2\lambda)^3}, \quad (1)$$

where  $\rho$  is the reactivity in units of  $10^{-5}$ ,  $M^2$  is the neutron migration area in  $\text{cm}^2$ ,  $k_\infty$  is the neutron multiplication constant in an infinite system, and  $\lambda$  is the extrapolation length in cm. When the solution is added to a critical reactor the total reactivity becomes

$$\rho = \frac{2\pi^2 M^2}{k_\infty} \int_{H_{\text{sup}}}^H \frac{dh}{(h+2\lambda)^3} \quad (2)$$

or

$$\rho = \frac{\pi^2 M^2}{k_\infty} \left[ \frac{1}{(H+2\lambda)^2} - \frac{1}{(H_{\text{sup}}+2\lambda)^2} \right], \quad (3)$$

where  $H_{\text{sup}}$  is the height of the active zone of the supercritical reactor which becomes critical when the absorbing rod is inserted into the active zone. From equation (1) we have

$$\rho = \frac{1}{2} \left( \frac{\partial\rho}{\partial h} \right) (H+2\lambda)^3 \times \left[ \frac{1}{(H+2\lambda)^2} - \frac{1}{(H_{\text{sup}}+2\lambda)^2} \right]. \quad (4)$$

Experimental values of  $(\partial\rho/\partial h)$  and  $H$  were analyzed by the method of least squares, and the resulting data were used to plot  $H$  as a function of  $(\partial\rho/\partial h)^{-1/3}$  (Fig. 1). This yielded

$$\begin{aligned} \frac{\partial\rho}{\partial h} \cdot (H+2\lambda) &= 336 \pm 16 \text{ and } 2\lambda \\ &= 5.4 \pm 0.2 \text{ cm.} \end{aligned}$$

#### Effectiveness of a Central Absorbing Rod

Results of experiments and calculations on the efficiency of a central absorbing rod are shown in Figs. 2-6. The corresponding calculations of the increase in the critical height  $\Delta H = H^r - H$  were performed for a bare reactor. The critical dimen-

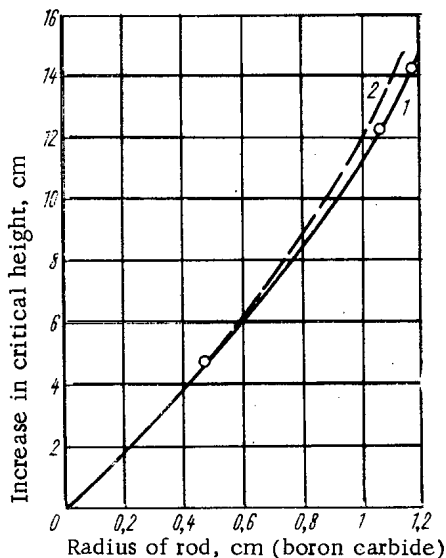


Fig. 3. Dependence of the effectiveness of a central absorbing boron carbide rod on its radius in a bare cylindrical reactor ( $d = 400$  mm,  $C = 38$  g/liter,  $H = 41.3$  cm): 1) experiment, rods clad in 0.3-0.5 mm of steel; 2) calculation without allowance for the steel cladding.

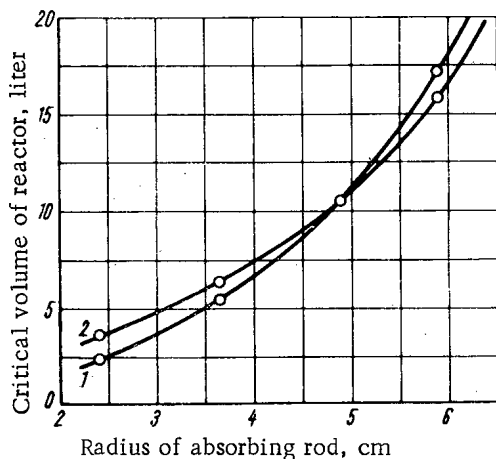


Fig. 5. Effectiveness of boron carbide and cadmium rods filled with water, as a function of radius (bare reactor;  $d = 400$  mm,  $C = 136$  g/liter, critical volume of reactor without rod 25.6 liters): 1) rods in the form of water-filled cadmium tubes (0.5 mm of cadmium, thickness of steel cladding 1 mm); 2) boron carbide rods (thickness of steel cladding 1 mm).

A comparison of the effectiveness of rods filled with boron carbide powder and cadmium rods filled with water is shown in Fig. 5. It is clear that for diameters up to 90 mm, a solid rod with boron carbide is more effective.

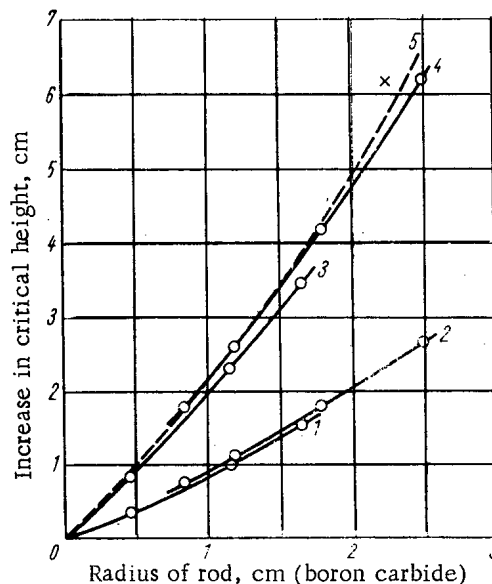


Fig. 4. Effectiveness of a central absorbing boron carbide rod as a function of its radius (bare reactor,  $d = 400$  cm,  $H = 24.3$  cm for  $C = 72$  g/liter, and  $H = 19.2$  cm for  $C = 286$  g/liter): 1,2) experiment, rods clad in 0.3-0.5 and 4 mm of steel respectively ( $C = 286$  g/liter); 3,4) experiment, rods clad in 0.3-0.5 and 4 mm of steel respectively ( $C = 72$  g/liter); 5) calculation ignoring the steel cladding ( $C = 72$  g/liter); X) calculation with allowance for the steel cladding ( $C = 72$  g/liter).

effect of the steel tank, a special calculation was performed of the effectiveness of a two-layer rod, consisting of 45 mm in diameter of boron carbide and a 4 mm steel cladding, with allowance for multiple scattering of the neutrons in the rod using the method described in [5]. It is evident from Figs. 3 and 4 that the 2-group calculations led to a rod effectiveness which was somewhat high.

For a uranium concentration of 38 g/liter, the discrepancy between calculated and experimental data is 2-9%; for  $C = 72$  g/liter, the calculated values for the effectiveness of rods with 0.3-0.5 mm cladding is higher by 10% than the experimental result. When the steel envelope is taken into account the discrepancy between the calculated and experimental values becomes 11%. It follows that 2-group calculations can be used to estimate the rod effectiveness. Experiments and calculations performed for a rod of boron carbide having a diameter of 4.5 cm showed that for a given rod size its effectiveness falls somewhat with decreasing envelope thickness. The steel cladding gives rise to two opposite effects: (1) it screens the boron carbide and (2) it displaces the solution. The latter effect is found to predominate (see Figs. 2 and 4).



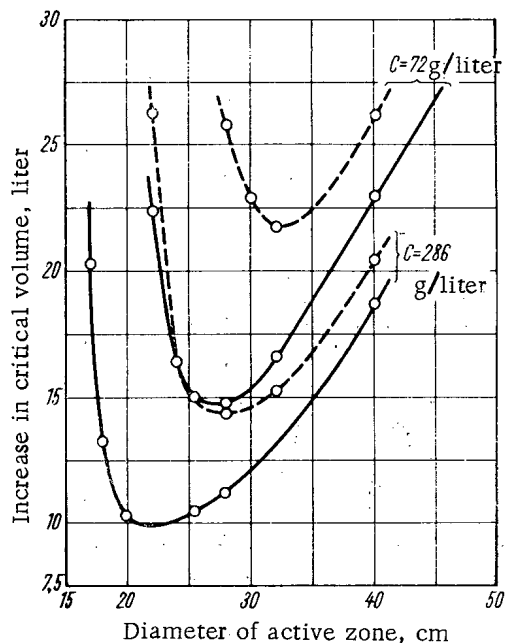


Fig. 6. Critical volume of cylindrical reactor, with absorbing rods (-----) and without (—) as a function of active-zone diameter (reactor with reflector; diameter of absorbing rod (boron carbide) 50 mm; thickness of steel cladding 4 mm).

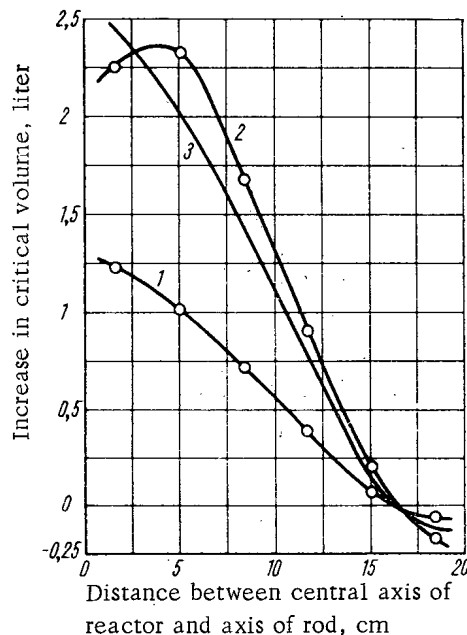


Fig. 7. Effectiveness of one and of two absorbing rods as a function of their position along the radius of the active zone (bare reactor:  $d = 400$  mm,  $C = 286$  g/liter, diameter of boron carbide 24 mm, thickness of cladding 4 mm): 1) one rod, 2) two rods, 3) single-rod effectiveness multiplied by two.

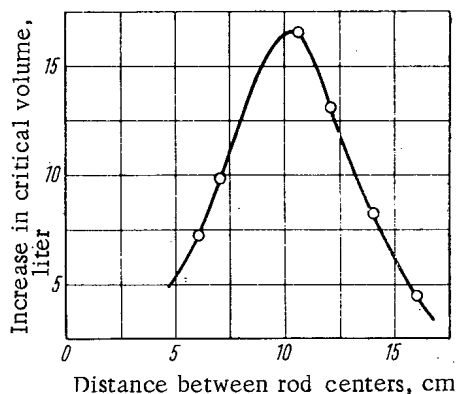


Fig. 8. Effectiveness of 7 rods (1 central and 6 eccentric) as a function of their mutual separation (reactor with reflector:  $d = 400$  mm,  $C = 286$  g/liter, diameter of boron carbide rod 50 mm, thickness of steel cladding 4 mm).

When the outer diameter of the absorber increases, the rod effectiveness becomes the same. Further increase in the diameter makes the cadmium tube filled with water more effective. When the rod diameters reach about 100 mm, which corresponds to  $\sim 2\sqrt{\tau_{H_2O}}$ , where  $\tau_{H_2O}$  is the neutron age, the absorber efficiencies become equal. A series of experiments was also carried out to determine the critical volumes of cylindrical reactors with and without a central absorbing rod, as a function of the active zone diameter. The reactors had lateral and bottom water reflectors. The active zone diameters were 160–500 mm. The data obtained in these experiments (Fig. 6) show that as the active zone diameter decreases, the critical volumes of the solution with rod and without rod increase and become infinite at certain values of the diameters. For smaller diameters the reactor can only be subcritical.

#### Effectiveness of a Group of Absorbing Rods

Figure 7 shows the efficiency of one and of two rods as functions of position in the active zone of the reactor.

Curve 1 corresponds to an experimental determination of the effectiveness of a single rod as it is displaced from the center of the active zone to its periphery. This gives rise to a reduction in the rod effectiveness. The positive effect of rod reactivity on the boundary of the active zone is due to the fact that the rod acts not only as a reflector but in addition modifies the form of the reactor by displacing a part of it, and this leads to an increase in the reactivity. Curve 2 (Fig. 7) shows the effectiveness of two rods symmetrically located with respect to the reactor axis. Curve 3 shows the single rod effectiveness multiplied by two, with the rod located on the same radius as the two symmetrical rods.

TABLE 1. Effectiveness of a Group of Rods Distributed Symmetrically on a Circle of Radius 192 mm

Number of rods	2	3	4	6
Increase in critical volume, liter (concentration of uranium = 72 g/liter)	3.0	9.4	17.8	91.9
Increase in critical volume, liter (uranium concentration = 286 g/liter)	2.2	2.6	5.6	11.3

Note: reactor with reflector, d = 400 mm, diameter of boron carbide 50 mm, thickness of steel cladding 4 mm.

TABLE 2. Effectiveness of Regular Arrays of Rods for Different Numbers of Rods

Parameter	Diameter of boron carbide 17 mm, thickness of steel cladding 4 mm					Diameter of boron carbide 12 mm, thickness of steel cladding 4 mm					
	60					40					
Rod separation, mm . . . . .	60					40					
Number of rods . . . . .	7	12	13	18	36	6	7	18	36	6	18
Increase in critical volume, liter. . . . .	2.73	4.45	5.23	8.05	17.9	2.18	2.20	7.00	24.75	1.48	4.55

Note: reactor with reflector, d = 400 mm, uranium concentration = 286 g/liter, critical volume of reactor without rods 18.2 liter.

TABLE 3. Effectiveness of Regular Sets of Rods for Different Number of Rods

Rod separation, mm		60				40	
Number of rods . . . . .	6	18	1	6	7	18	36
Increase in critical volume, liter. . . . .	3.40	15.10	0.80	3.40	3.50	18.90	58.90

Note: reactor with reflector, d = 320 mm, uranium concentration 286 g/liter, critical volume of bare reactor 13.1 liter, diameter of boron carbide 17 mm, thickness of steel cladding 4 mm.

When the distance between the rods is small, interference is negative, but in the remaining cases it is positive. Maximum interference is obtained with rod separation of about 10 cm. An analogous effect is observed in measurements on the effectiveness of 7 rods (Fig. 8). The measurements were performed for a fixed central rod and a simultaneous displacement of six symmetrically located rods. It was shown that the maximum effectiveness of such a group of rods is observed when the distance between the centers of the rods is 10 cm, just as in the case of two rods.

The effectiveness was also determined for a group of rods arranged symmetrically on a circle of radius approximately equal to 0.5 of the radius of the active zone (except for a group of 4 rods when one rod lay at the center of the active zone). The results of these experiments are given in Table 1. When the diameter of the active zone is 400 mm, the insertion of six rods increases the critical volume of the reactor by 65% or more, depending on the concentration of uranium in the solution.

Tables 2 and 3 show the results of experiments involving the insertion of rods into the active zone between the center and the periphery. This gave rise to a two-zone reactor with the central zone filled uniformly with rods, and a circular peripheral zone without rods. The ratio of the volumes of these zones could be varied by increasing the number of rods. Experiments showed that the use of a group of rods leads to a considerable increase in the critical volume and may be recommended as a method of ensuring nuclear safety in technological equipment.

## LITERATURE CITED

1. V. K. Markov, Uranium and the Methods for its Determination [in Russian], Moscow, Atomizdat (1960).
2. Krasik and Radkovskii, in Proceedings of the Second International Conference on the Peaceful Uses of Atomic Energy, Geneva, 1955, 5 [in Russian] (1958), p. 248.
3. G. I. Marchuk, Design Calculations for Nuclear Reactors [in Russian], Moscow, Gosatomizdat (1961).
4. A. I. Novozhilov and S. B. Shikhov, Atomnaya Énergiya, 8, 209 (1960).
5. E. I. Grishanin, Atomnaya Énergiya, 16, 234 (1964).

RELATIVE VAPOR PRESSURE DIFFERENCES OF  $B^{11}F_3 - B^{10}F_3$ 

(UDC 621.039.332/546.27)

I. B. Amirkhanova, A. V. Borisov, I. G. Gverdtsiteli,  
and A. T. Karamyan

Translated from *Atomnaya Énergiya*, Vol. 19, No. 1,  
pp. 20-24, July, 1965

Original article submitted July 1, 1964; Final editing December 14, 1964

The relative vapor pressure differences of the isotopic molecules  $B^{11}F_3 - B^{10}F_3$  were measured in the temperature range 147-247.7°K. The enrichment factor decreases from  $20 \cdot 10^{-3}$  (147.0° K) to  $1.1 \cdot 10^{-3}$  (247.7° K).

Within the limits of the experimental error (2-4%), liquid solutions of  $B^{11}F_3 - B^{10}F_3$  are ideal. Within the measured temperature interval, corrections were calculated for the enrichment factors, related to the nonideality of the gas phase.

When other parameters of the process of rectification of  $BF_3$  are available (height of the theoretical plate, throughput of the packing, etc.), the data obtained permit an estimation of the efficiency of the process of separation of  $B^{11}F_3 - B^{10}F_3$  at various pressures.

In the calculation of separating columns for the production of the isotopes  $B^{10}$  and  $B^{11}$  by distillation of  $BF_3$ , it is necessary to have information on the separation factors within a rather wide temperature range. The data available in the literature are insufficient for this purpose. The values of the relative volatility of  $B^{11}F_3$  and  $B^{10}F_3$  have been determined by various methods [1-5], but all the measurements were performed within a small temperature range -160-173° K (the boiling point of  $BF_3$  is equal to 172.4° K [6]), and there are considerable discrepancies among the results obtained by different authors. In view of this, measurement of the relative volatility of  $B^{11}F_3 - B^{10}F_3$  and establishment of the dependence of this quantity on the temperature are of great practical importance.

Just as before [5], we used a differential method. Its essence consists of a direct measurement of the difference in the saturated vapor pressures of the isotopes at a fixed temperature. In view of the smallness of such a difference, high requirements are set for stabilization of the temperature. The temperature drop between samples should not exceed  $\sim 10^{-3}$  degree during the time required for taking the experimental point. As a result of this, the maximum possible thermal insulation of the pressure pickup is required, and at the same time, a short time of establishment of the equilibrium temperature (of the order of several minutes) is needed.

Various types of cryostats have been tested. At pressures below 1 atm, the measurements were conducted on the instrument of [5], where the pickup of the pressures of  $B^{11}F_3 - B^{10}F_3$  is placed in a bath with liquid ethylene, and the temperature is stabilized by regulating the vapor pressure of ethylene. Such cryostats, convenient within a narrow temperature range, require a set of thermostatically controlling liquids when the temperature region is expanded.

The cryostat described below permits the production of a stable temperature from -195.8° C to zero °C, with fluctuations of no more than  $10^{-3}$  degree. The pressure pickup (Fig. 1) consists of a copper block, 50 mm in diameter, 30 mm high, with two circular chambers, placed one in the other. It is placed in a copper reservoir of a gas thermometer, filled with helium. The gas thermometer is a sensitive element of the temperature regulator, is bathed by nitrogen vapors, and is equipped with a heater. When the temperature is varied, the helium pressure in the gas thermometer varies; heating is turned on or off with the aid of the relays and contacts of the manometer, and the temperature in the volume is thereby maintained with an accuracy of  $10^{-3}$  degree.

The level of liquid  $N_2$  in the cryostat is kept constant automatically with the aid of a Bellows valve. The absolute vapor pressures of the isotopes are measured with standard manometers, while the pressure difference is

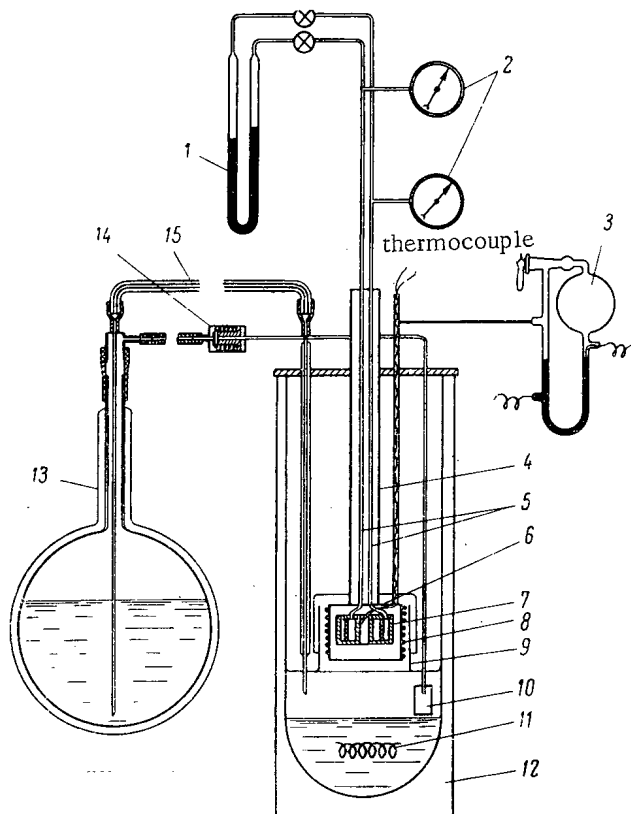


Fig. 1. Scheme of setup for measuring the vapor pressures of the isotopes  $B^{11}F_3$ - $B^{10}F_3$ : 1) differential manometer; 2) standard manometers; 3) contact manometer; 4) vacuum sleeve; 5) steam delivery tubes; 6) gas thermometer; 7) pressure pickup; 8) heater of gas thermometer; 9) guide of flow of nitrogen vapors; 10) pickup registering level of liquid  $N_2$ ; 11) evaporator of liquid  $N_2$ ; 12) Dewar flask; 13) Dewar flask with  $N_2$ ; 14) Bellows valve; 15) overflow tube.

Then measured amounts of  $BF_3$  of the same isotopic composition were condensed into pressure pickup chambers cooled to the required temperature, and when temperature equilibrium was reached, the zero point of the instrument was checked.

The saturated vapor pressure difference of  $B^{11}F_3$  and  $B^{10}F_3$  was measured analogously. For this purpose, a preparation enriched in  $B^{11}F_3$  was condensed into one of the chambers of the pressure pickup, while a preparation enriched in  $B^{10}F_3$  was condensed into the second chamber. The temperature dependence of  $\Delta P/P$  was then recorded.

By measuring  $\Delta P/P$  as a function of  $T$  by this method within a definite temperature interval for samples with different contents of the isotopes, we obtained the dependence of  $\Delta P$  on the isotope concentration.

In most of these experiments, the vapor pressures of liquid boron trifluoride, enriched in  $B^{10}F_3$ , and  $BF_3$  with a natural content of 18.6%  $B^{10}F_3$ , were compared. In this case, samples with maximum enrichment in  $B^{10}F_3$  were measured, and then mixtures were prepared with a reduced  $B^{10}F_3$  concentration. The concentrations of the mixtures were evaluated according to data on the pressures and volumes of the gases to be mixed and were measured more exactly on a mass spectrometer.

The saturated vapor pressure differences of mixtures of the isotopes  $B^{11}F_3$ - $B^{10}F_3$ , with  $B^{10}$  concentrations equal to 2.5-86.5; 13.0-96.9; 18.6-86.5; 18.6-81.6; 18.6-59.2; 18.6-34.3% at pressures from 70 to 626 mm Hg, were measured on the instrument described in [5]. The error in the measurements of  $\Delta P$  in these experiments was no more than 0.02-0.03 mm Hg, while the absolute pressures were measured with mercury manometers with an accuracy of 1 mm Hg.

measured with a differential mercury manometer with readings on a KM-6 cathetometer. Such a system permits measurement of the pressure with an accuracy of  $10^{-1}$  mm Hg when the absolute pressures are varied from 1 to 50 atm.

Purification of  $BF_3$ . It is known that the relative difference in the vapor pressures of the isotopes,  $\epsilon_0 = \Delta P_0/P_0$ , is of the order of 1%. Hence, for measurement of  $\epsilon_0$  with an accuracy of 1%, the presence of impurities more volatile or comparable in volatility with  $BF_3$  at a given temperature should not exceed  $\sim 10^{-2}\%$ .

One of these substances is  $SiF_4$  (at  $T=172.4^\circ K$ , the value of  $P=400$  mm Hg).

The ability of  $BF_3$  to form a complex with anisole was used for its purification. The impurities that do not form chemical compounds with anisole ( $SiF_4$ ,  $N_2$ ,  $O_2$ , HF), are removed by evacuation. Mass spectrometric measurements showed that after purification the total amount of impurities did not exceed 0.4%; moreover, the  $SiF_4$  content was of the order of hundredths of a percent. The purification of  $BF_3$  was also performed by distillation.  $BF_3$  containing no more than 0.5% impurities was loaded into the column. The final purity was verified by a comparison of the vapor pressures of two samples of  $BF_3$  with the same isotopic content at a given temperature, using a differential manometer on the setup described in [5].  $\Delta P/P$  was measured on samples whose vapor pressure difference did not exceed 0.05-0.1 mm Hg.

Measurement Procedure and Results. Before the measurements of  $\Delta P/P$  were begun, the setup was evacuated with a diffusion pump to a residual pressure of  $\sim 10^{-5}$  mm Hg. After this it was washed with a small amount of the  $BF_3$  to be measured and again evacuated.

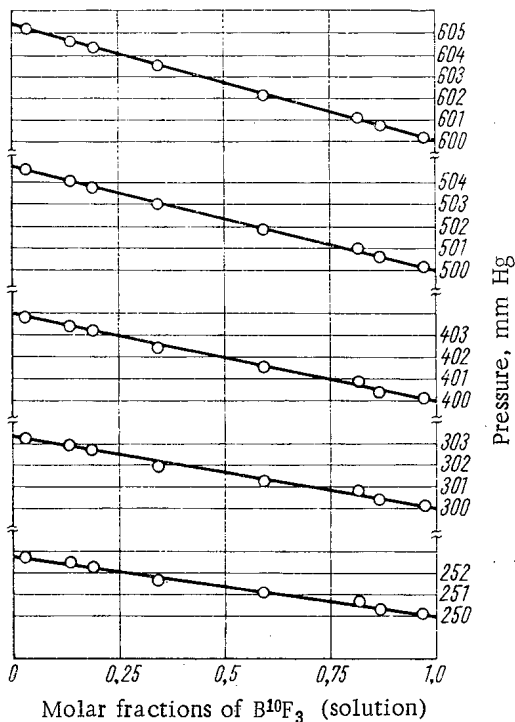


Fig. 2. Vapor pressure isotherms of B<sup>11</sup>F<sub>3</sub>-B<sup>10</sup>F<sub>3</sub>.

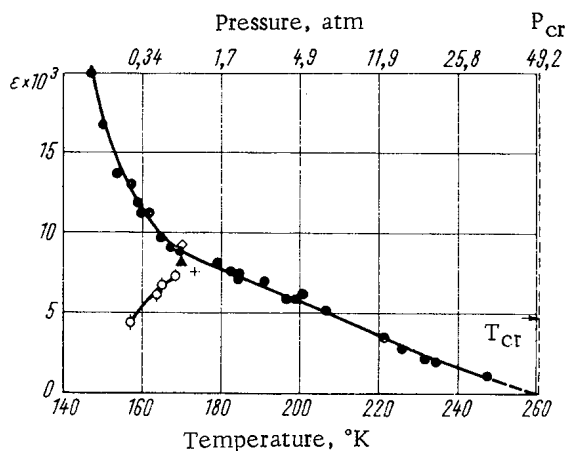


Fig. 3. Comparison of the dependence of the enrichment factor of the isotopes B<sup>11</sup>F<sub>3</sub>-B<sup>10</sup>F<sub>3</sub> on the temperature (pressure) with the literature data: ○) [4]; ▲) [1]; +) [3]; ●) data of the authors of this work; □) [2].

In this equation, the difference of the second virial coefficients of the isotopes B<sub>1</sub>-B<sub>2</sub> (the activity coefficients of B<sup>11</sup>F<sub>3</sub>-B<sup>10</sup>F<sub>3</sub> in liquid solution γ<sub>1</sub>-γ<sub>2</sub>) are neglected, and α = P<sub>01</sub>/P<sub>02</sub> ≈ 1. The second virial coefficients of BF<sub>3</sub> at temperatures of 147-247°K were calculated on the basis of the Lennard-Jones potential of intermolecular interaction, using the tables of [9]. The force constants of the Lennard-Jones intermolecular potential in the calculation of B were taken from [10], where the second virial coefficient of BF<sub>3</sub> was determined by measuring the compressibility of BF<sub>3</sub> at temperatures of 293.2-343.2° K. According to [10], E/k = 178° K; σ = 4.38 · 10<sup>-8</sup> cm. Here B is the minimum potential energy of the interaction, corresponding to the state of equilibrium; σ is the collision diameter of the molecule; k is Boltzmann's constant.

The saturated vapor pressure differences of mixtures with concentrations 3.0-87.8% B<sup>10</sup> and 3.0-95% B<sup>10</sup> were measured on the cryostat described in this communication (see Fig. 1) within the pressure interval 25 080-1216 mm Hg (33.0-1.60 atm). The accuracy of the measurements of ΔP on this instrument was ~0.1 mm Hg, while the accuracy of the reading of the absolute pressures was 0.02 atm.

The vapor pressure isotherms of B<sup>11</sup>F<sub>3</sub>-B<sup>10</sup>F<sub>3</sub> were constructed on the basis of the data obtained for temperatures of 160-170° K (Fig. 2). As can be seen from Fig. 2, solutions of the isotopes B<sup>11</sup>F<sub>3</sub>-B<sup>10</sup>F<sub>3</sub> are ideal within the limits of error of the measurements (2-4%).

The enrichment factors at pressures of 1 atm and below are calculated according to equation [5]

$$\epsilon_0 = \frac{P_1 - P_2}{P_2(C_1 - C_2)}, \quad (1)$$

where P<sub>1</sub> and P<sub>2</sub> are the saturated vapor pressures of mixtures with concentrations C<sub>1</sub> and C<sub>2</sub>. The equation is correct for ideal solutions in both phases. By definition, ε<sub>0</sub> = P<sub>01</sub>-P<sub>02</sub>/P<sub>02</sub>, where P<sub>01</sub> and P<sub>02</sub> are the saturated vapor pressures of B<sup>11</sup>F<sub>3</sub> and B<sup>10</sup>F<sub>3</sub>, respectively, and according to Raoult's law, ε<sub>0</sub> = P<sub>1</sub>-P<sub>2</sub>/P<sub>02</sub>(C<sub>1</sub>-C<sub>2</sub>). When P<sub>02</sub> is replaced by the measured P<sub>2</sub>, at a B<sup>10</sup>F<sub>3</sub> concentration of the order of 80% even at low pressures, the difference of ε<sub>0</sub> from such a replacement does not exceed tenths of a percent.

Since we demonstrated the ideality of the solutions of B<sup>11</sup>F<sub>3</sub>-B<sup>10</sup>F<sub>3</sub> in the liquid experimentally, and the deviation from ideality decreases with increasing temperature [7], to obtain exact values of the separation factors it is necessary to consider the deviation from ideality in the gas phase, especially at increased pressures.

Such an estimate can be made if the values of the virial coefficients of B<sup>11</sup>F<sub>3</sub>-B<sup>10</sup>F<sub>3</sub> are known within the temperature interval of interest to us. In the case considered, the equation of state of the gas phase with the second virial coefficient B can be used with accuracy sufficient for estimating the corrections [8]. Then, using the results of [8], we obtain an expression for the enrichment factor:

$$\epsilon = \epsilon_0 + \frac{\Delta P_0 B}{RT}. \quad (2)$$

Second Virial Coefficient of  $\text{BF}_3$  and Corrections to the Enrichment Factors  $\epsilon_0$ , Related to Nonideality of the Gas Phase ( $\epsilon_0 - \epsilon$ ), as a Function of the Temperature T

T, °K	$\frac{P_{01}-P_{02}}{\Delta P_0}$ , mm Hg	$P_2$ , mm Hg	B, cm <sup>3</sup> / mole	$\epsilon_0 \cdot 10^3$	$(\epsilon_0 - \epsilon) \cdot 10^3$
147,0	1,42	70	-374,0	20,0±3	0,05
150,1	1,67	100	-360,0	16,7±2	0,06
153,6	2,08	150	-345,0	13,7±1,3	0,07
157,2	2,63	200	-333,0	13,1±1,0	0,1
158,8	2,74	230	-327,5	11,9±0,7	0,1
159,6	2,85	250	-324,9	11,4±0,6	0,1
161,6	3,40	300	-318,0	11,3±0,6	0,1
164,8	3,94	400	-307,6	9,8±0,4	0,1
167,3	4,66	500	-299,8	9,3±0,3	0,1
169,5	5,32	600	-293,0	8,9±0,3	0,1
179,1	10,1	1216	-266,0	8,3±0,4	0,2
182,6	11,7	1497	-257,0	7,8±0,4	0,3
183,7	10,9	1520	-254,0	7,15±0,3	0,3
184,1	11,8	1620	-253,3	7,3±0,4	0,3
184,3	12,7	1641	-253,0	7,7±0,4	0,3
189,6	16,1	2250	-240,0	7,15±0,3	0,3
191,1	17,4	2416	-237,4	7,2±0,4	0,3
197,1	20,3	3252	-224,5	6,2±0,2	0,4
198,6	21,5	3480	-221,5	6,2±0,2	0,4
200,7	24,9	3914	-217,4	6,4±0,2	0,4
206,7	28,2	5122	-206,0	5,5±0,2	0,4
221,6	37,1	9591	-181,6	3,9±0,2	0,5
225,8	36,0	11400	-175,0	3,2±0,3	0,4
231,8	37,0	14440	-167,9	2,6±0,3	0,4
234,4	39,0	16000	-165,3	2,4±0,2	0,4
247,7	38,0	25080	-148,0	1,5±0,4	0,4

A more exact calculation of the enrichment factors requires experimental data on the virial coefficients of  $\text{B}^{11}\text{F}_3$ - $\text{B}^{10}\text{F}_3$  at temperatures of 147-247° K. For this purpose, an experiment is prepared on the measurement of the viscosity of gaseous  $\text{B}^{11}\text{F}_3$ - $\text{B}^{10}\text{F}_3$ .

Figure 3 presents the dependence of the enrichment factor on the temperature, and a comparison with the literature data. In the temperature region that we studied  $\text{B}^{11}\text{F}_3$  is the more volatile compound. The enrichment factor decreases with increasing temperature.

The sign of the correction to  $\epsilon_0$  in equation (2) is determined by the second virial coefficient. For  $\text{B}^{11}\text{F}_3$ - $\text{B}^{10}\text{F}_3$ , the corrections related to nonideality of the gas phase reduce the "ideal" enrichment factor  $\epsilon_0$ . But nonetheless, equation (1) can be used to calculate the enrichment factor with an accuracy of 2% at a pressure of 2-3 atm (see Fig. 3 and Table). At higher pressures, equation (2) must be used.

The dependence of  $\epsilon$  on the temperature obtaining analytically takes the form

$$\left. \begin{array}{l} 147^\circ \text{ K} \\ 172^\circ \text{ K} \end{array} \right\} \epsilon = \frac{128}{T^2 - 14250}; \quad (3a)$$

$$\left. \begin{array}{l} 172^\circ \text{ K} \\ 247^\circ \text{ K} \end{array} \right\} \epsilon = \frac{4.52}{T} - 17.135 \cdot 10^{-3}. \quad (3b)$$

The average deviations of the quantities calculated according to equations (3a), (3b) from the experimental values are no greater than 5%.

The maximum deviations of the quantities calculated according to equation (3) from the experimental values are no greater than 4%.

The results of [2], where  $\epsilon$  was measured by a differential method, coincide with our data (see Fig. 3). The data of [1, 3], although differing somewhat from ours in the quantitative aspect, possess the same sign of the temperature variation.

In [4],  $\epsilon$  was measured by the method of Rayleigh distillation, and an inverse dependence on the temperature obtained, in contrast with the results of the present publication. One of the causes of such a discrepancy may be the error related to the nonequilibrium occurrence of the process of evaporation during Rayleigh distillation [11]. Moreover, the "nonequilibrium" correction to the enrichment factor, which increases with decreasing temperature, lowers the enrichment factor. According to the calculations that we cited in [11], the nonequilibrium correction to  $\epsilon$  may reach the enrichment factor when the temperature is lowered by one order of magnitude, which qualitatively explains the discrepancy indicated above.

The results cited in this communication on the dependence of  $\epsilon$  on T, when other parameters of the process of rectification of  $\text{BF}_3$  are available, such as, for example, the height of the theoretical plate, throughput of the packing, make it possible to evaluate the efficiency of the process of separation of  $\text{B}^{11}\text{F}_3$ - $\text{B}^{10}\text{F}_3$  at various pressures. We are now conducting experiments on the separation of  $\text{B}^{11}\text{F}_3$ - $\text{B}^{10}\text{F}_3$  at pressures of ~1-4 atm.

G. L. Kakuliya took part in the measurements. The mass spectrometric measurements were performed by L. I. Chernova under the supervision of K. G. Ordzhonikidze. The authors would like to express their gratitude to Yu. V. Nikolaev, V. V. Boiko, and N. E. Menabde for their participation in the discussion of the work.

## LITERATURE CITED

1. J. K. Muhlenfordt, G. G. Sievert, and T. A. Gagois, In the Book: Transactions of the All-Union Scientific and Technical Conference on the Use of Radioactive and Stable Isotopes [Russian translation], Moscow, Izd. AN SSSR, (1958) p. 127.
2. J. Muhlenfordt et al., Proceedings of the Symposium on Isotope Separation, Amsterdam (1957), p. 408.
3. P. Nettley et al., Ibidem, p. 385.
4. N. N. Sevryugova, O. V. Uvarov, and N. M. Zhavoronkov, Zh. Fiz. Khimii, 34, 1004 (1960).
5. A. V. Borisov and I. G. Gverdsiteli, Zh. Fiz. Khimii, 35, 1212 (1961).
6. D. R. Stell, Tables of Vapor Pressures with Individual Substances [Russian translation], Moscow, Izd. Inostr. Lit. (1949).
7. I. M. Lifshits and G. I. Stepanova, In the Collection: Problems of Kinetics and Catalysis, IX. Isotopes in Catalysis [in Russian], Moscow, Izd. AN SSSR, (1957) p. 354.
8. A. M. Rozen, Theory of Separation of Isotopes in Columns [in Russian], Moscow, Atomizdat (1960), p. 37.
9. J. Girschfelder, G. Curtiss, and R. Bird, Molecular Theory of Gases and Liquids [Russian translation], Moscow, Izd. Inostr. Lit. (1961), p. 854.
10. C. Raw, J. Chim. Phys., 34, 1452 (1961).
11. I. B. Amirkhanova et al., Dokl. AN SSSR, 149, 351 (1963).

---

All abbreviations of periodicals in the above bibliography are letter-by-letter transliterations of the abbreviations as given in the original Russian journal. Some or all of this periodical literature may well be available in English translation. A complete list of the cover-to-cover English translations appears at the back of this issue.



A METHOD OF DETERMINING THE CONCENTRATIONS  
OF SHORT-LIVED DAUGHTER PRODUCTS OF RADON  
IN AIR BY THE  $\alpha$ - AND  $\beta$ -RADIATIONS

(UDC 543.52)

V. G. Labushkin and L. S. Ruzer

Translated from Atomnaya Énergiya, Vol. 19, No. 1,  
pp. 24-28, July, 1965

Original article submitted July 3, 1964; Final revision December 14, 1964

A new method for measuring the concentration of RaA, RaB, and RaC in air is proposed, based on the measurement of the  $\alpha$ - and  $\beta$ -activity of a filter immediately after pumping air through. This method makes it possible to obtain more accurate results, to shorten the measurement time and to take account of the effect of self-absorption of the  $\alpha$ -radiation.

It is well-known that the principal danger in breathing air containing radon and its daughter products is due to RaA, RaB, RaC and RaC'; their presence in the dose is several orders of magnitude greater than that of radon. Measurement of the concentration of these isotopes in air is one of the most urgent problems in radiometry of aerosols.

In order to determine the concentration of RaA, RaB, RaC, and RaC', methods of measuring the  $\alpha$ -activity of the deposit on a filter paper are usually used [1, 2].

These methods are used for the daily dosimetric monitoring of the content of short-lived daughter products of radon in the atmosphere of mining undertakings. In these undertakings the monitoring equipment must be portable, light, simple to operate and capable of functioning in considerable  $\gamma$ -fields. A high accuracy is not required for this equipment.

The problem of measuring the concentration of RaA, RaB, and RaC in air is discussed in this paper and a new spectrometric method of increased accuracy is proposed, based on the simultaneous measurement of the  $\alpha$ - and  $\beta$ -activity of each of the daughter products deposited on a filter. In this case, when the parent substance is long-lived, expressions for the activities of RaA, RaB, and RaC on the filter at the instant of completion of filtration,  $A_A(\theta, 0)$ ,  $A_B(\theta, 0)$ , and  $A_C(\theta, 0)$ , can be obtained from the equation for a chain of radioactive transformations [3].

Each of the daughter products will be deposited on the filter at a constant rate  $qv_t\delta\eta_i/\lambda_i$  (where  $v_t$  is the rate of pumping through of the air) in liter/min;  $\delta$  is the collection factor;  $\eta_i$  is the equilibrium ratio of the  $i$ -th daughter product;  $\eta_i = q_i/q$ ;  $q_i$  is the concentration of the  $i$ -th isotope in the air, Ci/liter which corresponds to the rate of decay of the long-lived parent substance. The activity of RaC on the filter,  $A_C(\theta, t)$ , corresponding to the filtration time  $\theta$  and the time  $t$  elapsed from the instant of completion of filtration to the instant of measuring the activity, is made up from the activity of RaC deposited as a result of filtration, taking into account its decay  $A_C^C(\theta, t)$ , and the activity of RaC formed by the decay of RaA and RaB accumulated on the filter during the time of air filtration  $\theta$ ,  $A_C^A(\theta, t)$  and  $A_C^B(\theta, t)$  respectively.

The activity of RaB on the filter,  $A_B(\theta, t)$ , in its turn comprises the activity of RaB deposited by air filtration,  $A_B^B(\theta, t)$ , and the activity of the RaB produced by decay of RaA accumulated on the filter during the time of air filtration  $\theta$ ,  $A_B^A(\theta, t)$ . By applying the well-known expressions for a chain of radioactive transformations [4] successively to RaA, RaB, and RaC we obtain the general relationships for the activity of each of the radon decay products accumulated on the filter.

TABLE 1. Comparison of the Errors (in %) of Various Methods of Measuring the Activity of a Deposit of Radon Decay Products on a Filter

$q_A : q_B : q_C$	Measurements of total $\alpha$ -activity of the filter during 5, 15 and 30 min (Tzivoglou's procedure)			Measurement of the total $\alpha$ -activity of the filter during 1, 15 and 60 min			Measurement of the total $\beta$ -activity of the filter during 5, 15 and 30 min			Measurement of the $\alpha$ - and $\beta$ -activity of each daughter product		
	$\Delta q_A/q_A$	$\Delta q_B/q_B$	$\Delta q_C/q_C$	$\Delta q_A/q_A$	$\Delta q_B/q_B$	$\Delta q_C/q_C$	$\Delta q_A/q_A$	$\Delta q_B/q_B$	$\Delta q_C/q_C$	$\Delta q_A/q_A$	$\Delta q_B/q_B$	$\Delta q_C/q_C$
1:1:1	300	53	75	120	23	37	6430	680	180	10	11	13
1:0.8:0.6	210	49	89	79	22	44	2980	690	195	10	11	13
1:0.5:0.5	160	57	80	58	27	40	4070	700	190	10	12	13
0.5:0.7:0.7	440	54	35	150	22	37	8810	680	180	10	11	12
1:0.1:0.01	35	57	460	19	56	200	690	900	420	10	22	49

Since there are  $\alpha$ ,  $\beta$ , and  $\gamma$ -emitters amongst the short-lived daughter products of radon and there is a strict relationship between their activities on the filter, then the concentrations of RaA, RaB, and RaC in the air can be determined, in principle, by measuring the activity of the filter deposit by any of the forms of radiation mentioned. There are several versions of the measurement: 1) measurement of the total  $\alpha$ -activity of the filter at different instants of time  $t$  after completion of filtration; 2) measurement of the total  $\beta$ - or  $\gamma$ -activity for different values of  $t$ ; 3) measurement of the activity of each of the daughter products  $A_A(\theta, t)$ ,  $A_B(\theta, t)$ ,  $A_C(\theta, t)$ , and  $A_C(\theta, t)$ . The measurement error in each of these versions depends on the ratio of the concentrations  $q_A : q_B : q_C$ , the choice of the times at which the activity measurements are undertaken, and other factors.

In order to calculate the errors of these three methods we shall assume that the activity of the deposit on the filter is measured with an accuracy of  $\pm 10\%$ , which corresponds essentially to the accuracy of the instruments used. Table 1 shows the magnitudes of the errors for the cases mentioned above for various ratios of the measured concentrations of RaA, RaB, and RaC -  $q_A : q_B : q_C$ . It can be seen that the most accurate is the individual measurement of the activity of each of the daughter products on the filter.

The choice of the time at which the activity measurements is carried out must satisfy the conditions for obtaining the least values of the statistical and methodological errors. As detailed consideration showed, both these conditions are satisfied for  $t \approx 0$ . Thus, it is desirable to measure the activity immediately after completion of filtration.

It should be mentioned that in determining the concentrations of RaA, RaB, and RaC only by the  $\alpha$ -activity, it is necessary to take into account the self-absorption of the  $\alpha$ -radiation, especially in cases when a test is selected in places with high dust content in the air. The measurement of the activity of each of the daughter products on the filter enables a correction  $P$  to be introduced into the self-absorption of the  $\alpha$ -activity by simultaneous measurement of the  $\alpha$ -activity of RaC' and the activity of RaC, which are in equilibrium between themselves.

On the basis of what has been said above, the conclusion can be drawn that the most accurate method is the method of individual measurement of the  $\alpha$ - and  $\beta$ -activity of each of the radon daughter products on the filter immediately after completion of filtration.

#### Determination of the Concentrations of RaA, RaB, and RaC by the $\alpha$ - and $\beta$ -Activity

It is well-known that the short-lived  $\alpha$ -emitters in the radon series are RaA and RaC' with energies of 6.00 and 7.68 MeV respectively, the short-lived  $\beta$ -emitters RaB and RaC with maximum energies 0.65 and 3.17 MeV respectively. In consequence of the considerable difference between the energies of these emitters, the activity of each of the daughter products on the filter can be measured relatively simply (by means of a scintillation spectrometer).

In order to determine  $q_A$ ,  $q_B$ , and  $q_C$  in c/liter, it is necessary to calibrate the appropriate equipment with standard aerosols of radon daughter products. This method presents great difficulties.

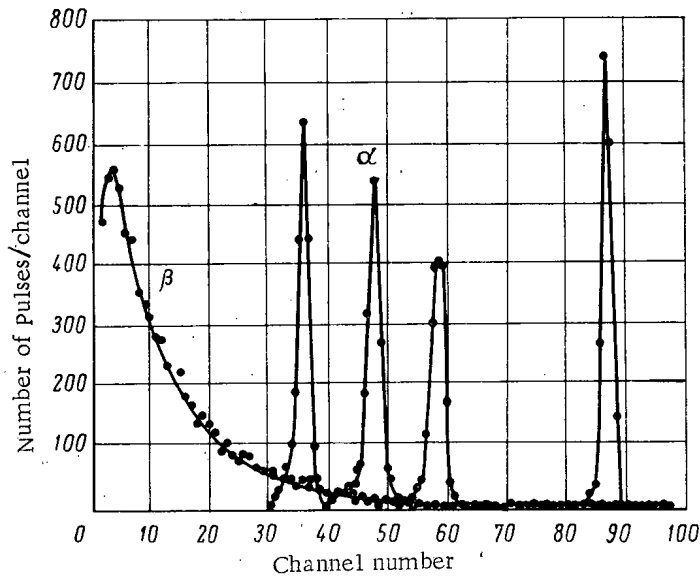


Fig. 1. Spectrum of  $\alpha$ - and  $\beta$ -radiation from a nonemanating  $Ra^{226}$  source.

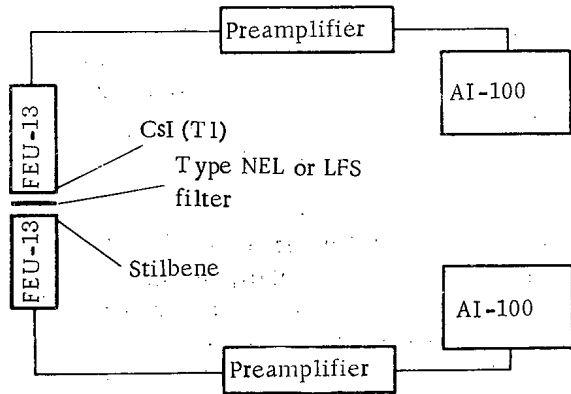


Fig. 2. Block diagram of experimental equipment.

Figure 1 shows the spectrum of a specially-prepared nonemanating  $\alpha$ - and  $\beta$ -source from  $Ra^{226}$ . A scintillation spectrometer [CsI(Tl) crystal with a thickness  $\sim 100 \mu$ ] and a semiconductor spectrometer were used for plotting the  $\alpha$ -spectra. In the first case the resolution was  $\sim 9\%$  and in the second case  $\sim 1\%$ . For plotting the  $\beta$ -spectra, stilbene with a thickness of 13 mm was used. It can be seen from Fig. 1, that the Ra, Rn, RaA, and RaC' lines are well-resolved on the spectrogram.

In measuring  $A_A$ ,  $A_{C'}$ ,  $A_B$ , and  $A_C$  by the  $\alpha$ - and  $\beta$ -spectrometric method, the number of pulses  $N_A(T_i, T_k)$  due to RaA on the filter and the results of a similar measurement of radium source  $N_A^0(T_i, T_m)$  for  $\theta = 5$  min are connected by the relationship:

$$\frac{N_A(T_i, T_k)}{N_A^0(T_i, T_m)} A_A^0(T_m - T_i) = v_i \delta q_A 13.15 (e^{-\lambda_A T_i} - e^{-\lambda_A T_k}), \quad (1)$$

where  $T_i$  and  $T_k$ ,  $T_i$  and  $T_m$  are respectively the time of start and time of completion of the activity measurement of each isotope on the filter and in the standard source. For the  $\alpha$ -radiation from RaC' we obtain

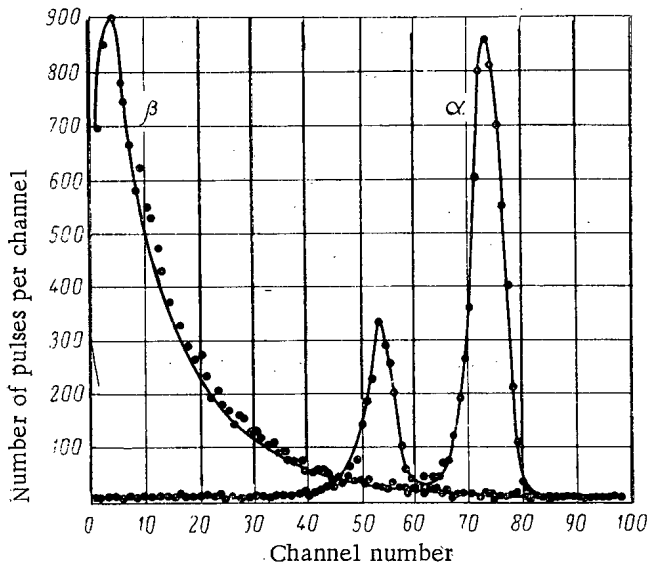
$$\frac{N_{C'}(T_i, T_k)}{N_{C'}^0(T_i, T_m)} A_{C'}^0(T_m - T_i) = v_i \delta \{ q_A [0.31 (e^{-\lambda_A T_i} - e^{-\lambda_A T_k}) + 88.18 (e^{-\lambda_B T_i} - e^{-\lambda_B T_k}) - 66.50 (e^{-\lambda_C T_i} - e^{-\lambda_C T_k})] + q_B [685 (e^{-\lambda_B T_i} - e^{-\lambda_B T_k}) - 493 (e^{-\lambda_C T_i} - e^{-\lambda_C T_k})] + q_C \cdot 130.2 (e^{-\lambda_C T_i} - e^{-\lambda_C T_k}) \}; \quad (2)$$

and for the  $\beta$ -radiation from RaB:

TABLE 2. Comparison of Methods for Measuring the Concentration of Radon Decay Products in Air

Number of experiment	Measurement method	$q_A : q_B : q_C$	Concentration, Ci/liter		
			$q_A$	$q_B$	$q_C$
1	A	1 : 0,36 : 0,22	—	—	—
	B	1 : 0,30 : 0,23	$1,59 \cdot 10^{-10}$	$0,47 \cdot 10^{-10}$	$0,38 \cdot 10^{-10}$
2	A	1 : 0,97 : 0,85	—	—	—
	B	1 : 0,84 : 1,17	$2,42 \cdot 10^{-10}$	$2,03 \cdot 10^{-10}$	$2,82 \cdot 10^{-10}$
3	A	1 : 0,67 : 0,40	—	—	—
	B	1 : 0,40 : 0,67	$1,70 \cdot 10^{-10}$	$0,68 \cdot 10^{-10}$	$1,15 \cdot 10^{-10}$
4	A	1 : 1,22 : 0,89	—	—	—
	B	1 : 0,85 : 1,56	$1,44 \cdot 10^{-10}$	$1,23 \cdot 10^{-10}$	$2,25 \cdot 10^{-10}$
5	A	1 : 1,68 : 1,35	—	—	—
	B	1 : 1,25 : 1,57	$2,05 \cdot 10^{-9}$	$2,57 \cdot 10^{-9}$	$3,21 \cdot 10^{-9}$
6	A	1 : 0,47 : 0,47	—	—	—
	B	1 : 0,30 : 0,55	$1,13 \cdot 10^{-9}$	$0,34 \cdot 10^{-9}$	$0,62 \cdot 10^{-9}$

\*A —Measurement of total  $\alpha$ -activity (Tsvoglou's procedure); B—Measurement of  $\alpha$ - and  $\beta$ -activity of each isotope

Fig. 3.  $\alpha$ - and  $\beta$ -radiation spectra of the active filter deposit.

(thin filter designed for  $\alpha$ -spectrometry) by means of a rotary air-blower at a rate of 20 liter/min. Measurement of the  $\alpha$ -activity of the filter was carried out by means of the equipment mentioned above; the  $\alpha$ - and  $\beta$ -activities of the filter were measured simultaneously from both sides.

In order to determine  $q_A$ ,  $q_B$ , and  $q_C$  (in Ci/liter) relative measurements of the filter and the radium nonemanating source were made. In order to eliminate the effect of the geometry factor the area of the filter was equal to the area of the radium source. The  $\alpha$ - and  $\beta$ -spectrograms of the filter are shown in Fig. 3.

The number of pulses recorded for the time of obtaining the spectrum,  $\Delta T = T_K - T_i$  is equal to the areas of the respective peaks belonging to RaA and RaC'. The nonemanating  $\alpha$ -emitting source was prepared in such a way that the Ra<sup>226</sup>, Ra<sup>222</sup>, RaA and RaC' were in equilibrium with one another.

$$\frac{N_B(T_p, T_q)}{N_B^0(T_i, T_m)} A_B^0 (T_m - T_i) = v_t \delta \{q_A [23.3 (e^{-\lambda_B T_p} - e^{-\lambda_B T_q}) - 1.7 (e^{-\lambda_A T_p} - e^{-\lambda_A T_q})] + q_B \cdot 181 \} \times (e^{-\lambda_B T_p} - e^{-\lambda_B T_q}). \quad (3)$$

The formula for determining  $N_C(T_i, T_K)$  by  $\beta$ -radiation is identical with Eq. (2).

The choice of the time interval  $\Delta T = T_K - T_i$  is determined by the requirement for obtaining a specified statistical accuracy for measuring the activity of RaA, RaB, and RaC.

#### Measurement Procedure and Experimental Results

The equipment used for determining experimentally the concentration of RaA, RaB, and RaC is shown as a block diagram in Fig. 2.

The radon daughter products were deposited by pumping a specified volume of air from a chamber containing radon through a Type NEL or LFS filter

The RaA activity on the filter is determined by comparing the number of pulses from RaA on the filter and from the radium source, and the value of  $q_A$  in Ci/liter is found by formula (1).

In order to determine  $q_B$ , we use the spectrograms shown in Figs. 1 and 3. Using a monoenergetic source of  $Cs^{137}$  conversion electrons with an energy of 0.624 MeV, we find the edge of the RaB  $\beta$ -spectrum. Having determined the areas of the RaB and RaC spectra on the filter and on the source and having compared these areas with one another, we find  $q_B$  and  $q_C$  by formulas (3) and (2). The concentration of RaA, RaB, and RaC are determined in Ci/liter, because all the conditions necessary for carrying out the relative measurements are taken into account.

Table 2 shows the results of measuring  $q_A$ ,  $q_B$ , and  $q_C$  by Tsivoglou's procedure and the procedure based on measurement of the  $\alpha$ - and  $\beta$ -activity of the filter. Comparison of the results with respect to the relative concentrations  $q_A : q_B : q_C$  (where  $q_A$  is assumed to be unity) is given as an illustration, because the determination of the quantity  $q_A$  by Tsivoglou's procedure leads to a large error and normalization of the daughter products with respect to it is hardly valid.

Shifts of equilibrium (see Table 2) to the side of subsequent radon decay products can be explained by diffusion deposition of RaA in the delivery tubes, which occurred in our experiments. By carrying out supplementary experiments it was established that in the chamber containing the radon, from which the samples were taken, there is about 30% of "free atoms" of RaA. As a result of filtration of the air, a considerable portion of these atoms is deposited on the inside walls of the sampling system.

It follows from the work carried out that the more accurate method of determining the concentration of RaA, RaB, and RaC in air is the individual measurements of the activity of each of the daughter products of radon on the filter immediately after completion of filtration. These measurements can be carried out over 2-3 min for a filtration time of 5 min, a pumping speed of 20 liter/min and concentration of radon daughter products of 0.1 to 1 MPC (maximum permissible concentration). Consequently, the stated method is more rapid than the previously-used one. The required concentrations  $q_A$ ,  $q_B$ , and  $q_C$  are determined directly in Ci/liter.

The simultaneous measurements of the  $\alpha$ -activity of RaC' and the  $\beta$ -activity of RaC enable a correction to be introduced for the absorption of the  $\alpha$ -radiation by the filter, by the aerosol and by the inert dust deposited on the filter during collection of the sample. By the proposed procedure, using a solid  $Ra^{226}$  preparation, research projects can be carried out on the physics of aerosols and the calibration of aerosol radiometers used for determining the concentration of radon daughter products.

In conclusion, the authors tender their sincere appreciation to the staff of the Radium Institute, Academy of Sciences USSR (D. M. Ziv, E. A. Volkova, and Yu. V. Mazurek) for preparing the nonemanating source of  $Ra^{226}$ .

#### LITERATURE CITED

1. E. Tsivoglou, H. Ayer, and D. Holaday, *Nucleonics*, **11**, No. 9, 40 (1953).
2. K. Markov, N. Ryabov, and K. Stac', *Atomnaya Énergiya*, **12**, 315 (1962).
3. L. S. Ruzer, Dissertation, MIFI (1961).
4. V. I. Gol'danskii, A. V. Kutsenko, and M. I. Podgoretskii, *Statistics of Calculations in the Recording of Nuclear Particles* [In Russian], Moscow, Fizmatgiz (1959).

## RADIOACTIVE FALLOUT ON THE TERRITORY OF THE USSR IN 1963

(UDC 551.577.7)

S. G. Malakhov, G. A. Sereda, V. F. Brendakov, T. V. Polyakova,  
R. I. Pervunina, V. I. Svisheva, and V. N. Churkin

Translated from *Atomnaya Énergiya*, Vol. 19, No. 1,  
pp. 28-35, July, 1965

Original article submitted August 20, 1964; Final revision submitted February 1, 1965

Summarized data are given in this paper concerning radioactive fallout of fission products and their content in soil in the USSR in 1963. On the basis of a study of the isotopic composition of the radioactive fallout, assumptions are made concerning their relationships to actual test series. An estimate is given of the total quantity of  $\text{Sr}^{90}$  deposited in the northern hemisphere in 1962 and 1963.

Fallout samples were collected on Marley tiles with an area of  $0.3 \text{ m}^2$ ; the exposure was of 24 h duration. The collection efficiency was assumed equal to 0.36 [1]. The ashes obtained from burning the tiles, which had been set out at 10-20 points of an appropriate administrative region, oblast or Republic were analyzed radiochemically and spectrometrically. Normally, the ash collected from these stations was accumulated over 3 months, carefully mixed and only after this was it admitted for analysis. The determination of  $\text{Ce}^{144}$ ,  $\text{Ce}^{141}$ , and  $\text{Zr}^{95}$  in the sample was undertaken by the  $\gamma$ -spectrometric method using a 100-channel amplitude analyzer and a NaI(Tl) crystal with a diameter of 70 mm and a height of 50 mm. Separation of  $\text{Sr}^{90}$  from the sample was accomplished radiochemically by the method described in [2]. The error for the radiochemical analysis of  $\text{Sr}^{90}$  was not more than 15% and for the  $\gamma$ -spectrometric analysis of  $\text{Ce}^{141}$ ,  $\text{Ce}^{144}$ , and  $\text{Zr}^{95}$  it was 10-15%. The amount of  $\text{Sr}^{90}$  in the surface layer of soil with a thickness of 10 cm was determined in accordance with the recommendations of [3].

Data are presented in this paper, averaged mainly over a latitude belt of  $10^\circ$  and taking account of the areas of the territories or Republics. Similar data for 1962 can be found in [4, 5].

#### Deposition of $\text{Sr}^{90}$ , $\text{Ce}^{144}$ , and $\text{Zr}^{95}$ in Various Territories of the USSR

Data are given in Table 1 concerning the intensity of  $\text{Sr}^{90}$ ,  $\text{Ce}^{141}$ ,  $\text{Ce}^{144}$ , and  $\text{Zr}^{95}$  fallout in territories of the USSR. The measurement results are averaged quarterly and along different latitude belts. A seasonal trend is noted with a maximum in the second and third quarters. In 1959-1961 this maximum usually arrived in the first and second quarter [6, 7]. A latitude trend is also noted; the maximum fallouts are observed in the belt  $40-60^\circ$  latitude north and they are reduced to the north and south of these latitudes.

Table 2 gives the average values of the intensity of radioactive fallout of fission products over the USSR as a whole and separately for the European part, Siberia and the Far East, and they are compared with the analogous data for 1962 [4, 5].

In Table 3 the  $\text{Sr}^{90}$  fallouts are compared for the years 1959, 1962, and 1963 and gives average data fallout of this isotope in the USSR and at a number of sites in other countries. The following conclusions can be drawn from consideration of the table.

1. The levels given for fallout of radioactive fission products on the territory of the Soviet Union from 1959 to 1963 are approximately the same as the levels of fallout in other countries [4, 8-12]. The average values for 1963 are approximately one and one-half times higher than those according to the data of the American HASL Service.

2. In 1963 the maximum intensity of  $\text{Sr}^{90}$  fallout in comparison with previous years was noted. Thus, for the first half of 1963 the fallout in many regions was even greater than for the whole of 1962 or 1959. On the average, throughout the USSR the quantity of  $\text{Sr}^{90}$  deposited from the atmosphere in 1963 [ $22.5 \mu\text{Ci}/\text{km}^2 \cdot \text{year}$ ] was more than twice as large as in 1962 [ $9.6 \mu\text{Ci}/\text{km}^2 \cdot \text{year}$ ] and more than three times as large as in 1959 [ $5.9 \mu\text{Ci}/\text{km}^2 \cdot \text{year}$ ].

TABLE 1. Intensity of Radioactive Fallout of  $\text{Sr}^{90}$ ,  $\text{Ce}^{144}$ ,  $\text{Ce}^{141}$ , and  $\text{Zr}^{95}$  as a Function of Geographical Latitude (European part of the USSR and Central Asia),  $\mu\text{Ci}/\text{km}^2 \cdot \text{month}$

Isotope	Quarter of the year	Geographical latitude, °N			
		70-60	60-50	50-40	40-37
$\text{Sr}^{90}$	I	0.7	1.1	1.1	1.2
	II	2.7	3.4	3.3	2.2
	III	2.6	2.9	2.9	1.1
	IV	0.5	0.7	0.8	0.6
	Total for year*	19.5	24.3	24.3	15.3
$\text{Ce}^{144}$	I	11.7	26.8	14.5	21.3
	II	36.3	58.2	44.6	40.2
	III	37.1	40.7	50.0	12.0
	IV	11.2	13.4	13.2	7.9
	Total for year*	190	264	242.0	146.7
$\text{Zr}^{95}$	I	26.0	21.0	16.0	20.7
	II	13.0	23.0	22.0	27.0
	III	7.7	7.4	9.2	2.4
	IV	0.8	0.9	0.9	1.8
$\text{Ce}^{141}$	I	8.8	19.0	18.4	13.1
	II	15.8	13.6	24.2	25.1

\* In  $\mu\text{Ci}/\text{km}^2$  year, taking account of radioactive decay; reduced to January 1, 1964.

TABLE 2. Average Intensity of  $\text{Sr}^{90}$ ,  $\text{Ce}^{141}$ ,  $\text{Ce}^{144}$ , and  $\text{Zr}^{95}$  Fallout on the Territory of the Soviet Union in 1962-1963,  $\mu\text{Ci}/\text{km}^2 \cdot \text{month}$

Region of measurement	Isotope	1st Quarter	2nd Quarter	3rd Quarter	4th Quarter	Total for the year $\mu\text{Ci}/\text{km}^2$
USSR (average for 1963)	$\text{Sr}^{90}$	1.1	3.0	2.8	0.7	22.5
	$\text{Ce}^{144}$	22.8	42.6	39.2	12.3	-
	$\text{Zr}^{95}$	18.0	19.3	7.1	0.8	-
USSR (average for 1962) European part of USSR (1963)	$\text{Sr}^{90}$	0.23	1.5	0.8	0.7	9.6
	$\text{Sr}^{90}$	1.0	3.1	2.8	0.7	22.5
	$\text{Ce}^{144}$	23.1	41.5	38.2	11.9	-
Siberia and Far East (1963)	$\text{Zr}^{95}$	13.8	16.0	5.8	0.9	-
	$\text{Sr}^{90}$	-	-	2.8	0.6	-
	$\text{Ce}^{144}$	-	-	50.8	10.0	-
	$\text{Zr}^{95}$	-	-	6.6	0.6	-

TABLE 3. Fallout Density of Sr<sup>90</sup> in the Soil of Various Regions of the Northern Hemisphere in 1959, 1962, 1963 [1, 4, 8-12],  $\mu\text{Ci}/\text{km}^2$ 

Region of measurement	1959	1962	First half of 1962	Second half of 1962	First half of 1963	Second half of 1963	1963
Tokyo	8.1	8.09	4.9	3.19	11.4	—	—
Milford Haven (Great Britain)	5.7	9.3	4.5	4.8	12.1	—	—
Reykjavik	—	15.1	8.5	6.6	10.2	—	—
Ottawa	8.4	19.7	10.6	9.1	21.8	—	—
Gibraltar	12.2	16.1	8.7	7.4	18.5	—	—
New York	8.6	11.0	6.0	5.0	13.5	10.2	23.7
Pittsburg (USA)	7.7	10.7	5.5	5.2	9.7	—	—
Westwood (New Jersey, USA)	9.1	13.2	7.7	5.5	13.6	11.7	24.7
Louisville (Kentucky, USA)	6.2	9.5	6.3	3.2	15.5	—	—
Vienna	4.7	6.1	3.3	2.8	10.5	4.3	15.8
USSR (on the average)	5.9	9.6	5.1	4.5	12.0	4.3	22.5

TABLE 4. Content of Ce<sup>144</sup> + Pr<sup>144</sup>, Zr<sup>95</sup> + Nb<sup>95</sup>, Ru<sup>106</sup> + Rh<sup>106</sup>, Sr<sup>90</sup> + Y<sup>90</sup>, Cs<sup>137</sup> and Sb<sup>125</sup> in Soil from Different Latitude Belts of the USSR on July 1, 1963,  $\mu\text{Ci}/\text{km}^2$ 

Latitude, °N., lat.	Ce <sup>144</sup> + Pr <sup>144</sup>	Sb <sup>125</sup>	Ru <sup>106</sup> + Rh <sup>106</sup>	Cs <sup>137</sup>	Zr <sup>95</sup> + Nb <sup>95</sup>	Sr <sup>90</sup> + Y <sup>90</sup>	Total
30-40	640	52	420	95	520	100	1827
40-50	630	47	410	95	550	90	1822
50-60	620	46	405	93	550	88	1846
60-70	400	38	240	60	230	70	1038
Average over USSR	570	46	370	86	460	88	1668

TABLE 5. Quantity of Ce<sup>144</sup> + Pr<sup>144</sup> and Sr<sup>90</sup> Deposited in the First Half of 1963, from the Total Content of Fission Products in Soil (on July 1, 1963), %

Latitude, °N., lat.	Ce <sup>144</sup> + Pr <sup>144</sup>	Sr <sup>90</sup>
30-40	47	20
40-50	48	30
50-60	66	30
60-70	60	30

The highest fallout level is noted in the second and third quarters of 1963. The differences mentioned are associated with the different yields of the nuclear tests carried out in 1958, 1961, and 1962.

#### Content of Radioactive Fission Products in Soil

The content of Ce<sup>144</sup> + Pr<sup>144</sup>, Zr<sup>95</sup> + Nb<sup>95</sup>, Ru<sup>106</sup> + Rh<sup>106</sup>, Sr<sup>90</sup> + Y<sup>90</sup>, Cs<sup>137</sup>, and Sb<sup>125</sup> in soil on July 1, 1963 is given in Table 4. For comparison we note that according to data from the HASL Laboratory [13], the following quantity of Sr<sup>90</sup> was contained in soils from the northern hemisphere

in July 1963 to March 1964: 32  $\mu\text{Ci}/\text{km}^2$  in the belt 60-70° lat. N.; 51  $\mu\text{Ci}/\text{km}^2$  in the belt 50-60° lat. N.; 58  $\mu\text{Ci}/\text{km}^2$  in the belt 40-50° lat. N.; 47  $\mu\text{Ci}/\text{km}^2$  in the belt 30-40° lat. N. Taking into account that samples of the soils in this case were taken later than in our project, the agreement of the results must be acknowledged as satisfactory. The average content of Sr<sup>90</sup> in the soil (44  $\mu\text{Ci}/\text{km}^2$ ) coincides approximately with the total fallout of Sr<sup>90</sup> for all the year of carrying out the nuclear tests. Thus, for Tokyo this total to August 1, 1963 amounted to 45.2  $\mu\text{Ci}/\text{km}^2$  and for Milford Haven (Great Britain) it was 49.4  $\mu\text{Ci}/\text{km}^2$  [8, 9].

An attempt was made to estimate the quantity of individual isotopes in the soil, deposited in the first half of 1963. For this purpose the data of Tables 1 and 4 were compared and the quantity of deposited Ce<sup>144</sup> was reduced to July 1, 1963. The results of the determination of Sr<sup>90</sup> and Ce<sup>144</sup> are given in Table 5. Approximately 50-60% of the Ce<sup>144</sup> atoms and 30% of the Sr<sup>90</sup> atoms from the total content of these isotopes in soil was deposited from the atmosphere during January to July 1963. The results obtained agree with certain other estimates. Thus, in Tokyo and Milford Haven during the six months being considered, approximately 25% of the total quantity of Sr<sup>90</sup> fallout in the previous years was deposited [8, 9].



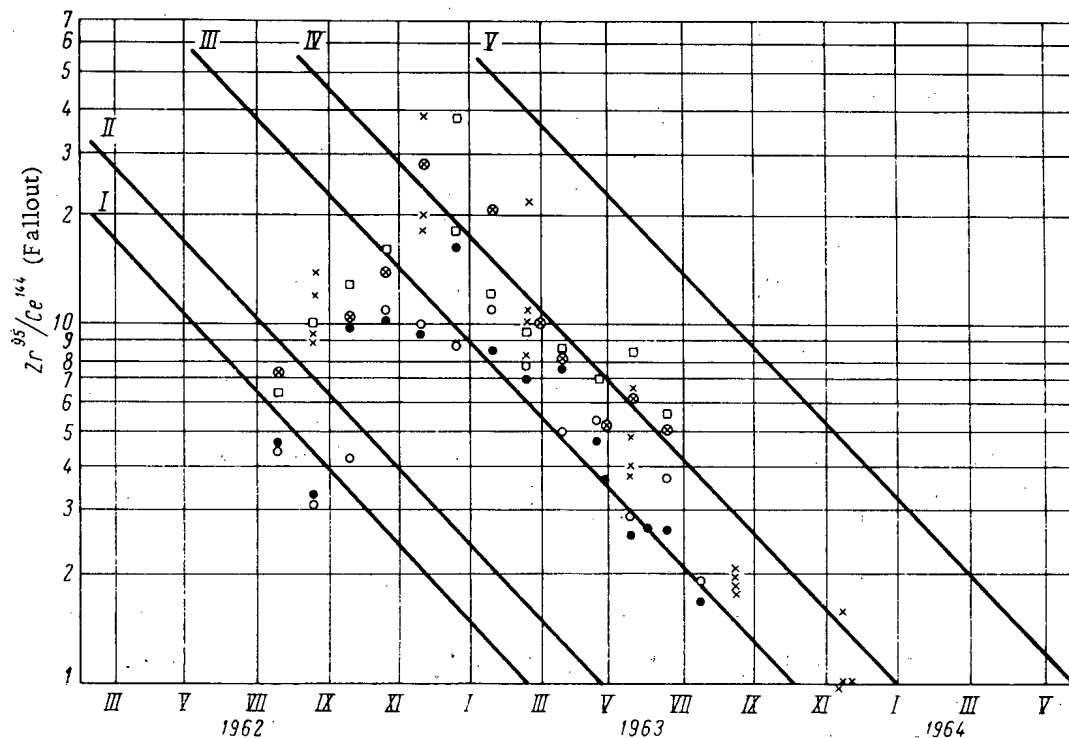


Fig. 1: Ratio of  $Zr^{95}/Ce^{144}$  activity in radioactive fallout in 1962-1964; X) USSR, fallout (see Table 1); O) Milford Haven (Great Britain), precipitation; ●) Chilton (Great Britain), precipitation; □) Richmond (USA), precipitation; ⊗) New Jersey (USA), precipitation.

The total activity of the isotopes mentioned above in soil amounts to  $1.66 \text{ Ci/km}^2$ . It is only a little less than the total contamination of soil by fission products, since it includes the isotopes which are most important in a quantitative respect and which are characteristic for mixtures of fission products with a growth of several months to 2-5 years.

In order to compare the level of radioactive soil contamination, we present data from measurements in Leningrad [14]. In the Leningrad region from 1954 to 1959, the cumulative buildup of  $Sr^{90}$  fallout amounted to  $14.3 \mu\text{Ci/km}^2$ ,  $Cs^{137} - 27.6 \mu\text{Ci/km}^2$ , the quantity of  $Ce^{144} + Pr^{144}$  accumulated towards the middle of 1959 was equal to  $120 \mu\text{Ci/km}^2$ ,  $Zr^{95} + Nb^{95}$  was  $90 \mu\text{Ci/km}^2$ . The maximum buildup of total  $\beta$ -activity in soil in 1958-1959 amounted to  $0.8 \mu\text{Ci/km}^2$  in Kjeller [15] and in Podmoskov'e it was  $0.6 \mu\text{Ci/km}^2$  [16].

The radioactive contamination of soil in 1963 did not have such clear latitude variations as the distribution of radioactive fallout in general. Only north of  $60^\circ$  lat. N. is a lower content of the individual isotopes in soil noted in comparison with more southerly latitudes. This fact is difficult to explain. However, it should be noted that in previous years over the territories of the USSR, the normal latitude distribution of radioactive fallout with a maximum between  $40-60^\circ$  lat. N. was often significantly distorted. Such was the case, for example, in 1962 [4, 5]. On the other hand, data concerning fission product fallout from the atmosphere and their content in soil south of  $40^\circ$  lat. N. are relatively small and they all refer to a latitude belt  $40-37^\circ$  lat. N.

#### Concerning the Ratios of the Activities of Individual Isotopes in Radioactive Fallout

Figures 1 and 2 show the ratios of the activities of  $Zr^{95}/Ce^{144}$  and  $Ce^{144}/Sr^{90}$  in fallout in 1962-1964. The straight lines plotted on these same graphs correspond to different assumptions of the dates of the nuclear tests: 15 September and 1 November 1961 (lines I and II), 1 March and 1 August 1962 (lines III and IV) and 1 January 1963 (line V). The initial ratios of the activities of  $Zr^{95}/Ce^{144}$  and  $Ce^{144}/Sr^{90}$  were assumed to be equal to 5.7 and 45 respectively. The lines mentioned demarcate, as it were, regions associated with nuclear test series in 1961-1962. For comparison, we show on the same graphs the results of measurements at a number of points beyond the limits of the Soviet Union [8, 11]. The data given enable the following conclusions to be drawn.

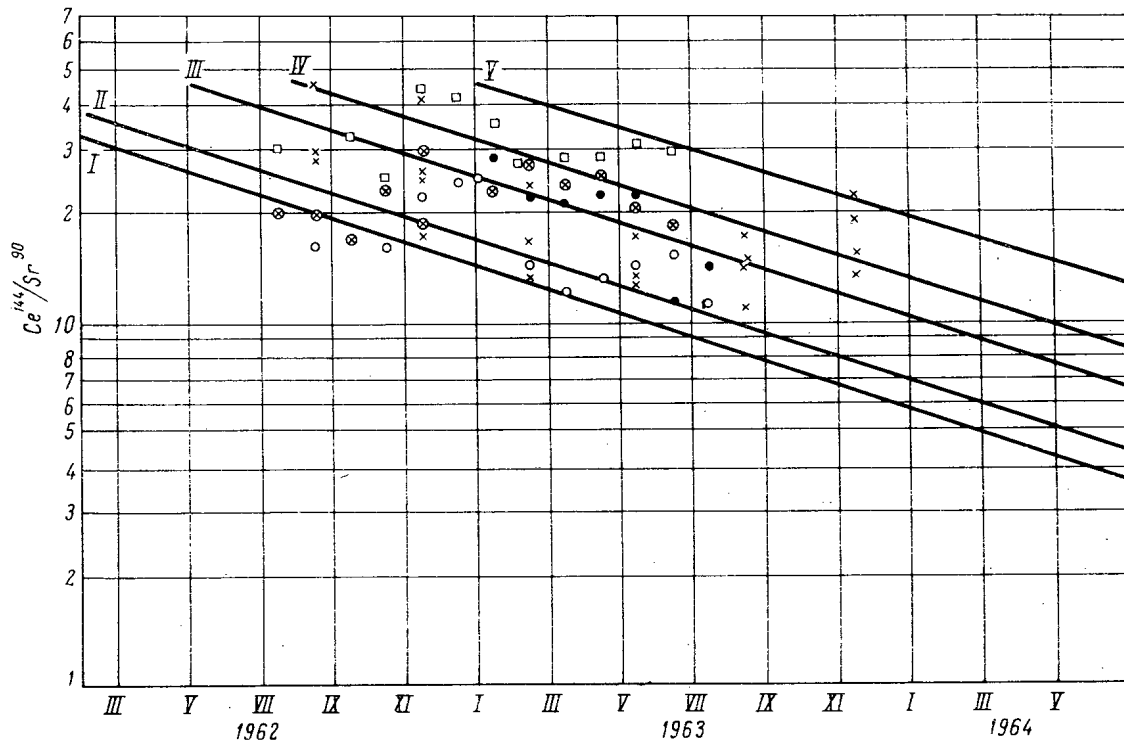


Fig. 2. Ratio of  $Ce^{144}/Sr^{90}$  activity in radioactive fallout in 1962-1964: X) USSR, fallout (see Table 1); O) Milford Haven (Great Britain), precipitation; ⊙) Abingdon (Great Britain), precipitation; ○) Westwood, New Jersey (USA), precipitation; □) Richmond, California (USA), precipitation.

1) Judging from the  $Zr^{95}/Ce^{144}$  ratio, the assumed time of formation of the fission products detected in the atmospheric boundary layer and in the fallout in 1963 is related to May-August 1962. Most likely, a mixture of fission products from several series of nuclear tests in 1961 and 1962 was deposited from the atmosphere.

2) The  $Ce^{144}/Sr^{90}$  ratio fluctuates strongly and differs significantly at the various observation points. The assumed time of formation in this case is also found to be significantly dissimilar for different points and periods of observation.

The above fact can be explained by many reasons. It is possibly the effect of measurement errors or the presence of products from different types of test (Small changes in the  $Ce^{144}/Sr^{90}$  ratio lead to considerable changes in the estimate of the growth of fission products). It is quite probable that there are different fractions of fission products from individual tests in the total mixtures of these products, depending on the site and time of taking the samples. Fractionation of isotopes as a result of dispersal and deposition of aerosols from the atmosphere cannot be excluded (different rates of deposition, rainout and trapping of the aerosols). It is not possible to isolate a single cause as the principal cause, because of the absence of supplementary experimental data. The simultaneous effect of all the reasons mentioned also cannot be excluded.

3) The increase in the last quarter of 1963 of the mid-quarter  $Ce^{144}/Sr^{90}$  ratio of fallout on the territories of the USSR is noteworthy (see Fig. 2). According to measurement data above San Angelo (USA, State of Texas, 31° lat. N.), a similar increase in this ratio was also noted in the stratosphere (Fig. 3 [12]) during the second half of 1963 compared to the first half of 1964.

It is interesting that this effect also occurred in previous years. An increase in the  $Ce^{144}/Sr^{90}$  ratio in radioactive fallout on the territories of the USSR in the summer of 1961 was noted in [4]. In Fig. 4 a graph is drawn of the  $Ce^{144}/Sr^{90}$  ratio in 1960-1961 in radioactive fallout and in the atmospheric boundary layer of air for a number of points of the northern hemisphere [14, 17, 18]. In this case the lines I, II, and III correspond to changes in the  $Ce^{144}/Sr^{90}$  ratio for the tests carried out on November 1, July 1 and January 1, 1958. The increase of the ratio in the third quarter of 1961 can be seen clearly, which, according to measurement data in Leningrad, was also seen in autumn 1960.

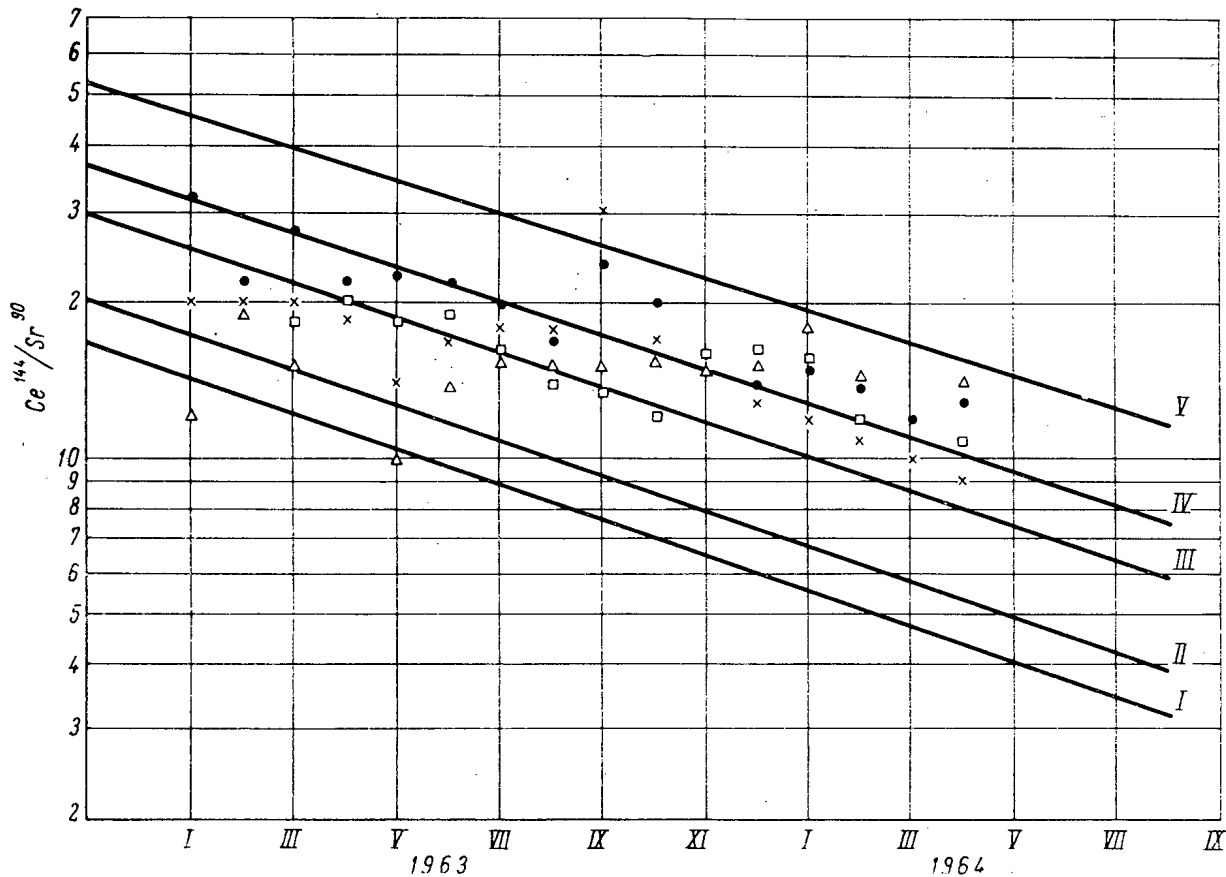


Fig. 3.  $Ce^{144}/Sr^{90}$  ratio in aerosol samples from the stratosphere in 1963-1964 (35° N. lat.).

It can be confirmed that the increase in the  $Ce^{144}/Sr^{90}$  ratio in the atmospheric boundary layer of air in the summer of 1961 is connected with the entry of fission products into the lower layers of the atmosphere, which had been injected into the mesosphere as a result of high-altitude tests. It is well-known that the first sign of the appearance in the boundary layer of the atmosphere of the northern hemisphere of fission products from the high-altitude tests of 1958 (the appearance of  $Rh^{102}$ ) was detected during the year after their appearance, autumn-winter 1959-1960. The entry of large quantities of these products into the lower layers of the stratosphere of the polar and temperate latitudes occurred during autumn-winter of 1960-1961, but into the boundary layer of air in the third quarter of 1961 [19-21].

According to [22], a gradual increase of the  $Ce^{144}/Sr^{90}$  ratio was observed in the stratosphere at temperate and polar latitudes of the northern hemisphere at the end of 1959 and the beginning of 1960, and in the layer located at an altitude of 18-21 km it remained higher than in the lower layers. The increase was associated with radioactive aerosols arriving from the mesosphere as a result of the high altitude tests (established by the change of concentration of  $Rh^{102}$ ).

By analogy with 1960-1961 it would be thought that in the autumn-winter of 1963-1964 fission products, which were injected at the time of the tests into the higher layers of the stratosphere and possibly into the mesosphere, reached the atmospheric boundary layer of air in significant quantities. It should not be excluded that this circumstance served as the reason for the longer lasting maximum of fission product fallout and its movement in the second-third quarter in 1963 in comparison with 1959. The reason for the increase in the  $Ce^{144}/Sr^{90}$  ratio in the fission products from the high-altitude tests should be found in the appearance of fractionation and separation of  $Ce^{144}$  and  $Sr^{90}$  as a result of the formation and propagation in the atmosphere of radioactive aerosols from nuclear tests. The oxides of  $Sr^{90}$  are more volatile than the oxides of  $Ce^{144}$ ; moreover, the gaseous precursor of  $Sr^{90}$  has a longer half-life than the precursor of  $Ce^{144}$ . Hence it follows that  $Ce^{144}$ , in comparison with  $Sr^{90}$ , will be found mainly in the coarser particles [23]. Then the fraction of  $Ce^{144}$ , deposited locally, will be significantly higher than the local depositions of  $Sr^{90}$ , but in the fission products which have been propagated globally the  $Ce^{144}/Sr^{90}$  ratio is found to be

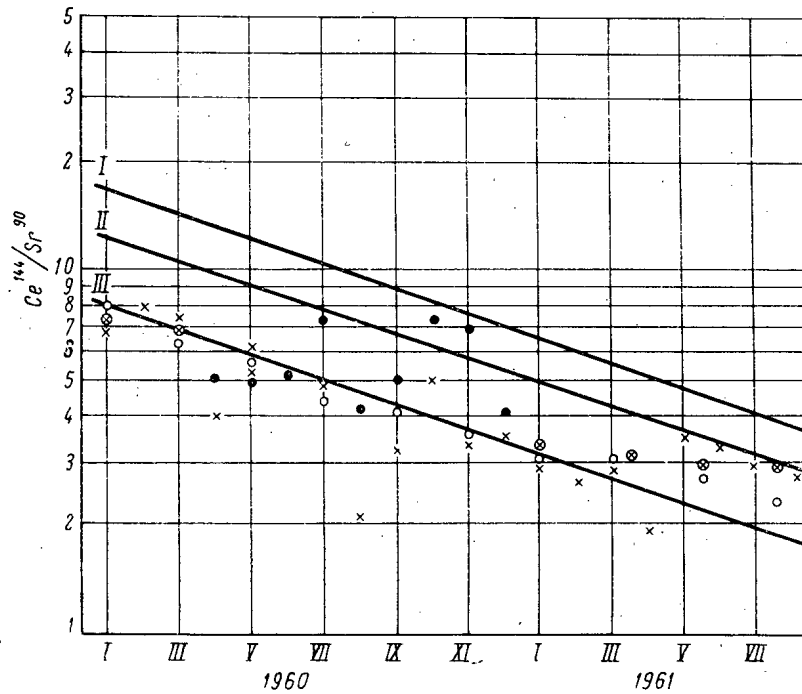


Fig. 4. Relative activity of  $Ce^{144}/Sr^{90}$  in the atmospheric boundary layer of air and in fallout in 1960-1961:  $\circ$ ) Leningrad, air; X) Milford Haven, precipitations;  $\circ$ ) Moosonee (Canada), air;  $\circ$ ) Washington (USA), air.

too low. Precisely these very low values of  $Ce^{144}/Sr^{90}$  were observed in the stratosphere at equatorial latitudes during the whole of 1958, despite the series of nuclear tests in the region of the Pacific Ocean [22]. The absence of local fallout in the case of the high-altitude tests and the high sedimentation rate of an aerosol enriched in  $Ce^{144}$  was due to the increase in the  $Ce^{144}/Sr^{90}$  as a result of fission products reaching the lower stratosphere and then the troposphere. On the other hand, the increase of the ratio being considered can be explained also by a simple "young" mixture of fission products i.e., by a significant reduction of their assumed average increase as a result of the arrival of relatively "fresh" fission products from a high altitude.

#### Estimation of the Total Quantity of $Sr^{90}$ Deposited in the Northern Hemisphere in 1962 and 1963

An attempt was made to estimate the total quantity of  $Sr^{90}$  deposited in the northern hemisphere in 1963 on the basis of data concerning the distribution of the annual fallout of  $Sr^{90}$  over different latitude belts of the Soviet Union (see Table 1). Since we did not undertake the measurements south of  $37^\circ$  lat. N. and north of  $70^\circ$  lat. N., the assumption was made in estimating the total quantity of  $Sr^{90}$  deposited that the fraction of  $Sr^{90}$  deposited in the belt  $70-30^\circ$  lat. N., relative to the following at other latitudes in 1963, was the same as in 1959 [24].

The average annual fallout density of  $Sr^{90}$  in a  $10^\circ$  wide belt (see Table 1) was multiplied by the total area of the ground in this belt and the quantity of  $Sr^{90}$  deposited in the corresponding latitude belt was obtained. Thus, it was estimated that in 1963 in the northern hemisphere 3.3 MCi of  $Sr^{90}$  were deposited and 1.4 MCi of  $Sr^{90}$  in 1962. Altogether, over the two years the atmosphere of the northern hemisphere was purified from 4.7 MCi of  $Sr^{90}$ . For comparison, we show that according to data from [13, 25] the total quantity of  $Sr^{90}$  deposited in the northern hemisphere in 1962 and 1963 amounted to 1.3 and 2.3 MCi respectively. The discrepancy between the results is related to their rough approximate nature as well as to the fact that the sample collecting points were located in completely different physical-geographical regions of the USA and the USSR. In addition, the methods of fallout collection were also different in both cases.

Altogether, about 6 MCi of  $Sr^{90}$  [13] were contained in the atmosphere of the northern hemisphere on January 1, 1963 (up to an altitude of 30 km). Thus, during 1963, approximately 0.6-0.4 of the total accumulation of this isotope was deposited from the atmosphere. If we assume that the atmospheric purification takes place according to a first-order law of kinetics, then the average time of residence of  $Sr^{90}$  in the atmosphere,  $\tau$  (per annum) can be

calculated by the formula  $\tau = T_{1/2} / 0.69 = 1 / \ln J/J - F$  [13]. Here,  $T_{1/2}$  is the period of half-cleansing of the atmosphere from the radioactive contamination (in years); J is the quantity of radioactive substances in the atmosphere at the beginning of the year; F is the quantity of radioactive substances deposited during the year. Hence, we obtain  $\tau \approx 1.2$  to 2.0 years and  $T_{1/2} = 0.9$  to 1.4 year. This value is higher than the average time of residence in the atmosphere of the  $Sr^{90}$  injected in 1958 into the stratosphere in the temperate and high latitudes of the northern hemisphere ( $T_{1/2} \approx 0.5$  to 0.6 year) and, probably, it is associated with the fact that the altitude of injection of fission products into the stratosphere in the temperate and high latitudes of the northern hemisphere in 1962 was, on an average, higher than in 1958.

Knowing the  $Sr^{90}$  content in soils of different latitude belts of the USSR on July 1, 1963 (see Table 4), and assuming that the quantity of  $Sr^{90}$  deposited in the second half of 1963 from the atmosphere is one-half of the accumulation of  $Sr^{90}$ , the maximum level of this isotope in the soils of the USSR in the next one to two years can be estimated. In this case, if no new tests are carried out, it will be approximately 60-70  $\mu Ci/km^2$  without taking fallout into account.

## LITERATURE CITED

1. V. M. Shubko,  $Sr^{90}$  Fallout on the Surface of the Territories of the USSR [in Russian], Moscow, Izd-vo AN SSSR (1959).
2. V. I. Baranov and V. D. Vilenskii, Radiokhimiya, 4, 486 (1962).
3. A. K. Lavrukina, T. V. Malysheva, and F. I. Pavlotskaya, Radiochemical Analysis, [in Russian], Moscow, Izd-vo AN SSSR (1963), p. 192.
4. V. M. Shubko and A. M. Eremycheva, Documents OOH A/AC 82/g/L-916 (1963); A/AC 82/g/L-706 (1961).
5. S. G. Malakhov, E. N. Davydov, and N. A. Karagod, Document OOH A/AC 82/g/L-902 (1963).
6. E. Hardy and W. Collins, Radiolog. Health Data, IV, No. 1 (1963).
7. Fallout program; Quarterly summary report, HASL-146 (1964).
8. R. Cambray, E. M. R. Fisher, and G. Spicer, AERE-R-4392 (1963).
9. Y. Mijake, K. Saruhashi, and Y. Katsuragi, Papers Meteorol. and Geophys., 24, 3 (1963).
10. H. Crooks, R. Osmond, and E. M. R. Fisher, AERE-R-3349 (1960).
11. Fallout program; Quarterly summary report; HASL-142 (1964).
12. Fallout program; Quarterly summary report; HASL-149 (1964).
13. Report of the U. N. scientific committee on the effects of atomic radiation, New York (1964), p. 48.
14. Radioactive Contamination of the Environment, Collection pod red, V. P. Shvedova and S. I. Shirokova, [in Russian], Moscow, Gosatomizdat (1962).
15. T. Hvinden, Radioactive fallout in Norway, July 1959 to July 1960; Report F-404.
16. S. Malakhov, Document OOH A/AC 82/g/L-614 (1960).
17. R. Crooks, et al., AERE R-3766 (1961).
18. L. Lockhart et al., Radiolog. Health Data, IV, 71 (1963).
19. M. Kalkstein, Science, 137, 645 (1962).
20. P. Gustafson, S. Brar, and M. Kerrigan, J. Geophys. Res., 67, 4641 (1962).
21. M. Leo and A. Walton, Science, 140, 1398 (1963).
22. A. Stebbins and R. Minx, The high altitude sampling program. Radiation standards including fallout. Hearings before the Joint committee on atomic energy, Congress of the United States, Part II (1962), p. 649.
23. E. Freiling, TID-7632 (1962), p. 47.
24. E. Hardy and W. Collins, Radiolog. Health Data, 4, No. 1 (1963).
25. W. Collins, Ibid., 5, 163 (1964).

## NOTES ON ARTICLES RECEIVED

SHAPING OF THE THERMAL NEUTRON FLUX IN HETEROGENEOUS  
NUCLEAR REACTORS BY PROFILING THE FUEL CHARGE

(UDC 621.039.512.45)

E. I. Inyutin

Translated from *Atomnaya Énergiya*, Vol. 19, No. 1,  
p. 36, July, 1965

Original article submitted August 3, 1964; Abstract submitted April 21, 1965

One of the possible ways of improving the efficiency in utilizing the nuclear fuel in thermal reactors is to equalize the energy release per unit mass of fuel. The use of fuel elements with an equal fuel concentration in

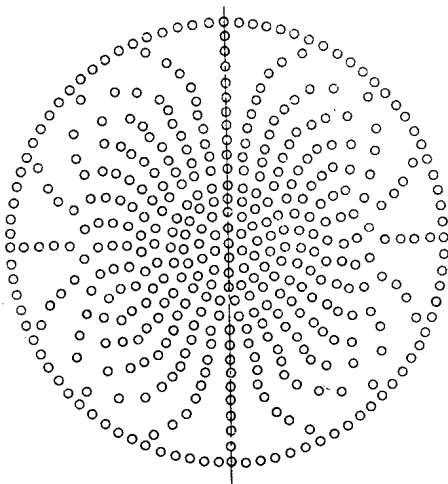


Fig. 1. Arrangement of fuel elements (the line marks the direction in which the neutron fluxes were measured).

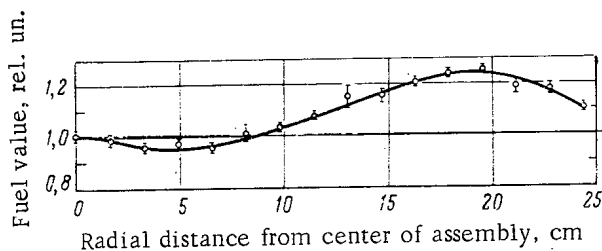


Fig. 3. Relative effect of the fuel on the reactivity along the radius of an assembly with an aqueous moderator.

elements at the boundary between the core and the reflector was varied in experiments. Ordinary water or monoisopropylidiphenyl was used as the moderator.

We determined the critical charges of the profiled systems, the radial distributions of thermal and epicalcium neutron fluxes, the relative fuel value, and the relative effect of the cadmium absorber on the reactivity of the critical assembly. Some of the experimental results are given in Figs. 2 and 3.

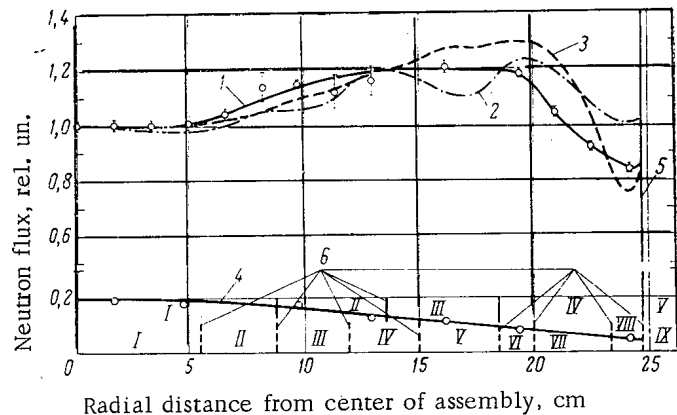


Fig. 2. Radial distribution of neutron fluxes in assemblies with aqueous moderators. 1) Thermal neutron flux (experiment); 2) same (calculation in the five-zone approximation); 3) same (calculation in the nine-zone approximation); 4) epicalcium neutron flux (experiment); 5) core boundary; 6) zone boundaries (calculation).

such reactors makes it possible to utilize all the elements at the maximum load under equal cooling conditions. Additional profiling of the fuel charge—along the length of fuel elements—may be necessary in reactors for direct conversion of thermal into electric energy.

The present article describes critical experiments with profiled uranium-hydrogenous assemblies. Tubular fuel elements with uniform  $U_3O_8$  filling (10% enriched uranium) were used. The fuel charge was arranged according to the scheme shown in Fig. 1. The number of fuel

Calculations of profiled systems were performed. A better agreement between the calculation and the experimental results was observed for critical assemblies with a moderator consisting of ordinary water than for critical assemblies with monoisopropyldiphenyl.

EQUALIZATION OF THE VOLUME ENERGY RELEASE IN HETEROGENEOUS  
THERMAL REACTORS BY PROFILING THE FUEL CHARGE

(UDC 621.039.512.45)

E. I. Inyutin

Translated from *Atomnaya Énergiya*, Vol. 19, No. 1,  
pp. 37-38, July, 1965

Original article submitted August 3, 1964; Abstract submitted June 21, 1965

Equalization of the energy release per unit volume of the core in nuclear power reactors is provided for the purpose of securing the maximum power in a core with certain given dimensions.

The article describes critical experiments where the energy release throughout the core volume was equalized by arranging fuel elements with a constant fuel content in a lattice with variable square spacings. The experiments

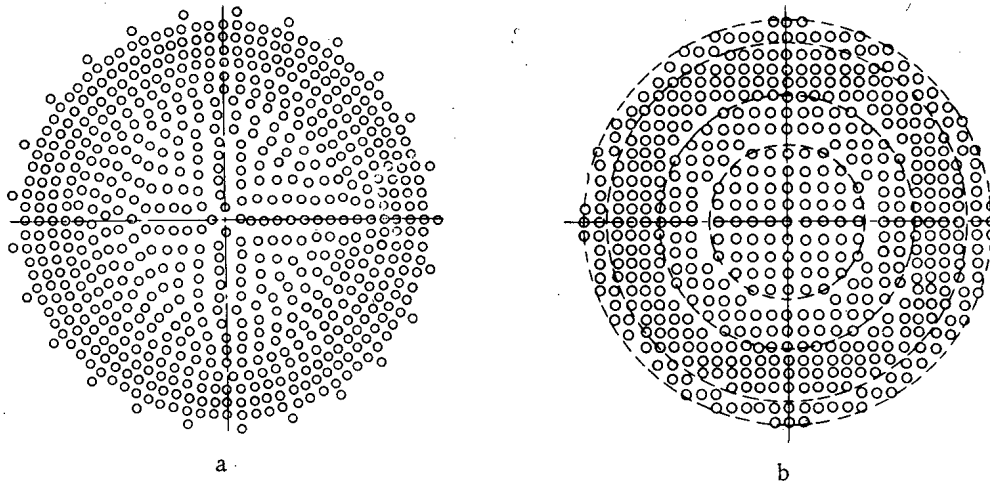


Fig. 1. Fuel element arrangements. a) Critical assembly with "continuous" profiling of the fuel charge; b) five-zone critical assembly (the zone boundaries are marked by dashed lines).

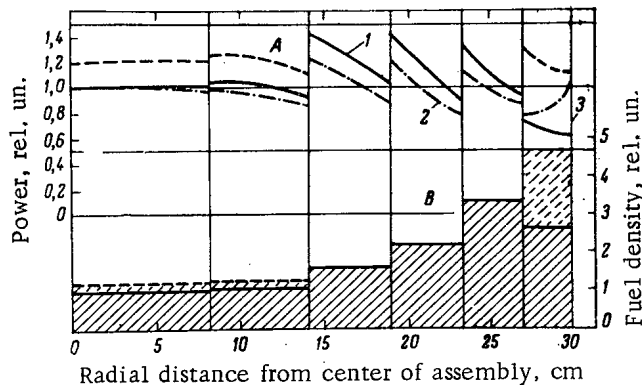


Fig. 2. Distributions of the energy release A and of the fuel density B in a seven-zone reactor. 1) Experiment; 2) calculation (the dashed curves mark the corrected distributions of fuel and energy release densities); 3) core boundary.

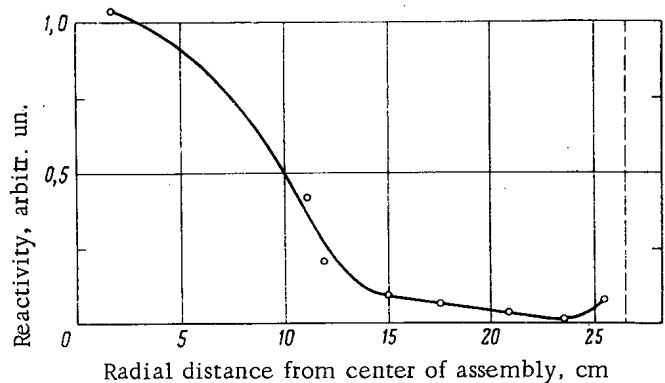


Fig. 3. Relative effect of uranium on the reactivity of a critical assembly with "continuous" profiling of the fuel charge. The dashed line denotes the core boundary.



were performed by using the critical assembly mentioned in the preceding abstract and the same fuel elements. Ordinary water was used as the moderator. The experiments were performed on three cores; two of them are shown in Fig. 1.

We determined the critical charges of profiled assemblies, the distributions of thermal and episcadmium neutron fluxes, and the relative fuel values along the core radius. It was assumed that the energy release was proportional to the product of the thermal neutron flux and the fuel concentration. Some of the experimental results are shown in Figs. 2 and 3.

The results of numerical calculations were compared with experimental data.

## EQUALIZED THERMAL NEUTRON FLUX IN AQUEOUS URANIUM REACTORS

(UDC 621.039.512.45)

E. I. Inyutin, V. P. Kochergin, and I. P. Markelov

Translated from *Atomnaya Énergiya*, Vol. 19, No. 1,  
p. 38, July, 1965

Abstract submitted March 12, 1965

The problem of equalizing the thermal neutron flux in the cores of heterogeneous nuclear reactors (where the fuel fission takes place mainly in the thermal region of the neutron spectrum) is of interest in connection with the possibility of more efficient utilization of the nuclear fuel.

The article provides the results of an analysis of alternative calculations of aqueous uranium thermal reactors with equalized thermal neutron fluxes. The published data can be used for determining the most suitable parameter ranges in which to perform more precise calculations of profiled aqueous uranium lattices.

The calculations were performed in the 18-group approximation by means of an electronic computer for the one-dimensional problem in a cylindrical geometry according to a five-zone program. The flux was equalized by simultaneously profiling the fuel charge and the moderator density (by varying the lattice spacing).

The alternative calculations of reactors with equalized neutron fluxes were performed for lattices using  $U^{235}$  fuel and a moderator consisting of ordinary water. Structural materials similar to those used in M-10 fuel elements were utilized [1]. The calculations were performed under the assumption that each zone was homogenized.

It was shown in [2, 3] that the calculation method used yielded results which agreed within  $\pm 10\%$  with the distribution of the thermal neutron flux in profiled heterogeneous aqueous uranium lattices.

The cores in all reactors had the same height (100 cm) and variable diameters (30-100 cm). The enrichment of fuel with respect to  $U^{235}$  varied from 5 to 90%. The fuel charge was profiled with respect to four zones; the fifth (external) zone served as the reflector (15 cm of water). The variation of the fuel concentration from one zone to another was linear.

The interdependence of the various characteristics of multizone reactors was illustrated by means of a number of graphs. These graphs make it possible to determine the dimensions of the core of a reactor with a plane-parallel flux having an assigned effective multiplication constant, and the required fuel enrichment for the assigned shape of the charge profile (or to find the charge profile necessary for equalizing the flux in the case where the fuel enrichment is assigned), to estimate the number of regions into which the core must be divided in profiling, etc.

The simple method of fuel charge profiling (based on the linear law) that we used can often satisfy the requirements for flux equalization and simplify the choice of a profiled system.

## LITERATURE CITED

1. E. I. Inyutin et al., Report No. 359, submitted by the USSR at the Third International Conference on the Peaceful Uses of Atomic Energy (Geneva, 1964).
2. E. I. Inyutin, See abstract of deposited article No. 23/3037 in the present issue.
3. E. I. Inyutin, See abstract of deposited article No. 24/3038 in the present issue.

DETERMINING THE SELF-ABSORPTION OF  $\alpha$ -RADIATION  
IN A SAMPLE DURING AIR FILTRATION

(UDC 543.52)

V. G. Labushkin, N. M. Polev, and L. S. Ruzer

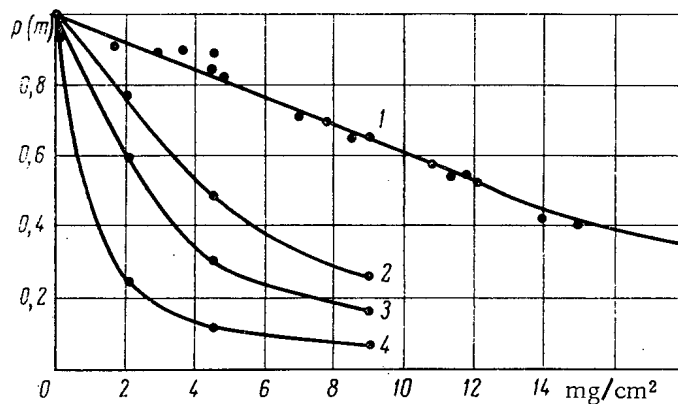
Translated from *Atomnaya Énergiya*, Vol. 19, No. 1,

p. 39, July, 1965

Original article submitted March 19, 1965

One source of error in measurements of the concentration of  $\alpha$ -active aerosols in air is absorption of  $\alpha$ -radiation in the sample layer.

This paper contains experimental measurements of the absorption coefficient for  $\alpha$ -particles from RaC' in a specimen with dust content on the filter of 0-18 mg/cm<sup>2</sup>. The measurements were made with artificial aerosols of



Curve of  $p$  versus  $m$  for various discrimination thresholds: 1) 1 V; 2) 50 V; 3) 60 V; 4) 70 V.

ammonium chloride formed by the interaction of gaseous HCl and ammonia. The coefficient of absorption of  $\alpha$ -particles from RaC' was measured by comparison of the  $\alpha$ -particle count of RaC' with the  $\beta$ -particles from RaC in equilibrium with it.

The results are plotted as the curve of  $p = p(m)$ , where  $p$  is the fraction of RaC'  $\alpha$ -particles leaving the specimen layer,  $m$  the thickness of the dust deposit in mg/cm<sup>2</sup> (see figure). This can be used as a calibration curve either for correcting the  $\alpha$ -radiation from RaC' or for determining the dust content of air. The value of  $p$  thus measured is found from the corresponding value of  $m$  and the calibration curve.

This method can be used to measure the concentration of long-lived  $\alpha$ -emitters (Pu<sup>239</sup>, Po<sup>210</sup>, etc.) in air; to get acceptable statistical accuracy a large quantity of air must be passed through the filter. For example, when the concentration of Pu<sup>239</sup> in the air is  $2 \cdot 10^{-15}$  curie/liter, to deposit  $10^{-10}$  curie on the filter it is necessary to pass 50 m<sup>3</sup> air. In this case, with dust content of 0.5 mg/m<sup>3</sup> and filter area 3 cm<sup>2</sup>, a dust layer of 8 mg/cm<sup>2</sup> is deposited on the filter, and even with minimum discrimination threshold the self-absorption in the dust layer is  $\sim 40\%$ .

To measure the concentration of long-lived  $\alpha$ -emitters, the sample is usually kept for long enough to allow decay of the short-lived daughter products of radon and thoron, and the activity of the long-lived isotope then measured.

The retention period can be used to measure the absorption coefficient for  $\alpha$ -radiation from R&C' in the sample by the method described above, followed by calculation of the  $\alpha$ -radiation absorption of the long-lived isotope.

SCATTERING OF  $\beta$ -RADIATION FROM THIN SPECIMENS  
BY MATERIAL EQUIVALENT TO TISSUE

(UDC 543.52)

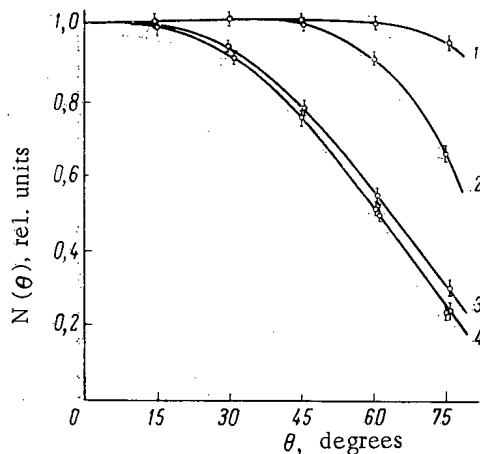
M. A. Malevich and Yu. M. Shtukkenberg

Translated from *Atomnaya Énergiya*, Vol. 19, No. 1,  
p. 40, July, 1965

Original article submitted April 1, 1965

The authors describe experiments on the scattering of  $\beta$ -radiation from thin specimens by a medium simulating tissue ( $Z_{\text{eff}} \approx 7$ ). The spectra were studied by means of a semicircular magnetic  $\beta$ -spectrometer with resolution 1.6%. The measuring chamber was maintained at  $\sim 10^{-4}$  mm Hg. A special structure enabled the source to be set up at angles  $\theta$  from 0 to 90°.

The authors measured the  $\beta$ -radiation spectra of the radioactive isotopes  $S^{35}$  ( $E_{\text{max}} = 0.17$  MeV),  $Tl^{204}$  (0.78 MeV),  $Sr^{89}$  (1.5 MeV) and  $P^{32}$  (1.7 MeV), with media of various depths and with  $\theta = 0, 15, 30, 45, 60$  and  $75^\circ$ , and also the reverse scattering spectra of  $\beta$ -radiation. With increasing penetration into the medium, the shape of the  $\beta$ -spectra varies with  $\theta$ ; the limiting energy decreases and so does the number of particles going through the absorber.



Angular distribution of  $\beta$ -radiation from  $P^{32}$  after passage through a layer of material equivalent to tissue: (1, 2, 3) for thickness 3.8, 32.1, 110.5  $\text{mg}/\text{cm}^2$ , respectively; (4) for thickness 172.4, 250 358.5  $\text{mg}/\text{cm}^2$ .

It is shown that the angular distribution of scattered  $\beta$ -radiation is independent of  $E_{\text{max}}$ ; for thicknesses less than the half-value layer it is related to the filter thickness (see diagram).

With further increases of the filter thickness, a diffuse distribution is set up; in this case, for any  $\theta$  the yield of  $\beta$ -particles per unit solid angle obeys the equation

$$N(\theta) \approx f(E_{\text{max}}) \cos \theta.$$

The function  $f(E_{\text{max}})$ , which characterizes the passage of the  $\beta$ -particles at  $\theta = 0^\circ$ , is found from the experimental data.

The authors study the way in which the energy composition and number of reverse scattered  $\beta$ -particles vary with the thickness of the reflecting material and with  $\theta$ .

The experimental data for the number of particles reflected through an angle of  $180^\circ$ , plotted against the filter thickness and the limiting energy of the  $\beta$ -spectrum of the incident radiation, obey the relation

$$\frac{N+N_1}{N} = 1.15 - 0.15 \exp\left(-0.03 \frac{t}{E_{\text{max}}}\right),$$

where  $N$  and  $N_1$  are the number of incident and reflected particles, and  $t$  is the filter thickness in  $\text{mg}/\text{cm}^2$ .

## LETTERS TO THE EDITOR

MEASUREMENT OF THE MEAN NUMBER OF FISSION NEUTRONS EMITTED  
BY  $U^{235}$  AND  $Pu^{239}$  ON THE CAPTURE OF A SINGLE 24 KeV NEUTRON

(UDC 539.173.84)

A. A. Van'kov and Yu. Ya. Stavisskii

Translated from *Atomnaya Énergiya*, Vol. 19, No. 1,  
pp. 41-42, July, 1965

Original article submitted November 9, 1964

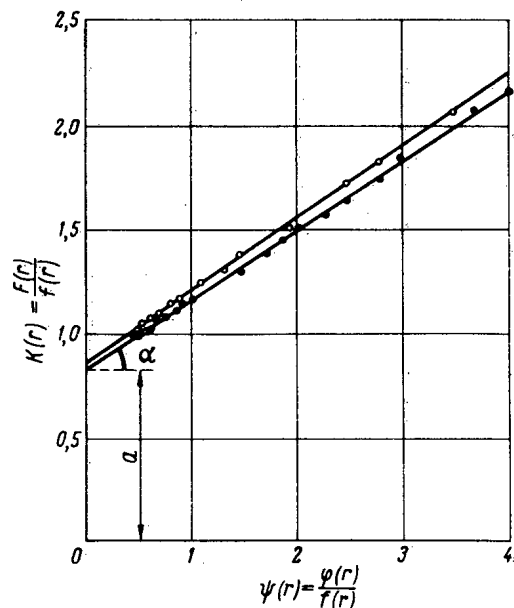
Experimental determinations of the mean number of secondary fission neutrons are based on measurements of the balance between the absorption of neutrons from the source and the appearance of fission neutrons.

To separate these two groups of neutrons, we used the difference between their moderation lengths in water. The detector system was a water tank with a spherical cavity of diameter 1 m. At the center of the cavity an Sb-Bè-photoneutron source was fixed [1]. Changes in the count rate when the source was surrounded by a spherical layer of fissionable isotope were measured by means of a movable system of small fission chambers placed in the water. The  $U^{235}$  and  $Pu^{239}$  specimens had internal and external diameters of 30 and 50 mm, respectively.

Let  $\delta$  be the fraction of photoneutrons absorbed by the specimen, and  $\nu_{\text{eff}}$  the number of secondary fission neutrons per single act of absorption. Then  $F(r)$ , the count rate of a fission chamber at a distance  $r$  from the source with the specimen can be written as:

$$F(r) = (1 - \delta) f(r) + \delta \epsilon \nu_{\text{eff}} \varphi(r), \quad (1)$$

where  $f(r)$  and  $\varphi(r)$  are the normalized radial distributions of the thermalized neutron fluxes in water, due to the photoneutron source and the fission-neutron source respectively, as found at the center of the tank cavity;  $\epsilon$  is the multiplication constant for fission neutrons in the specimen.



Experimental points corresponding to equation

(2). ○  $Pu^{239}$ ; ●  $U^{235}$ .

Relation (1) can be written as the equation of a straight line with parameters  $a$  and  $b$  (here,  $b = \tan \alpha$  is the slope of the line):

$$K(r) = a + b \psi(r), \quad (2)$$

where

$$K(r) = \frac{F(r)}{f(r)}, \quad \psi(r) = \frac{\varphi(r)}{f(r)}; \quad a = 1 - \delta;$$

$$b = \delta \epsilon \nu_{\text{eff}}$$

The function  $K(r)$  represents the change in count rate of the fission chamber at point  $r$  when the specimen is enclosed; the

	$U^{235}$	$Pu^{239}$
$\nu_{\text{eff}}$	$1.79 \pm 0.06$	$2.15 \pm 0.06$
$\delta_{\nu} / \delta_f$	$0.352 \pm 0.040$	$0.349 \pm 0.040$
$\delta_f + \delta_{\nu}$	$2.95 \pm 0.17$	$2.75 \pm 0.16$

function  $\psi(r)$  represents the change in count rate when the source is replaced by a fission-neutron source of equal intensity; it was found from subsequent measurement and normalization of the radial distribution of the thermalized neutron flux in the tank, due to the photoneutron source and the fission-neutron source. The latter was obtained by means of a uranium converter, placed at the center of the tank, onto which was directed a sharply collimated beam of thermal neutrons from the reactor. The diagram shows the experimental points corresponding to equation (2). Parameters  $a$  and  $b$  were determined by the method of least squares. In processing the results, corrections were made for the presence of 10%  $U^{238}$  as impurity in the  $U^{235}$ , for the presence of satellite groups of photoneutrons with energy 380 keV (4%), for absorption in the material of the source, and for the different fission-neutron spectra of  $U^{235}$  and  $Pu^{239}$ . Control experiments and approximate calculations showed that it is possible to neglect certain side-effects—namely, inelastic scattering of neutrons in the specimen, depression of thermal neutrons in the tank, and the collimator effect.

Calculations of neutron kinetics in spherical shells, performed with computers by the Monte Carlo method [2], have enabled us to determine  $\epsilon$ , the multiplication constant for fission neutrons, and also  $\sigma_f + \sigma_\gamma$ , the absorption cross-section for photoneutrons, starting from the experimental values of  $\delta$ . By comparing our data with the known values of  $\nu$ , the mean number of fission neutrons, we found the values of  $\sigma_\gamma / \sigma_f$  and  $\sigma_f$ : Our values of  $\nu_{eff}$  agree satisfactorily with the data for  $U^{235}$  and  $Pu^{239}$  in [3, 4]. A comparison of our values for  $\sigma_\gamma / \sigma_f$  with the results of time-of-flight measurements [5] reveals agreement for both isotopes.

The authors wish to thank A. I. Leipunskii and O. D. Kazachkovskii for their kind cooperation and attention, A. I. Abramov and V. N. Andreev for interesting comments, F. F. Mikhailus for compiling the program by which the neutron kinetics were calculated, and Yu. M. Nikitin, V. V. Piskunova and L. E. Fedorov for helping with the measurements.

#### LITERATURE CITED

1. Yu. Ya. Stavisskii et al., "Atomnaya Energiya," 15, 489 (1963).
2. T. S. Belanova, A. A. Van'kov, F. F. Mikhailus, and Yu. Ya. Stavisskii, "Atomnaya Energiya," 19, 3 (1965).
3. P. E. Spivak et al., "Atomnaya Energiya," No. 3, 21 (1956).
4. V. N. Andreev, "Atomnaya Energiya," 4, 185 (1956).
5. I. Hopkins and B. Diven, Nucl. Sci. and Engng, 12, 169 (1962).

## FAST NEUTRON CAPTURE CROSS SECTION FOR RHENIUM

(UDC 539.172.4:539.17.02)

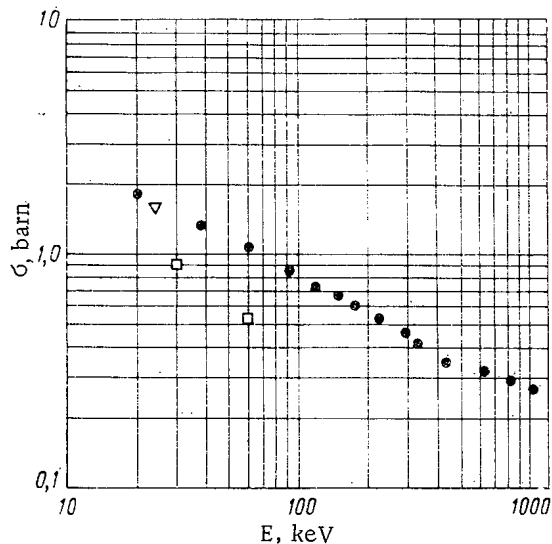
Yu. Ya. Stavisskii, A. V. Shapar' and R. N. Krasnokutskii

Translated from *Atomnaya Énergiya*, Vol. 19, No. 1,  
pp. 42-43, July, 1965

Original article submitted August 26, 1964

By registering the prompt  $\gamma$ -radiation, we have measured the energy/cross section relationship for radiative capture of fast neutrons by the natural isotope mixture of rhenium. The neutron source was the reaction  $T(p, n)He^3$  in the target of a Van de Graaff accelerator. The mean neutron energy scatter was  $\pm 16$  keV. The capture  $\gamma$ -rays were detected by means of a scintillation counter with  $CaF_2$  crystal.

The cross section curve was measured in annular geometry: the  $CaF_2$  crystal was shielded from the direct beam by a lead cone, and was placed inside a ring of the element being studied. The rhenium specimens had thickness  $6 \cdot 10^{22}$  atom/cm<sup>2</sup>. The noise/signal ratio was below 30%. The energy dependence of the radiative capture cross section was determined by comparison with the curve for fission cross section of  $U^{235}$ , as given in [1]. The error in an individual measurement was 7%.



Energy/radiative capture cross section relationship of rhenium for neutrons. Sources:  $\circ$ ) Present authors;  $\nabla$ ) [3];  $\square$ ) [4].

were irradiated with thermal neutrons in the beam from a horizontal channel of a thermal column of a BR-5 reactor. The induced  $\beta$ -activity was measured by end-window  $\beta$ -counters.

In processing the results we used data from [2] on the cross-section of  $I^{127}$ , and values of the absorption cross-sections of the rhenium isotopes for thermal neutrons from [1]. The capture cross-section of the natural rhenium isotope mixture for neutrons of energies  $600 \pm 100$  keV was found to be  $325 \pm 60$  mbarn.

Our results are shown on the graph. The error of an individual determination of the rhenium cross section is 22%. For comparison, the graph also shows data due to other authors.

To determine the absolute value by the activation method, we measured the capture cross section for both isotopes of rhenium at neutron energy 600 keV.

Our method was different from the usual activation methods: irradiation by thermal and fast neutrons was carried out in essentially different conditions. This is associated with the marked instability of a flux of fast neutrons from the target of a Van de Graaff accelerator, which makes it practically impossible to repeat the same conditions in irradiation by thermal neutrons. In irradiating the specimens by fast neutrons, we allowed for the change in the neutron flux with time. During irradiation by thermal neutrons, the flux was taken as a constant. The capture cross sections of the isotopes were determined by comparison with the cross sections of  $I^{127}$  for irradiation by fast and thermal neutrons.

To increase the neutron yield we used a relatively thick target; and the energy scatter was  $\pm 100$  keV. During irradiation by fast neutrons, the irradiation time necessary for separation of the two rhenium isotopes was 20 h, while for thermal neutrons it was 2 h. The specimens



LITERATURE CITED

1. J. Hughes and R. Schwartz, Atlas of Neutron Cross Sections, [Russian translation], Moscow, Atomizdat (1959).
2. Yu. Ya. Stavisskii, V. A. Tolstikov, and V. N. Kononov, "Atomnaya Energiya," 10, 158 (1961).
3. R. Macklin, N. Lazar, and W. Lion, Phys. Rev., 107, 504 (1957).
4. I. Gibbons et al., Phys. Rev., 122, 182 (1961).

FISSION CROSS SECTION OF  $U^{235}$  FOR RESONANCE ENERGY NEUTRONS

(UDC 539.17.02:539.173.4)

Wang Shih-Ti, Wang Yung-Ch'ang, E. Dermendzhiev, and Yu. V. Ryabov

Translated from Atomnaya Énergiya, Vol. 19, No. 1,  
pp. 43-45, July, 1965

Revised and re-submitted November 24, 1964

Many authors [1-4] have made determinations of the level parameters of  $U^{235}$ . Their results, however, fail to agree. We have measured the fission cross section of  $U^{235}$  in the resonance region, using a new experimental method, our aim being to get additional information on the level parameters.

The fission cross section was measured by the time-of-flight method. The resonance neutron source was the pulsed fast reactor of the United Institute of Nuclear Research [5]. The flight distance was 1000 m. The time spectrum was recorded by a 2048-channel time analyzer with channel width  $32 \mu\text{sec}$  for the 2-20 eV energy region and  $16 \mu\text{sec}$  for the energy region above 20 eV. This gave a resolution of  $\sim 0.04 \mu\text{sec/m}$ . Fission was recorded by a detector [6] consisting of a cylindrical tank with a liquid scintillator containing cadmium. The specimen was placed on the axis of the cylindrical tank with nearly  $4\pi$  geometry. The detector body was scanned by thirty two FEU-24 photomultipliers. Detection was based on the fact that fission is accompanied by the emission of prompt  $\gamma$ -rays and neutrons. The  $\gamma$ -rays from fission were detected with high efficiency. The fission neutrons, moderated by the hydrogen-containing scintillator medium, were captured by the cadmium nuclei and gave  $\gamma$ -radiation with total energy  $\sim 9 \text{ Mev}$ , which was also recorded by the detector. Each delayed coincidence corresponded to an act of fission.

The mean lifetime of a neutron in the detector was less than  $10 \mu\text{sec}$ . The efficiency of the detector for fission in various series of measurements was 30-50%. It was constant in the resonance region, as the total energy and multiplicity of fission  $\gamma$ -rays and the mean number of prompt neutrons emitted in one act of fission ( $\bar{\nu}$ ) do not change appreciably from one resonance to another for any one isotope [7]. In addition, the high efficiency of the detector for fission neutrons makes it insensitive to small variations in  $\bar{\nu}$ .

To reduce the background due to recycled neutrons, the measurements in the energy region up to 20 eV were with a cadmium filter in the beam, and those above 20 eV with a boron filter. The background of chance delayed

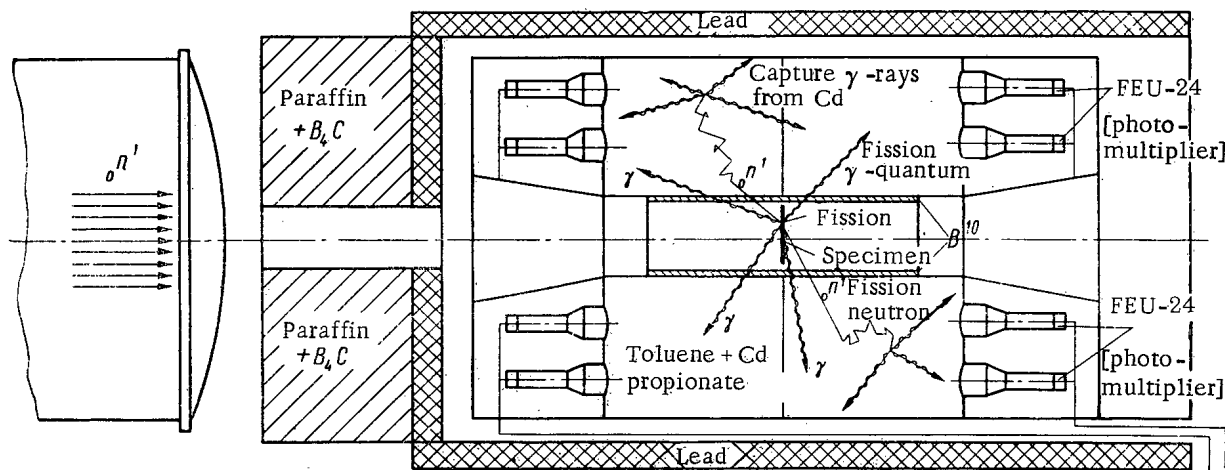


Fig. 1. Longitudinal cross section of detector and its position in the neutron beam.

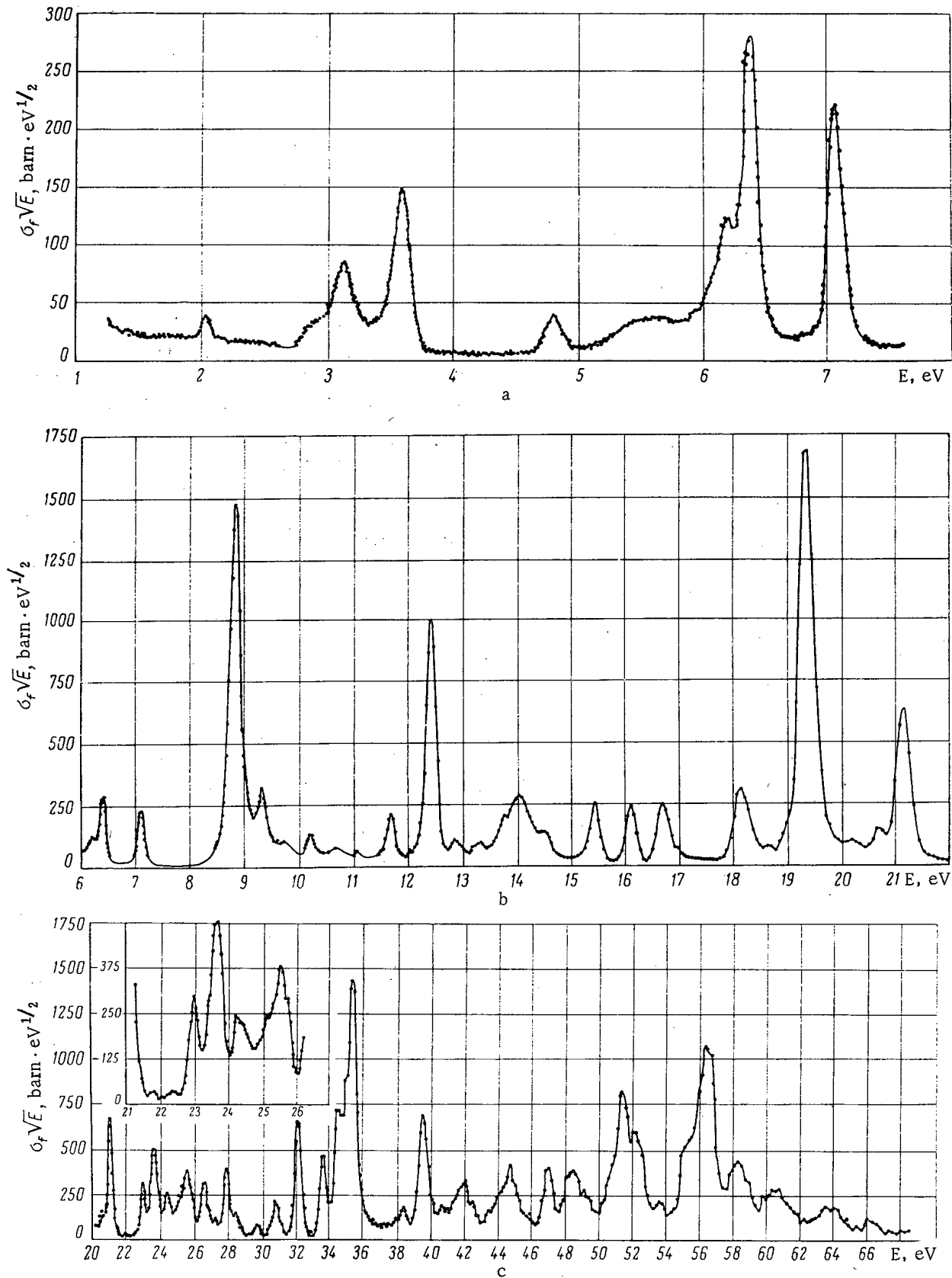


Fig. 2. Effective fission cross section of  $U^{235}$ . Neutron energies, eV: a)  $\sim 2-8$ ; b)  $\sim 6-22$ ; c)  $\sim 20-70$ .

Values of  $\sigma_0 \Gamma_f$ 

E, eV	$\sigma_0 \Gamma_f$ , barn. eV	E, eV	$\sigma_0 \Gamma_f$ , barn. eV
2,026±0,004	1,47±0,05	21,13±0,05	33,0±1,0
2,84±0,02	1,15	22,99±0,06	13,0±0,3
3,136±0,006	7,90±0,6	23,43±0,15	4,5
3,584±0,006	10,3±0,5	23,68±0,07	30,3
4,81±0,01	2,6±0,2	24,25±0,07	7,5
5,45	2,1±0,3	24,41±0,15	3,9
5,82	1,6	25,16±0,16	7,4
6,20±0,01	4,0	25,56±0,10	11,0
6,40±0,01	11,5±0,4	25,84±0,15	3,0
7,095±0,015	9,1±0,4	26,55±0,07	15,3
8,77±0,02	106±4	27,16±0,07	3,9
9,30±0,03	13,1±0,5	27,86±0,07	17,8
9,73±0,06	4,3	28,45±0,09	4,6
10,2±0,03	4,6	28,85±0,09	2,0
11,66±0,04	10,3±0,3	29,69±0,09	2,9
12,39±0,04	47,0±2,0	30,55±0,20	4,1
12,82±0,04	3,1	30,86±0,10	6,8
13,28±0,05	3,0	32,10±0,09	37,8
13,67±0,10	3,7	33,58±0,09	25,7
13,98±0,05	30,2	34,45±0,14	31,7
14,50±0,06	7,3	34,90±0,20	12,8
15,42±0,05	10,4±0,4	35,27±0,10	107,0
16,08±0,05	9,6±0,3	38,40±0,11	13,4
16,66±0,06	13,7±0,6	39,47±0,14	38,7
18,05±0,06	17,3±0,7	47,06±0,14	22,6
19,30±0,05	112,0±4,0	70,62±0,26	66,0
20,10±0,08	3,5	72,49±0,28	34,0
20,62±0,06	5,8		

coincidences, which must increase at the resonances, was determined by measurements with delays four or five times greater than the mean lifetime of a neutron in the detector. The background count of the detector was not more than 1-2% of the count of strong  $U^{235}$  resonances. The specimens consisted of  $U^{235}$  oxide of thicknesses  $8 \cdot 10^{19}$ ,  $4 \cdot 10^{20}$ , and  $10^{21}$  nuclei/cm<sup>2</sup>, deposited on aluminum substrates.

Figure 1, shows the longitudinal cross section of the detector and its position in the neutron beam.

Figure 2 gives the fission cross section  $\sigma_f \sqrt{E}$  for neutron energies 2-70 eV. The fission cross section was calibrated directly from the thermal cross section which was taken as 582 barn. It displays weak resonances at 9.7, 10.65, 11.05, 18.7, 21.85, and 22.40 eV. Some of these were observed only in measurements of the total  $U^{235}$  cross section by the transmission method. Well-known factors hinder the determination of the level positions in the region of "poor" resolution. However, we reckoned that the 24.32 eV level consists of two levels at 24.25 and 24.41 eV, while in the 25-26 eV region there are three levels at 25.16, 25.56, and 25.84 eV. In agreement with [8], we found that in the 5-6 eV region there are two levels at 5.45 and 5.82 eV. The statistical accuracy of our work was about  $\pm 0.6\%$  for the 1500 barn, eV<sup>1/2</sup> level and about  $\pm 3.0\%$  for the 25 barn, eV<sup>1/2</sup> level. The method of getting  $\sigma_0 \Gamma_f$  for an isolated resonance was described in detail in [9, 10].

The table gives values of  $\sigma_0 \Gamma_f$  obtained as the means of measurements with specimens of various thicknesses. For the level with  $n\sigma_0 \approx 1$  the data were processed with values of  $g \Gamma_n$  taken from [3, 4, 8]. The error is given in each case when the accuracy in determining  $\sigma_0 \Gamma_f$  was better than 10%. It is difficult to estimate the errors for closely spaced levels (13.67, 13.98, and 14.50 eV), and also for the levels in the energy region above 23 eV, owing to a certain arbitrariness in discerning their areas. The results agree with [11].

In conclusion, the authors wish to thank F. L. Shapiro, L. B. Pikel'ner, and I. V. Kirpichnikov for valuable advice and comment, and Yu. I. Kolgin and T. S. Afanas'eva for help with the measurements and data processing.

## LITERATURE CITED

1. A. Michaudon et al., Rapport CEA, No. 1098, France, Saclay (1959).
2. C. Bowman, G. Auchampaugh, and S. Fultz, Phys. Rev., 130, 1482 (1963).
3. V. V. Vladimirkii et al., In "Proc. of the Second International Conference on the Peaceful Uses of Atomic Energy" [in Russian], (Geneva 1958), T. 1. Moscow, Atomizdat (1959), p. 504.
4. W. Havens et al., Phys. Rev., 116, 1538 (1959).
5. G. E. Blokhin et al., "Atomnaya Energiya," 10, 437 (1961).
6. Wang Shih-Ti and Yu. V. Ryabov, OIYaI Preprint No. 1685 (1964).
7. L. Bollinger et al., Bull. Amer. Phys. Soc., Ser. I, 165 (1956).
8. V. Pilcher et al., Phys. Rev., 103, 1342 (1956).
9. D. Zelinger et al., ZhETF, 45, 1295 (1963).
10. O. Simpson et al., Phys. Rev., 103, 971 (1956).
11. A. Michaudon et al., J. Phys. et Radium., 21, 429 (1960).

RELATIVE YIELDS OF DELAYED NEUTRONS IN THE FISSION OF  $U^{235}$  AND  $U^{238}$ 

(UDC 539.125.5:539.163.1)

B. P. Maksyutenko

Translated from Atomnaya Énergiya, Vol. 19, No. 1,  
p. 46, July, 1965

Original article submitted March 2, 1964; final form February 6, 1965

The relative yields of delayed neutrons from  $U^{235}$  on its fission by neutrons of maximum energy 6.0 MeV were studied. A metallic sample of uranium enriched to 90%  $U^{235}$  was used. The total disintegration curve was obtained by making twenty measurements and contained 700,000 pulses. Decomposition into components was effected on an electronic computer by the matrix inversion method for given values of half-life periods. Owing to the difficulty of cutting off the deuteron beam rapidly on the Van de Graaff accelerator, we were unable to separate out groups with a half-life period smaller than 2.0 sec (the background after irradiation lasted 5 sec).

The measurements made in the present investigation, in the same way as earlier measurements [1], indicate a smooth variation of the yield ratio as a function of the energy of the neutrons causing the fission (Table 1). We obtained analogous results for  $U^{238}$  in the energy range 2.3 to 5.5 MeV, i.e., between the first and second "steps" in the fission cross section [3].

We studied the relative yields of delayed neutrons at the fission threshold for  $U^{238}$ . The sample was irradiated by neutrons with maximum energy 1.75 MeV obtained in the reaction  $T(p, n) He^3$  on the Van de Graaff generator.

TABLE 1. Relative Yields of Delayed Neutrons from  $U^{235}$ 

Half-life period, sec	Relative yield of group
55,0	1
24,0	$2,83 \pm 0,03$
15,5	$2,32 \pm 0,04$
5,2	$4,26 \pm 0,17$
2,2	$10,23 \pm 0,92$

TABLE 2. Yield of Delayed Neutrons at the Fission Threshold of  $U^{238}$ 

Half-life period, sec	Relative yield of group
55,0	1
24,0	$9,07 \pm 0,13$
15,5	$2,692 \pm 0,044$
5,2	$8,42 \pm 0,17$
2,2	$23,3 \pm 1,0$

A thick target ( $20 \text{ mg/cm}^2$ ) was used. The disintegration curve had a rather greater statistical accuracy than in the previous measurements, and was analyzed in an analogous way. The results of the experiments appear in Table 2. Comparison with the data of [2] for  $E_n = 2.3 \text{ MeV}$  (top of the first step in the fission cross section) shows a sharp change in the ratio of the yields. This is apparently connected with the channel effects.

## LITERATURE CITED

1. B. P. Maksyutenko, ZhETF, 35, 815 (1958).
2. B. P. Maksyutenko, Bulletin of the Information Center on Nuclear Data [in Russian], No. 1, Moscow, Atomizdat (1964), p. 266.

## DISTRIBUTION OF NEUTRONS IN A STRAIGHT CYLINDRICAL CHANNEL

(UDC 621.039.538 : 539.125.52)

E. A. Kramer-Ageev, V. N. Markov, V. P. Mashkovich,  
V. K. Sakharov, and V. M. Sakharov

Translated from *Atomnaya Énergiya*, Vol. 19, No. 1,  
pp. 46-48, July, 1965

Original article submitted July 15, 1964

The passage of radiation through inhomogeneities in shielding, and in particular through slots and channels, is a quite important, though comparatively little-studied question in shielding from radiation. A number of papers have been devoted to this problem, among which the most fundamental and interesting are, for example, [1-5].

In the present investigation we studied the energy and space distribution of neutrons in a straight cylindrical channel of diameter 14.4 cm and length 150 cm passing through a water shield. Source of neutrons was an isotropic Po- $\alpha$ -Be disk source which was simulated by an isotropic Po- $\alpha$ -Be point source emitting  $2 \cdot 10^7$  neutrons/sec.

The arrangement of the experimental apparatus is shown in Fig. 1. During the measurements, for each fixed position of the detector  $z$ , the point source was moved along the  $r$  axis over the range  $0 \leq r \leq R$ . For discrete positions of the source the spectrum of fast neutrons  $\Phi(E_n, z, r)$  was taken. From the data so obtained the fast-neutron spectrum can be determined as a function of  $z$  for each radius  $R$  from the formula

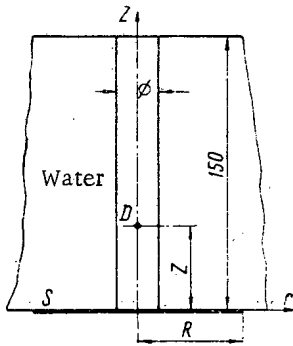


Fig. 1. Scheme of experimental system  
(D= detector, S= source).

$$\Phi(E_n, z) = 2\pi \int_0^R \Phi(E_n, z, r) r dr.$$

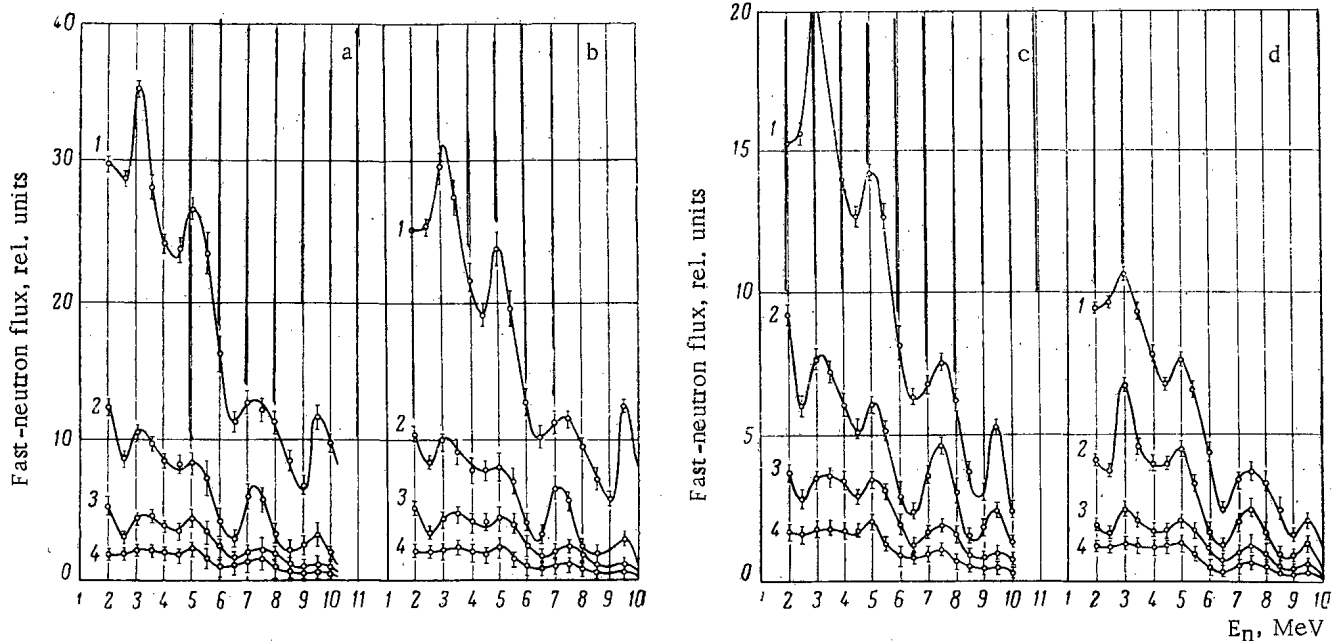


Fig. 2. Fast-neutron spectra for isotropic disk sources of radius  $R$  equal to a) 30, b) 20, c) 10, and d) 7.2 cm for various distances  $z$  (cm): 1) 35, 2) 55, 3) 80, 4) 105.

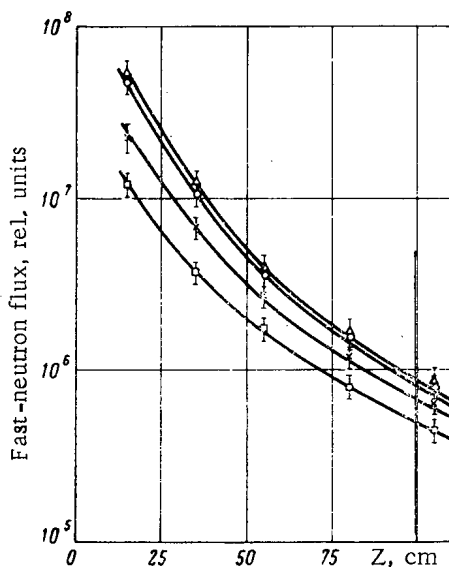


Fig. 3. Distribution of fast-neutron fluxes over the depth of the channel for isotropic disk sources of various radii  $R$  (cm):  $\Delta$ ) 30;  $\circ$ ) 20;  $\times$ ) 10;  $\square$ ) 7.2; continuous curve gives computed results. (Experimental and computed data normalized at  $z = 35$  cm and  $R = 7.2$  cm).

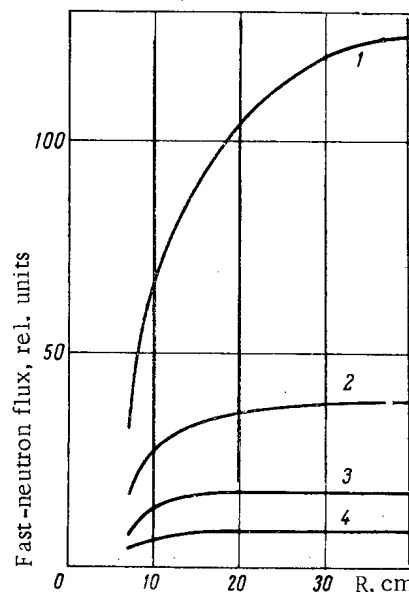


Fig. 4. Fast-neutron flux as a function of  $R$  for various  $z$  (cm): 1) 35, 2) 55, 3) 80, 4) 105.

The spectral distribution of the fast neutrons ( $E_n > 2$  MeV) was measured with a single-crystal neutron spectrometer, with division according to pulse shape [6]. The spectrum was analyzed by the method of count efficiencies [7].

The detector for intermediate neutrons was a thermal-neutron counter surrounded by a paraffin sphere of diameter 6.3 cm [8].

Analysis of the fast-neutron spectra given in Fig. 2, for isotropic disk sources shows that, within the limits of experimental error ( $\pm 8\%$ ), no deviations from the spectrum of the Po- $\alpha$ -Be source occurred.

The measured relationship for the fast-neutron flux as a function of  $z$  agrees with that calculated by the radial-analysis method [3] within 15% (Fig. 3). This deviation lies entirely within the experimental and computing errors. The variation of the fast-neutron flux with source radius for various depths is shown in Fig. 4. We see that, as  $z$  increases, the dimensions of the source which may be treated as infinite diminish.

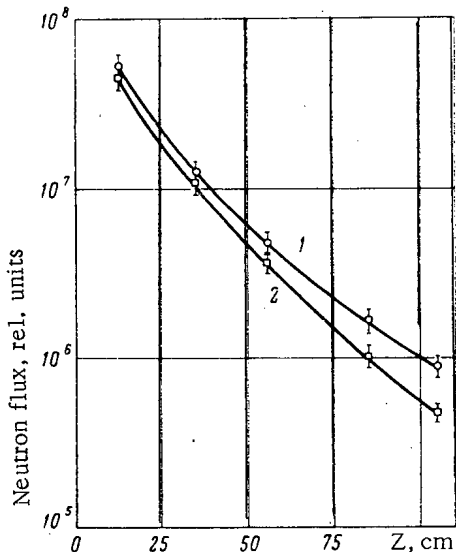


Fig. 5. Variation of 1) fast- and 2) intermediate-neutron flux with  $z$  for  $R = \infty$ .

[8] and also the known fast-neutron fluxes and the expected form of the spectrum, we determined the distribution of the intermediate-neutron flux ( $1 \text{ eV} < E_n < 0.5 \text{ MeV}$ ) over the channel depth (Fig. 5). The flux was impoverished with respect to neutrons of intermediate energies as the detector moved away along the channel. The intermediate-neutron flux fell with  $z$  on a  $1/z^3$  law, beginning from  $z = 45$  cm.

In conclusion the author expresses deep thanks to O. I. Leipunskii for valuable discussions and criticism of the results.

LITERATURE CITED

1. A. Simon and C. Clifford, Nucl. Sci. and Engng, 1, 103 (1956).
2. Shielding of Nuclear Reactors, Editor T. Rockwell [Russian translation], Moscow, IL (1958).
3. Reactor Handbook, V. III, Part B, Shielding Ed. E. Blizard, ORNL, New York-London (1962).
4. R. Schamberger, E. Shore, and H. Sleeper, The transmission of neutrons and  $\gamma$ -rays through hair slots, US AEC, Report BNL-2019-BNL-2028 (1954).
5. F. Shore and R. Schamberger, The transmission of neutron through ducts in Water, US AEC, Report BNL-390 (1956).
6. G. G. Doroshenko et al., Collection "Questions of Dosimetry and Shielding from Radiation" [in Russian], No. 2 Moscow, Gosatomizdat (1963), p. 179.
7. V. G. Zolotukhin et al., Ibid., p. 146.
8. S. Basson, Neutron Dosimetry, V. II. International Atomic Energy Agency, Vienna (1963), p. 241.



VARIATION OF THE YIELD OF THE  $(\alpha, n)$  REACTION  
WITH THE ENERGY OF THE  $\alpha$  PARTICLES

(UDC 539.172.16)

E. M. Tsenter and A. B. Silin

Translated from *Atomnaya Énergiya*, Vol. 19, No. 1,  
pp. 48-50, July 1965.

Original article submitted July 27, 1964; final form January 6, 1965

The neutron yield resulting from the  $(\alpha, n)$  reaction is of interest for many practical questions, in particular for a number of control problems [1-4]. For the solution of certain questions of geochemistry and geophysics we need data on the yield of the  $(\alpha, n)$  reaction for various elements [6-10].

An empirical formula

$$n = 0.152E^{3.56} \quad (1)$$

is given in [11] for the relation between the neutron yield for beryllium and the energy of the  $\alpha$ -particles.

Formula (1) is derived from three values of  $\alpha$ -particle energy:

$$E_{\alpha} = 5.14M \text{ eV (Pu}^{239}\text{);}$$

$$E_{\alpha} = 5.48M \text{ eV (Am}^{241}\text{);}$$

$$E_{\alpha} = 6.11M \text{ eV (Cm}^{242}\text{).}$$

Analogous empirical formulas of the type

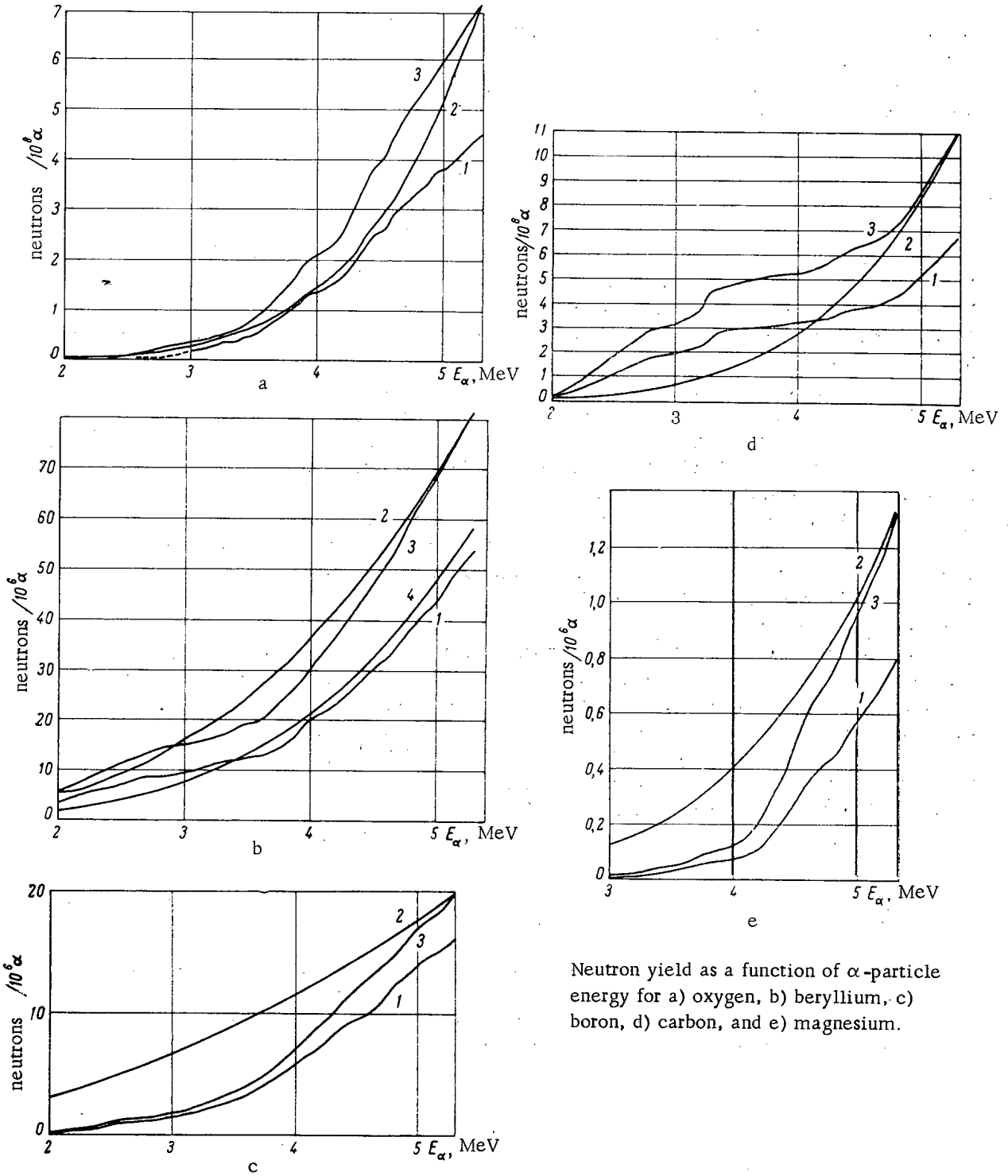
$$Q = kE^n \quad (2)$$

are given for a number of materials in [12, 13]. For determining the parameters  $k$  and  $n$ , the authors of these papers used values of  $Q$  obtained with emitters  $\text{Po}^{210}$  ( $E_{\alpha} = 5.3 \text{ MeV}$ ),  $\text{RaC}'$  ( $E_{\alpha} = 7.68 \text{ MeV}$ ), and  $\text{Rn} + \text{RaA} + \text{RaC}'$  ( $E_{\alpha}$  respectively 5.5, 6, and 7.68 MeV).

These formulas cannot be used without special verification for the energies of  $\alpha$ -particles coming outside the range given above. The necessity of such verification is further confirmed by the fact that the formulas in question correspond to curves with monotonically-rising first derivatives with respect to energy. In general this monotonic feature cannot arise, owing to the resonance peaks in the curve relating the cross section of the reaction to the energy of the  $\alpha$ -particles.

For Be, B, C, O, and Mg, curves relating the cross section of the  $(\alpha, n)$  reaction to energy up to 5.3 MeV occur in the literature [14, 15]. From these cross sections the variation of neutron yield with  $\alpha$ -particle energy can be calculated. The data necessary for calculating the  $\alpha$ -particle energy loss per unit distance were obtained by recalculating the energy loss in air [16] from known values of the relative atomic slowing-down powers, which we regard as constant in the energy range in question.

For  $\text{O}^{18}$  the  $\sigma(E)$  relationship is given in [14, 15]. Supposing that the  $(\alpha, n)$  reaction in oxygen is connected mainly with  $\text{O}^{18}$  [17], the results of such a calculation (see Figure a, curve 1) may be compared with experimental data obtained on a natural mixture of oxygen isotopes [18, 19]. The calculated value of 4.5 neutrons per  $10^8 \alpha$ -particles of energy 5.3 MeV (recalculated for a natural mixture of oxygen isotopes) deviates from the experimental value for this point [18, 19] (7 neutrons per  $10^8 \alpha$ -particles) by  $\sim 35\%$ . The latter value, obtained by various authors as a result of direct experiments, is more reliable than our value calculated from the cross sections of [15], the accuracy of which is no better than 25%. Clearly, curve 1 should reflect the form of the relation between the neutron yield and the  $\alpha$ -particle energy correctly, and we shall obtain a curve closer to the correct one if we normalize curve 1 to the experimental value at the point 5.3 MeV (curve 3, Fig. a). Curve 2 in the figure was obtained from



Neutron yield as a function of  $\alpha$ -particle energy for a) oxygen, b) beryllium, c) boron, d) carbon, and e) magnesium.

formula (2). Calculations for Be, B, C, and Mg were also made from the cross sections indicated in [14, 15], and analogous graphs (Fig. b, c, d, and e) were constructed; these are distinguished, as in Fig. a, by the respective numbers 1, 2, 3. Figure b also shows a curve 4, constructed from formula (1).

Formula (2) for oxygen might be compared with the data given in [20]. The authors reports on two new neutron sources developed by S. Amiel and A. Nier. One of these sources is  $Po^{210}-O^{18}$  (neutron yield 30 neutrons per  $10^6$   $\alpha$ -particles, mean energy approximately 2.4 MeV). In [17] a value of 31 neutrons per  $10^6$   $\alpha$ -particles is given for the neutron yield from a  $Po^{210}-O^{18}$  source. In 1959 data were published on the  $\gamma$ -radiation [21] and the neutron spectrum [22] of the  $Po^{210}-O^{18}$  neutron source. The maximum of the curve lay at 2.4 MeV. Data on the neutron yield from a  $Th^{228}-O^{18}$  source (1500 neutrons per  $10^6$   $\alpha$ -particles) in [20] are dubious. The energy of  $\alpha$ -particles of

$\text{Th}^{228}$  and its disintegration products are 5.4, 5.7, 6.3, 6.8, 6.08, and 8.8 MeV [23], some 13% falling to the share of the latter group. For the  $\alpha$ -particles of RaC ( $E = 7.68$  MeV), the yield on converting to  $\text{O}^{18}$  is 280 neutrons per  $10^6$   $\alpha$ -particles [12]. Judging by the  $\alpha$ -particle spectrum, the neutron yield of the  $\text{Th}^{228}$ - $\text{O}^{18}$  source should be still smaller than that of the RaC'- $\text{O}^{18}$  source. Thus, the value of 1500 neutrons per  $10^6$   $\alpha$ -particles given in [20] is roughly one order too high.

## LITERATURE CITED

1. V. V. Ivanov et al., "Atomnaya energiya," 7, 166 (1959).
2. I. N. Plaksin, V. N. Smirnov, and L. P. Starchik, "Dokl. AN SSSR," 127, 618 (1959).
3. I. N. Plaksin, V. N. Smirnov, and L. P. Starchik, "Dokl. AN SSSR," 128, 1208 (1959).
4. I. N. Plaksin, V. N. Smirnov, and L. P. Starchik, "Atomnaya energiya," 9, 361 (1960).
5. A. Blanc et al., Proceedings of the second International conference on the Peaceful Uses of atomic energy, V. 23, (1958), p. 269.
6. D. Cartwright, M. Todd, and B. Ukaea, Nucl. Power, 6, 66, 79 (1961).
7. G. V. Gorshkov and N. M. Lyatkovskaya, "Dokl. AN SSSR," 133, 92 (1960).
8. G. V. Gorshkov and N. M. Lyatkovskaya, "Dokl. AN SSSR," 25, 745 (1939).
9. L. L. Kashkarov and V. V. Cherdyn'tsev, "Geokhimiya," No. 7, 632 (1958).
10. I. Pine and P. Morrison, Phys. Rev., 86, 606 (1952).
11. I. Marion and I. Fowler, Fast neutron Physics, Interscience Publishers, Inc., New York (1960), p. 12.
12. G. V. Gorshkov, V. A. Zyabkin, and O. S. Tsvetkov, "Atomnaya energiya," 13, 475 (1962).
13. G. V. Gorshkov and O. S. Tsvetkov, "Atomnaya energiya," 14, 550 (1963).
14. T. Banner et al., Phys. Rev., 102, 1348 (1956).
15. J. Boir and H. Willard, Phys. Rev., 128, 299 (1962).
16. E. Segre, Experimental Nuclear Physics [Russian translation], Vol. 1, Moscow, IL (1955), p. 154.
17. I. A. Serdyukova, A. G. Khabakhpashev, and E. M. Tsenter, "Izv. AN SSSR, Ser. fiz.," 21, 1017 (1957).
18. E. Segre, Experimental Nuclear Physics [Russian translation], Vol. 2, Moscow, IL (1955), p. 311.
19. G. V. Gorshkov, V. A. Zyabkin, and O. S. Tsvetkov, "Atomnaya energiya," 13, 65 (1962).
20. G. Ben-David, Neutron dosimetry, Vol. II, IAEA, Vienna (1963), p. 407.
21. E. M. Tsenter, A. G. Kabakhpashev, and I. A. Pyrkin, ZhETF, 37, 1138 (1959).
22. A. G. Kabakhpashev, "Atomnaya energiya," 7, 71 (1959).
23. D. Strominger, J. Hollander, and G. Seaborg, Rev. Mod. Phys., 30, No. 2, Part II (1958).

All abbreviations of periodicals in the above bibliography are letter-by-letter transliterations of the abbreviations as given in the original Russian journal. Some or all of this periodical literature may well be available in English translation. A complete list of the cover-to-cover English translations appears at the back of this issue.

MATRIX ANALYSIS OF DATA OBTAINED BY MEANS OF A SINGLE-CRYSTAL  
FAST-NEUTRON SCINTILLATION SPECTROMETER

(UDC 539.108 : 539.125.5)

G. G. Doroshenko, V. G. Zolotukhin, and B. A. Efimenko

Translated from *Atomnaya Énergiya*, Vol. 19, No. 1,

pp. 51-56, July, 1965

Original article submitted September 22, 1964

In this paper we calculate matrices for analyzing measurements of fast-neutron spectra. As shown in [1, 2], the matrix method of count efficiencies enables the energy resolution of the spectrometer to be taken directly into account in the elements of the direct matrix. The count efficiencies of recording for a stilbene crystal (height 30 mm, diameter 30 mm) in the energy range 1 to 18 MeV, allowing for the energy resolution, were calculated from the shapes of the  $K_0(E_p, E)$  lines found by the Monte Carlo method for 55 values of initial neutron energies [3, 4].

The shapes of the  $K(E_p, E)$  lines, allowing for energy resolution, were determined from the expression

$$K(E_p, E) = \frac{dV}{dE_p} \int_0^E \frac{K_0(E'_p, E)}{\sqrt{2\pi\sigma^2(E'_p)}} e^{-\frac{[V(E'_p) - V(E'_p)]^2}{2\sigma^2(E'_p)}} dE'_p \quad (1)$$

where  $V(E_p)$  is the mean pulse amplitude from a proton with energy  $E_p$ ,  $\sigma(E'_p)$  is the standard deviation of the distribution of pulses from monoenergetic protons.

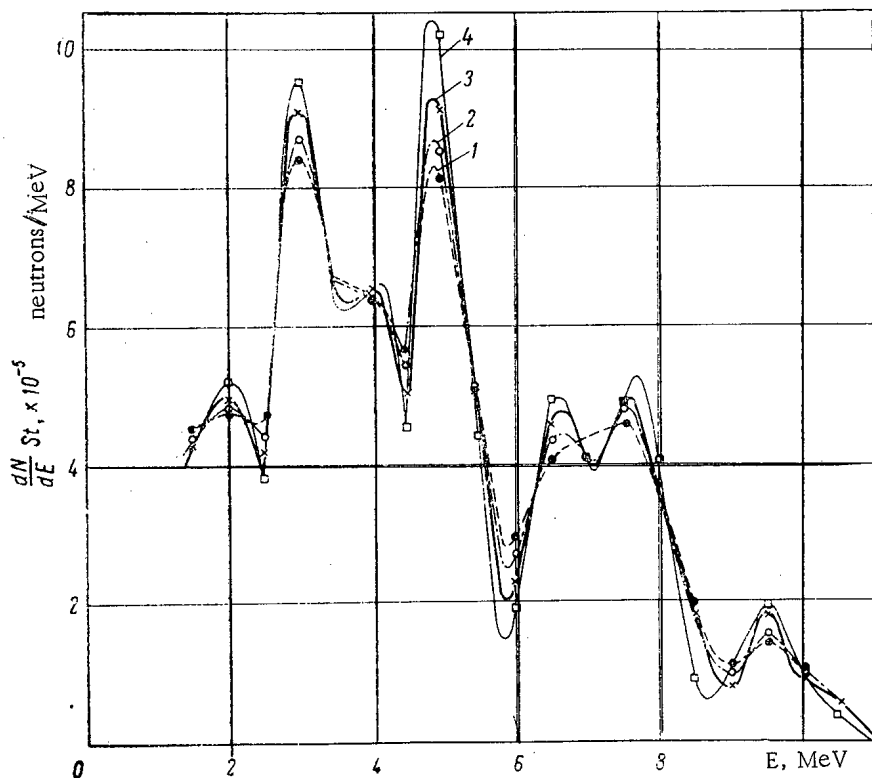


Fig. 1. Neutron spectrum of a Po-Be source analyzed by the matrix method, allowing for energy resolution ( $S$  = area of scintillator,  $t$  = time of measurement). Resolution parameter  $\sigma_0$ : 1) 0; 2) 0.07; 3) 0.13; 4) 0.19.

TABLE 1. Direct Matrix of Count Efficiencies for Stilbene Crystal

$B_i$	$E_R$															
	1,5	2,0	2,5	3,0	3,5	4,0	4,5	5,0	5,5	6,0	6,5	7,0	7,5	8,0	8,5	9,0
1,0	142 048	181 900	190 142	188 581	183 438	177 548	171 120	164 230	156 904	151 502	146 301	139 738	134 601	129 934	124 341	119 519
1,5		90 206	130 262	145 471	149 445	149 603	149 117	144 893	140 515	135 277	132 164	128 198	123 812	120 105	115 882	111 719
2,0			61 146	97 612	113 150	121 447	125 770	125 094	124 154	121 126	118 149	116 619	113 023	110 317	107 461	104 159
2,5				44 772	73 552	90 971	101 408	105 428	107 646	106 919	105 760	105 035	102 380	100 565	98 891	96 683
3,0	151 336				33 663	58 933	75 614	84 670	90 423	92 617	93 388	94 030	91 815	90 923	90 464	89 061
3,5	3 008	90 900				27 552	48 285	63 192	72 589	77 915	80 609	82 949	81 987	81 071	82 069	81 454
4,0		2 281	61 266				23 145	40 564	53 834	62 344	67 651	71 777	72 139	72 434	73 883	74 210
4,5			1 898	44 181				19 584	34 279	45 690	54 291	59 962	62 115	63 665	66 019	66 888
5,0	155 556			1 525	33 564				16 867	29 532	39 810	48 039	51 895	54 511	58 245	59 606
5,5	6 035	90 200			1 294	27 643				14 372	25 707	35 620	40 858	45 279	50 052	52 515
6,0		4 727	61 142			1 169	23 129				12 594	23 149	29 805	35 974	41 681	45 242
6,5			3 944	44 078			1 086	10 570				11 386	19 449	26 315	32 755	37 537
7,0	154 912			3 199	33 447			982	16 837				9 740	17 160	23 980	29 563
7,5	9 478	87 621			2 754	27 505			903	14 442				8 625	15 753	21 848
8,0		7 484	60 812			2 504	23 006			823	12 591				7 753	14 420
8,5			6 332	43 991			2 300	19 486			757	11 350				7 043
9,0				5 194	33 423			2 124	16 777			707	9 364			
9,5					4 564	27 510			1 947	14 403			605	8 424		
10,0						4 118	23 012			1 786	12 555			571	7 818	
10,5							3 784	19 520			1 642	11 309			552	6 999
11,0								3 504	16 841			1 560	9 374			512
11,5									3 206	14 500			1 356	8 425		
12,0										2 974	12 667			1 268	7 810	7 010
12,5											2 720	11 430			1 236	1 150
13,0												2 618	9 538			
13,5													2 314	8 578		
14,0														2 148	7 956	
14,5															2 096	7 171
15,0																1 967
15,5																
16,0																
16,5																
17,0																
17,5																

Note. Numbers are magnified  $10^6$  times. To obtain a spectrum in units of neutrons/MeV · cm<sup>2</sup> · sec, the results of the analysis must be divided by 3.53 t, where t is the time of measurement in sec.

TABLE 2. Inverse-Transpose Matrix of Second Differences for a Stilbene Crystal with  $\sigma_0 = 0$ 

$B_i$	$E_R$															
	1,5	2	2,5	3	3,5	4	4,5	5	5,5	6	6,5	7	7,5	8	8,5	9
1	14,080															
1,5	-0,232	22,171														
2	2,157	-2,889	32,709													
2,5	1,079	2,987	-5,894	44,671												
3	0,759	1,598	1,373	-8,262	59,412											
3,5	0,079	1,410	1,804	0,083	-8,257	72,590										
4	0,934	0,718	1,347	3,737	-4,907	-6,257	86,412									
4,5	0,465	-0,278	1,440	0,884	4,533	-5,662	-6,160	102,124								
5	0,017	0,251	1,113	0,673	3,326	4,421	-10,780	-3,300	118,575							
5,5	-2,002	0,332	0,064	0,519	2,657	5,824	-2,086	-6,622	-6,666	139,159						
6	0,089	-2,655	-0,171	1,561	-0,363	1,343	8,810	-2,533	-9,046	-5,735	158,806					
6,5	0,107	0,332	-1,508	0,230	0,021	3,407	0,340	4,929	1,256	-8,463	-5,258	175,654				
7	0,100	-0,357	0,371	-3,388	0,138	0,130	0,823	9,219	1,277	-9,604	-10,566	0,559	205,339			
7,5	-0,221	-0,014	-0,519	2,311	-8,516	0,735	3,094	0,514	1,182	6,555	-9,012	-12,621	2,143	231,884		
8	-0,273	0,411	-0,483	0,071	-0,417	-3,024	-2,051	4,384	2,258	10,744	-2,125	-12,030	-6,080	-7,388	257,965	
8,5	-0,603	-0,486	0,686	0,505	-2,938	1,523	-0,365	-4,126	2,096	8,462	6,855	-5,820	-8,095	-1,329	-12,233	283,970
9	-0,043	-0,274	-0,142	0,768	-1,384	2,522	-1,775	-2,881	-1,180	2,704	3,235	12,555	-11,510	-5,296	-15,401	-3,889
9,5	0,137	-1,016	2,113	-1,759	-0,491	2,289	-2,161	2,258	-4,619	2,079	-3,749	11,803	-2,046	0,756	-8,453	-5,025
10	-2,381	1,598	0,556	-1,600	1,535	-0,340	-0,952	-2,131	-0,936	-2,003	-3,248	-3,631	14,148	1,765	-11,516	-6,568
10,5	0,271	0,914	-2,802	0,461	2,252	-0,535	-0,820	0,085	0,712	0,260	-9,469	-4,669	19,980	-10,730	18,808	-14,463
11	-0,844	0,372	-0,449	-0,472	0,421	-1,614	2,622	-0,998	-7,354	7,484	-5,156	-3,580	5,155	4,698	-4,421	4,036
11,5	0,113	-0,395	0,276	-0,375	0,314	-2,411	-0,350	0,761	1,401	-3,987	4,446	-3,221	-3,612	2,422	11,140	-0,439
12	0,050	-0,368	-0,050	1,127	-2,864	-0,117	0,919	-0,419	1,791	-1,499	-0,088	-0,513	-0,730	1,270	0,164	7,336
12,5	0,291	-0,660	0,318	0,778	-2,049	-0,560	3,107	-3,575	-1,665	4,529	-5,957	-3,921	4,893	10,677	-17,313	3,980
13	0,135	-0,631	0,356	0,459	-2,235	0,333	0,728	-2,367	-1,260	4,781	-6,097	0,407	2,300	5,070	-9,955	3,858
13,5	-0,058	-0,574	0,345	0,157	-2,499	1,287	-2,046	-0,693	-0,489	4,419	-5,636	5,505	-1,027	-2,208	0,033	3,979
14	0,195	-0,579	0,111	0,040	-1,749	-0,219	-1,112	0,481	-2,264	4,294	-2,465	1,865	-0,403	-5,842	4,508	0,141
14,5	0,502	-0,591	-0,148	-0,031	-0,094	-1,981	0,270	1,529	-4,168	4,037	1,046	-2,684	0,632	-9,094	8,408	-4,113
15	-0,270	-0,084	-1,072	1,184	-1,756	-0,569	0,350	-0,531	-2,195	1,777	-1,895	1,058	-2,033	-4,955	7,698	-4,667
15,5	-1,186	0,480	-2,045	2,543	-2,765	1,192	0,310	-3,022	0,349	-0,773	-5,531	5,774	-5,402	0,267	6,449	-4,806
16	-0,667	0,188	-1,158	0,165	-1,113	1,207	-1,886	-1,814	1,196	-1,089	-5,237	0,881	-0,801	2,356	1,306	-8,959
16,5	0,003	-0,187	-0,097	-2,563	0,741	1,193	-4,335	-0,311	1,845	-1,146	-4,540	-4,897	4,357	4,290	-4,131	-13,298

Note. To obtain a spectrum in units of neutrons/MeV · cm<sup>2</sup> · sec, the results of the analysis must be divided by 7.06 t.

$E_h$

	9,5	10,0	10,5	11,0	11,5	12,0	12,5	13,0	13,5	14,0	14,5	15,0	15,5	16,0	16,5	17,0	17,5	18,0
115 195	110 660	106 670	102 823	99 168	95 734	92 779	89 070	86 482	83 895	81 161	78 427	76 089	73 752	71 798	69 842	67 899	65 956	
108 288	104 453	100 490	97 637	94 148	91 285	88 598	85 255	82 882	80 510	78 016	75 523	73 254	70 984	69 218	67 454	65 640	63 825	
101 377	98 214	95 206	92 330	89 376	86 819	84 440	81 392	78 718	76 118	73 807	71 698	69 590	67 679	65 769	64 217	62 666	61 091	59 516
94 542	92 185	89 529	86 935	84 539	82 405	80 332	77 825	75 716	73 807	71 698	69 590	67 679	65 769	64 217	62 666	61 091	59 516	
87 693	85 808	83 797	81 934	79 765	77 964	76 205	73 812	72 136	70 461	68 558	66 656	64 965	63 274	61 794	60 314	58 865	57 417	
80 776	79 651	78 196	76 797	75 039	73 563	72 035	69 968	68 543	67 119	65 426	63 733	62 200	60 667	59 362	58 058	56 685	55 312	
74 020	73 546	72 478	71 524	70 264	69 145	68 031	66 207	65 059	63 911	62 396	60 882	59 521	58 160	56 969	55 780	54 555	53 331	
67 114	67 275	66 773	66 257	65 571	64 789	64 031	62 490	61 579	60 670	59 383	58 098	56 856	55 615	54 545	53 475	52 390	51 304	
60 360	61 164	61 133	61 009	60 766	60 455	59 984	58 654	58 067	57 481	56 391	55 302	54 181	53 061	52 167	51 273	50 304	49 335	
53 744	54 943	55 412	55 825	55 910	56 097	55 939	54 921	54 617	54 313	53 389	52 467	51 524	50 583	49 834	49 085	48 220	47 355	
47 163	48 947	49 740	50 637	51 334	51 695	51 866	51 241	51 208	51 175	50 450	49 725	48 916	48 108	47 481	46 855	46 177	45 379	
40 414	42 823	44 101	45 421	46 524	47 415	47 827	47 450	47 688	47 926	47 413	46 901	46 273	45 646	45 146	44 647	44 056	43 465	
33 558	36 825	38 545	40 460	41 861	43 015	43 810	43 788	44 293	44 798	44 430	44 063	43 666	43 269	42 880	42 491	42 019	41 548	
26 292	30 434	33 103	35 614	37 281	38 678	39 797	40 222	40 901	41 581	41 427	41 274	41 041	40 807	40 604	40 401	40 019	39 637	
19 391	24 128	27 322	30 305	32 576	34 405	35 778	36 562	37 466	38 370	38 423	38 477	38 441	38 406	38 373	38 269	38 169	37 979	
12 646	17 817	21 513	25 215	27 784	30 088	31 729	32 740	33 961	35 182	35 477	35 773	35 888	36 004	36 055	36 107	35 946	35 786	
6 280	11 715	15 954	19 804	23 072	25 594	27 690	29 148	30 572	31 996	32 496	32 997	33 269	33 542	33 752	33 963	33 948	33 933	
	5 718	10 519	14 644	18 306	21 242	23 551	25 507	27 133	28 760	29 505	30 251	30 687	31 124	31 523	31 922	32 004	32 087	
$\sigma_0=0,07$		5 230	9 722	13 518	16 895	19 322	21 696	23 600	25 504	26 501	27 499	28 093	28 688	29 278	29 868	30 055	30 242	
6 294			4 820	8 894	12 625	15 297	17 908	20 065	22 222	23 453	24 685	25 515	26 345	27 008	27 670	27 982	28 294	
475	5 821			4 420	8 314	11 403	14 284	16 586	18 889	20 407	21 926	22 925	23 925	24 703	25 482	25 953	26 424	
	449	5 200			4 117	7 476	10 628	13 100	15 573	17 315	19 058	20 309	21 560	22 461	23 363	23 946	24 630	
$\sigma_0=0,13$		426	4 556			3 780	7 026	9 747	12 468	14 376	16 285	17 703	19 122	20 146	21 171	21 860	22 550	
6 315			386	4 329			3 482	6 398	9 313	11 409	13 505	15 163	16 701	17 889	19 079	19 859	20 639	
1 075	5 830			373	4 010			3 245	6 169	8 458	10 748	12 475	14 203	15 574	16 945	17 804	18 608	
	1 030	5 242			354	3 757			3 029	5 545	8 061	9 927	11 793	13 237	14 681	15 744	16 808	
$\sigma_0=0,19$		968	4 565			344	3 473			2 815	2 687	4 841	6 995	8 735	10 475	11 792	13 108	
6 479			879	4 361			322	3 249				2 453	4 631	6 501	8 370	9 746	11 122	
1 850	5 981			849	4 051			309	3 027	2 851			2 300	4 273	6 246	7 730	9 214	
	1 764	5 382			814	3 795			296	286	2 675			2 162	4 155	5 775	7 394	
		1 657	4 697			788	3 507				2 675				2 050	3 775	5 500	
			1 538	4 521			747	3 289			275	2 486				1 936	3 638	
				1 475	4 213			716	3 072			261	2 398				1 841	
					1 420	3 950			687	2 891			245	2 173				
						1 365	3 656			664	2 709			238	2 049			
							1 302	3 439			640	2 524			234	1 940		
								1 250	3 224			611	2 340			239	1 832	
									1 208	3 033			579	2 217				
										1 164	2 844			558	2 096			
											1 129	2 657			539	2 015		
												1 084	2 470			520	1 867	
													1 042	2 347				
														1 016	2 224			
															978	2 104		
																951	1 983	

$E_h$

	9,5	10	10,5	11	11,5	12	12,5	13	13,5	14	14,5	15	15,5	16	16,5	17
318.471																
-15.539	349.773															
-8.715	-3.946	382.409														
-15.513	-1.384	-6.506	414.938													
2.647	-12.827	-12.899	-5.069	452.489												
0.195	-6.293	4.239	-11.391	-8.793	485.791											
8.430	-18.108	-12.427	3.679	-27.847	10.795	529.101										
15.725	-1.511	-17.720	4.016	-6.375	-8.284	-9.421	574.382									
9.161	1.865	-5.842	1.009	-17.033	-1.486	-32.225	16.285	616.333								
1.341	3.732	7.726	2.219	-30.932	8.045	-0.728	-1.355	-22.586	660.284							
9.023	6.197	1.288	6.735	-24.263	5.222	-0.807	-8.853	-40.749	19.937	710.480						
-0.819	8.731	-7.220	16.945	-15.448	1.288	-4.542	-14.881	5.083	-10.649	5.817	744.324					
1.065	-2.562	1.783	4.523	-0.531	-1.234	5.970	-18.481	8.792	-16.918	-36.340	19.723	815.328				
3.021	-15.490	12.889	-10.431	14.739	-3.180	17.731	-21.300	7.197	-20.280	0.715	-10.945	-10.989	869.565			
2.757	2.896	5.314	-12.172	16.457	-13.101	14.779	6.037	-10.448	-29.169	12.484	-3.391	-44.382	20.513	925.069		
2.148	23.835	-3.986	-12.626	17.028	-23.892	11.404	35.296	-29.435	-38.499	22.490	6.597	-12.009	5.388	-24.819	975.609	

TABLE 3. Inverse-Transpose Matrix for a Stilbene Crystal with  $\sigma_0 = 1.13$

$B_i$	$E_k$									
	1,5	2,0	2,5	3,0	3,5	4,0	4,5	5,0	5,5	
1,0	13.991	-1.061	0.097	-0.010	0.001	-0.004	-0.001			
1,5	-1.235	25.217	-2.297	0.248	-0.029	0.832	0.009			
2,0	2.659	-6.252	39.116	-4.217	0.497	-0.062	0.009	-0.001		
2,5	0.611	5.705	-13.895	56.167	-6.613	0.832	-0.117	0.018	-0.003	
3,0	0.869	0.690	4.993	-19.271	75.881	-9.546	1.337	-0.208	0.035	
3,5	-0.200	1.704	1.362	3.062	-20.931	93.988	-13.163	2.044	-0.340	
4,0	1.112	0.902	0.613	5.869	-4.817	-21.447	114.863	-17.837	3.044	
4,5	0.419	-0.795	2.058	-0.918	8.417	-6.212	-24.727	138.877	-23.702	
5,0	0.357	0.169	1.439	0.500	2.419	8.584	-13.262	-25.104	164.988	
5,5	-2.909	1.473	-0.276	0.069	3.875	8.689	-4.241	-4.924	-35.289	
6,0	0.874	-4.653	0.357	2.541	-1.359	-2.692	17.670	-5.159	-7.845	
6,5	-0.163	2.045	-3.232	1.858	-1.342	7.342	-5.302	6.714	4.312	
7,0	0.437	-1.881	2.996	-3.615	5.548	-3.373	0.152	16.579	0.189	
7,5	-0.526	0.767	-2.590	8.960	-18.902	5.427	6.364	-7.083	0.377	
8,0	-0.226	0.920	-0.726	-2.309	6.002	-7.268	-6.280	12.814	-1.252	
8,5	-0.771	-1.270	1.710	1.841	-7.905	4.936	2.872	-11.597	3.737	
9,0	-0.329	0.961	-2.351	2.807	-1.774	3.823	-3.001	-4.583	0.173	
9,5	1.477	-3.135	4.638	-3.213	-1.900	5.378	-5.442	7.168	-11.589	
10,0	-4.237	3.662	0.177	-3.093	4.250	-2.621	-0.551	3.225	0.802	

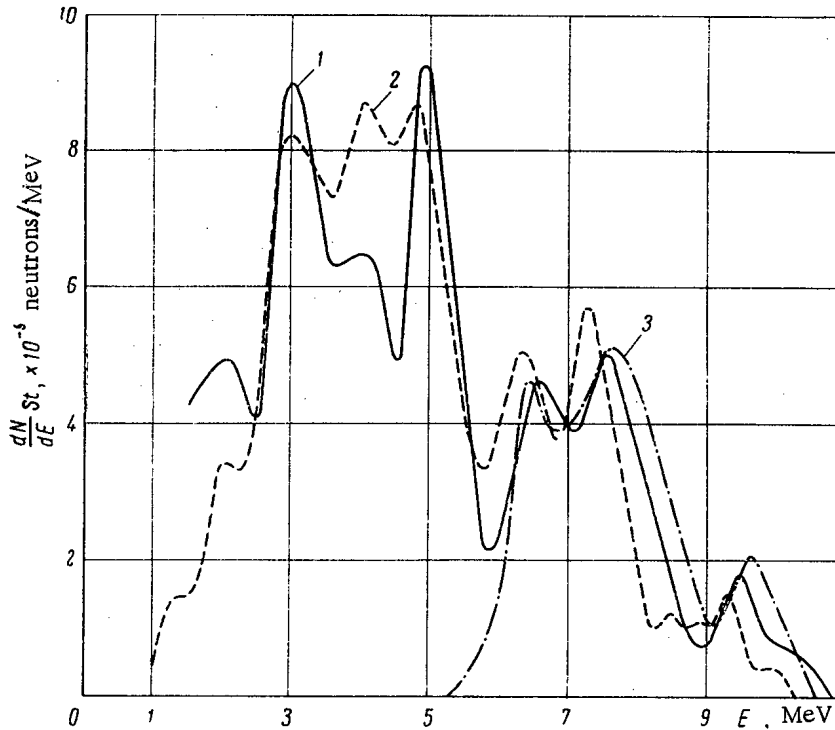


Fig. 2. Neutron spectra of Po-Be source obtained 1) by the matrix method with  $\sigma_0 = 0.13$  (data of present paper), 2) by the photographic-plate method [8], and 3) theoretically [9].

$E_k$									
6,0	6,5	7,0	7,5	8,0	8,5	9,0	9,5	10,0	10,5
0,001									
-0,007	0,001								
0,065	-0,013								
-0,570	0,115	0,003	-0,001	-0,001					
4,438	-0,897	-0,025	0,006	0,012	-0,003	0,001			
-30,895	6,246	0,191	-0,047	-0,081	0,021	-0,006	0,002	-0,001	
198,963	-40,225	-1,332	0,330	0,521	-0,134	0,038	-0,011	0,004	-0,001
-45,223	235,541	8,581	-2,128	16,570	0,785	-0,220	0,066	-0,020	0,006
0,535	-60,362	-50,246	12,462	-3,053	-4,258	1,196	-0,357	0,111	-0,035
-22,301	17,430	-67,637	330,203	-83,098	21,355	-5,997	1,791	-0,555	-0,173
18,086	-22,225	-85,599	-90,480	383,494	-98,554	27,675	-8,267	2,563	-0,799
15,433	-2,887	272,706	14,962	-104,500	432,201	-121,367	36,254	-11,241	3,502
10,150	13,613	-21,669	-14,801	38,900	-142,469	494,396	-147,682	45,789	-14,266
1,354	-1,131	-12,141	-25,374	-8,000	-1,719	-121,404	555,764	-172,315	53,685
10,831	-16,958	20,900	-19,320	10,607	-10,132	15,918	-160,387	628,177	-195,712
-7,324	2,049	32,265	42,548	-2,164	-22,700	-8,809	25,011	-183,252	662,054
		-25,995							

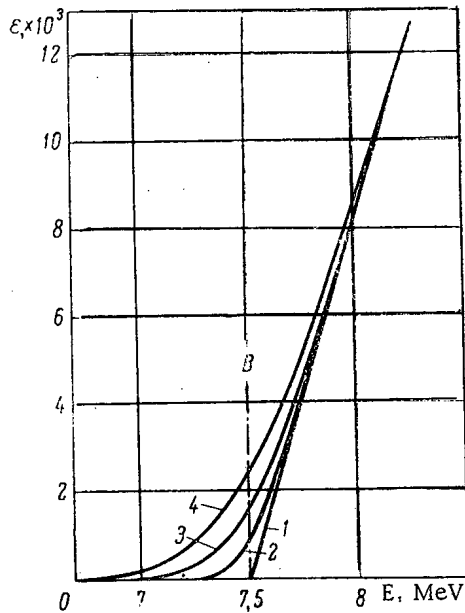


Fig. 3. Recording count efficiency for a detector with a stilbene crystal, allowing for resolution, for threshold  $B = 7.5$  MeV. Resolution parameter  $\sigma_0$ : 1) 0; 2) 0.07; 3) 0.13; 4) 0.19.

The energy dependence of the standard deviation, according to [5], has the form

$$\sigma(E_p) = \sigma'_0 \sqrt{E_p} \tag{2}$$

Taking the energy dependence of the light yield in the form  $S = kE^{3/2}$ , we obtain a connection between  $\sigma'_0$  and  $\sigma_0$ :

$$\sigma_0 = \frac{3}{2} \sigma'_0$$

Calculations were made for three values of the resolution parameter: 0.07, 0.13, and 0.19. The energy dependence of the recording count efficiency with a fairly small step was determined by corresponding interpolation of integrals from the diffuse line shapes (1). Figure 3 gives the calculated energy dependence of the recording count efficiency, allowing for energy resolution, for a stilbene crystal 30 mm in height and diameter.

In order to make allowance for the energy resolution in obtaining the matrix, the system of linear algebraical equations in the method of count efficiencies was written in the form



$$N(B_i) = \int_0^{E_{\max}} f(E') \epsilon(E', B_i) dE'$$

$$\approx f(E_i) \left[ \int_0^{B_i} \epsilon(E', B_i) dE' + \frac{1}{2} \epsilon(E_i, B_i) \Delta E \right] + f(E_{i+1}) \epsilon(E_{i+1}, B_i) \Delta E + \dots + f(E_n) \epsilon(E_n, B_i) \Delta E \quad (4 < i < n), \quad (3)$$

where  $B_i$  is the energy threshold of the counter. All the points of the trapezium quadrature formula (except the first) coincided with the positions of energy thresholds. In order to improve the conditioning of the system of equations [2], the first point was placed where the efficiency was practically zero. Thus the number of columns in the matrix became  $n-1$ . In order to obtain a square matrix, the last equation of system (3), together with the corresponding right-hand side, was discarded. As a result of these operations, the small diagonal elements of the  $n$ -th-order square matrix become subdiagonal elements in an  $n-1$ -th-order square matrix; this in general improves the conditioning of the system of equations.

Table 1 presents a direct 32-nd-order matrix\* for  $\Delta E = 0.5$  MeV and  $\sigma_0 = 0$ . The matrix for any nonzero value of  $\sigma_0$  is obtained by substituting the diagonal and adding the subdiagonal elements. The same table shows the diagonal and subdiagonal elements for the above-mentioned values of constant  $\sigma_0$ ; intermediate values of  $\sigma_0$  may be obtained by interpolation.

Table 2 shows a 32- $n$ -order inverse-transpose matrix of second differences [1] for  $\Delta E = 0.5$  MeV and  $\sigma_0 = 0$ ; Tables 3 and 4 give 19-th-order inverse-transpose matrices of second differences for  $\sigma_0$  equal to 0.13 and 0.07 respectively. The system of equations for  $\sigma_0 = 0.19$  is poorly conditioned even in the case of a 19-th-order matrix. In this case we must use the method of regularization [6, 7], for which each apparatus spectrum is analyzed on a computer.

Figure 1 shows results of analyzing the fast-neutron spectrum of a Po-Be source by means of matrices corresponding to the above values of constant  $\sigma_0$ , the regularization method being used for the case of  $\sigma_0 = 0.19$ . We see from Fig. 1 that allowing for the resolution of the detector enables the fine structure of the neutron spectrum from the Po-Be source to be revealed. The resolution of the detector in the present case is characterized by the constant  $\sigma_0 = 0.13$ . Comparing our spectrum with that obtained in [8], we find good agreement and fine structure of the same kind (Fig. 2). Also in this figure we have the results of calculations for the part of the energy spectrum corresponding to the formation of the  $C^{12}$  nucleus in the ground state [9]. We see that the peaks at neutron energies 6.6, 7.6, and 9.5 MeV.

\*All the tables give data for a stilbene crystal 30 mm in height and diameter.

TABLE 4. Inverse-Transpose Matrix for a Stilbene Crystal with  $\sigma_0 = 0.07$

$B_i$	1.5	2.0	2.5	3.0	3.5	4.0	4.5	5.0	5.5	6.0	6.5	7.0	7.5	8.0	8.5	9.0	9.5	10.0	10.5	
1.0	13.772	-0.482	0.109	-0.001	-0.002	-0.004	-0.007	-0.012	-0.01	-0.03	-0.04	-0.06	-0.08	0.01	0.01	0.01	0.01	0.02	0.03	0.03
1.5	0.439	23.287	-0.932	0.043	0.002	0.004	0.007	0.012	0.01	0.03	0.04	0.06	0.08	0.10	0.10	0.10	0.10	0.10	0.10	0.10
2.0	2.228	4.114	35.273	-1.643	0.043	0.004	0.007	0.012	0.01	0.03	0.04	0.06	0.08	0.10	0.10	0.10	0.10	0.10	0.10	0.10
2.5	0.918	4.128	9.462	12.379	65.688	-3.382	0.150	0.027	0.01	0.03	0.04	0.06	0.08	0.10	0.10	0.10	0.10	0.10	0.10	0.10
3.0	0.776	1.305	2.627	12.379	65.688	3.382	0.150	0.027	0.01	0.03	0.04	0.06	0.08	0.10	0.10	0.10	0.10	0.10	0.10	0.10
3.5	0.008	1.470	1.823	12.379	65.688	3.382	0.150	0.027	0.01	0.03	0.04	0.06	0.08	0.10	0.10	0.10	0.10	0.10	0.10	0.10
4.0	0.979	0.788	1.047	4.694	5.891	6.454	12.091	114.961	7.266	0.03	0.04	0.06	0.08	0.10	0.10	0.10	0.10	0.10	0.10	0.10
4.5	0.452	0.448	1.599	4.694	5.891	6.454	12.091	114.961	7.266	0.03	0.04	0.06	0.08	0.10	0.10	0.10	0.10	0.10	0.10	0.10
5.0	0.112	0.253	1.232	0.495	3.290	5.891	12.091	114.961	7.266	0.03	0.04	0.06	0.08	0.10	0.10	0.10	0.10	0.10	0.10	0.10
5.5	0.283	3.293	-0.075	1.927	2.730	5.891	12.091	114.961	7.266	0.03	0.04	0.06	0.08	0.10	0.10	0.10	0.10	0.10	0.10	0.10
6.0	0.079	0.766	1.962	0.363	2.730	5.891	12.091	114.961	7.266	0.03	0.04	0.06	0.08	0.10	0.10	0.10	0.10	0.10	0.10	0.10
6.5	0.167	0.830	1.173	4.883	1.311	4.299	11.525	3.122	10.19	16.97	183.26	14.12	1.24	0.01	0.01	0.01	0.01	0.01	0.01	0.01
7.0	0.287	0.185	1.096	4.234	1.311	4.299	11.525	3.122	10.19	16.97	183.26	14.12	1.24	0.01	0.01	0.01	0.01	0.01	0.01	0.01
7.5	0.267	0.583	0.648	4.234	1.311	4.299	11.525	3.122	10.19	16.97	183.26	14.12	1.24	0.01	0.01	0.01	0.01	0.01	0.01	0.01
8.0	0.675	0.637	0.921	0.811	4.049	3.986	3.011	6.107	1.60	12.72	11.74	2.92	13.77	5.89	27.48	30.01	24.05	0.02	0.02	0.02
8.5	0.043	0.080	0.613	1.300	4.049	3.986	3.011	6.107	1.60	12.72	11.74	2.92	13.77	5.89	27.48	30.01	24.05	0.02	0.02	0.02
9.0	0.434	1.501	2.767	2.230	1.656	3.133	2.187	3.467	2.53	9.11	8.64	7.30	18.12	15.31	16.16	16.16	16.16	16.16	16.16	16.16
9.5	2.862	2.183	0.526	2.083	2.261	3.019	3.009	3.503	2.659	2.00	5.66	18.80	15.31	2.13	7.93	31.23	380.78	37.17	42.88	42.88
10.0						0.873	-0.995	2.659	-0.12	-2.97	-5.32	18.80	15.31	1.43	-14.74	-6.11	-4.53	-31.07	-465.23	-465.23

agree closely both with the experimental data obtained on photographic plates and with the theoretical spectrum calculated with due allowance for the anisotropy of the angular distribution of neutrons formed in the reaction  $\text{Be}^9(\alpha, n)\text{C}^{12}$ .

The results obtained indicate great possibilities for the matrix analysis of spectra for quite bad detector-line shapes, as well as the possibility of taking the energy resolution strictly into account in the elements of the direct matrix. A similar method may also be used in analyzing  $\gamma$ -quantum spectra measured by detectors with organic and inorganic scintillators.

#### LITERATURE CITED

1. G. G. Doroshenko et al., "Izv. AN SSSR. Ser. Fiz.", 27, 1308 (1963).
2. G. G. Doroshenko et al., "Atomnaya énergiya", 16, 218 (1964).
3. V. G. Zolotukhin et al., "Atomnaya énergiya", 15, 194 (1963).
4. V. G. Zolotukhin and G. G. Doroshenko, "Atomnaya énergiya", 18, 287 (1965).
5. V. A. Dulin et al., "Pribory i tekhnika eksperimeta", No. 2, 35 (1961).
6. D. Phillips, J. Assoc. Comput. Machinery, 9, 84 (1962).
7. A. N. Tikhonov, "Dokl. AN SSSR", 151, 501 (1963).
8. L. Medvetski, "Atomnaya énergiya", 13, 583 (1962).
9. H. Broek and C. Anderson, Rev. Scient. Instrum., 31, 1063 (1960).

---

All abbreviations of periodicals in the above bibliography are letter-by-letter transliterations of the abbreviations as given in the original Russian journal. *Some or all of this periodical literature may well be available in English translation.* A complete list of the cover-to-cover English translations appears at the back of this issue.

ANALYSIS OF SYSTEMATIC ERROR IN DIFFERENTIATING APPARATUS SPECTRA  
MEASURED BY MEANS OF A SINGLE-CRYSTAL FAST-NEUTRON SPECTROMETER

(UDC 539.16.08: 539.125.5)

V. G. Zolotukhin, G. G. Doroshenko, and B. A. Efimenko

Translated from *Atomnaya Énergiya*, Vol. 19, No. 1,

pp. 56-59, July, 1965

Original article submitted September 22, 1964

The characteristics of the scintillation detector as a spectrometer have been considered in a number of papers [1-5]; they include the line shape and the recording efficiency. The conditions which must be satisfied for the simplest approximation (single scattering at protons) to be applicable have been found, as well as quantitative corrections which, in the opinion of the authors, eliminate a large proportion of the error produced by distortions of the rectangular energy distribution of the recoil protons due to multiple scattering and the end effect. The basic equation

$$P(E_p) = \int_{E_p}^{E_{\max}} f(E') K(E_p, E') dE', \quad (1)$$

where  $P(E_p)$  is the observed distribution of the total energy of the recoil protons due to neutrons with spectrum  $f(E)$ , and  $K(E_p, E')$  is the analogous distribution from monoenergetic neutrons, after differentiation with respect to  $E_p$  may be put in the form

$$f_H(E_p) = f(E_p) \frac{K(E_p, E_p)}{K_H(E_p, E_p)} \times \left[ 1 - \int_{E_p}^{E_{\max}} \frac{f(E')}{f(E_p)} \frac{\partial K(E_p, E')}{\partial E_p} \frac{dE'}{K(E_p, E_p)} \right], \quad (2)$$

where

$$f_H(E_p) = -\frac{\partial P(E_p)}{\partial E_p} \frac{1}{K_H(E_p, E_p)}; \quad K_H(E_p, E_p) = \frac{1 - e^{-H\Sigma_H(E_p)}}{E_p};$$

$H$  is the thickness of the scintillator, and  $\Sigma_H(E_p)$  is the macroscopic cross section of n-p scattering.

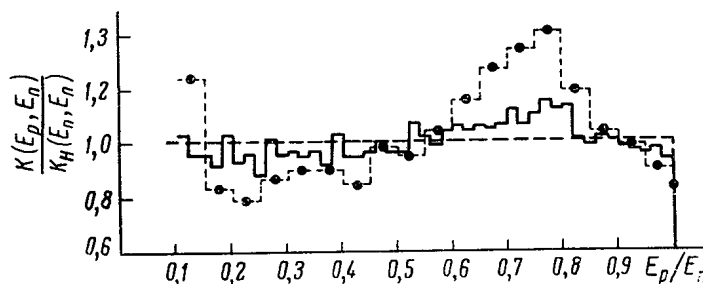
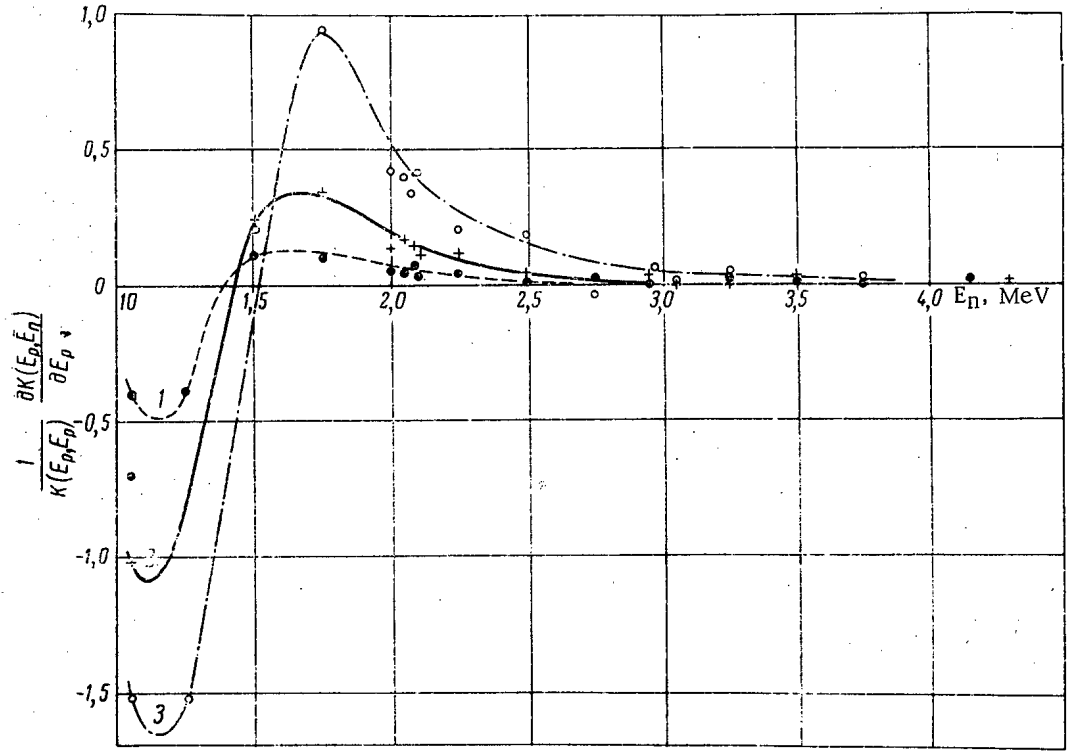
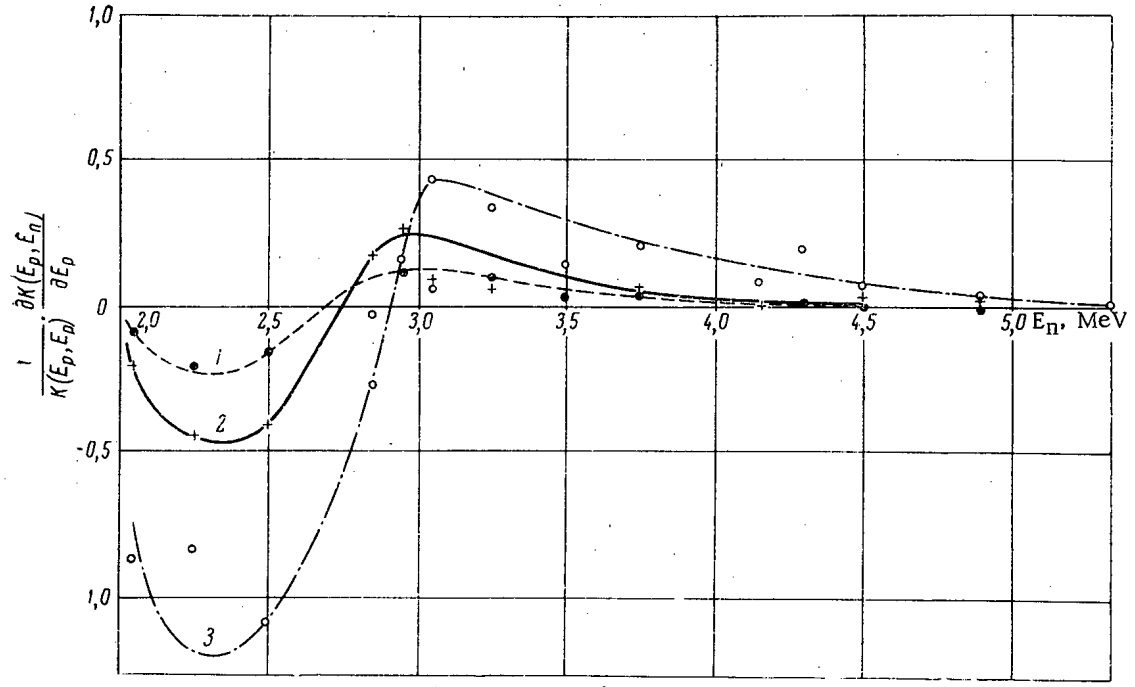


Fig. 1. Line shape of a detector with a stilbene crystal (height and diameter both 30 mm) for neutron energy 1.0 MeV (broken-line histogram) and 4.15 MeV (continuous-line histogram).



a



b

Fig. 2. Values of  $1/K(E_p, E_p) \cdot \partial K(E_p, E_n)/\partial E_p$  as a function of  $E$  for  $E_p = 1.05$  MeV (a) and  $E_p = 2.05$  MeV (b). Curves 1, 2, and 3 relate to crystals of diameter 30 mm and height 10 mm, diameter 30 mm and height 30 mm, and diameter 70 mm and height 70 mm respectively.

The deviation of the coefficient of  $f(E_p)$  on the right hand side of (2) from unity characterizes the influence of the distortions of the rectangular line shape resulting from the effects in question. If we neglect the integral in the square brackets, then the correction reduces to the calculation of  $K(E_p, E_p)/K_H(E_p, E_p)$ , equal to the proportion in which the height of the plateau at  $E_p = E$  rises or falls. This correction was calculated in [3] on the assumption that the light output was linear, taking account of only two-fold scattering of neutrons at protons.

Detailed calculations of the  $K(E_p, E)$  line shape for a stilbene crystal, which we made by the Monte Carlo method, enable us to estimate the error of the approximation

$$f(E_p) \approx - \frac{1}{K_H(E_p, E_p)} \frac{\partial P(E_p)}{\partial E_p}$$

A detailed description of the computing method and of certain results is given in [6-8].

Figure 1 shows the shape of the line  $K(E_p, E_n)/K_H(E_n, E_n)$  for a cylindrical stilbene crystal. The presence of a contribution from multiple scattering appears in the form of a rise in probability density. It is an important point that this rise, owing to the considerable nonlinearity of the stilbene light yield (varying roughly as  $E_p^{3/2}$ ) does not appertain to the region of  $E_p = E$ , as would be the case if there were a linear relation between the energy of the recoil proton and the amplitude of the light pulse, but to the region  $E_p \approx 0.75 E$ . Furthermore, at  $E_p = E$  there is a fall in the height of the plateau, so that the quantity

$$Q = \frac{K(E, E)}{K_H(E, E)}$$

is smaller than unity. This fall in height may easily be calculated if we consider that a neutron with energy  $E$  may give recoil protons with total energy  $E$ , either as a result of the first head-on collision [the probability of which is  $(\Sigma_H/\Sigma_t)(1 - e^{-H\Sigma_t}) \frac{dE_p}{E}$ ], or as a result of multiple scattering at protons leading to the appearance of a light pulse corresponding to proton energy  $E$ . Owing to the nonlinear light yield the latter possibility is not realized, so that

$$Q = \frac{(1 - e^{-H\Sigma_t(E)})}{(1 - e^{-H\Sigma_H(E)})} \frac{\Sigma_H(E)}{\Sigma_t(E)} \approx 1 - \frac{H\Sigma_c(E)}{2}, \quad (3)$$

where  $\Sigma_c(E) = \Sigma_t(E) - \Sigma_H(E)$  is the macroscopic cross section for the interaction of neutrons with carbon nuclei. Formula (3) is confirmed by exact calculation in cases where the end effect is unimportant.

The values of the quantity  $1/K(E_p, E_p) \cdot \partial K(E_p, E_n)/\partial E_p$ , found by numerical differentiation of the histograms, are given in Fig. 2a and b for various dimensions of the stilbene crystals and energies  $E_p$  equal to 1.05 and 2.05 MeV. By means of these curves and formulas (2) and (3), for a specific form of spectrum we may calculate the errors introduced into the method of differentiating the apparatus spectrum by neglecting multiple scattering.

It should be noted that these errors depend considerably on the form of the spectrum. For a "white" spectrum [ $f(E_p)/f(E) = \text{const} = 1$ ] the errors are substantially compensated. Below we give some results for the errors introduced by multiple scattering into the method of differentiation, as given by formulas (2) and (3), as well as data obtained in [3] for a 30 x 30 mm crystal (%):

E, MeV	Data obtained in accordance with [3]	Data of the present paper
1,0	+23,4	-8
2,0	+18,0	-3,5

Thus, for smooth slowly-changing spectra, the errors of the method of differentiation connected with multiple scattering certainly lie within the limits of the errors due to statistics, accuracy of calibration, etc.

It may be shown that for the end effect the following formula is valid

$$f_H(E_p) = f(E_p) \left\{ 1 - \frac{R(E_p)}{H} + \int_{E_p}^{E_{\max}} \frac{f(E')}{f(E_p)} \cdot \frac{R(E')}{H} \left[ \frac{4}{3E'} + \frac{7}{6} \frac{E_p^{3/2}}{(E')^{5/2}} \right] dE' \right\}, \quad (4)$$

where  $R(E')$  is the range of a proton with energy  $E'$ . Here also there is a certain compensation of the error for  $E_p \neq E_{\max}$ . For a crystal with  $H \geq 30$  mm and  $E_p < 14$  MeV, we may neglect the end effect.

Summarizing our discussion on the accuracy of the method of differentiation, we note that for slowly-changing spectra the mathematical errors associated with the distortion of the line shape lie below a few percent, while for rapidly-changing neutron spectra the error of the differentiation method may reach considerable values. In the latter case it is desirable to develop matrix methods for solving equation (1), taking account of the actual spectrometer line shape as well as its energy distribution.

#### LITERATURE CITED

1. C. Swartz and G. Owen, *Fast Neutron Physics*, Pt. 1 215 (1960).
2. B. V. Rybakov and V. A. Sidorov, *Spectrometry of Fast Neutrons* [in Russian], Moscow, Atomizdat (1958).
3. H. Broek and C. Anderson, *Rev. Scient. Instrum.*, 31, 1063 (1960).
4. V. A. Dulin et al., "*Pribory i tekhnika éksperimenta*," 2, 35 (1961).
5. J. Hardy, *Rev. Sci. Instrum.*, 29, 705 (1958).
6. V. G. Zolotukhin et al., "*Atomnaya énergiya*," 15, 194 (1963).
7. V. G. Zolotukhin et al., *Collection "Questions of Dosimetry and Shielding from Radiation"* [in Russian], Editor V. I. Ivanov, Moscow, Gosatomizdat (1963), p. 146.
8. V. G. Zolotukhin and G. G. Doroshenko, "*Atomnaya énergiya*," 18, 287 (1965).

ANALYSIS OF THE SPECTRA OF INSTANTANEOUS NEUTRONS  
FROM THE SPONTANEOUS FISSION OF  $Cf^{252}$

(UDC 539.173.7/546.799.8)

A. E. Savel'ev

Translated from *Atomnaya Énergiya*, Vol. 19, No. 1,

pp. 59-61, July, 1965

Original article submitted July 9, 1964

Spectra of neutrons from the spontaneous fission of  $Cf^{252}$  were measured in [1] for various angles  $\theta_L$  with respect to the direction of the light fragment. Assuming the evaporation theory to be valid, the authors of [1] analyzed the spectra obtained and came to the conclusion that the spectra of the light and heavy fragments were isotropic to  $\sim 10\%$  in their center-of-mass systems, and that on average the light fragments emitted 1.16 times as many neutrons as the heavy.

For analyzing the data of [1], it is supposed in the present work that the fission-neutron spectrum is isotropic in the center-of-mass system (c.m.s.) of the fragment. This assumption enables us to reduce the neutron spectra of the light and heavy fragments to the c.m.s. from solely kinematical considerations.

Let the isotropic spectra in the c.m.s. of the light and heavy fragments be denoted by functions  $\mathcal{P}_L(\epsilon, A_L)$  and  $\mathcal{P}_H(\epsilon, A_H)$ , where  $A_L$  and  $A_H$  are the mass numbers of the light and heavy fragments respectively,  $\epsilon$  is the energy of the neutron in the system of the fragment. Let us transform these spectra into the laboratory system of coordinates.

The energy of the neutron in the c.m.s. of the light fragment is connected with its energy in the laboratory system by the relation

$$\epsilon = \epsilon_L + w_L - 2\sqrt{\epsilon_L w_L} \cos \theta_L, \quad (1)$$

where  $w_L(A_L)$  is the kinetic energy of the fragment calculated for one nucleon. The corresponding Jacobian of the transformation has the form

$$J_{L1} = \frac{\epsilon_L^{1/2}}{(\epsilon_L + w_L - 2\sqrt{\epsilon_L w_L} \cos \theta_L)^{1/2}}. \quad (2)$$

Analogous relationships for the heavy fragment are obtained from equations (1) and (2) on replacing  $\theta_L$  by  $\pi - \theta_L$  and  $w_L$  by  $w_H$ .

Allowing for (1) and (2), the neutron spectrum in the laboratory system of coordinates is determined from the expression

$$\begin{aligned} \mathcal{P}(\epsilon, \theta_L) = & \frac{\sqrt{\epsilon_L}}{\alpha_L} \int_{A_{1L}}^{A_{2L}} \psi_L(A_L) \times \frac{\mathcal{P}_L(\epsilon_L + w_L - 2\sqrt{\epsilon_L w_L} \cos \theta_L, A_L)}{(\epsilon_L + w_L - 2\sqrt{\epsilon_L w_L} \cos \theta_L)} dA_L \\ & + \frac{\sqrt{\epsilon_L}}{\alpha_T} \int_{A_{1H}}^{A_{2H}} \psi_H(A_H) \times \frac{\mathcal{P}_H(\epsilon_L + w_H + 2\sqrt{\epsilon_L w_H} \cos \theta_L, A_H)}{(\epsilon_L + w_H + 2\sqrt{\epsilon_L w_H} \cos \theta_L)^{1/2}} dA_T, \end{aligned} \quad (3)$$

where  $\psi_L$  and  $\psi_H$  are the mass distributions of the light and heavy fragments and  $\alpha_i = \int_{A_{1i}}^{A_{2i}} \psi_i(A_i) dA_i$  ( $i=L, H$ ).

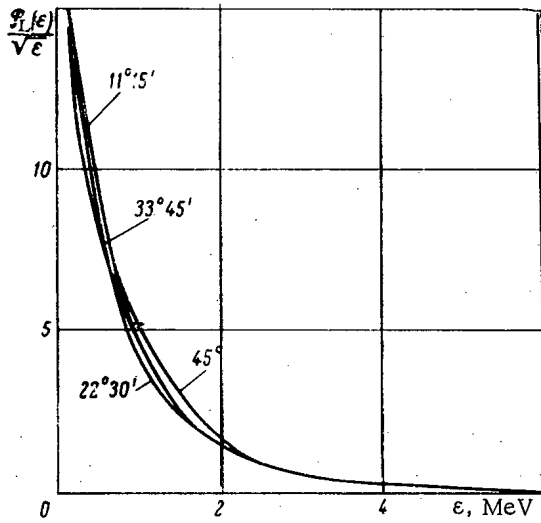


Fig. 1. Neutron spectra of the light fragment in the c.m.s.

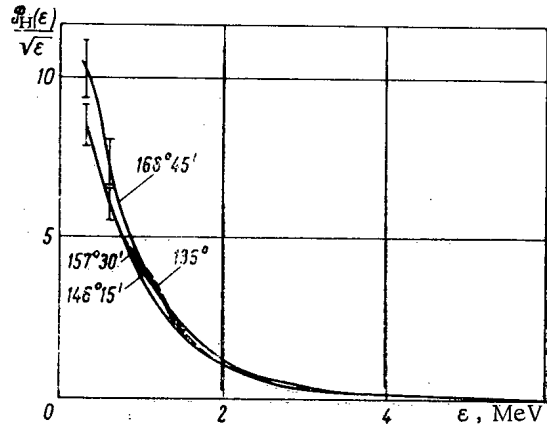


Fig. 2. Neutron spectra of the heavy fragment in the c.m.s.

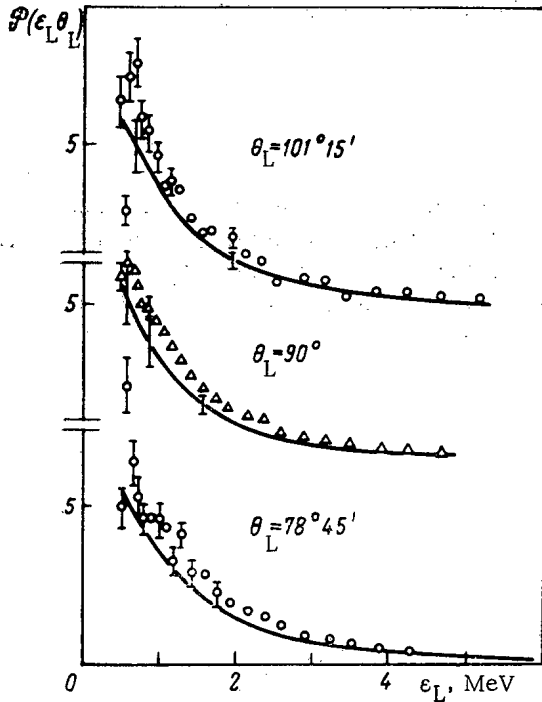


Fig. 3. Neutron spectra of light fragment in the laboratory system of coordinates.

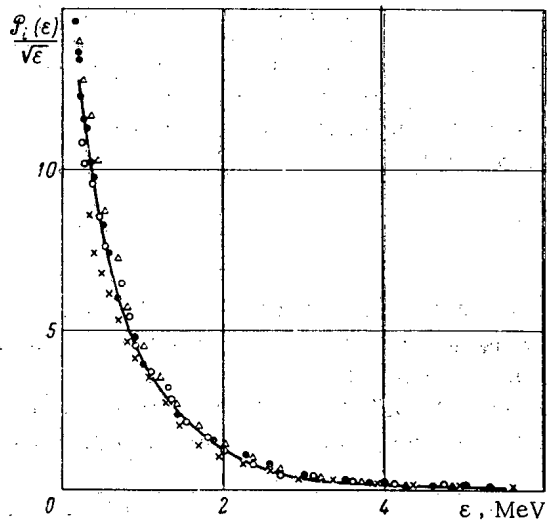


Fig. 4. Comparison between the neutron spectra of the light and heavy fragments in the c.m.s. and calculated results based on the statistical theory of the nucleus:  $\circ, \ominus$  light fragments;  $\Delta, \times$  heavy fragments.

The functions  $\psi_i/\alpha_i$  form sharp peaks around the most probable values of the masses of the light and heavy fragments. Replacing these by  $\delta$  functions, we obtain

$$\begin{aligned}
 \rho(\epsilon_L, \theta_L) \approx & \sqrt{\epsilon_L} \left[ \frac{\rho_L(\epsilon_L + \bar{w}_L - 2\sqrt{\epsilon_L \bar{w}_L} \cos \theta_L, \bar{A}_L)}{(\epsilon_L + \bar{w}_L - 2\sqrt{\epsilon_L \bar{w}_L} \cos \theta_L)^{1/2}} \right. \\
 & \left. + \frac{\rho_H(\epsilon_L + \bar{w}_H + 2\sqrt{\epsilon_L \bar{w}_H} \cos \theta_L, \bar{A}_H)}{(\epsilon_L + \bar{w}_H + 2\sqrt{\epsilon_L \bar{w}_H} \cos \theta_L)^{1/2}} \right], \quad (4)
 \end{aligned}$$

where  $\bar{w}_L = 1.02$  MeV,  $\bar{w}_H = 0.58$  MeV [1]. By comparing (4) with the experimental data of [1] we can find functions  $\rho_L(\epsilon, A_L)/\sqrt{\epsilon}$  and  $\rho_H(\epsilon, A_H)/\sqrt{\epsilon}$ , i.e., reduce the neutron spectra to the c.m.s. of each of the fragments. Let  $\theta_L = 0$ ,  $\epsilon_L = 1$  MeV; then the argument of the first term on the right-hand side of relation (4) is close to zero, and that of the second term equals  $\sim 3.2$  MeV. If we take account of the estimates made in [1], then this means that for  $\epsilon_L > 1$  MeV the contribution of the heavy fragment to the total spectrum may, to an accuracy of a few percent,



be neglected. This is also valid for  $\varepsilon_L > 1.5$  MeV in the angular range  $0 \cong \theta \cong 45^\circ$ . Analogously for  $\varepsilon_L > 1.5$  MeV and  $180^\circ \cong \theta \cong 135^\circ$  we may neglect the contribution of the light fragment to the total spectrum.

If it is justifiable to suppose that the neutron spectrum in the c.m.s. of a fragment is isotropic, then the functions  $\mathcal{P}_i(\varepsilon, \bar{A}_i)/\sqrt{\varepsilon}$  ( $i$  fixed) obtained from data at different angles should coincide. The function  $\mathcal{P}(\varepsilon, \bar{A}_L)/\sqrt{\varepsilon}$  was obtained from neutron spectra measured at angles  $\theta_L$  equal to  $11^\circ 15'$ ,  $22^\circ 30'$ ,  $33^\circ 45'$ , and  $45^\circ$ . The corresponding curves coincide within the limits of experimental and computing errors (Fig. 1). Figure 2 shows curves representing  $\mathcal{P}_H(\varepsilon, \bar{A}_H)/\sqrt{\varepsilon}$ ; these are obtained from data measured at angles  $\theta_L$  equal to  $135^\circ$ ,  $146^\circ 15'$ ,  $157^\circ 30'$ , and  $168^\circ 45'$ . All the curves coincide except the one corresponding to  $\theta_L = 168^\circ 45'$  (for  $\varepsilon < 1$  MeV this lies above the rest). The deviation of this curve from the others, however, passes insignificantly outside the experimental and computing errors.

Transforming the neutron spectra of the light and heavy fragments given in Fig. 1 and 2 from the c.m.s. to the laboratory system of coordinates and comparing the calculated spectra with the experimental, measured at angles  $\theta_L$  in the neighborhood of  $90^\circ$ , we are easily convinced that the deviation of the computed spectra from the experimental lies practically within the limits of experimental and computing errors (Fig. 3). Thus we may conclude that in the c.m.s. of the light and heavy fragments the neutron spectra are isotropic within 10 to 15%.

It is interesting to compare the reduced neutron spectra of the light and heavy fragments with each other and with calculated data based on the statistical theory of the nucleus.

Figure 4 presents the spectra of the light and heavy fragments; we see that the spectra coincide to a high accuracy. Since they are normalized to the same number of fissions [1], this means that the light and heavy fragments on average emit the same number of neutrons. The continuous line shown in Fig. 4 was obtained from Le Couteur's formula [2]

$$\frac{P(\varepsilon)}{\sqrt{\varepsilon}} \approx B \exp \left\{ -\frac{\varepsilon}{\tau^*} \right\}, \quad B = \text{const.} \quad (5)$$

This gives the cascade neutron spectrum, valid for initial excitation energies of the fragments exceeding twice the binding energy and for a cross section, corresponding to the formation of the compound nucleus from neutron and fragment, independent of the neutron energy. In order to make equation (5) agree with the spectra shown in Fig. 4, we must choose  $\tau^* = 0.72$  MeV. It follows that, if Cameron's formula [3] for the binding energy is correct, the light and heavy fragments have excitation energies 15.4 and 13.9 MeV respectively.

#### LITERATURE CITED

1. Bowman et al., Phys. Rev., 126, 2120 (1962).
2. K. Le Couteur, Proc. Phys. Soc., 65, 718 (1962).
3. Cameron, Canad. J. Phys., 35, 1021 (1957).

PRODUCTION OF  $Al^{26}$  ON IRRADIATING MAGNESIUM  
WITH 20 MeV DEUTERONS

(UDC 539.172:13)

N. N. Krasnov, P. P. Dmitriev, Yu. G. Sevast'yanov,  
and A. S. Bezmaternykh

Translated from Atomnaya Énergiya, Vol. 19, No. 1,  
pp. 62-63, July, 1965  
Original article submitted July 20, 1964

The only long-living radioactive isotope of aluminum was discovered in 1954 [1]. Its half-life period is  $\sim 8 \cdot 10^5$  years, so that obtaining significant activity of  $Al^{26}$  presents certain difficulties.

In order to obtain great activity of  $Al^{26}$  the most productive are the following two methods: 1) irradiation of magnesium with deuterons, using reactions  $Mg^{25}(d, n)Al^{26}$  and  $Mg^{26}(d, 2n)Al^{26}$ , and 2) irradiation of aluminum with protons, using the reactions  $Al^{27}(p, pn)Al^{26}$  and  $Al^{27}(p, 2n)Si^{26} \rightarrow Al^{26}$ . The authors studied the first method, which enables  $Al^{26}$  with a higher specific activity to be obtained than with the second. Moreover, in this case the isotope  $Na^{22}$ , which has wide practical application, is formed at the same time as the  $Al^{26}$ .

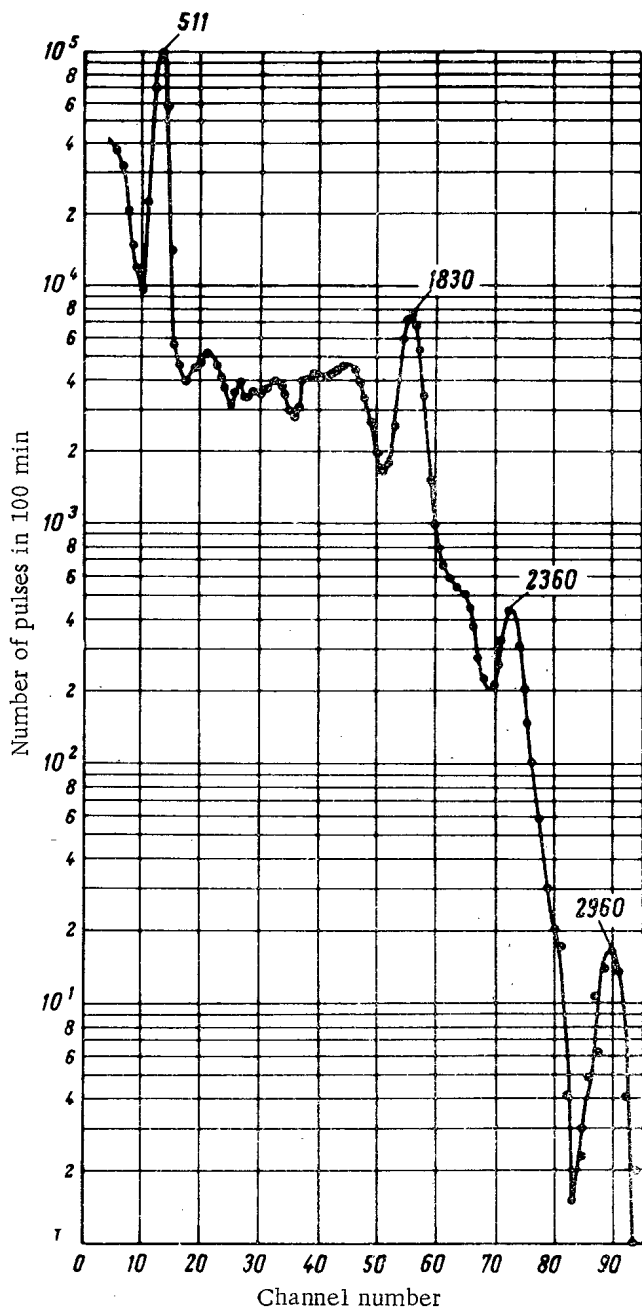
The irradiation was effected on the 1.5 m cyclotron of the Physico-Power Institute of the State Committee for the Use of Atomic Energy, USSR, with a deuteron energy of 20 MeV and beam current 300  $\mu A$ . A rotating target with a head in the form of a hemisphere made of MA8-type magnesium was used; the diameter of the head was 90 mm. Below we give the chemical composition of the MA8 magnesium.

The total current to the target was 12 000  $\mu A \cdot h$ . The target was dissolved in hydrochloric acid. The characteristics of the working solution were: volume 500 ml, Mg concentration 75 mg/mliter, acidity with respect to HCl 0.1 N.

The method of separating radiochemically-pure aluminum included the following stages:

- 1) precipitation of aluminum hydroxide by dilute ammonia with methyl-red indicator [2];
- 2) obtaining soluble aluminates on addition of 10% NaOH with subsequent introduction of precipitable alkali "back carriers":  $Fe^{-3}$ ,  $La^{-3}$ ,  $Y^{-3}$  (5 mg each) [3];
- 3) purification with anion exchanger Dowex 1X8 on passing 8N HCl solution with "back carriers"  $Co^{-2}$ ,  $Cu^{-2}$ ,  $Zn^{-2}$  (5 mg each) introduced into it through the resin [4];
- 4) displacer chromatography in cation exchanger Dowex 50X8 on desorption of hydrochloric acid of various concentrations (0.5, 1.0, 2.0 N) [5]; aluminum fraction collected on washing out 2.0 N HCl.

Com- po- nent	Mg	Mn	Ce	Al	Zn	Si	Fe	Cu	Be
Con- tent, %	97- 98	1,5- 2,5	0,15- 0,55	0,3- 0,3	0,15	0,05	0,05	0,05	0,02



Gamma spectrum of  $\text{Al}^{26}$  obtained on a scintillation spectrometer.

At all stages of purification, the discarded solutions were analyzed for aluminum content by a colorimetric method by means of aluminone [2]. The  $\text{Al}^{26}$  so obtained in the form of  $\text{AlCl}_3$  solution was concentrated to a volume of 2 mliters. The losses of  $\text{Al}^{26}$  in separation were 25 to 30%. The coefficient of purification from  $\text{Na}^{22}$  was not smaller than  $10^8$ .

The figure shows the  $\gamma$ -spectrum of  $\text{Al}^{26}$  taken on a scintillation  $\gamma$ -spectrometer with a  $\text{NaI(Tl)}$  crystal. Marked on the spectrum are the main  $\gamma$ -lines of  $\text{Al}^{26}$ : 511 keV (annihilation radiation), 1830 keV, 2960 keV, and also an addition peak of the  $\gamma$ -lines 511 and 1830 keV, corresponding to energy 2350 keV. A detailed description of the  $\gamma$ -spectrum of  $\text{Al}^{26}$  obtained on the scintillation spectrometer is given in [6], where the energy and origin of the apparatus peaks observed between the 511- and 1830-keV  $\gamma$ -lines are indicated. (The values of  $\gamma$ -line energy given in the figure are taken from this paper).

The activity of the  $\text{Al}^{26}$  source was measured in two ways: 1) by comparing the intensities of the 511-keV  $\gamma$ -lines of  $\text{Al}^{26}$  and a calibrated  $\text{Na}^{22}$  source; 2) by comparing the intensities of the 1830-keV  $\gamma$ -lines of  $\text{Al}^{26}$  and a calibrated  $\text{Y}^{88}$  source.

The volumes of the  $\text{Na}^{22}$  and  $\text{Y}^{88}$  solutions and the shapes of the vessels were the same as for the  $\text{Al}^{26}$ . Their activities differed from that of  $\text{Al}^{26}$  by not more than two or three times. The activity of the  $\text{Al}^{26}$  measured by the first method was  $(0.0193 \pm 0.002) \mu\text{Ci}$  and by the second  $(0.0187 \pm 0.002) \mu\text{Ci}$ . Allowing for the radiochemical losses, the yield of  $\text{Al}^{26}$  at  $E_\alpha = 20 \text{ MeV}$  will equal  $(2.24 \pm 0.8) \cdot 10^6 \mu\text{Ci}/\mu\text{A} \cdot \text{h}$ , or  $5 \pm 1.7$  disintegrations/ $\text{min} \cdot \mu\text{A} \cdot \text{h}$ . The error in determining the yield ( $\sim 30\%$ ) is due to the errors in measuring the  $\mu\text{A} \cdot \text{h}$ , the activity of the  $\text{Al}^{26}$ , and the loss of  $\text{Al}^{26}$  in the separation process. For comparison we note that the  $\text{Al}^{26}$  yield at  $E_\alpha = 15 \text{ MeV}$  in [6] was  $1.4 \pm 0.13$  disintegrations/ $\text{min} \cdot \mu\text{A} \cdot \text{h}$ .

The authors are grateful to Z. P. Dmitriev for making the spectrometer measurements.

#### LITERATURE CITED

1. J. Simonton et al., *Phys. Rev.*, **96**, 1711 (1954).
2. E. V. Alekseevskii et al., *Quantitative Analysis* [in Russian], Moscow-Leningrad, Goskhimizdat (1953).
3. V. F. Gillebrandt et al., *Practical Handbook on Inorganic Analysis* [in Russian], Moscow, Goskhimizdat (1960).
4. K. Kraus and G. Moore, *J. Amer. Chem. Soc.*, **75**, 1460 (1953).
5. F. Strelow, *Anal. Chem.*, **33**, 542 (1961).
6. T. Kohman et al., *Aluminum-26. Proceedings of the International Conference on Radioisotopes in Scientific Research. Band 1, Paris (1957).*

SEPARATION OF  $\text{Na}^{22}$  FROM A MAGNESIUM  
TARGET IRRADIATED BY DEUTERONS

(UDC 541.15)

Yu. G. Sevast'yanov and A. S. Bezmaternykh

Translated from *Atomnaya Énergiya*, Vol. 19, No. 1,  
pp. 63-64, July, 1965

Original article submitted August 14, 1964

The separation of radioactive  $\text{Na}^{22}$  from a cyclotron-irradiated high-efficiency industrial-magnesium target [1] is associated with the removal of large quantities ( $\sim 50$  g) of magnesium. The usual ion-exchanger methods of separating  $\text{Na}^{22}$  from magnesium with this magnesium content requires considerable volumes (tens of liters) of washing solutions and occupies considerable time. One method proposed is to eliminate the main bulk of the magnesium (94 to 97%) by precipitating as magnesium sulfate from aqueous-acetone solutions. Subsequent purification of the  $\text{Na}^{22}$  from magnesium is effected by ion exchange.

At the present time radioactive  $\text{Na}^{22}$  is obtained by irradiating a magnesium target with deuterons accelerated in a cyclotron, using the nuclear reaction  $\text{Mg}^{24}(\text{d}, \alpha)\text{Na}^{22}$ . There are several papers on the separation of  $\text{Na}^{22}$  from irradiated magnesium without a carrier. In [2], the separation of  $\text{Na}^{22}$  and magnesium is effected by precipitating  $\text{Mg}(\text{NH}_4)_4(\text{CO}_3)_2 \cdot 4\text{H}_2\text{O}$ , which does not capture the  $\text{Na}^{22}$ . Another method [3] is based on the precipitation of the magnesium as  $\text{Mg}(\text{OH})_2$  by gaseous ammonia. In the majority of papers [4, 5],  $\text{Na}^{22}$  is separated from magnesium by ion exchange. Studies had to be made in order to elucidate the possibility of using these methods in the chemical treatment of targets in the 1.5 m cyclotron of the Physico-Power Institute [6].

In the present investigation, we used a rotating target with a head of hemispherical shape made of alloy MA8. The diameter of the head was 90 mm. The composition of alloy MA8 (balance Mg) was:

Com- po- nent	Mn	Ce	Al	Zn	Cu	Be	Ni	Si	Fe	Others
Con- tent, %	1.5- 2.5	0.15- 0.35	0.3	0.3	0.05	0.02	0.01	0.15	0.05	0.3

The irradiation was effected on the inner beam of the cyclotron with deuteron energy 20 MeV at current 300  $\mu\text{A}$ . The area of irradiation was  $\sim 50$  to 70  $\text{cm}^2$ . Experiments on the dissolution of alloy MA8 in various acids showed sulfuric acid to be the most appropriate. In fact, use of any of the known methods [2-5] of separating  $\text{Na}^{22}$  from magnesium requires a minimum concentration of free acid. In such conditions, the possible hydrolysis of magnesium salts leads to hydrolysis of manganese salts, the residue of which may capture considerable quantities (up to 10 or 15%) of  $\text{Na}^{22}$ . The hydrolysis of solutions of magnesium sulfate is insignificant, and by dissolving the magnesium target made from MA8 alloy in sulfuric acid we can obtain stable solutions with magnesium concentration 60 to 70 mg/mliter at  $\text{pH} = 2$  to 3.

Dissolution of the irradiated targets showed that, for a quantitative (95 to 98%) recording of the activity of  $\text{Na}^{22}$ , practically complete dissolution of the magnesium target (40 to 70 g dissolved magnesium) was needed. Use of the generally-accepted ion-exchange method for separating the  $\text{Na}^{22}$  from the magnesium with such quantities

of the latter leads to considerable volumes (tens of liters) of eluting solutions and a long-drawn-out experiment. Thus, for example, in separating  $\text{Na}^{22}$  from 1 g of irradiated magnesium, the total volume of the eluting solution of 0.1 N HCl was  $\sim 1.5$  liter for a washing rate of 1.2 to 1.5 mliter/min. It is therefore desirable to study suitable methods for eliminating the main quantity of dissolved magnesium.

Experiments were made on model solutions of magnesium sulfate obtained by dissolving MA8 alloy in sulfuric acid with magnesium concentration 60 to 70 mg/mliter (pH = 2 to 3). The magnesium content was determined by complexometric titration, and the amount of  $\text{Na}^{22}$  introduced was found by measurement with an end-window counter and scintillation spectrometer. Attempts to remove the main bulk of the magnesium by the methods of [2, 3] gave no positive results. As shown by the experimental data, the completeness of the precipitation of magnesium in the form of  $\text{Mg}(\text{OH})_2$  [3] is insufficient; washing  $\text{Na}^{22}$  out from the residue of  $(\text{NH}_4)_2\text{Mg}(\text{CO}_3)_2 \cdot 4\text{H}_2\text{O}$  requires large volumes of washing water. Subsequent purification of the  $\text{Na}^{22}$  from magnesium is complicated by the large content of ammonium salts. Moreover, the presence of a considerable amount of  $\text{Mn}^{2+}$  in solution hinders the precipitation of  $\text{Mg}(\text{OH})_2$  or  $(\text{NH}_4)_2\text{Mg}(\text{CO}_3)_2 \cdot 4\text{H}_2\text{O}$ . It is known that magnesium sulfate is insoluble in acetone. Bearing this in mind, experiments were made to find the optimum conditions for precipitating magnesium sulfate from water-acetone mixtures. The results of the experiment are given below and in the table.

Volumetric ratio of aqueous phase and acetone	1 : 0,5	1 : 1	1 : 1,5	1 : 2
Amount of magnesium remaining in solution, % of original	10	5-8	2-3	1

It follows from the data presented that for a selected ratio between the aqueous and organic phases (1 : 1.5) the solution is significantly freed from magnesium. A larger ratio of the acetone to the water phase somewhat increases the percentage removal of magnesium in the form of  $\text{MgSO}_4$ , but leads to the formation of a poorly filtering residue. The capture of  $\text{Na}^{22}$  by the magnesium sulfate residue (see table) precipitating on addition of acetone reaches 20%; subsequent reprecipitation of the residue, however, leads to almost complete washing out of the  $\text{Na}^{22}$ .

In final form, the method of separating  $\text{Na}^{22}$  without a carrier reduces to the following. The previously-weighed magnesium target was dissolved in dilute sulfuric acid. The acid was poured gradually and the loss in activity of the target monitored. The solution (volume 500 to 600 mliter, with magnesium concentration 60 to 70 mg/mliter, pH = 2 to 3) was filtered through a Schott No. 1 filter and placed in an apparatus analogous to that described in [7], furnished with a mechanical agitator and a Schott No. 1 filter sealed to the bottom. Into the apparatus was poured 900 mliter of acetone, and the precipitated pulp of  $\text{MgSO}_4$  residue was stirred for 15 to 20 min. The magnesium sulfate residue was filtered off, dissolved in a minimum amount of hot water ( $\sim 400$  mliter), and the operation of precipitation repeated. The united first and second water-acetone filtrates (2300 to 2400 mliter) were passed through an ion-exchange column with Dowex 50X8 resin (100 to 200 mesh) of diameter 1.5 cm and

Data on the Precipitation of Magnesium Sulfate from Water-Acetone Mixtures

Concen. of magnesium in original solution, mg/liter	Volume of original aqueous solution, mliter	Distribution of magnesium, % of original			Distribution of $\text{Na}^{22}$ , % of original			Total volume of water-acetone filtrate, mliter
		first filtrate	second filtrate	first and second filtrates	first filtrate	second filtrate	residue (reject) $\text{MgSO}_4$	
34	225	2.2	0.8	3.0	88.5	9.5	2.0	900
34	290	1.5	1.4	2.9	86.0	13.0	1.5	1100
49	180	1.0	1.5	2.5	80.5	18.0	1.5	700
62	125	1.4	1.6	3.0	87.0	11.5	1.5	500
62	135	1.8	0.6	2.4	79.5	19.0	2.0	550

height 50 cm at a rate of 1.5 to 2.0 mliter/min. (from the zero fraction acetone suitable for subsequent precipitations may be distilled in quantity up to 70% of the original amount). The desorption of  $\text{Na}^{22}$  was effected by 0.1 N HCl at a rate of 1.0 to 1.5 mliter/min in a volume 500 to 600 mliter. The eluent containing  $\text{Na}^{22}$  was carefully concentrated in a quartz flask in a water bath and treated with concentrated  $\text{HNO}_3$  to remove organic impurities. The excess nitric acid was removed by repeated evaporation with water; the resultant weakly acid solution (pH = 2) was the final product. The concentration of  $\text{Na}^{22}$  activity was 0.3  $\mu\text{Ci/mliter}$ ; the magnesium content in this was  $\leq 1 \mu\text{g/mliter}$ ; the radiochemical purity was greater than 99% and the yield 95 to 97%. The method was tested on a magnesium target with activity 50 mg-equiv- $\text{Na}^{22}$ .

The authors express thanks to P. P. Dmitriev for help and consultation in carrying out the radiometrical measurements, and also to B. S. Kir'yanov and V. P. Sharov for taking part in discussion of the results.

#### LITERATURE CITED

1. N. N. Krasnov, N. A. Konyakhin, and V. M. Tuev, "Pribory i tekhnika éksperimenta" (in press).
2. J. Irvine and K. Clarke, J. Chem. Phys., 16, 686 (1948).
3. I. Grúverman and P. Kruger, Internat. J. Appl. Radiation and Isotopes, 5, 21 (1959).
4. V. Linnenbom, J. Chem. Phys., 20, 1637 (1952).
5. I. Inorg. and Nucl. Chem., 16, 356 (1960).
6. N. N. Krasnov et al., "Pribory i tekhnika éksperimenta" (in press).
7. S. A. Grachev et al., "Radiokhimiya," 3, 116 (1961).

INTERNATIONAL COMPARISONS OF THE SPECIFIC ACTIVITIES OF  $P^{32}$ ,  $Co^{60}$ ,  
AND  $Tl^{204}$  SOLUTIONS AND OF THE ACTIVITY OF "SOLID"  $Co^{60}$  SOURCES

(UDC 539.16.08)

A. A. Konstantinov, V. V. Perepelkin, and A. E. Kochin

Translated from *Atomnaya Énergiya*, Vol. 19, No. 1,

pp. 65-67, July, 1965

Original article submitted July 9, 1964; revised form January 21, 1965

International comparisons to determine the activity of various radioactive sources, carried out in accordance with the program of the International Bureau of Weights and Measures, have been recommended by the International Commission for Radiological Units and Measurements to the national metrological laboratories which use radioactive standards.

Examination of the data from international comparisons allows one to establish the reliability of methods used for standardization and to check the accuracy and prevalence of the various methods. Further, international comparisons make it possible to compare conditions (for example,  $\gamma$  and  $\beta$  background) and parameters of the equipment used in the different national laboratories. International comparisons are an objective check on the work of the national laboratories in the standardization of various radioactive sources.

The D. I. Mendeleev All-Union Scientific Research Institute of Metrology (VNIIM) first participated in international comparisons of radioactive sources in January 1961, and by May 1963 had participated in four international comparisons to determine the specific activities of  $P^{32}$ ,  $Co^{60}$ ,  $Tl^{204}$ , and  $Co^{60}$  solutions. At this same institute international comparisons were made of the activities of "solid"  $Co^{60}$  sources, i.e., specially prepared sources of  $Co^{60}$  on thin films. In determining the specific activities of  $P^{32}$  and  $Tl^{204}$  solutions, the absolute  $\beta$ -counting method employing a  $4\pi$  proportional counter was used. In determining the specific activity of  $Co^{60}$  solutions, the  $4\pi$  counting and  $4\pi$   $\beta$ - $\gamma$  coincidence methods were used. In determining the activity of "solid"  $Co^{60}$  sources, the  $4\pi$   $\beta$ - $\gamma$  and  $\beta$ - $\gamma$  coincidence methods were used.

In the international comparisons which were carried out in January 1961, 12 countries participated; some countries such as England, Canada, France, and West Germany were represented by two laboratories [1]. All the national laboratories used the  $4\pi$  counting method for the comparison; in addition,  $4\pi$  proportional counting was used in many laboratories, and only in the French laboratories was  $4\pi$  Geiger-Muller counting used. The prominent national laboratories NPL (England) and PTB (West Germany) also used ionization chambers in addition to  $4\pi$  proportional counting. Some national laboratories used liquid and plastic scintillation counting to duplicate the  $4\pi$  counting.

While this comparison was being carried out, the  $4\pi$  proportional counter with fixed gas pressure [2] which was used at VNIIM was checked out. Since  $P^{32}$  has a "hard" spectrum with a maximum energy of 1.7 MeV, the corrections for self-absorption and for absorption of  $\beta$  particles in the film are very small and do not contribute a significant error to the measurements that are obtained. The specific activity we found for the  $P^{32}$  solution, 10.79  $\mu$ Ci/g, agreed almost exactly with the average value for all countries (10.76  $\mu$ Ci/g) and was in good agreement with the results of the leading national laboratories [1]. The deviation of our result from the average was 0.03% (Fig. 1).

The next international comparison in which VNIIM participated was carried out in January 1962. In it, 21 laboratories from 18 countries participated.  $Co^{60}$  was selected as the nuclide whose specific activity in solution it was necessary to determine. The measurement of this  $\beta$  emitter with great accuracy by the  $4\pi$  counting method is accompanied by great difficulty because of the low endpoint energy of the  $\beta$  spectrum (0.306 MeV). Because of the difficulty in accurately determining the self-absorption of  $Co^{60}$   $\beta$  particles, the  $4\pi$  counting method was used by only six of the national laboratories [3]. Because of its convenient decay scheme, this nuclide can be measured

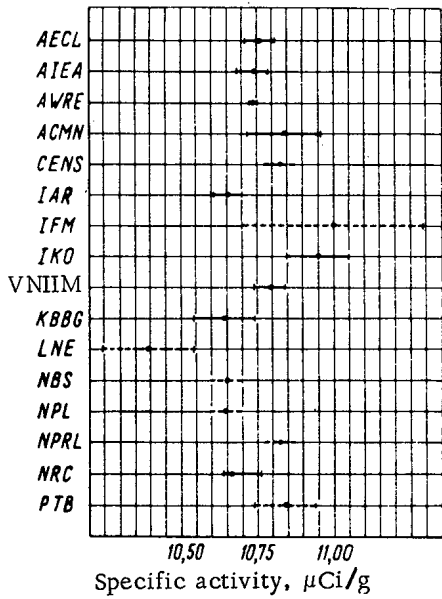


Fig. 1. Results of international comparison of the specific activity of P<sup>32</sup> solution (January 1961).

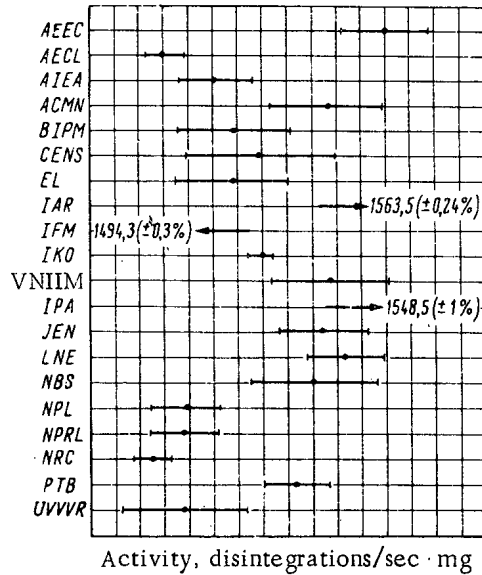


Fig. 2. Results of international comparison of the specific activity of Co<sup>60</sup> solution (March-April 1963).

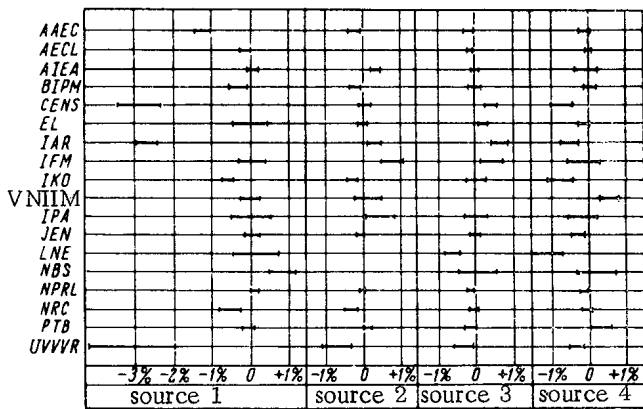


Fig. 3. Results of international comparison of the activity of "solid" Co<sup>60</sup> sources (March-April, 1963).

very accurately by the coincidence method. The result obtained at VNIIM by the 4π counting method, 4.700 μCi/g, was in complete agreement with the result obtained by the 4π β-γ coincidence method, and was in good agreement with the overall average value for the results of all the national laboratories (4.699 μCi/g [3]). The deviation of our result from the average was 0.02%.

In May 1962, VNIIM participated in international comparisons to determine the specific activity of a Tl<sup>204</sup> solution [4]. In these comparisons, 21 laboratories from 18 countries participated. Our determination of the specific activity of Tl<sup>204</sup> solution gave somewhat different results for two ampoules: 100.4 and 101.3 μCi/g. However, the average value of 100.9 μCi/g was in good agreement with the overall average value for all the laboratories (101.4 μCi/g [4]); the deviation of our result from the average was 0.5%.

Realizing the special interest of the national metrological laboratories in accurate measurements of the activity of Co<sup>60</sup> sources, the International Bureau of Weights and Measures carried out two more comparisons at the beginning of 1963. To eliminate errors which might arise from the preparation of sources from solutions, comparison was made not only for Co<sup>60</sup> solutions but also for "solid" Co<sup>60</sup> sources which were prepared on backing made of metallized thin films. In these comparison, 20 laboratories from 17 countries participated [5]. The activity of the Co<sup>60</sup> sources was measured at VNIIM by the 4π β-γ and the β-γ coincidence methods. The deviation of the value for the specific activity of Co<sup>60</sup> solutions obtained at VNIIM in 1963 from the average for all laboratories was 0.23% [5] (Fig. 2).

For solid Co<sup>60</sup> sources, the deviations (Fig. 3) were: 0.02% for source 1 (No. 51811, high activity, covered on both sides with film); 0.15% for source 2 (No. 5203, medium activity); and 0.5% for source 4 (No. 5173, low activity). It is clear that the deviation of our results did not exceed 0.25%. Source 4 was an exception; the deviation of its results, 0.5%, is explained by the large γ background in the VNIIM laboratory room where the international comparison were performed, because accuracy in the determination of activity for weak sources strongly depends on the magnitude of the γ background.



Examination of the results of international comparisons and of the results for determinations of the activity of one and the same source by two independent methods ( $4\pi$  counting method [6] and coincidence method) makes it possible to estimate the systematic error of each method, which did not exceed 0.1% for the measuring equipment at VNIIM.

List of Laboratories Participating in International Comparisons

AAEC—Australian Atomic Energy Commission, Lucas Heights, Australia.  
 AECL—Atomic Energy of Canada, Ltd., Chalk River, Ontario, Canada.  
 AEE—Atomic Energy Directorate, Bombay, India.  
 IAEA—International Agency for Atomic Energy, Vienna, Austria.  
 AWRÉ—Atomic Weapons Research Establishment, Aldermaston, England.  
 BCMN—Central Bureau for Nuclear Research, Geel, Belgium.  
 BIPM—International Bureau of Weights and Measures, Sevres, France.  
 CENS—Center for Nuclear Research, Saclay, France.  
 CFN—Center for Nuclear Physics, Lisbon, Portugal.  
 DAECRE—Research Institute of the Danish Atomic Energy Commission, Riso, Denmark.  
 EL—Electrotechnical Laboratory, Tokio, Japan.  
 GWI—Gustav Werner Institute of Radiochemistry, Uppsala, Sweden.  
 IAR—Institute of Applied Radioactivity, Leipzig, East Germany.  
 IFM—Institute of Physics and Mathematics, Santiago, Chile.  
 IKO—Scientific Research Institute for Nuclear Physics, Amsterdam, Holland.  
 VNIIM—D. I. Mendeleev All-Union Scientific Research Institute of Metrology, Leningrad, USSR.  
 IPA—Institute of Atomic Physics, Bucharest, Rumania.  
 IR—Radium Institute, Vienna, Austria.  
 IRK—Institute of Radioactivity and Nuclear Physics, Vienna, Austria.  
 IRPAR—Institute for the Investigation, Production, and Application of Radioactive Isotopes, Prague, Czechoslovakia.  
 JEN—Atomic Energy Council, Madrid, Spain.  
 KBBG—Society for the Construction and Operation of Nuclear Reactors, Karlsruhe, West Germany.  
 LNE—National Testing Laboratory, Paris, France.  
 NBS—National Bureau of Standards, Washington, USA  
 NPL—National Physical Laboratory, Teddington, England.  
 NPRL—National Physical Research Laboratory, Pretoria, South Africa.  
 NRC—National Research Council, Ontario, Canada.  
 PTB—Federal Physico-Technical Institute, Braunschweig, West Germany.  
 UVVVR—see IRPAR.

LITERATURE CITED

1. Bureau International des Poids et Mesures. Resultats de la Comparaison du Phosphore 32, Comite International des Poids et Mesures, Paris, Gauthier—Vilars (1963).

2. A. A. Konstantinov, Trudy VNIIM, 30, 90 (1957).
3. A. Kotchine, Rapport sur la comparaison internationale du cobalt 60, Comite international des poids et mesures, Paris (1963).
4. I. Roy and L. Cavallo, Rapport sur la comparaison international du thallium 204. Comite international des poids et mesures. Paris (1963).
5. A. Rytz and I. Roy, Rapport Preliminaire sur la comparaison international de la methode  $4\pi\beta\text{-}\gamma$  (PC), au moyen du  $^{60}\text{Co}$ , Pavillon de Breteuil Sevres, France (1963).
6. A. A. Konstantinov and A. E. Kochin, Trudy institutov Goskomiteta standartov, mer i izmeritel'nykh priborov pri SM SSSR, No. 69 (129), Moscow, Standartgiz (1962), p. 13.

## ASYMPTOTIC FORM OF THE SCATTERING LAW FOR SLOW NEUTRONS

(UDC 539.121.7)

L. V. Maiorov

Translated from *Atomnaya Énergiya*, Vol. 19, No. 1,  
pp. 67-69, July, 1965  
Original article submitted June 15, 1964

The asymptotic behavior of the slow neutron scattering law [1]  $S(\alpha, \beta)$  for large  $\alpha$  has been investigated [1-3]. An asymptotic formula was obtained in [2] which did not satisfy the principle of detailed balance but which had a clear physical significance (scattering in a free gas). The asymptotic formula obtained in [1], on the other hand, satisfied the principle of detailed balance, but, as noted in [4], did not have so clear a physical meaning. Naturally, both formulas differ from one another, and also from the asymptotic expansion obtained in [3] by means of the method of steepest descent.

Since there was no discussion in the published literature as to the region of the  $\alpha, \beta$  plane in which these expansions are valid and in what sense they differ from one another, we shall derive a general asymptotic formula for the slow neutron scattering law which is valid in the entire  $\alpha, \beta$  plane and which is applicable to a number of other physical problems, a review of which can be found in [2], for example. In addition, all the well known expansions [1-3] can be obtained as particular cases of the general asymptotic formula. Limits of the remainder terms of the expansion are also presented; previously, these were not given or were incorrect [2].

General asymptotic formula for the scattering law. In the noncoherent Gaussian approximation, the scattering law for slow neutrons can be written in the form of an integral

$$S(\alpha, \beta) = \frac{1}{2\pi} e^{-\alpha\Delta\left(-\frac{i}{2}\right)} \int_{-\infty}^{\infty} e^{\alpha\Delta(t)} e^{i\beta t} dt. \quad (1)$$

Here the following notation is used:

$$\alpha = \frac{E_0 + E - 2 \cos \theta \sqrt{EE_0}}{MT}; \quad \beta = \frac{E_0 - E}{T};$$

$T$  is the temperature of the medium;  $M$  is the mass of the scattering atom;  $E_0$  and  $E$  are the initial and final neutron energies;  $\Delta(t)$  is expressed through the function  $p(\beta)$  introduced in [1] and characterizing the dynamic properties of the scattering medium by means of the relation

$$\Delta(t) = \int_{-\infty}^{\infty} f(\beta) e^{i\beta t} dt. \quad (2)$$

Further

$$f(\beta) = \frac{p(\beta)}{\beta^2}; \quad \Delta^{(n)}(i\tau) = (-i)^n \int_{-\infty}^{\infty} f(\beta) e^{\beta\tau} d\beta = (-i)^n f_n(\tau). \quad (2')$$

Following [3], we shift the contour of integration in (1) parallel to the axis by a distance  $\tau$  (in the following,  $\tau$  will be considered as an arbitrary parameter). Keeping (2) and (2') in mind, and making the obvious transfor-

mations, we obtain

$$S(\alpha, \beta) = \frac{e^{-\beta\tau}}{\sqrt{\alpha f_2(\tau)}} e^{-\alpha \left[ \Delta \left( -\frac{i}{2} \right) - \Delta(i\tau) \right]} \psi_\tau(\alpha, x), \quad (3)$$

where

$$x = \frac{\beta - \alpha f_1(\tau)}{\sqrt{\alpha f_2(\tau)}}, \quad (4)$$

$$\psi_\tau(\alpha, x) = \frac{1}{2\pi} \int_{-\infty}^{\infty} e^{\alpha \varphi \left( \frac{t}{\sqrt{\alpha f_2(\tau)}}, \tau \right)} e^{ixt} dt; \quad (5)$$

$$\varphi(t, \tau) = \Delta(t + i\tau) - \Delta(i\tau) - t\Delta'(i\tau). \quad (6)$$

In the appendix, it is shown that for an arbitrary scattering system different from an Einstein crystal (whose normal frequency spectrum can be represented as the sum of  $\delta$  functions), on the basis of the central limit theorem in Cramer's formulation, (see [5], p. 121), the asymptotic expansion

$$\int_{-\infty}^x \psi_\tau(\alpha, x) dx = \frac{1}{\sqrt{2\pi}} \int_0^x e^{-x^2/2} dx + e^{-x^2/2} \sum_{r=1}^{k-3} \frac{P_{3r-1}(\tau, x)}{\alpha^{r/2}} + R_k(\tau, \alpha, x), \quad (7)$$

is valid, where  $P_{3r-1}(x)$  is a polynomial of degree  $3r-1$  with respect to  $x$ ,  $k \geq 3$  and can be chosen as large as is convenient.

For  $R_k(\tau, \alpha, x)$  the limit

$$|R_k(\tau, \alpha, x)| \leq \frac{A_k(\tau)}{\alpha^{\frac{k-2}{2}}} \quad (8)$$

holds uniformly in  $x$ .

Differentiating (7) wrt.  $x$ , we obtain the general asymptotic formula for the scattering law in which  $\tau$  is an arbitrary parameter [6]:

$$\begin{aligned} S(\alpha, \beta) = S_\tau(\alpha, \beta) &\equiv \frac{e^{-\beta\tau}}{\sqrt{2\pi\alpha f_2(\tau)}} e^{-\alpha \left[ \Delta \left( -\frac{i}{2} \right) - \Delta(i\tau) \right]} \left\{ e^{-x^2/2} \right. \\ &\times \left[ 1 + \frac{g_3(\tau) H_1(x)}{3! [\alpha f_2(\tau)]^{1/2}} + \frac{1}{\alpha f_2(\tau)} \left( \frac{g_4(\tau) H_4(x)}{4!} \right. \right. \\ &+ \left. \left. \frac{10g_3^2(\tau) H_6(x)}{6!} \right) + \frac{1}{[\alpha f_2(\tau)]^{3/2}} \left( \frac{g_5(\tau) H_5(x)}{5!} \right. \right. \\ &\left. \left. + \frac{35}{7!} g_3(\tau) g_4(\tau) H_7(x) + \frac{280}{9!} g_3^3(\tau) H_9(x) \right) + \dots \right] + r_h(\tau, \alpha, x) \left. \right\}. \end{aligned} \quad (9)$$

Here,  $g_n(\tau) = f_n(\tau)/f_2(\tau)$ ;  $H_n(x)$  are Hermite polynomials;

$$r_h(\tau, \alpha, x) = \frac{d}{dx} R_h(\tau, \alpha, x).$$

If the scattering law has no singularities,  $r_k(\tau, \alpha, x)$  is uniformly bounded:

$$|r_k(\tau, \alpha, x)| \leq \frac{b_k(\tau)}{\alpha^{\frac{k-2}{2}}}. \quad (10)$$

However, the limit (10) is incorrect in the case of scattering by a crystal, for example, since a  $\delta$  function corresponding to elastic scattering enters into  $r_k(\tau, \alpha, x)$ . In this case, as in all such cases, the uniform limit (8) is valid.

We point out an important property of general asymptotic formula which reflects the symmetry of the scattering law (principle of detailed balance). Since  $g_n(\tau) = (-1)^n g_n(-\tau)$  and  $H_n(x) = (-1)^n H_n(-x)$ ,

$$S_\tau(\alpha, \beta) = S_{-\tau}(\alpha, -\beta). \quad (11)$$

Region of applicability of the general asymptotic formula. For arbitrary choice of  $\tau$ , formulas (9)-(11) are true for the entire plane. However, nontrivial information about the scattering law can be obtained from these formulas only in the situation where the expression  $r_k(\tau, \alpha, x)/e^{-x^2} \rightarrow 0$  when  $\alpha \rightarrow \infty$ , i.e., when the leading terms of the expansion decrease more slowly than the neglected ones. This requirement leads to the condition that  $x$  must remain bounded when  $\alpha \rightarrow \infty$ , namely:

$$|x| = \left| \frac{\beta - \alpha f_1(\tau)}{\sqrt{\alpha f_2(\tau)}} \right| \leq \varepsilon. \quad (12)$$

Here  $\tau$  determines the particular form of the general asymptotic formula, and  $\varepsilon$  is an assigned number which is as large as is convenient. The inequality (12) delineates a region in the  $\alpha, \beta$  plane which contracts to the line  $\beta/\alpha = f_1(\tau)$  for  $\alpha \rightarrow \infty$ . In addition, it is clear that the smaller  $\varepsilon$  is, the less the maximum of  $|r_k(\tau, \alpha, x)|$  is in the region  $|x| \leq \varepsilon$  (further, we always have  $|r_k| \leq b_k(\tau)/\alpha^{k-2/2}$ ). Thus, for a fixed number of terms, formula (9) becomes more exact with smaller  $\varepsilon$ .

Application of the asymptotic formula for calculating the scattering law. Let it be required to calculate the scattering law for sufficiently large  $\alpha$  along the lines  $|\beta|/\alpha = C$  is given. Find the root  $\tau_0$  of the equation  $f_1(\tau) = C$ . Then not only for the rays  $|\beta|/\alpha = C$  but for the entire region

$$|x| = \left| \frac{|\beta| - \alpha f_1(\tau_0)}{\sqrt{\alpha f_2(\tau_0)}} \right| \leq \varepsilon \quad (13)$$

(where  $\varepsilon$  is an arbitrary number) the asymptotic formula

$$S(\alpha, \beta) = \frac{e^{-|\beta|\tau_0}}{\sqrt{2\pi\alpha f_2(\tau_0)}} e^{-\alpha \left[ \Delta \left( -\frac{i}{2} \right) - \Delta(i\tau_0) \right]} \times \left\{ e^{-x^2/2} \left[ 1 + \frac{g_2(\tau_0) H_1(|x|)}{3! [\alpha f_2(\tau_0)]^{1/2}} + \dots \right] + r_k(\tau, \alpha, x) \right\}, \quad (14)$$

is valid, and the remainder term is bounded modulo by the function  $\xi_k(\varepsilon, \tau)/\alpha^{k-2/2}$  which depends only on  $\tau$  and  $\varepsilon$  [ $\xi_k \leq b_k(\tau)$ ]. The  $\beta$ -symmetric writing of formula (9) in the form (14) follows from relation (11) which is a consequence of the principle of detailed balance.

Special cases. 1. Putting  $\tau = 1/2$  in (13) and (14), we obtain an asymptotic expansion of the scattering law which agrees with the formula of Nelkin and Parks [2] for  $\beta > 0$  (for simplicity, we give here, and in the following, only the first term of the expansion):

$$S(\alpha, |\beta|) = \frac{e^{-|\beta|/2}}{\sqrt{2\pi\alpha f_2(\tau_0)}} \left\{ \exp \left[ -\frac{(|\beta| - \alpha)^2}{2\alpha f_2(1/2)} \right] + \frac{\xi_1(\alpha, \beta)}{\alpha^{1/2}} \right\}, \quad (15)$$

( $\xi_1 \leq b_1$ ).

Thus, (15) satisfies the principle of detailed balance, in contrast to the Nelkin-Parks formula. In addition, the correct limit for the remainder term in (14) differs from the limit given in [2].

2. When  $\tau = 0$ , the formula of [1] follows from (13) and (14):

$$S(\alpha, \beta) = \frac{e^{-\alpha \left[ \Delta \left( -\frac{i}{2} \right) - \Delta(0) \right]}}{\sqrt{2\pi\alpha f_2(0)}} \left( e^{-\beta^2/2} + \frac{\xi_1}{\alpha^{1/2}} \right), \quad (16)$$

$$|\xi_1| \leq b_1.$$

3. Taking an arbitrary value for  $\tau$  and setting  $\varepsilon = 0$  in (13), we obtain from (14) the Egelstaff-Schofield formula [3] which was formally derived by means of the method of steepest descent without the limit of the remainder term. Since  $H_{2n+1}(x) = 0$ , terms with fractional powers of  $\alpha$  vanish in (14) for  $\varepsilon = x = 0$ .

Following from what has been said above, all three special asymptotic expansions are valid in a region given by inequality (13) for the corresponding choice of  $\varepsilon$  (in the sense that they give nontrivial information about the scattering law in this region).

In conclusion, the author takes pleasure in expressing his gratitude to V. F. Turchin for a number of critical comments and for a discussion of the results and to O. B. Moskalev for his consideration of this work.

#### APPENDIX

The function  $\psi_\tau(\alpha, x)$  is positive. Its moments can be computed in the following manner:

$$\begin{aligned} \gamma_n &= \int_{-\infty}^{\infty} x^n \psi_\tau(\alpha, x) dx = i^n = \int_{-\infty}^{\infty} e^{\alpha \psi \left( \frac{t}{\sqrt{\alpha f_2(\tau)}}, \tau \right)} \delta^{(n)}(t) dt = \\ &= (-i)^n \left[ \exp \left\{ \alpha \psi \left( \frac{t}{\sqrt{\alpha f_2}}, \tau \right) \right\} \right]_{t=0}^{(n)}. \end{aligned} \quad A1$$

Since in accordance with (A1) all moments  $\gamma_n$  of the function  $\psi_\tau(\alpha, x)$  exist, then, in particular,  $\gamma_0 = 1$ ,

$\gamma_1 = 0$ , and  $\gamma_2 = 1$ . Therefore,  $\int_{-\infty}^x \psi_\tau dx$  satisfies the requirement which probability distribution functions must satisfy

in order that the central limit theorem of probability theory in Cramer's formulation (see [5], p. 121, theorem 30) be valid, from which it follows that the asymptotic expansion (7) with remainder term limit (8) is true in the case where the characteristic function  $e^\phi$  is such that

$$\lim_{|t| \rightarrow \infty} e^\Phi < 1. \quad A2$$

It follows from (6) that inequality (A2) can be violated only in the situation where  $f(\varepsilon)$  is represented by a sum of  $\delta$  functions of the form  $\delta(\varepsilon - \varepsilon_i)$ , i.e., for an Einstein crystal (or more precisely, for a scatterer with optical vibrations not smeared out in energy).

#### LITERATURE CITED

1. P. Egelstaff, Proc. Simp. Vienna (1960), p. 25.
2. M. Nelkin and D. Parks, Phys. Rev., 119, 1060 (1960).
3. P. Egelstaff and P. Schofield, Nucl. Sci. Engng, 12, 260 (1962).
4. Kh. Purokhit, In Neutron Thermalization [in Russian] Moscow, Atomizdat (1964).
5. H. Cramer, Random Variables and Probability Distributions [Russian translation], Moscow, Izd-vo inostr. lit., (1947).
6. H. Cramer, Mathematical Methods of Statistics [Russian translation], Moscow Izd-vo inostr. lit. (1948).

PHYSICAL CHARACTERISTICS OF A CRITICAL ASSEMBLY  
WITH BERYLLIUM OXIDE MODERATOR

(UDC 621.039.519.4)

S. S. Lomakin

Translated from Atomnaya Énergiya, Vol. 19, No. 1,

pp. 69-71, July, 1965

Original article submitted July 28, 1964; revised form December 12, 1964

Experiments and calculations have been described [1] which deal with a critical assembly having a beryllium moderator. In this paper a report is given of work that was undertaken to determine the neutron-physical characteristics of a critical assembly with beryllium oxide moderator.

The critical assembly investigated, which was in the form of a parallelepiped, was built of blocks and plates of beryllium oxide and of flat fuel elements which were located between the moderator blocks in horizontal planes, so that a plane lattice was produced. The moderator block dimensions were  $100 \times 100 \times 50$  mm, the plates were  $100 \times 50 \times 15$  mm (density  $2.8 \text{ g/cm}^3$ ). The fuel elements were manufactured with a teflon-4 base [2]. The assembly was made up mainly of moderator blocks which were stacked in layers. The approach to the critical state was carried out with the help of moderator plates by increasing the height of the assembly. Under each moderator block there were three fuel element plates.

The characteristics of the assembly, for which the ratio of the atomic concentration of beryllium and  $\text{U}^{235}$  was 3272, are given below:

Lattice spacing . . . . .	50 mm
Number of fuel elements under moderator block	3
Amount of $\text{U}^{235}$ . . . . .	3409 g
Geometric parameter, $\kappa^2$ . . . . .	$0.438 \pm 0.005 \text{ cm}^{-2}, \times 10^2$
Calculated value of $k_{\text{eff}}$ :	
with experimental values of $\tau$ and $\mu$	0.999
multigroup calculation . . . . .	0.967

The assembly had upper and lower reflector face plates 25 mm thick.

The effect of neutrons reflected from the walls and the structure of the test stand on the critical dimensions of the assembly was determined experimentally. To accomplish this, the assembly was surrounded by a layer of cadmium, and the perturbing structural elements of the test stand were removed. The resulting corrections are taken into account in the value given for  $\kappa^2$ .

The supercriticality of the assembly was measured for small changes in its height with various geometric dimensions of the assembly under study. The resulting data, analyzed by the least squares method, is shown in Fig. 1 where  $H = -2.37 + 14.729 \times (\Delta H / k_{\text{eff}} \Delta \rho)^{1/3}$  is the height of the core in cm. The relationship shown, which, according to [1], can be written in the form

$$H = [2\pi^2 (\tau + L^2/1 + \kappa^2 L^2)]^{1/3} (\Delta H / k_{\text{eff}} \Delta \rho)^{1/3},$$

was used to determine the value of  $\tau$  which turned out to be  $112 \pm 2.5 \text{ cm}^2$ .

From the criticality condition  $k_{\text{eff}} = k_{\infty} e^{-\kappa^2 \tau / 1 + \kappa^2 L^2}$ , where  $k_{\infty} = \eta \theta \rho \mu$ , it was found that  $k_{\infty} = 2.07 \pm 0.06$ .

To determine the geometric parameter of a homogeneous system, an assembly was constructed in which the number of fuel elements per layer and the lattice spacing were doubled. In this case the fuel concentration remained unchanged. The geometric parameter for a homogeneous system was determined by extrapolating the resulting geometric parameters to zero amount of fuel elements (Fig. 2).

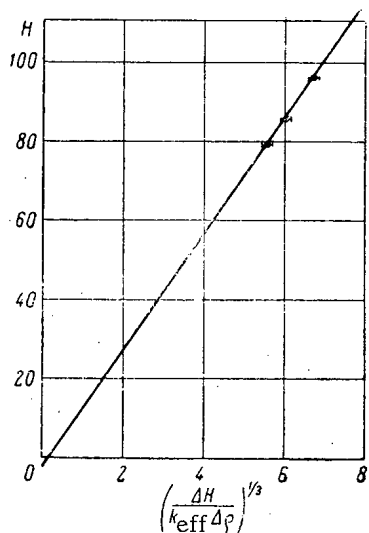


Fig. 1. Dependence on  $(\Delta H/k_{eff} \Delta \rho)^{1/3}$  of the core height of an assembly with beryllium oxide moderator having three fuel elements per layer.

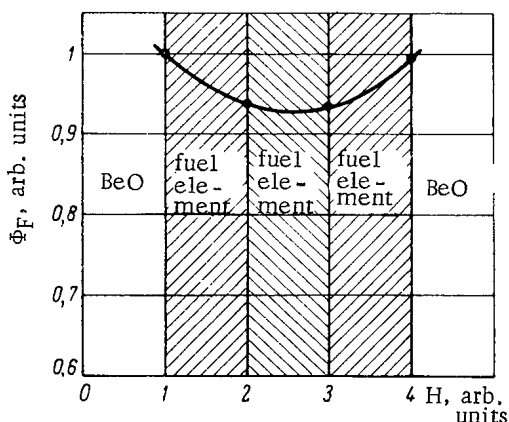


Fig. 3. Distribution of thermal neutron density in a layer with three vertically arranged fuel elements.

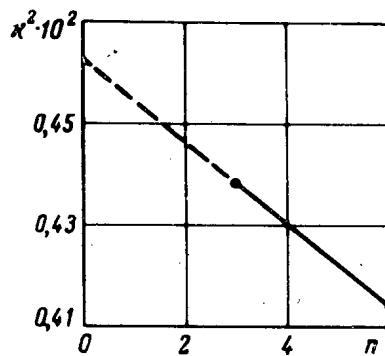


Fig. 2. Dependence of geometric parameter  $\kappa^2$  on  $n$  fuel elements per layer for constant fuel concentration.

Calculations for a critical assembly were also carried out using parameters obtained by the multigroup method [3]. The magnitude of fuel self-shielding was calculated in the  $P_3$  approximation, by the Monte Carlo method, and by the technique presented in [4]. In addition, the internal self-shielding coefficient was obtained from measurements of the thermal neutron distribution in a fuel element layer (Fig. 3). Data are given below for the values of the fuel self-shielding coefficients for a layer consisting of three fuel elements:

Calculation using the technique of [4]	Monte Carlo calculation	$P_3$ approximation	Measured internal self-shielding coefficient	Value assumed for calculation of $k_{eff}$
0.885	0.890	0.916	0.94	0.885

With the assumed self-shielding coefficient the assembly was calculated like a homogeneous one. The result of the calculation is given above. The contribution to the multiplication coefficient from the  $Be(n, 2n)$  and  $Be(n, \alpha)$  reactions was also calculated by the method presented in [1] including scattering by oxygen; the magnitude of the effect proved to be 1.06.

It is of interest to compare the data that was obtained with the results of other authors. To do this, the measured value of  $\tau$  was recalculated for a beryllium oxide density of  $2.79 \text{ g/cm}^3$  (the moderating contribution of teflon-4, for which the calculated value of  $\tau = 410.8 \text{ cm}^2$ , was taken into account). Up to an energy of 0.2 eV, it turned out that  $\tau$  amounted to  $105.6 \text{ cm}^2$ . According to [5], the value of  $\tau$  up to 0.3 eV was  $104.5 \pm 2 \text{ cm}^2$ . From a measured value for  $k_{\infty}$ , the value of  $\mu$  [the effect of the  $Be(n, 2n)$  reaction] was determined by calculation involving the factors  $\eta$ ,  $\theta$ , and  $p$ . It was 1.07. It was found in [6] that  $\mu = 1.054$  for a system of beryllium oxide and slightly enriched uranium. In such a system, it should be noted that inelastic scattering of fission neutrons in uranium lumps reduces the effect of the  $Be(n, 2n)$  reaction by 10-20%. In [7], a value of  $1.08 \pm 0.02$  is presented for  $\mu$ , which was obtained for beryllium oxide by converting the data from an experiment with a beryllium sphere.

In conclusion, the author is deeply grateful to N. N. Ponomarev-Stepnoi for directing the work, to V. A. Khodakov for supplying the results of Monte Carlo self-shielding calculations, and to V. G. Kosovskii for help in performing the critical experiment.



LITERATURE CITED

1. N. N. Ponomarev-Stepnoi and S. S. Lomakin, *Atomnaya Energiya*, 16, 228 (1964).
2. N. N. Ponomarev-Stepnoi, S. S. Lomakin, and Yu. G. Degal'tsev, *Atomnaya Energiya*, 15, 259 (1963).
3. G. I. Marchuk, *Methods of Reactor Calculations* [in Russian], Moscow, Gosatomizdat (1961).
4. E. Cohen, *Nucl. Sci. and Engng.*, 4, 225 (1958).
5. I. F. Zhezherun, *Atomnaya Energiya*, 13, 258 (1962).
6. P. Benoist, et al., Paper No. 1192, presented by France at the Second International Conference on the Peaceful Use of Atomic Energy (Geneva 1958).
7. I. F. Zhezherun, *Atomnaya Energiya*, 15, 505 (1963).

THE PROBLEM OF  $\gamma$ -RAY PENETRATION THROUGH SHIELDS

(UDC 539.122:539.121.72)

S. M. Ermakov and É. E. Petrov

Translated from *Atomnaya Énergiya*, Vol. 19, No. 1,  
pp. 71-73, July, 1965

Original article submitted August 13, 1964; revised form November 30, 1964

In this paper, an effect is described which is associated with the penetration of  $\gamma$ -rays through plane shields consisting of two components: a primary water layer and a secondary lead layer.

The effect consists of the following: for incidence of hard  $\gamma$ -rays at large angles to the normal, an increase in the thickness of the water layer can lead to an increase in the intensity of the radiation penetrating the shield.

Consider the physical picture of the phenomenon. If a  $\gamma$ -ray flux is obliquely incident on a plane layer of lead, this flux can be considerably attenuated even by a thin layer, the attenuating properties of the layer being enhanced for increasing angles of incidence. This is particularly apparent at high energies of the incident radiation since scattering anisotropy and absorption cross section increased with increasing energy, i.e., the  $\gamma$ -rays traverse a longer path in the layer and are absorbed with higher probability. Now place a water layer in front of the lead layer. In this case, on the one hand, the  $\gamma$ -rays will be reflected with greater probability from such a double-layered shield, leading to further attenuation of the penetrating radiation; on the other hand, they will be less obliquely incident on the lead, which can lead to reduced attenuation of the penetrating radiation. In addition, the  $\gamma$ -rays scattered in the water and penetrating to the surface of the lead have a lower energy than the primary  $\gamma$ -rays. Further, if they are scattered at large angles and have energies less than 3 MeV (the energy at which the linear attenuation coefficient for lead has a minimum), this will lead to large attenuation of the radiation. If the  $\gamma$ -rays are scattered at small angles and have energies greater than 3 MeV, that can lead to a relative reduction in radiation attenuation behind the shield because the absorption cross section for these energies falls with decreasing energy. In some cases, therefore, the intensity of obliquely incident radiation behind a shield is increased by the addition of a water layer.

The effect mentioned was observed in the analysis of the results of Monte Carlo calculations for the penetration of  $\gamma$ -radiation through multi-layer shields.

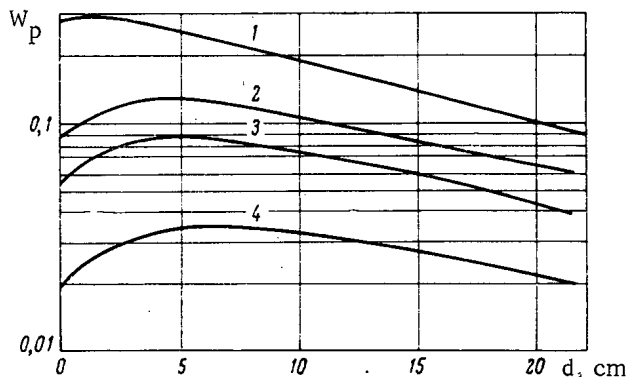


Fig. 1. Variation of  $W_p$  as a function of water layer thickness for various lead thicknesses: 1) 3 mm; 2) 7 mm; 3) 10 mm; 4) 20 mm.

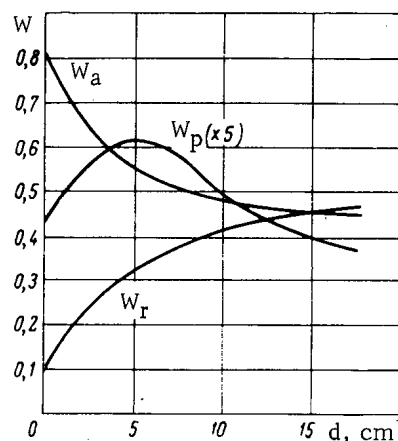


Fig. 2. Variation of  $W_p$ ,  $W_r$ , and  $W_a$  as a function of water layer thickness.

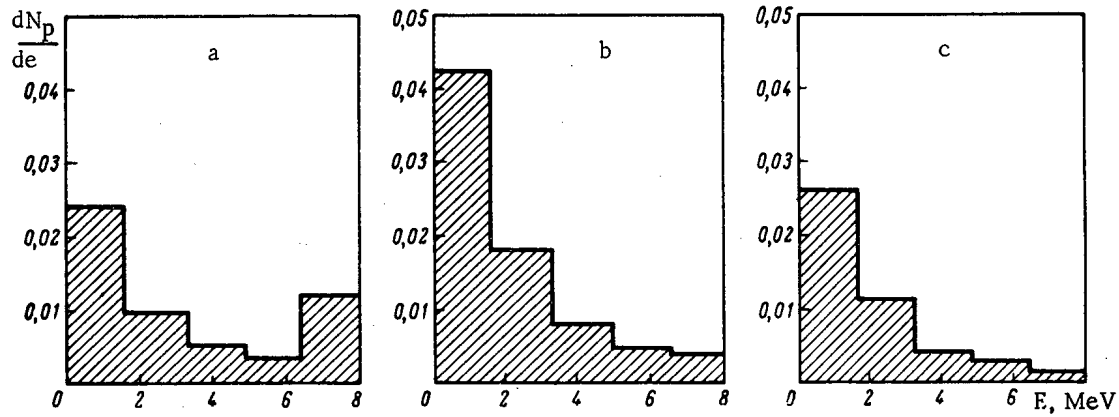


Fig. 3. Variation in the shape of the penetrating radiation spectrum as a function of water layer thickness: a) 0; b) 5 cm; c) 16 cm.

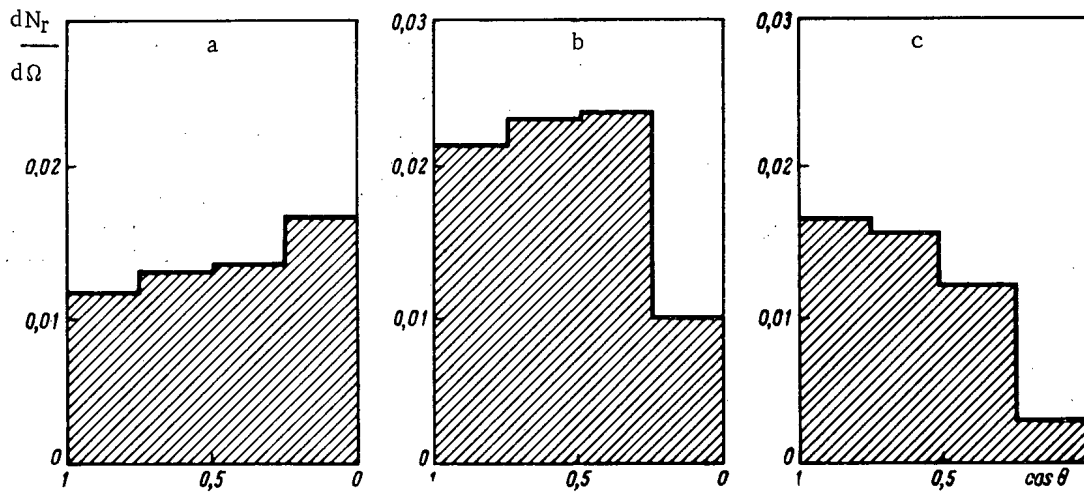


Fig. 4. Variation in the shape of the angular distribution of the penetrating radiation as a function of water layer thickness: a) 0; b) 5 cm; c) 16 cm.

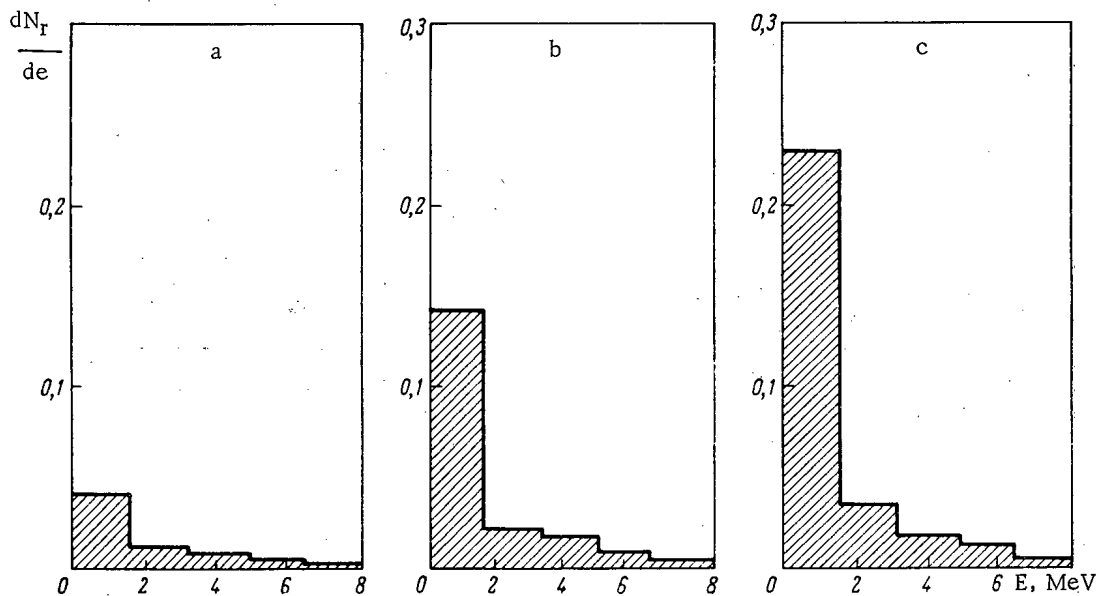


Fig. 5. Variation in the spectrum of reflected  $\gamma$ -rays as a function of water layer thickness; a) 0; b) 5 cm; c) 16 cm.

In the statistical simulation, the following types of photon interactions with matter were included: Compton scattering, and the absorption resulting from photoeffect and from pair production. Statistical simulation of this kind has been described in the literature\* therefore we mention only that the computation was performed with the inclusion of statistical weights. In the calculation of each sample, 4000 particle "histories" were followed; the statistical error of all the results obtained describing energy and angular distributions did not exceed 10% of the maximum value of the quantity under consideration (even in the worst cases). For integral characteristics (such as the probabilities for penetration through the layer, reflection from the layer, or absorption), the error was 1-2%.

The computations were performed for a monodirectional, monoenergetic source of radiation. The region in which the above described effect was observed was that for which the angle of incidence was greater than  $82^\circ$  (angle measured from the normal to the surface of the shield) and the energy greater than 6 MeV. In this region the intensity of penetrating radiation increased with increasing water layer thickness for any thickness of the lead layer.

Typical cases are shown in Figs. 1 and 2 (energy of  $\gamma$ -ray source 8 MeV, angle of incidence  $85^\circ$ ) of the increase in radiation intensity caused by a shield for increasing thickness  $d$  of the water layer. It is clear from Fig. 1 how the probability of  $\gamma$ -ray penetration through a shield varies with increasing thickness of the water layer for various thicknesses of the lead layer.

The changes in radiation characteristics ( $W_p$ , penetration probability;  $W_r$ , reflection probability;  $W_a$ , absorption probability) with increasing thickness of the water layer are shown in Fig. 2. The thickness of the lead layer in this case was 7 mm.

The variations in the shape of the energy spectrum of the penetrating  $\gamma$ -rays, of the angular distribution of the total penetrating flux, and of the energy spectrum of the reflected  $\gamma$ -rays are shown in Figs. 3-5, all quantities in these figures being normalized to one incident quantum. These figures clearly illustrate the physical picture of the effect described.

The authors consider it their obligation to thank N. F. Kham'yanov, who carried out the necessary calculations on an electronic computer.

---

\*See, for example, the paper by T. Ishii, T. Secine, K. Ono, A Monte Carlo Calculation of Gamma Ray Scattering on the Teidac Computer, Codes for Reactor Computations, Vol. I, Vienna, IAEA (1961), p. 53.

CALORIMETRIC DETERMINATION OF ABSORPTION OF A DOSE  
OF IONIZING RADIATION FROM A REACTOR BY COMPENSATION  
OF THE HEAT EVOLVED IN THE SPECIMEN

(UDC 621.039.55:536.629)

V. S. Karasev and V. M. Kolyada

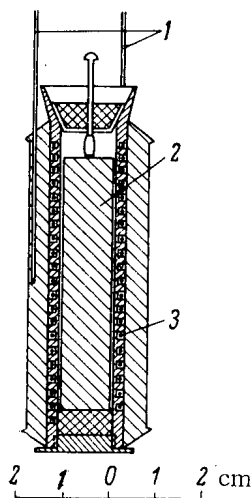
Translated from *Atomnaya Énergiya*, Vol. 19, No. 1,  
pp. 74-75, July, 1965

Original article submitted July 15, 1964

In investigations of the radiation resistance of materials, the absorption of energy from ionizing radiation is used as a measure of the action of irradiation on the physico-mechanical, chemical and other properties of the materials. In addition, to ensure that irradiation takes place at the desired temperature, we must know the dose, the heat evolved in the specimen, and the construction of the ampoule for irradiation. Theoretical calculations of the absorbed dose give only approximate answers, as the spectra of reactor radiations used for this purpose are not accurately known. It is therefore desirable to make direct calorimetric measurements.

In experiments with a VVR-M high-intensity reactor\*, the use of the previously employed calorimeters is limited or prohibited by the high heat evolution in the irradiated specimens. An exception is the use of the isothermal method [1] with the RFT reactor, where the total heat evolved in the specimen was calculated from data on the temperature drop in the air gap between the specimen and the channel wall. The accuracy of estimate of the absorbed dose here was 16%.

In this paper we shall describe a method by which the absorption rate of a high dose can be measured with great accuracy without the need for calculations involving the thermo-physical constants of the materials. For this purpose we used the method of electrical compensation of the heat evolved in a specimen in an isothermal calorimeter; this method is reliable and accurate, as shown by preliminary calibration outside the reactor (for diagram of calorimeter, see figure).



Calorimeter: 1) thermocouples; 2) specimen; 3) heater.

During measurement of the absorbed dose, thermostating of the calorimeter was effected by the high thermal stability of the reactor, due to its efficient automatic power control and large thermal capacity. Observations showed that the temperature of the water in the primary reactor circuit, which intensively cooled the channel with the calorimeter and was in this case the working fluid of the thermostat, varied by less than  $0.1^{\circ}\text{C}/\text{h}$ .

The method is based on the fact that in isothermal conditions the energy of the ionizing radiation absorbed by the specimen per unit time is, in the absence of the specimen from the calorimeter, equal to the electrical power of the compensating heater, provided that the temperature of the calorimeter surface (as measured by the thermocouples) is the same in both cases.

To determine the optimum construction of the calorimeter, we made calculations which were confirmed by experiments. The calorimeter was enclosed in a jacket simulating the loading channel, and was placed in a

\*Water-moderated water-cooled power reactor.

TABLE 1. Experimental Estimation of Accuracy of Simulation of Irradiated Specimen

Power of heater, watt	Mean reading of thermocouple, mV	Power of electrical heating coil simulating specimen, watt	Mean reading of thermocouple, mV
10,70	3,062	10,20	2,931
16,52	4,325	16,86	4,360
30,50	6,650	30,50	6,560

TABLE 2. Results of Measurements with Specimen Simulator

Power of heater, watt	Power of electrical heating coil simulating specimen, watt	Mean reading of thermocouple at surface of calorimeter, mV
20,00	5,40	5,921
25,40	0,00	5,935

Experimental measurements of the dose absorption rates of specimens of lead, tin, and steel (height 55 mm, diameter 9.5 mm) were made at the center of the working part of the metal-handling channel. During the measurements the reactor power was kept constant at 0.85 Megawatt. It was found that, for lead, tin, and steel 3, for reactor power 10 megawatt, the dose absorption rates were 0.665, 0.509, and 0.425 Mrad/sec respectively.

Estimates of the dose absorption rates of these materials for  $\gamma$ -rays and fast neutrons can be made on the basis of a method previously described (see reference). On comparing our results with data from work with an RFT [research] reactor, it is found that the total absorption with the same neutron flux from the VVR-M reactor is significantly greater. This is explained by the fact that the heat-evolving elements in the RFT reactor are surrounded by graphite blocks, so that the density of  $\gamma$ -quanta in the reactor channel, which makes the main contribution to the heat evolved, is markedly less than in the VVR-M reactor.

## LITERATURE CITED

1. N. F. Pravdyuk, V. N. Kuznetsov, and N. I. Laletin, *Atomnaya Énergiya*, 9, 380 (1960).

water thermostat in which the temperature was kept close to that of the reactor cooling water to within 0.1° C. The temperature at the calorimeter surface was plotted against the reactor power, and this was then repeated with a nichrome coil heater replacing the specimen.

As shown by the results in Table 1, the data did not differ by more than 3%. The experimentally determined sensitivity of the calorimeter at the working temperature was on average 0.180 mV/watt. The emf of the thermocouple was measured potentiometrically to within 0.006 mV, and the heater power to within 0.05 watt.

Table 2 gives the results of experiments in which the measuring process was simulated. The electrical power dissipated in the calorimeter heater corresponded approximately to the radiation energy absorbed by the calorimeter structure. When the temperature was constant, compensation measurements were made with the specimen simulator.

The data in Tables 1 and 2 show that the construction of the calorimeter makes it possible to measure the absorption of radiation energy in the specimen to within 3-5% by compensation of the heat evolved by means of a heater placed in the calorimeter.

THE UKP-30 000 ISOTOPE APPARATUS FOR  $\gamma$ -IRRADIATION

(UDC 621.039.83)

G. N. P'yankov, M. A. Barashkin, and N. V. Kulyupina

Translated from *Atomnaya Énergiya*, Vol. 19, No. 1,

pp. 75-76, July, 1965

Original article submitted August 3, 1964

In radiation chemistry, especially in the handling of radioactive materials, it is often necessary to irradiate various materials of thicknesses over  $1 \text{ g/cm}^2$  with doses of  $10^8$ - $10^9$  rad and over.

The isotope and x-ray apparatus described in the literature cannot usually produce doses higher than 1000-1300 rad per sec [1, 2]. Doses of  $10^9$  rad thus, in the most favorable cases, require hundreds of hours. During this time it is necessary to keep constant observation, since specimens being irradiated may become very hot.

In comparison with other equipment of this type, the UKP-30 000 (Kiev Underwater Apparatus, 30,000 g-equiv. Ra) reduces the time required for large doses by a factor of 2-3. When using it continuous observation is unnecessary. It is completely safe in use and very simple to handle.

Figure 1 gives a diagram of the apparatus. The irradiation unit 1 is always kept under 4 meters of water 2 in the tank. The water acts as a biological shield. It also ensures constancy of the temperature of the irradiating unit and specimens. In case the water should leak away, there is a supplementary system with a float valve 3. This consists of a U-shaped lead screen of height 700 mm and thickness 150 mm with a pivoting lead lid of thickness 240 mm, fitted with a counterweight. The lid is balanced so that, in the raised position, it is supported by a 18 liter float. If the water level in the tank falls by about 300 mm, the equilibrium is broken and the lid falls by gravity onto the screen, shutting in the irradiator.

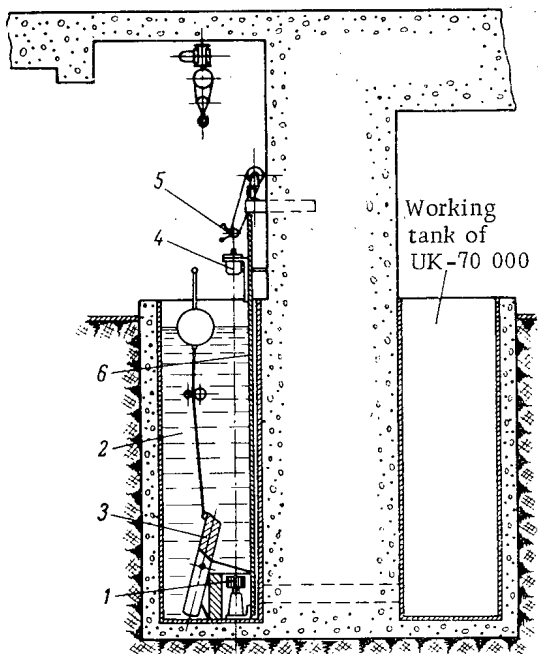


Fig. 1. UKP-30,000.

The UKP-30 000 irradiator is flat and has two rows. It comprises 22 standard cobalt sources each of intensity  $1500 \pm 300$  g-equiv. Ra, hermetically sealed in stainless steel cans of thickness 1 mm. The sources (with the cans) are of diameter  $11 \pm 0.15$  mm and height  $81.1 \pm 1.5$  mm. They are placed in stainless steel tubes of external diameter 14 mm and wall thickness 1 mm. The length of the irradiator is 160 mm. It is fixed securely to the bottom of the tank by means of a special holder. During preventive maintenance or repairs, etc., it can be removed to an adjacent tank in which is stored the irradiator from another high-power apparatus (UK-70 000). Similarly, the irradiator from the UK-70 000 can be transferred to the tank of the UKP-30 000. When the total activity in either basin is about 100,000 g-equiv. Ra, the radiation level at the water surface does not exceed the allowed value. The shaft of the flat irradiator from the UKP-30,000, which fits into the holder, is similar in construction and size to that of the UK-70 000 cylindrical irradiator; this makes them interchangeable and renders both irradiators more versatile.

The specimens are placed in a sealed 3-section cassette 4, which can be brought up to the irradiator by manual drive 5. The carriage which carries the cassette moves on rollers along a flat guide 6, pegged to the wall of the tank. The upper and lower positions of the cassette are fixed by stops and a locking mechanism on the hand drive. The cassette is made so that vacuum, excess pressure, and inert gas atmosphere, etc., can be created in its sections.

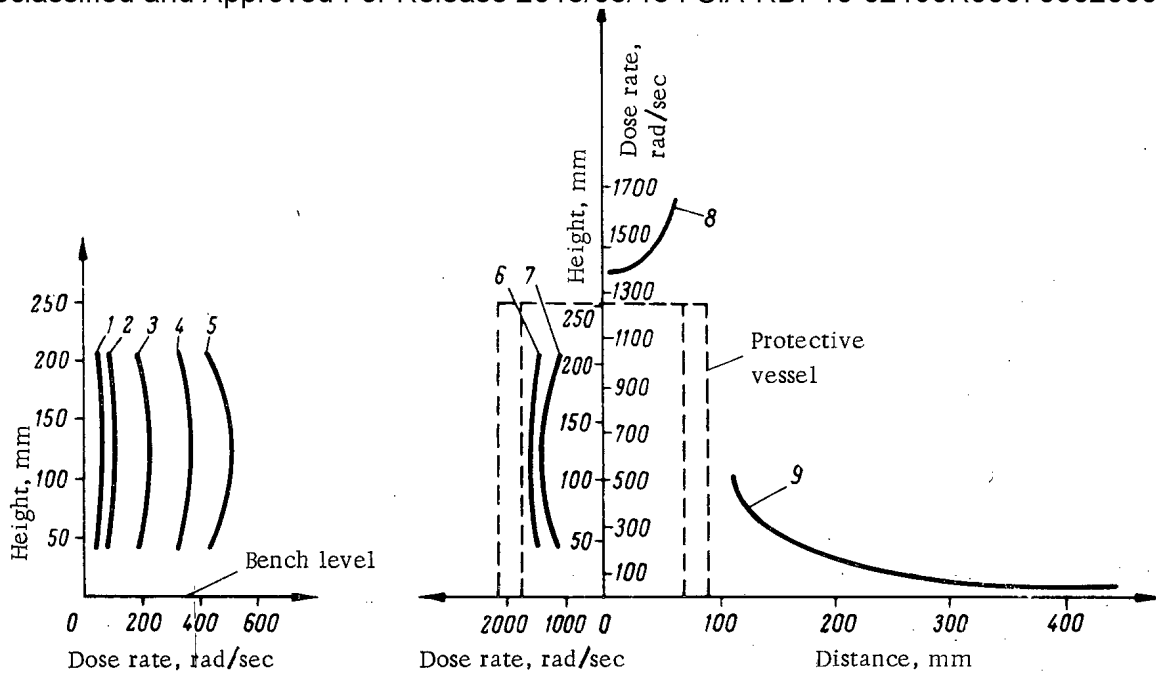


Fig. 2. Dose field of cassette.

The dose field of the UKP-30 000 was measured by chemical dosimetry. The measurement errors were below  $\pm 2\%$ . Figure 2 gives results of dosimetric measurements in the specimen cassette. It is seen that the highest dose rate (about 3000 r/sec) occurs in the middle section 1. It is proposed to increase the dose rate by altering the geometry of the irradiator and fitting it with  $\text{Co}^{60}$  sources, each of activity 3000 g-equiv. Ra [3].

Measurements in the cassette and irradiator showed that the temperatures of specimens with volumes up to  $50 \text{ cm}^3$  are practically constant throughout irradiation by dose rates of order  $10^8$ - $10^9$  rad, thanks to the thermostating action of the surrounding water. Continuous dosimetric monitoring of the water in the tanks shows that it does not become radioactive.

The following engineers from the Laboratory of Radiation Chemistry took part in the construction, assembly and adjustment of the UKP-30 000: I. G. Davidiuk, K. I. Subach, V. S. Kurennoi, M. V. Markov, M. M. Odnokon', A. I. Silenko, and N. R. Starichenko; A. N. Bordikova helped with the dosimetry.

In conclusion, the authors take this opportunity of thanking A. M. Kabakcha for constant interest and valuable advice.

#### LITERATURE CITED

1. Nucleonics, 21, 126 (1963).
2. A. Kh. Breger, Author's abstract of doctoral dissertation, Moscow, In-t elektrokhemii AN SSSR (1961).
3. V. I. Zatulovskii, In "Proceedings of All-Union Scientific-Technical Conference on the Applications of Isotopes and Nuclear Radiations. Preparation of Isotopes. Powerful gamma sources. Radiometry and Dosimetry" [in Russian], Moscow, Izd-vo AN SSSR (1958), p. 193.



THE UK-70 000 HIGH-POWER ISOTOPE APPARATUS FOR  $\gamma$ -IRRADIATION

(UDC 621.037.83)

G. N. P'yankov and N. V. Kulyupina

Translated from *Atomnaya Énergiya*, Vol. 19, No. 1,

pp. 77-78, July, 1965

Original article submitted August 3, 1964

Research developing in the Ukrainian Academy of Sciences on certain aspects of radiation chemistry required extensions of its experimental basis. The equipment constructed for this purpose included the UK-70 000 high-power irradiating unit (Kiev apparatus, 70,000 g-equiv. Ra), in which the  $\gamma$ -irradiator uses  $\text{Co}^{60}$  with total activity (on August 1, 1962) of 71,000 g-equiv. Ra (44 000 curies). In planning this equipment, much experimental work was done at the L. Ya. Karpov Physical Chemistry Institute, the Electro-Chemistry Institute of the USSR Academy of Sciences, and the All-Union Research Institute for Oil and Gas [1-4].

For the UK-70 000 we chose compound biological shielding; this was effected by building round the irradiator a concrete wall of thickness 2 m, a 1.5-m roof (the building is single storey) and a maze entrance closed by a metal door; at the storage position is a 4-m water layer.

The UK-70 000 apparatus (Fig. 1) consists of a "hot" room with water tank, an irradiator, an electro-mechanical system for raising and lowering the irradiator fitted with an emergency drop, an interlock, signalling and monitor system, a control panel, and pumping and ventilation equipment.

The hot room 1 is of concrete of size 4x4x2.9 m. Entry is through maze 2, closed on the outside by metal door 3. In the room is tank 4, with mirror, with water surface 1.5x1.5 m and depth 4.3 m. The main section of the tank is of welded stainless steel. The internal sides and bottom of the tank are faced with dutch tiles on a stainless steel grid. The lower part of the tank in the hot room is joined by sluice 5 to another similar tank 6 outside the room, surmounted by a monorail which goes outside the building and carries an electric crane 7, with load capacity of 2 t.

The irradiator consists of 30 aluminum tubes of external diameter 14 mm and wall thickness 1 mm, arranged round a cylindrical former of height 250 mm and internal diameter 140 mm. In each tube there are three standard sources, hermetically sealed into aluminum cans. The cans and sources are of standard size: diameter 11 mm, height 81.5 mm. The activities of the sources varied between 650 and 900 g-equiv. Ra. To obtain a uniform dose field, the sources with lowest activities were placed at the center of the irradiator.

The irradiator, under remote control, can be raised by crane 8 from the tank bottom to bench 9, where it enters safety container 10 which is fitted with a cooling system. The crane switches itself off at the upper and lower limits of the irradiator's travel. The whole system for raising and lowering the irradiator works either off the mains or from an emergency power supply. If a fault occurs, the irradiator can be dropped to the bottom of the tank by an electro-mechanical system, supplemented by an emergency hand winch. The

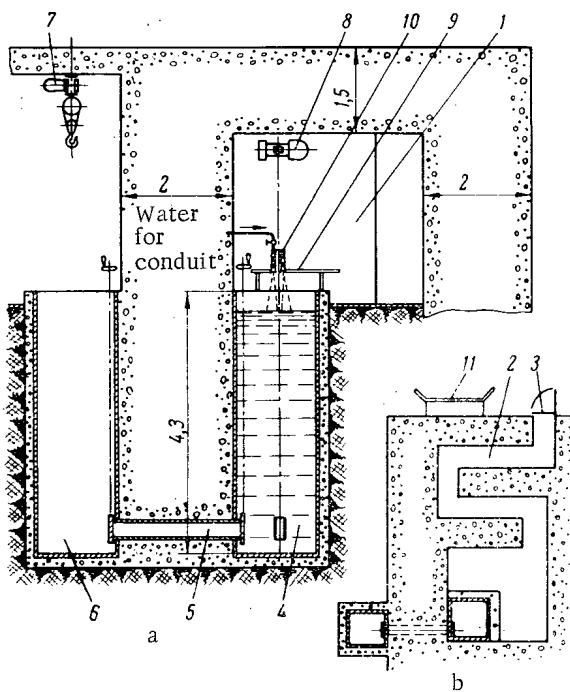


Fig. 1. UK-70 000. a) Vertical cross section; b) plan.

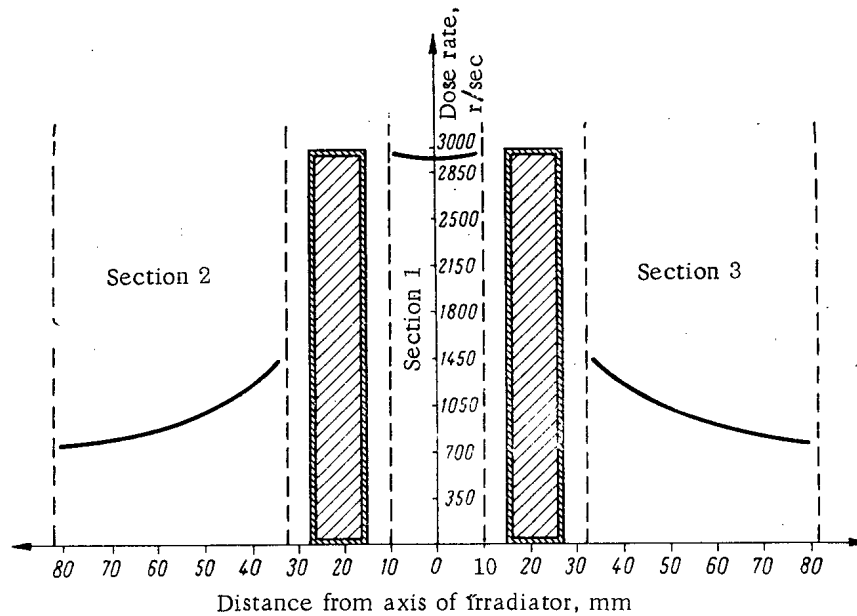


Fig. 2. Dose field of UK-70 000. Variation of dose rate with height above bench at various distances from irradiator axis in mm: 1) 400; 2) 320; 3) 180; 4) 125; 5) 110; 6,7) variation of dose rate with height inside protective vessel at 50 and 25 mm from its axis, respectively; 8,9) horizontal variation of dose rate inside protective vessel, half way up and on the bench, respectively.

position of the source and the water level in the tank are monitored by special devices. The system for raising and lowering the irradiator is electrically connected to the electro-mechanical interlock system for entry into the hot room. Thus one cannot enter the hot room when the irradiator is raised. The irradiator cannot be raised unless the door is shut by mechanical and electro-mechanical locks. The apparatus which signals the dose level is connected with a USID-12 stationary dosimeter, and a special siren warns of any attempts to open the door while the irradiator is raised. The USID-12 apparatus controls the radiation level both in the maze and outside the room. The electro-mechanical interlock system is regulated so that the door to the maze can be opened only 4 min after the irradiator is lowered. During this time, the ventilation system of the hot room removes ozone and oxides of nitrogen which are formed in large quantities during prolonged irradiation. In emergencies rapid access to the room can be obtained immediately after the irradiator is lowered. The irradiation of various specimens and the position of the irradiator are monitored by television cameras. To protect the chamber containing the optical transmitting equipment from the action of radiation, it is placed in the maze behind the concrete wall. It was thus necessary to mount a system of metal mirrors made of polished stainless steel in the room and maze.

The UK-70 000 is controlled entirely from panel 11 in the operating room. Tests of the biological shielding showed that in the working accommodation and near the outer walls the radiation level is close to the natural background and is 0.025 mr/h.

The dose field of the UK-70 000 was measured by chemical dosimetry. The errors were mostly below  $\pm 2\%$ . It was found that inside the protective vessel the maximum dose rate was 1800 r/sec (January 1963). On the bench, depending on the distance of the irradiator, it varied from 15-600 r/sec. Figure 2 shows the dose field.

Owing to absorption of radiation energy in the irradiator and the walls of the protective vessel, the active volume becomes heated. It was found that thermal equilibrium is attained after 3 h, when the temperature of the internal wall of the protective vessel is  $85^{\circ}\text{C}$  and the outer wall is at about  $65^{\circ}\text{C}$  (at the middle of the dose field). Direct cooling of the irradiator itself by a flow of 2-2.5 liters/min of mains water reduced the temperatures of both walls to room temperature practically instantaneously.

It appears that the compound biological shielding chosen for the UK-70 000 is very reliable and convenient in use.

Experience in the use of the UK-70 000 shows that the water in the tanks does not become radioactively contaminated by the  $\text{Co}^{60}$ .

Those taking part in the construction, assembly and adjustment of the UK-70 000 included I. G. Davidyuk, V. S. Kurennoi, M. Ya. Tereshchenko, I. N. Fedchishin, A. G. Puchkovskii, N. R. Starichenko, A. I. Silenko, M. M. Odnokon', Yu. I. Puzyrev, and A. P. Meleshevich; K. A. Zaitseva helped with the dosimetry.

#### LITERATURE CITED

1. V. I. Zatulovskii, In: "Proceedings of All-Union Conference on the Applications of Isotopes and Nuclear Radiations. Preparation of Isotopes. Powerful Gamma Sources, Radiometry and dosimetry" [in Russian], Moscow, Izd-vo AN SSSR (1958), p. 193.
2. A. V. Babushkin et al., Ibid., p. 189.
3. A. Kh. Vreger, Problems in Physical Chemistry [in Russian], No. 1, Moscow, Goskhimizdat (1958).
4. A. Kh. Vreger, In "Proceedings of Second All-Union Conference on Radiation Chemistry" [in Russian], Moscow, Izd-vo AN SSSR (1962).

THE ADVANTAGES OF RADIOMETRIC ENRICHMENT OF URANIUM  
ORES AND THE CHOICE OF OPTIMUM SEPARATION LEVEL

(UDC 622.7:553.495)

I. A. Andryushin, Yu. V. Roshchin, L. D. Chebotareva,  
and Yu. A. Érivanskii

Translated from *Atomnaya Énergiya*, Vol. 19, No. 1,  
pp. 79-80, July, 1965

Original article submitted September 9, 1964

It is important to determine the conditions under which it is advantageous to carry out radiometric enrichment and to select the optimum separation level: however, there is so far no single solution to this problem. As a rule, the optimum separation level is determined by the minimum net cost of the uranium obtained for any particular plant [1, 2]. However, it is not enough to allow only for the degree of recovery of uranium from the deposits [3]. The radiometric enrichment performances for minimum net cost for a given plant are not always optimal for a joint examination of several plants (in one field) with different technico-economic conditions of extraction and processing of the uranium ores. The method of determining the optimum separation level, in keeping with the requirement of maximum saving per ton of initial ore, is largely free from this short coming.

Level of economic effect of enrichment. The expenditure on winning, transporting and processing 1 ton of ore (without enrichment) is determined by the equation

$$A_1 = C_0 + C_t + C_h \text{ rub/ton} \quad (1)$$

and with enrichment

$$A_2 = C_0 + \gamma(C_t + C_h) + C_e \text{ rub/ton}, \quad (2)$$

where  $C_0$  is the cost of the ore in rub/ton,  $C_t$ ,  $C_h$ , and  $C_e$  are the costs of transportation, hydrometallurgical processing, and radiometric enrichment per ton of ore, respectively, in rub/ton, and  $\gamma$  is the yield of enriched ore in rel. units. In the first case the amount of uranium obtained per ton of ore is

$$Me_1 = \alpha \epsilon_h, \quad (3)$$

and in the second case

$$Me_2 = \alpha \epsilon_h' \epsilon, \quad (4)$$

where  $\epsilon_h$  and  $\epsilon_h'$  are the uranium extracted from the initial and enriched ores in the chemical concentrate, respectively, in rel. units;  $\epsilon$  is the amount of uranium passing into the enriched ore, in rel. units, and  $\alpha$  is the uranium content of the initial ore in kg/ton. If  $C$  is the distribution cost of 1 kg uranium (or the mean value of uranium in industry), then, in the absence of enrichment, the difference between the cost of the uranium per ton of initial ore and the expense of its production in a given plant (which we shall call the "profit"  $P$ ) will be

$$P_1 = CM e_1 - A_1 = \alpha \epsilon_h C - (C_0 + C_t + C_h); \quad (5)$$

with enrichment

$$P_2 = CM e_2 - A_2 = \alpha \epsilon_h' \epsilon C - [C_0 + \gamma(C_t + C_h) + C_e]. \quad (6)$$

The increment in profit due to ore enrichment will be

$$\Delta P = P_2 - P_1 = (C_t + C_h)(1 - \gamma) - \alpha C(\epsilon_h - \epsilon_h' \epsilon) - C_e, \quad (7)$$

which we shall call the economic effect of enrichment.

Conditions of advantage and optimum enrichment. Radiometric enrichment is advantageous if it leads to an increase in profit. The enrichment performance will be optimum if the increment in profit is a maximum. The conditions for advantage and optimum parameters can be written in the general form

$$(\Delta P)_{\max} > 0; \quad (8)$$

$$(C_t + C_h)(1 - \gamma) - \alpha C(\epsilon_h - \epsilon_h') - C = (\Delta P)_{\max} \quad (9)$$

Optimum separation level. The optimum separation level, according to (9), is found from the equation

$$\frac{\partial (\Delta P)}{\partial \beta} = 0, \quad (10)$$

where  $\beta$  is the separation level.

Remembering that  $\gamma = 1 - \int_0^{\beta} f(\beta) d\beta$  (I) and  $\epsilon = 1 - \frac{1}{\alpha} \int_0^{\beta} \beta f(\beta) d\beta$ , (II), where  $f(\beta)$  is the probability

density function of the distribution of uranium content in the volume elements of the ore, and assuming that the other quantities in (7) are independent of  $\beta$ , we get the equation

$$-(C_t + C_h) \frac{\partial \gamma_{\text{opt}}}{\partial \beta} + \alpha C \epsilon_h' \frac{\partial \epsilon_{\text{opt}}}{\partial \beta} = 0. \quad (11)$$

Substituting in (11) the values of the derivatives

$$\frac{\partial \gamma_{\text{opt}}}{\partial \beta} = -f(\beta) \text{ and } \frac{\partial \epsilon_{\text{opt}}}{\partial \beta} = -\frac{1}{\alpha} \beta_{\text{opt}} f(\beta_{\text{opt}}),$$

we get an expression for the optimum level of separation

$$\beta_{\text{opt}} = \frac{C_t + C_h}{C \epsilon_h'} \text{ kg/m}. \quad (12)$$

Thus the optimum separation level, which leads to maximum absolute economy (profit) per ton of initial ore, is independent of the ore contrast.

Conditions of advantage of enrichment with optimum indices. Knowing the optimum separation level, we can (from the contrast curves of the ore) determine the remaining technological indices of enrichment and estimate the advantage of carrying it out. Considering the approximate equation  $\epsilon_h = \epsilon_h'$ , (8) can be written as

$$(1 - \gamma_{\text{opt}}) > \frac{C_e}{C_t + C_h} + \frac{\alpha}{\beta_{\text{opt}}} (1 - \epsilon_{\text{opt}}), \quad (13)$$

where the  $(1 - \gamma)$  is the yield of tailings,  $(1 - \epsilon)$  the loss of uranium in tailings from radiometric enrichment. If (13) is not satisfied for optimal performances there is no economic advantage in radiometric enrichment.

If the price or mean value of uranium in industry is not stable, we can determine a variant of the performance corresponding to maximum economy per ton of initial ore, in contrast to the variant of obtaining uranium from a given plant without enrichment. Here the mean cost of the uranium is taken as its net cost for treatment without enrichment:

$$C = \frac{C_o + C_t + C_h}{\alpha \epsilon_h}, \quad (14)$$

while the optimum separation level is determined by the equation

$$\beta_{\text{opt}} = \alpha \frac{C_t + C_h}{C_o + C_t + C_h}. \quad (15)$$

As before, the yield of tailings leading to advantage in radiometric enrichment must satisfy (13), which, by (15), can be rewritten

$$(1 - \gamma_{\text{opt}}) > \frac{C_e}{C_t + C_h} + \left(1 + \frac{C_o}{C_t + C_h}\right) (1 - \epsilon_{\text{opt}}). \quad (16)$$

#### LITERATURE CITED

1. E. D. Mal'tsev, *Atomnaya Energiya*, 8, 121 (1960).
2. L. Ch. Pukhal'skii, *Theory of Contrast of Uranium Ores* [in Russian], Moscow, Atomizdat (1963).
3. P. Formery and V. Zeigler, *Proc. of the Second Intern. Conf. on the Peaceful Uses of Atomic Energy*, Geneva, UNO, Vol. 3 (1958), p. 105.

OPTIMAL INDICES OF RADIOMETRIC ENRICHMENT  
AND SUITABLE CONDITIONS FOR ITS USE ON AN ORE  
WITH LOG-NORMAL DISTRIBUTION OF URANIUM  
CONTENT IN ITS VOLUME ELEMENTS

(UDC 622.7:553.495)

Yu. V. Roshchin

Translated from *Atomnaya Énergiya*, Vol. 19, No. 1,

pp. 80-82, July, 1965

Original article submitted September 9, 1964

In many cases, the distribution of the useful-component content in deposits of non-ferrous, rare and noble metals is approximately represented by a log-normal distribution. In particular, tests of the log-normal theory of sampling [1] have showed that it is applicable to many uranium deposits in France [2]. It is therefore of interest to examine the contrast indices of uranium ores and the conditions for their radiometric enrichment in the case of log-normal distribution.

Various properties of the log-normal distribution. A content  $x$  ( $0 < x < \infty$ ) is a log-normal variate if  $\log x^*$  is distributed normally with mean  $\mu$  and variance  $\sigma^2$ , i.e., if  $\log x = N(\mu, \sigma^2)$ .

A knowledge of  $\mu$  and  $\sigma^2$  is sufficient for a description of all the properties of a log-normally distributed variate (for the properties of the log-normal distribution see, e.g., [3;5]). In this case the mean  $\alpha$  and coefficient of variation  $V$  of the content are given by

$$\alpha = \exp\left(\mu + \frac{1}{2}\sigma^2\right) = Me \exp \frac{\sigma^2}{2}; \quad (1)$$

$$V = (\exp \sigma^2 - 1)^{1/2}, \quad (2)$$

where  $Me = x_{0.5}$  is the median value of the content of initial ore in the volume elements. That fraction of the ore which consists of volume elements with content less than or equal to  $x$  is given by the distribution fraction

$$F(x) = \frac{1}{\sigma \sqrt{2\pi}} \int_0^x \frac{1}{x} \exp\left[-\frac{(\ln x - \mu)^2}{2\sigma^2}\right] dx. \quad (3)$$

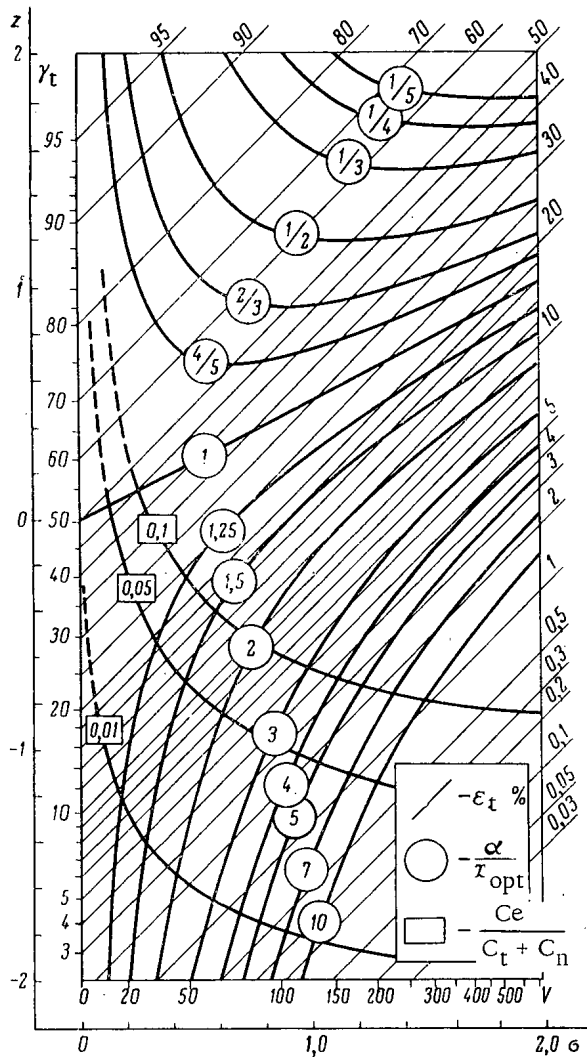
Let us introduce the normalized content

$$z = \frac{\ln x - \mu}{\sigma} \quad (4)$$

and denote the total weight of the ore by  $T$ . Then the weight of the volume elements with content in the range  $x_1 < x < x_2$ ,  $T(x_1, x_2)$ , and the mean content  $\alpha(x_1, x_2)$  and the quantity of metal  $Q(x_1, x_2)$  in the same range are given by

$$T(x_1, x_2) = T \int_{x_1}^{x_2} dF(x) = T [F(z_2) - F(z_1)]; \quad (5)$$

\*For simplicity we shall use  $\ln x$ .



Nomogram for determining optimum enrichment indices for various values of  $\alpha/x_{opt}$ , and minimum yield of tailings for various values of  $C_e/C_t + C_h$ , determining the advantageousness of enrichment.

We can get the uranium contents of the concentrate and tailings by putting in (6)  $x_1 = x_p$ ,  $x_2 = \infty$ , and  $x_1 = 0$ ,  $x_2 = x_p$ , respectively:

$$\{\beta_c\} = \alpha(x_p, \infty) = \alpha \frac{1 - F(z_p - \sigma)}{1 - F(z_p)} \quad (10)$$

$$\{\beta_t\} = \alpha(0, x_p) = \alpha \frac{F(z_p - \sigma)}{F(z_p)} \quad (11)$$

The coefficient of enrichment of the concentrate

$$\{K\} = \frac{\alpha(x_p, \infty)}{\alpha} = \frac{1 - F(z_p - \sigma)}{1 - F(z_p)} \quad (12)$$

\*Symbols in curly brackets are those used in L. Ch. Pukhal'skii's book [6].

$$\alpha(x_1, x_2) = \frac{\int_{x_1}^{x_2} x dF(x)}{\int_{x_1}^{x_2} dF(x)} = \alpha \frac{F(z_2 - \sigma) - F(z_1 - \sigma)}{F(z_2) - F(z_1)} \quad (6)$$

$$Q(x_1, x_2) = \alpha(x_1, x_2) T(x_1, x_2) = Q [F(z_2 - \sigma) - F(z_1 - \sigma)] \quad (7)$$

where  $Q = \alpha T$  is the total quantity of metal in the ore;

$$F(z) = \frac{1}{\sqrt{2\pi}} \int_{-\infty}^z \exp\left(-\frac{z^2}{2}\right) dz \text{ and } F(z - \sigma) = \frac{1}{\sqrt{2\pi}}$$

$\times \int_{-\infty}^{z - \sigma} \exp\left(-\frac{z^2}{2}\right) dz$  are the distribution functions of the variate  $N(0, 1)$ , tables of which can be found in any reference book on mathematical statistics.

Expressions for principal sorting indices in terms of distribution parameters. Using the basic relations in (1)-(7), let us express the indices of radiometric ore enrichment in terms of the sorting level  $\{\beta\}^* = x_p$ , where  $p$  is the order of the quantile determined by the relation  $p = F(z_p)$ , or in terms of the normalized sorting level  $z_p$  [cf. (4)] and the parameters  $\mu$  and  $\sigma^2$  of the log-normal distribution. We are considering the case of ideal sorting conditions, i.e., we are assuming that sorting is carried out with respect to the true content of the useful component in the ore's volume elements.

In (5) put  $x_1 = x_p$  and  $x_2 = \infty$ . We then get the yield of concentrate,

$$\{\gamma\} = \frac{T(x_p, \infty)}{T} = 1 - F(z_p) \quad (8)$$

and the yield of tailings

$$\{\gamma_t\} = \{1 - \gamma\} = F(z_p) \quad (9)$$



The degree of enrichment of uranium in the concentrate is

$$\{\varepsilon\} = 1 - F(z_p - \sigma). \quad (13)$$

The fraction of the uranium leaving in the tailings is

$$\{\varepsilon_t\} = 1 - \varepsilon = F(z_p - \sigma). \quad (14)$$

The figure gives a nomogram relating  $z$  and  $\gamma_t = F(z)$  to  $\sigma$  and  $V$  for various values of  $\varepsilon_t = F(z_p - \sigma)$  (denoted by the numbers on the family of parallel lines).

Determination of sorting indices for optimum separation level. Putting the optimum separation level  $x_{opt}$  in (4) and remembering (1) we get

$$z_{opt} = \frac{1}{\sigma} \ln \frac{x_{opt}}{\alpha} + \frac{\sigma^2}{2}, \quad (15)$$

where  $x_{opt}$ , as shown in [7], is independent of the form of the distribution and is determined by the equation

$$x_{opt} = \frac{C_t + C_h}{\varepsilon} \quad (16)$$

where  $C_t$  and  $C_h$  are the costs of transportation and metallurgical treatment per ton enriched ore,  $\varepsilon_h$  is the degree of extraction of uranium from the enriched ore in the chemical concentrate, and  $C$  the distribution costs of 1 kg uranium.

The figure shows a family of curves constructed from (15) and relating  $z_{opt}$ ,  $F(z_{opt})$ ,  $\sigma$ ,  $V$  and  $F(z_{opt} - \sigma)$  for various values of  $\alpha/x_{opt}$ . For example, if  $\alpha/x_{opt} = 4$  and  $\sigma = 1$  (corresponding to  $V \approx 130\%$ ), then  $z_{opt} = -0.9$ ,  $F(z_{opt}) = 0.18$  and  $F(z_{opt} - \sigma) = 0.03$ . From (8)-(14) it is easy to find the indices of the optimum sorting conditions:  $\gamma = 0.82$ ;  $\gamma_t = 0.18$ ;  $\beta_c = \alpha \cdot 1 - 0.03 / 1 - 0.18 = 1.18 \alpha$ ;  $\beta_c = \alpha \cdot 0.03 / 0.18 = 0.17 \alpha$ ;  $K = 0.97 / 0.82 = 1.18$ ;  $\varepsilon = 0.97$ ;  $\varepsilon_t = 0.03$ .

Determining the conditions for sorting. According to a number of factors, enrichment may, in given optimum conditions, be advantageous or disadvantageous. In [7] it is shown that radiometric enrichment is advantageous if the conditions satisfy the inequality

$$(\gamma_t)_{opt} > \frac{C_0}{C_t + C_h} + \frac{a}{x_{opt}} (1 - \varepsilon_{opt}), \quad (17)$$

where  $C_e$  is the cost of radiometric enrichment per ton initial ore.

On the figure are constructed curves

$$(\gamma_t)_{opt} = \frac{C_0}{C_t + C_h} + \frac{a}{x_{opt}} (1 - \varepsilon_{opt}), \quad (18)$$

which correspond to the least yield of tailings,  $(\gamma_t)_{opt} = F(z)$ , satisfying (17). Thus, for the conditions of the example given above, when  $C_e/C_t + C_h = 0.05$  it is advantageous to use sorting, since the "point" for the optimum conditions lies above the "advantageous sorting" line for  $C_e/C_t + C_h = 0.05$ , whereas for  $C_e/C_t + C_h = 0.1$  sorting is disadvantageous.

#### LITERATURE CITED

1. G. Matheron, Ann. mines, No. 9, (1957), p. 566.
2. P. Formery and V. Ziegler, Proc. of the Second Intern. Conf. on the Peaceful Uses of Atomic Energy, Geneva, UNO (1958), Vol. 6, p. 1246.
3. J. Aitchison and J. Brown, The Log-normal Distribution, Cambridge University Press (1957).
4. N. K. Razumovskii, The log-normal distribution law for a substance and its properties [in Russian], "Zap. Leningradskogo gornogo in-ta" T. 20, Leningrad (1948).
5. D. A. Rodionov, Distribution Functions for the Contents of Elements and Minerals in Igneous Rock [in Russian], Moscow, "Nauka" (1964).

6. L. Ch. Pukhal'skii, The Theory of Contrast of Uranium Ores [in Russian], Moscow, Gosatomizdat (1963).
7. I. A. Andryushin et al., The advantages of radiometric enrichment of uranium ores and the choice of optimum separation level [in Russian], "Atomnaya Energiya", 19, 79 (1965).

ISOTOPE SHIFT BETWEEN  $U^{234}$  AND  $U^{238}$  IN SECONDARY URANIUM  
MINERALS OF SOME HYDROTHERMAL DEPOSITS

(UDC 553.495)

P. I. Chalov, Ya. A. Musin, T. V. Tuzova, and K. I. Merkulova

Translated from *Atomnaya Énergiya*, Vol. 19, No. 1,  
pp. 82-84, July, 1965

Original article submitted September 9, 1964

According to the mechanism assumed to explain disturbances of isotope equilibrium between  $U^{234}$  and  $U^{238}$  in natural conditions [1], we should not expect the  $U^{234}/U^{238}$  ratio to deviate much from the equilibrium values for secondary uranium minerals in hydrothermal deposits. The results of [2] mainly confirm this thesis. The isotope ratio  $U^{234}/U^{238}$  has been further studied in uranium minerals in [3, 4].

In this report we compare the  $U^{234}/U^{238}$  ratios in secondary uranium minerals from two hydrothermal deposits which differ in the composition of the substance surrounding the uranium mineralization, and in consequence have two different types of oxidation zone [5]—mica and silicate-mica.

After preliminary separation of uranium and purification from other radioactive elements, the  $U^{234}/U^{238}$  ratio of the minerals was determined by  $\alpha$ -spectrometric measurements, using an ionization  $\alpha$ -spectrometer with resolution 60-70 keV (half-width) for the uranium isotope lines. The results were processed by the usual system for measurements of varied accuracy [6, 7].

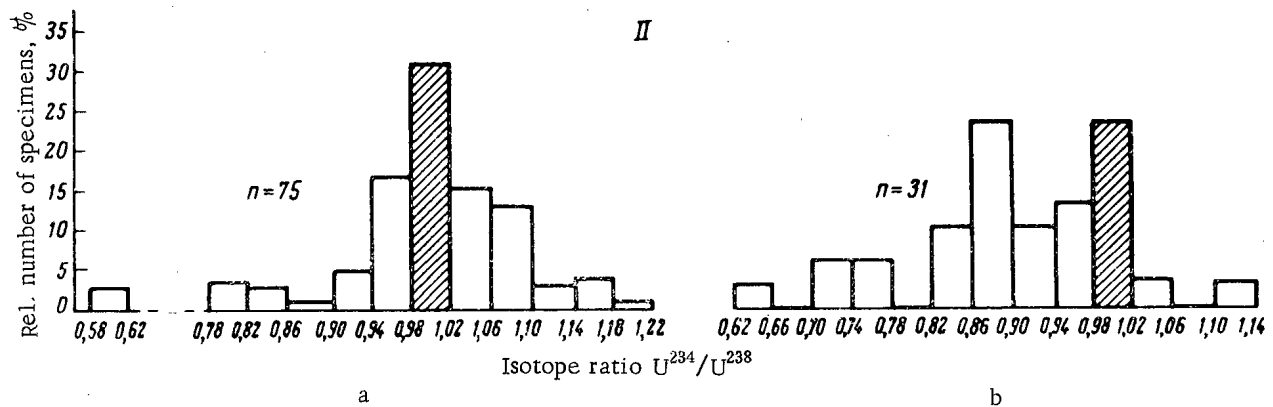
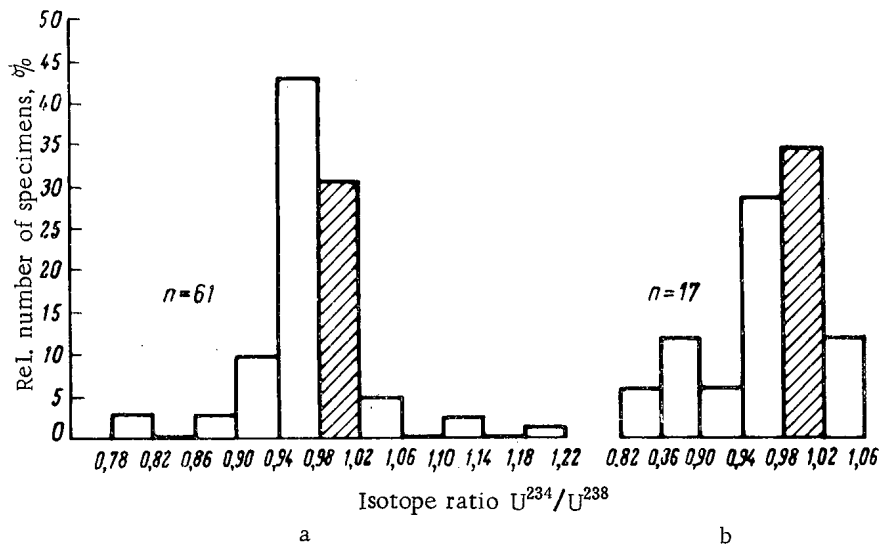
The isotope ratio was studied for 184 specimens of uranium minerals. The results are shown in the diagram as histograms of the distribution of the isotope shift. On the horizontal axis are plotted ranges of isotope shift, and on the vertical axis the relative numbers of specimens with  $U^{234}/U^{238}$  ratios in these ranges. The range 0.98-1.02 corresponds to the equilibrium ratio, as the greatest error in determining the isotope ratios was 2%.

Deposit with mica oxidation zone. In the oxidation zone of this deposit there are two main secondary minerals—autunite and metatorbernite; in the cementation zone are small quantities of residual and redeposited uranium oxide minerals.

In the majority of cases, the redeposited minerals of the deposit (see figure, I a) are characterized by equilibrium or slight deficiency of  $U^{234}$ ; only about 8% have excess  $U^{234}$ . The maximum number of specimens occurs in the range with isotope ratio between 0.94 and 0.98. The residual oxide minerals are characterized roughly by the same distribution of isotopes ratios (see figure Ib), differing only in the fact that the maximum number of specimens lies in the equilibrium range.

Before going on to consider the results, we shall note that the formation of equilibrium redeposited minerals from pitchblende or other equilibrium minerals is possible only by the latter's complete solution, as selective leaching leads, on the one hand, to the formation of redeposited minerals with isotope ratio  $U^{234}/U^{238}$  greater than unity, and, on the other, to deficiency of  $U^{234}$  in the leaching substance. Thus the data enable us to conclude that in this deposit the disintegration of pitchblende in supergene conditions took place preferentially by solution, and not by selective leaching. As a result, for the secondary minerals the oxidation zones at the moment of formation were equilibrial in the uranium isotopes. In some cases (about 30%), this ratio has been preserved to the present day, while in others there has been depletion of the secondary minerals'  $U^{234}$  owing to leaching of uranium after their formation.

This conclusion, following from an examination of isotope shift in the minerals, corresponds to geochemical conditions characteristic in general of deposits with mica oxidation zones, and in particular of the deposit here studied. In similar deposits, pitchblende is accompanied by large amounts of sulfides, so that during oxidation of the primary ores all the conditions favor the abundant formation of sulfuric acid. The latter can completely decompose pitchblende, preventing the separation of the uranium isotopes during transition to the liquid phase.



Distribution of  $U^{234}/U^{238}$  ratio of secondary minerals for deposits with mica (I) and silicate-mica (II) oxidation zones (n = number of specimens analyzed). a) Redeposited minerals; b) residual uranium oxide minerals.

Deposit with silicate-mica oxidation zone. The oxidation zone of this deposit reveals uranophane, and less widely distributed, autunite, tyuyamunite and phosphorus-arsenic uranites, and also residual uranium oxide minerals. In the redeposited minerals there is almost symmetrical distribution of isotope shift, with maximum in the equilibrium interval (see figure IIa). The equilibrium isotope ratio is seen in about one third of the specimens. For most of the residual uranium oxide minerals (about 70%) the  $U^{234}/U^{238}$  ratio is less than unity, while about 25% are equilibril (see figure IIb).

These data lead to the conclusion that in the second deposit uranium is widely leached not only out of the secondary minerals but also out of the pitchblende. This is evidently caused by the very small sulfide content in the primary ores of the deposit with silicate-mica oxidation zone, as a result of which sulfate decomposition of the pitchblende is not predominant.

Thus, in the deposit with mica oxidation zone, the redeposited minerals are most often characterized by deficiency of  $U^{234}$ , and in the deposit with silicate-mica oxidation zone by excess of  $U^{234}$ . Evidently the  $U^{234}/U^{238}$  ratio in the secondary minerals was, at the time of their formation, equilibril in the first deposit, but in the second deposit was preferentially characterized by excess of  $U^{234}$ . On subsequent leaching of  $U^{234}$  out of the redeposited minerals of both deposits, much more time (other things being equal) was naturally required to reduce the  $U^{234}/U^{238}$  ratio to below unity in minerals from the deposit with silicate-mica oxidation zone.

In characterizing the processes involved in disintegration of the primary uranium mineralization, the varying distribution of isotope shift in the residual uranium oxide minerals in the deposits is very significant. Most of the residual oxide minerals in the deposit with mica oxidation occur in or close to the equilibrium range (0.94-0.98), whereas for the deposit with silicate-mica oxidation zone, we find a marked scatter of isotope shift towards deficiency of  $U^{234}$ .

The data given show that in the supergene zone of hydrothermal uranium deposits, disintegration of pitchblende can take place in two ways, according to the geochemical conditions: either by complete solution of the mineral, or by prolonged selective leaching out of uranium. Predominance of one or other of these routes leads to a corresponding distribution in the isotope shift between  $U^{234}$  and  $U^{238}$  in the secondary minerals: this can act as an indication of the processes which took place during decomposition of the primary mineralization.

## LITERATURE CITED

1. V. V. Cherdyntsev, In "Proceedings of Third Session of Commission to Determine the Absolute Age of Geological Formations" [in Russian], Moscow, Izd-vo AN SSSR (1955), p. 175.
2. P. I. Chalov, "Geokhimiya," No. 2, 165 (1959).
3. Yu. V. Gromtsev et al., In "Topics in Ore Radiometry", ed. by V. L. Shashkin [in Russian], Moscow, Gosatomizdat (1962), p. 238.
4. K. E. Ivanov and R. K. Kudryashova, In symposium, "Topics in Applied Radiogeology", ed. by D. Ya. Surazhskii [in Russian], Moscow, Gosatomizdat (1963), p. 244.
5. G. S. Gritsaenko et al., In "Proceedings of Second International Conference on the Peaceful Uses of Atomic Energy", reports by Soviet scientists [in Russian], Vol.3, Moscow, Atomizdat (1959), p. 127.
6. A. Worthing and J. Heffner, Methods of Processing Experimental Data [Russian translation], Moscow Izd-vo inostr. lit. (1949).
7. B. M. Shigolev, Mathematical Treatment of Observations [in Russian], Moscow, Fizmatgiz (1962).

MEASURING LOW RADIUM ACTIVITIES BY MEANS  
OF A SCINTILLATION CHAMBER WITH AN ELECTROSTATIC FIELD

(UDC 543.52)

L. V. Gorbushina, G. S. Semenov, and V. G. Tyminskii

Translated from *Atomnaya Énergiya*, Vol. 19, No. 1,  
pp. 84-86, July, 1965

Original paper submitted October 31, 1964; revised January 25, 1965

The development of nuclear engineering has created the problem of determining small amounts of the isotopes of radium and its decay products in natural water or industrial effluent, or in the air of industrial buildings [1-4]. The sensitivity of commercial apparatus used to determine the activities of natural or artificial  $\alpha$ -radiators (emanation or aerosol) is often insufficient for this purpose [1]. One way of increasing the sensitivity of these devices is linked with the possibility of improving the sensitivity and efficiency of a scintillation chamber in detecting alpha radiation from the decay products of radon. For this purpose it is necessary to set up an electrostatic field inside the chamber and to make certain changes in the geometry of the detector's sensitive surface [3, 4].

The scintillation chamber with electrostatic field has the shape of a truncated cone, one end of which closed by a glass, the other being insulated from the chamber walls and kept at a negative potential. A positive potential is applied to the chamber walls (Fig. 1).

The  $\alpha$ -particle detector is zinc sulfide activated with silver (type K-9), which is applied to the insulated end face and inner surface of the chamber (except for the inspection glass); the zinc layer is less than  $30 \text{ mg/cm}^2$ . The charge atoms constituting the decay products of emanation (or other aerosols) are precipitated from the gas by the electrostatic field. The short-lived products of emanation decay are mainly charged positively at the moment of their formation: to collect them on the insulated end face this must therefore be charged negatively.

Experiments showed that the end face (the area of which constitutes 21% of the sensitive surface of the chamber) collects about 60% of the decay products of radon, thus making light collection possible. It is obvious that the efficiency of the  $\alpha$ -radiation from radon is independent of the applied voltage, since the emanation atoms are not linked with the aerosols and are uncharged. However, for charged aerosols in a chamber with an electrostatic field, the efficiency does depend on the voltage. This relation is plotted in Fig. 2, in which the abscissae are values of the negative potential applied to the end face of the chamber, and the ordinates are values of the efficiency for  $\alpha$ -radiation (K).

K increases as the potential is raised to 100 V, and then, up to 400 V, remains practically constant. At high voltages (1-2 kV) on the collector electrodes of the scintillation chamber, K may possibly increase somewhat owing to the registration of recoil atoms. In the first variant we chose an optimum potential applied to the end face (100 V). In this case, the effective recombination probability is small and lies below the statistical accuracy of measurement.

Characteristics of Various Chambers

Chamber type	Volume	Electrostatic field	Efficiency for $\alpha$ -radiation, %	Contribution of radon decay products to total count rate of $\alpha$ -emitters, %	Sensitivity, pulses/min per $10^{-10}$ curie radon
Standard	0.6	Absent	47	70	350
Non-standard	1.1	Same	43	75	290
Non-standard	1.1	Present	65-70	85	430

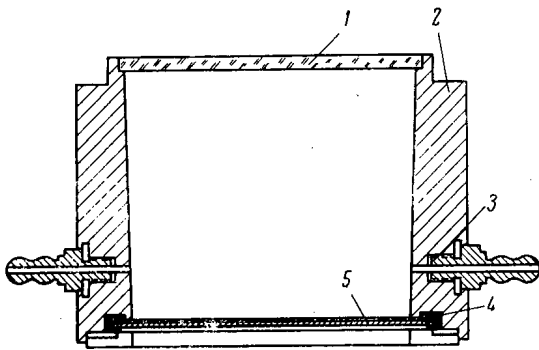


Fig. 1. Schematic cross section of chamber. 1) In-pection glass; 2) casing; 3) taps for introducing emanation; 4) insulating washer; 5) insulated face.

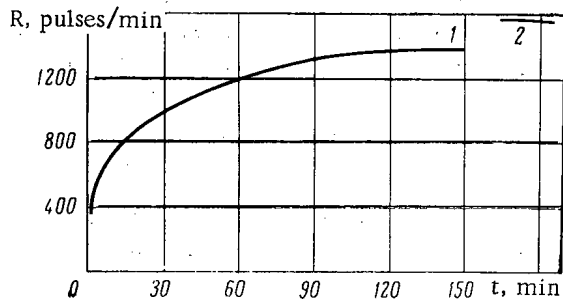


Fig. 3.  $\alpha$ -particle count rates for equilibrium radon before and after application of potential to chamber (curves 1 and 2, respectively).

by 57% of the original value. Figure 3 is a standardization curve for the RAL-1 device with a special chamber but without the electrostatic field. After 2.5 h, when radon was in equilibrium with its decay products, the voltage was connected to the chamber and the count rate rose abruptly owing to the increase in the efficiency of registration of  $\alpha$ -radiation from the radon decay products.

In order to determine the contributions made by radon and its decay products to the total  $\alpha$ -radiation of the equilibrium radon, 2.5-3 h after the radon was placed in the chamber (with or without field) the residual radon was pumped out and the activity of the decay products measured. As the decay products were firmly attached to the chamber wall, this measurement determines the amount of RaA, RaB, and RaC.

Similar experiments were performed repeatedly, and from their results were constructed average curves for the activity in standardized chambers with and without electrostatic fields, and also decay curves for the  $\alpha$ -activity of the decay products of radon after the emanation is pumped out of the chamber (Fig. 4). Here the abscissae are times, the ordinates are the measured activities. The origin (point 0) corresponds to the time of introduction of the radon to the chamber, the point 0' to beginning of measurement of the decay-product activity after pumping out the radon. Curves 1 and 1' were plotted with the electrostatic field, curves 2 and 2' without it. It was found that the contribution of the decay products to the measured total activity was about 80-85% with the field, and 75% without it (see table).

The background count for the chamber with electrostatic field was 1-3 pulses/min and increased somewhat after repeated use of the chamber owing to long-lived  $\alpha$ -emitters. With small amounts of radon, increase of background due to polonium does not take place at once. For complete decay of RaA, RaB, and RaC deposited on the chamber walls, it is sufficient to wait 5 h after a measurement.

The sensitivity of the scintillation chamber without the field is 290 pulses/min per  $10^{-10}$  curie radon, and with the field it increases to 430 pulses/min per  $10^{-10}$  curie radon. This increase, due to the presence of the field and a

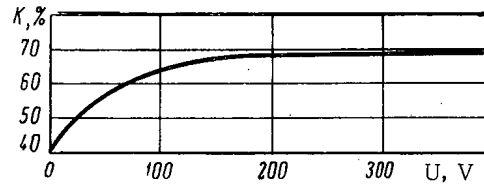


Fig. 2. Efficiency of scintillation chamber for  $\alpha$ -radiation, plotted against potential.

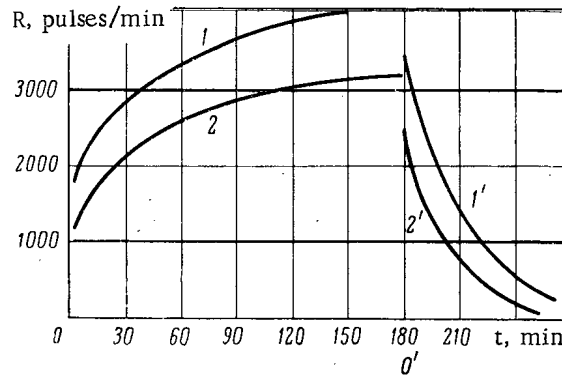


Fig. 4. Variation of  $\alpha$  count in standardized chamber with and without electrostatic field, and decay curves for  $\alpha$ -activity of decay products after removal of emanation from chamber.

From Fig. 2 it is seen that the efficiency of the chamber for  $\alpha$ -radiation rose from 43% without the electrostatic field to 65-70% with the field, i.e., on average,

slight increase of the chamber volume, is very significant, as the sensitivity of a counter of type RAL-1 with a standard scintillation chamber is 300 -350 pulses/min per  $10^{-10}$  curie radon.

Thus the sensitivity of any device with an  $\alpha$ -scintillation emanation chamber can be increased by slightly changing its construction and using an electrostatic field.

In conclusion the authors would like to thank V. L. Shashkin for helpful advice and assistance with the work.

#### LITERATURE CITED

1. V. A. Shashkin, Methods of Analyzing Natural Radioactive Elements [in Russian], Moscow, Gosatomizdat (1961).
2. H. Lucas, Rev. Scient. Instrum., 28, 680 (1957).
3. M. Curie, Radioactivity [Russian translation], Moscow, Fizmatgiz (1960).
4. A. Collinson and A. Hagne, Rev. Scient. Instrum., 40, 521 (1963).



## RADIATION CONDITIONS NEAR A VVR-M NUCLEAR REACTOR

(UDC 621.039.58)

P. V. Ramzaev, I. A. Belyaeva, V. N. Gus'kova, M. S. Ibatullin,  
Yu. O. Konstantinov, S. P. Nikolaev, and A. F. Oreshina

Translated from *Atomnaya Énergiya*, Vol. 19, No. 1,  
pp. 86-89, July, 1965

Original article submitted July 20, 1964

Practice in the use of research reactors in the USSR has shown that special attention is required only by gaseous radioactive waste, since the localization of liquid and solid wastes has been successfully dealt with. The system of collection and removal of liquid and solid wastes, with centralized burial sites, eliminates contamination of the biosphere, provided that certain rules are observed [1, 2]. Hence, the radiation conditions in the regions round research reactors are practically entirely determined by gaseous and aerosol discharges. These arise during ventilation of the cavities and channels of the reactor, pumping of the primary circuit, ventilation of cavities containing liquid wastes, and especially during de-aeration of water from the primary circuit to free it from oxyhydrogen gas. Fitting reactors with closed de-aeration circuits, and burn-up of oxyhydrogen gas, reduces the discharge of radioactive gases and aerosols through the ventilation system by a factor of more than 10; in our opinion, this adequately reduces the radioactivity of the air in the vicinity.

During the operation of a nuclear reactor with sealed fuel cans and efficient trapping of the disperse phase (aerosols) from the air released through the ventilation shaft, the radioactivity of the external medium is almost entirely due to  $\text{Ar}^{41}$  (if we neglect the exceedingly short-lived oxygen activity [3]). This isotope is formed by activation of  $\text{Ar}^{40}$  in the primary-circuit water and air spaces irradiated by neutron fluxes. The chemical inertness of argon prevents it from being accumulated in an organism or migrating along a biological chain [4]. The radiation hazard of  $\text{Ar}^{41}$  is therefore due to external  $\gamma$ -radiation; this facilitates monitoring of the external medium and reduces the possible dose acquired by the population.

If the sealed fuel cans leak, the wastes will contain fission products as well as  $\text{Ar}^{41}$ , and also (at first) radioactive isotopes of inert gases (xenon and krypton) and of iodine. Other fission products may also possibly be discharged into the atmosphere as aerosols, especially if filtering equipment is absent or inefficient.

Continuous monitoring of the relative activity of the primary-circuit water and waste, which is used in all Soviet research reactors, is very efficient and enables leaky fuel elements to be promptly removed from the core. On the whole, we failed to find fission products from the reactor ( $\text{I}^{131}$ ,  $\text{Sr}^{89}$ ,  $\text{Sr}^{90}$ ,  $\text{Cs}^{137}$ ,  $\text{Ce}^{144}$ , and  $\text{Y}^{91}$ ) in the external medium. A typical example is afforded by the results of some observations in an area of radius 20 km round a VVR-M research reactor of power 10 megawatts (see Fig. 1 and table). The physical and technical characteristics of the reactor are given in detail in [5].

From Fig. 1 and the table, it is seen that the fallout intensity of long-lived radioactive isotopes (total  $\beta$ -activity and  $\text{Sr}^{90}$ ) is approximately the same both near the reactor and at distant control points. This fallout is world-wide and its dynamics correspond to those of nuclear testing. Similar results were obtained from analyses of soil, vegetation, water and air for  $\text{Sr}^{90}$ ,  $\text{Sr}^{89}$ ,  $\text{Cs}^{137}$ ,  $\text{Ce}^{144}$ ,  $\text{Y}^{91}$ , and  $\text{I}^{131}$  and for total  $\alpha$ - and  $\beta$ -activity. The organization of safety zones around nuclear reactors gives an additional guarantee of the safety of the population, both during normal working and in an emergency. It must be noted that in the Soviet Union we have never had a single emergency in a research reactor which was accompanied by any appreciable contamination of the external medium whatever. In our opinion, the safety zones are therefore of more practical value during normal working of the reactor. Gaseous discharges from the ventilation shaft, encountering atmospheric currents, are scattered and form a discharge jet. Both the shape and size of the jet's projection on the local map and its radiation characteristics are very variable, and depend on the meteorological conditions, the height of the shaft, the rate of discharge and other factors.

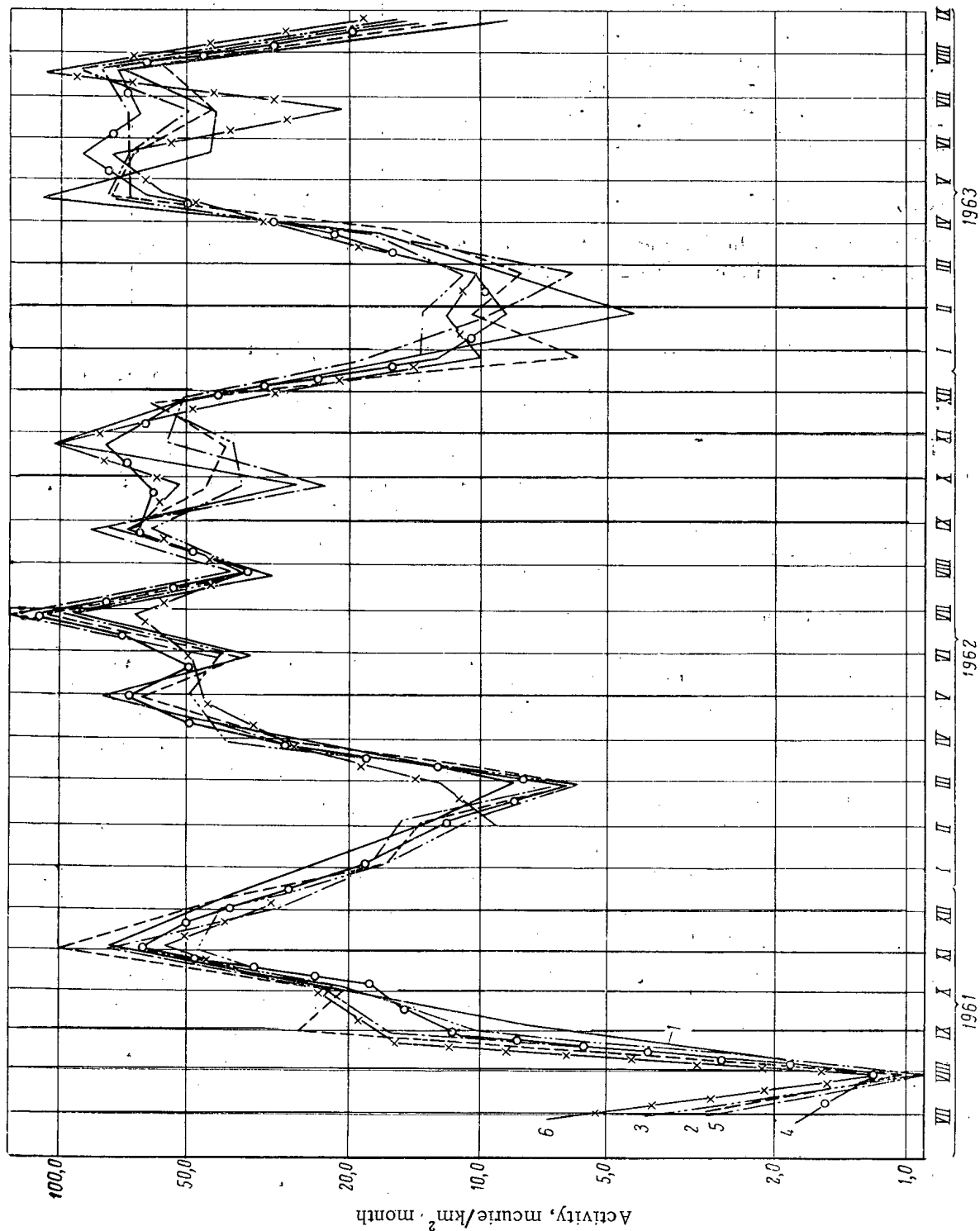


Fig. 1. Intensity of radioactive fallout (measured by total  $\beta$ -activity) in the vicinity of VVR-M nuclear reactor. Sample containers exposed monthly round perimeters at following distances from reactor: —○—) 2 km; - - -x - - -) 4 km; —x—) 20 km; —) 100 m; - - -) 500 m; ····) 1 km; —x—) 1 km.

Intensity of  $\text{Sr}^{90}$  Fallout Near VVR-M Reactor, mcurie/( $\text{km}^2 \cdot \text{month}$ )

Distance from reactor, km	Fallout intensity				Total of 16 months
	June-November, 1961	December, 1961 to April, 1962	May-August, 1962	September, 1962	
0.1	$\leq 3 \cdot 10^{-3}$	$2.5 \cdot 10^{-2}$	0.8	1.5	4.8
0.5	$\leq 3 \cdot 10^{-3}$	$0.7 \cdot 10^{-2}$	0.4	1.4	3.1
1.0	$\leq 3 \cdot 10^{-3}$	$2.7 \cdot 10^{-2}$	0.3	0.8	2.1
2.0	$\leq 3 \cdot 10^{-3}$	$5.1 \cdot 10^{-2}$	0.8	0.9	4.3
4.0	$\leq 3 \cdot 10^{-3}$	$2.4 \cdot 10^{-2}$	0.4	0.6	2.3
20.0 (Control)	$\leq 3 \cdot 10^{-3}$	$1.1 \cdot 10^{-2}$	0.3	2.3	3.6

Note. The errors of individual measurements are estimated at  $\pm 50\%$ . Six fallout samples were taken each month at each distance in the table.

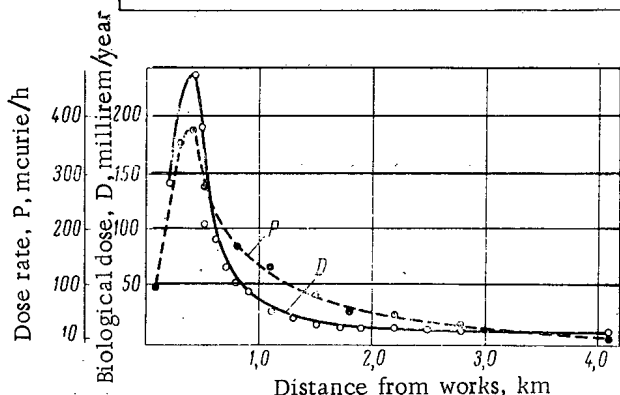


Fig. 2. Maximum  $\gamma$ -dose rate, P, and yearly biological dose, D, in district to lee side of VVR-M reactor without closed de-aeration circuit (dose from natural background excluded).

doses in the locality, given in this figure, were calculated for the prevailing wind direction, allowing for the actual operation of the reactor (working times and mean power 5 MW). From Fig. 2 it is seen that, even in the worst case, the boundary of the permissible dose (50 millirem/year) is about 1 km from the reactor on the leeward side. With lower discharge rates, this boundary moves closer to the reactor, and, when the closed de-aeration circuit is operating, the dose rate in the locality, even on the leeward side, nowhere reaches the limiting level and scarcely exceeds the natural background level by more than 2-4 mcurie/h.

For non-emergency operation of a nuclear reactor, the size of the safety zone must clearly be at least equal to the distance of the boundary corresponding to the limiting yearly dose of radiation. In practice, in choosing a site for a reactor it is difficult to take account of all the conditions influencing the limiting-dose boundary, so that the associated errors may be very great. For this reason, the sizes of safety zones in the Soviet Union are fixed only for the worst operating conditions, according to the type and power of the reactor. At the same time, the discharge of individual isotopes is limited [1, 2].

Guided by considerations of maximum care, and assuming that there is no threshold for genetic damage, we can make the most rigorous approach to determine the size of the safety zone: within it, the permissible hourly dose rate must not be exceeded. This approach facilitates dosimetric control.

From Fig. 2 it is seen that, for the VVR-M reactor, the boundary of limiting hourly dose rate occurs at a distance three or four times greater than that for the yearly dose rate. It is very desirable that this should be allowed for when building new reactors. As regards existing equipment, it is reasonable to employ technical methods for reducing the amount of discharge of radioactive isotopes to the locality.

The presence of  $\gamma$ -emitters (e.g.,  $\text{Ar}^{41}$ ) in the discharge enables us to use  $\gamma$ -counters to make rapid and fairly accurate determinations of the approximate projection of the jet on the locality. According to our observations, the radioactive jet can be recorded by existing  $\gamma$ -dosimetry methods up to 3.5 or 4 km from the discharge point (for a VVR-M reactor working at 10 MW with shaft height 60 m, and without a closed de-aeration circuit). The width of the jet is 300-1000 m, and its projection on the locality resembles an open fan.

For the reactor mentioned above, the greatest  $\gamma$ -dose rate, recorded on the axis of the jet, was 380 mcurie/h at 400 m from the shaft. Figure 2 gives the results of systematic dosimetry of the discharge jet in 1962 for the VVR-M reactor. The yearly biological

The isotope composition ( $\text{Ar}^{41}$ ) of the discharge, and also our observations on the components of the radioactive contamination of the soil, vegetation and water, enable us to use the safety zone territory round a research reactor (which in essence is a source of external radiation only by radioactive inert gases) for agricultural purposes. We can see no serious reason why this territory should not be used to grow crops (e.g., grain), but for safety purposes the harvest should be subjected to radiometric monitoring.

#### LITERATURE CITED

1. Health Rules for Planning and Operation of Nuclear Research Reactors No. 420-62 [in Russian], Moscow, Medgiz (1963).
2. Health Rules for Planning and Operation of Nuclear Power Stations, No. 392-62 [in Russian], Moscow, Medgiz (1962).
3. Yu. V. Sivintsev et al., *Atomnaya énergiya*, 10, 253 (1961).
4. Yu. V. Sivintsev, *Ibid.*, p. 631.
5. L. I. Rusinov et al., in "Proceedings of Second International Conference on the Peaceful Uses of Atomic Energy," reports of Soviet scientists [in Russian], Vol.2, Moscow, Atomizdat (1959), p. 293.

## SCIENCE AND ENGINEERING NEWS

### COLLABORATION OF THE SOCIALIST COUNTRIES IN NUCLEAR POWER DEVELOPMENT

Translated from Atomnaya Énergiya, Vol. 19, No. 1,  
p. 90, July, 1965

The first session of the working team on reactor science and reactor engineering and nuclear power was held in April 1965 at Dubna. The need to set up such a group under the aegis of the Permanent Commission on the Uses of Atomic Energy for Peaceful Purposes of the Council for Mutual Economic Aid [COMECON], capable of effectively expediting the coordination of the efforts of member-nations of COMECON in the field of reactor design and nuclear power engineering, arose in line with the common interest of nations of the socialist camp in the use of atomic energy to satisfy the continually and rapidly growing need of COMECON nations for electrical and heating power.

Participating in the sessions of this working team were specialists from Bulgaria, Hungary, East Germany, Poland, Rumania, the USSR, and the Czechoslovak Socialist Republic. Topics discussed included the 1965 plans of the working team, projects for planning and coordinating scientific and engineering research for the 1966-1967 period in the nuclear power field, and several others.

Delegates taking the floor stressed that extensive and intensive research underway in COMECON countries in reactor engineering, based on the science and research centers built in these countries in recent years, requires continual and effective coordination of work, mutual exchange of information, exchanges of field experience, correlation and synchronization with nuclear power development plans, for effective saving in forces, materials, and time. Priority is being given to nuclear power cost problems, since the tempo of nuclear power development and the effect brought about by the increased use of nuclear power in each country will depend in large measure on how suitable the choice of reactor types for nuclear power stations has been, what engineering cost advances have been achieved in power reactors to assure the gradual displacement of conventional fossil fuels by nuclear fuel in the total power picture of the COMECON nations. Practical measures were drawn up by the team as part of the solution of these problems, and prominent among these measures is the assignment of a minimum power generation cost savings level for nuclear power stations.

Some delegates also remarked that the general problem of work in the field of power reactor design is that of building and learning how to operate nuclear power stations based on fast reactors, long-term operation of which is independent of the initial fissionable materials employed. It is felt, however, that in the first stages of nuclear power development the coordinated efforts of member-nations of COMECON will be directed primarily toward the building of low-cost nuclear power stations based on thermal reactors.

There was confirmation of the general views shared by all the delegates on the basic trends in nuclear power development work. The discussion took place in a setting of comradeship and friendship.

After the sessions had been completed, the team members visited a few laboratories of the Joint Institute for Nuclear Research, where they were brought up to date on the nuclear physics facilities available there.

It can be stated without hesitation that the act of setting up this team on reactor science and engineering and nuclear power, and its first steps forward, characterize a new stage in the coordination of work and research in the member-nations of COMECON.

A MEETING OF IAEA EXPERTS ON NUCLEAR WATER DESALINIZATION

A. Loginov

Translated from Atomnaya Énergiya, Vol. 19, No. 1,  
pp. 90-93, July, 1965

The fifth conference of experts on nuclear power applications in water desalination met in Vienna in April 1965. The conference, called and sponsored by IAEA, attracted representatives of 17 countries, as well as from the UN and the IAEA itself.

Topics on the agenda of the conference were: a) a survey of various water desalination techniques; b) a review of results of a study of dual-purpose desalination plants using different types of reactors and conventional boilers; c) analysis of the potentialities of dual-purpose plants based on desalination techniques; d) single-purpose desalination plants using nuclear reactors; e) water desalination economics; f) survey of programs and projects drawn up by member-nations of the IAEA; g) the IAEA program in nuclear desalination.

Over 20 papers and reports were submitted to the conference.

A reasonable conclusion from the papers, statements, and discussions at the conference is that distillation techniques show the best promise in being sufficiently well developed and reliable for plants using nuclear sources of process heat at present and in the immediate future. But it would still be advisable to search out and investigate rival desalination techniques such as freeze-trapping, membrane technology, electrodialysis, and so forth.

It was stated that the choice of engineering characteristics must be based on a thorough analysis of the engineering cost picture of the desalination plants themselves.

A survey of the results of a study of dual-purpose desalinating plants employing different types of process heat sources revealed that the entire water supply complex of a concrete region as a whole, including the transportation or piping of the treated water to the consumer, must be considered in deciding plant performance characteristics.

Comparisons of dual-purpose plants using two methods of water supply showed that successful use of high-capacity desalination plants on a wide scale is still a long way off. The unit thermal rating of 2-3 thousand MW appears to be the most common one at present. As unit power is increased further, the problem of transporting the desalinated water to the consumer will come to the fore, and this will require additional capital investments.

Attainable steam heating temperatures run to 120°-130°C at the present time; attempts to find ways of raising the temperature are being pursued.

The report by the French delegation made it clear that expenditures on the evaporator plant take up a considerable fraction of the total capital invested in desalination facilities, and the vertical-tube evaporators are cheaper than flash evaporators, which hold out more promise in terms of expandable output. Close attention is being given to transients in the operation of dual-purpose plants. It is felt that a condenser-turbine loop might meet many of the requirements.

Reports by USA delegates cited cost data on nuclear dual-purpose desalination plants (Table 1) and desalination-only plants (Table 2).

Analysis of the market shows that in the immediate future there will be a demand for desalination plants of capacities up to 75,000 cubic meters daily, while larger plants will be needed only in a few regions.

The discussion made repeated mention of the fact that dual-purpose plants are the most promising ones, since they best answer the combined needs for fresh water and electric power. The Canadian heavy-water reactor was discussed in this context.

TABLE 1. Cost of Processed Water (cent/3.8 m<sup>3</sup>) Obtained from Dual-Purpose Plants ( $\varphi = 7000$  h/yr)

Electric power costs, c/kWh	Percent capital investment, %	From initial steam temperature to 320° C at thermal power (MW)				From initial steam temperature to 540° C at thermal power (MW)			
		200	600	1000	1500	200	600	1000	1500
Fossil-fueled plant									
0,365	7	55,1	44,0	43,0	40,8	58,0	42,3	41,6	38,4
	14	83,3	62,8	62,3	58,6	90,6	65,0	62,7	58,9
0,40	7	54,6	42,9	42,4	39,8	56,6	40,3	39,4	36,4
	14	82,4	61,7	61,0	57,4	89,1	63,0	60,3	57,9
0,60	7	51,5	36,5	35,6	33,0	48,9	28,8	24,1	22,9
	14	77,1	54,8	52,3	51,4	79,2	50,8	44,1	41,6
0,80	7	46,7	28,7	26,6	26,4	—	—	—	—
	14	71,2	47,0	41,9	40,8	68,1	—	—	—
1,0	7	43,4	—	—	—	—	—	—	—
	14	64,7	37,6	30,3	—	53,1	—	—	—
1,20	7	—	—	—	—	—	—	—	—
	14	54,8	—	—	—	—	—	—	—
Nuclear-reactor plants									
0,365	7	66,0	39,2	34,7	29,6	—	42,7	37,4	32,8
	14	—	69,3	62,4	54,1	—	79,9	72,4	63,9
0,40	7	65,5	38,2	33,5	29,0	—	40,7	34,8	30,6
	14	—	68,5	61,4	52,9	—	78,4	70,6	61,9
0,60	7	62,6	32,4	25,8	21,9	69,2	29,2	—	—
	14	—	63,6	54,4	47,8	—	68,5	57,7	49,8
0,80	7	59,2	25,2	—	—	60,8	—	—	—
	14	—	57,7	45,7	37,7	—	56,6	40,5	27,9
1,0	7	54,9	—	—	—	51,1	—	—	—
	14	100,9	51,1	36,2	—	—	41,6	—	—
1,20	7	50,3	—	—	—	33,9	—	—	—
	14	97,6	44,1	—	—	103,1	—	—	—

TABLE 2. Cost of Processed Water (cent/3.8 m<sup>3</sup>) from Single-Purpose Plants ( $\varphi = 7000$  h/yr)

Cost of purchased electric power, cent/kWh	Percent capital investment, %	From initial steam temperature to 320° C at thermal power (MW)				From initial steam temperature to 540° C at thermal power (MW)			
		200	600	1000	1500	200	600	1000	1500
Fossil-fueled plants									
0,6	4	48,2	42,5	40,2	39,8	49,1	43,0	40,7	40,2
	7	58,2	50,5	48,1	47,6	59,8	51,6	49,0	48,4
	14	79,7	67,4	64,7	64,1	83,1	69,9	66,7	66,0
Nuclear-reactor plants									
0,6	4	49,9	35,2	30,8	29,4	55,8	39,9	35,7	34,0
	7	65,6	45,8	40,8	38,3	72,4	51,8	46,6	44,3
	14	—	71,9	63,9	59,7	—	80,3	72,7	68,9

Italian delegates showed particular interest in the development of single-purpose desalinization plants. Southern Italy is currently experiencing an acute shortage of fresh water (running at 150,000 cubic meters daily). A desalinization plant of 6000 m<sup>3</sup> per day capacity powered by fossil fuels is currently in operation in Italy. The feeling is that the low-temperature organic-fueled organic-moderated reactor with aluminum-clad fuel will be the best reactor type for satisfying Italy's fresh water needs. A study is being made of the possible construction of a desalinization-only plant based on an organic-fueled organic-moderated reactor of 100 MW thermal rating (to be stepped up eventually to 200-300 MW).

The consensus of views is that this reactor type is quite suitable for low-capacity desalinization-only plants.

The conference noted the many approaches open in distributing expenses between electric power and water in desalinization process costs and in estimating capital expenditures and yearly production costs in dual-purpose facilities. The gist of the method employed in the USA is to consider fixed electric power costs as a by-product of the dual-purpose desalinization plant. At the same time, in the USSR equal importance is attached to electric power production and fresh water production from an economic standpoint, and this requires a rigorous distribution of production costs between the two aspects of production, under the assumption that the power source may be greater when used to produce electric power alone than when used in a dual-purpose plant. Facing these diametrically opposed approaches to estimating production costs in dual-purpose desalinization plants, we see that quantitative cost factors are not useful for comparison.

IAEA intends to prepare a report on the various methods used in estimating electric power costs and processed water costs, as part of its program of rendering assistance to member nations in the evaluation of nuclear desalinization plant projects.\*

Proposals on elaboration of a suitable method of cost calculations are to be found in the UNO papers. These contributions took up cost items to be considered in estimating desalinization process costs. Recommendations were given on approximate estimates for dual-purpose and single-purpose plants. The contribution also included a survey of engineering and cost factors relating to the choice and operation of desalinization plants (proper siting, soil requirements, collection and conveying of water, disposal of wastes, exploitation of by-products, etc.). Here some specific problems came into focus, of particular interest to developing nations undertaking desalinization programs, such as: inadequate training and skills in available work force, difficulties in obtaining replacements or in overhauling equipment in time to forestall shutdowns, and the need for exchange of experience with other nations on a wide scale.

Programs and projects undertaken by member nations of IAEA in utilization of nuclear reactors for water desalinization were heard at the conference.

An announcement was made of an agreement reached between the USSR and the USA in water desalinization, including the use of atomic energy, and of an agreement between the USA and Israel for a joint research program in this field.

A report by the Economic and Social Council of the UNO on desalinization of water in developing nations was heard; particular emphasis was placed on estimates of desalinization plants. The report covers siting and construction conditions for desalinization plants in 43 countries, analyzes 61 operating desalinization plants, and 19 new plants to be built. The perspectives and engineering feasibility of desalinization plant construction are being studied.

The presentation of the US desalinization technology development program noted that research on the reactor aspect of the program is being carried on by private firms under the leadership and guidance of the USAEC. Research centered on the desalinization facilities proper is handled by the Department of the Interior and the Office of Saline Water jointly. The USA intends to build two prototype plants with a heavy-water-moderated organic-cooled reactor. One plant is scheduled for completion in 1970. The thermal rating of the reactor is 1000 MW for a plant capacity of 190,000 cubic meters of processed water daily. The second plant using a 3500 MW(th) reactor is to be built by 1975. Construction of these prototype plants poses the problem of achieving commercially competitive nuclear dual-purpose plants by 1980.

Work on a desalinization plant research program is being carried out in Britain by the Atomic Energy Authority and Weir Westgarth Ltd. An AGR type reactor will be used in the desalinization plant to be sited on the sea-coast. The plant will have a capacity of  $\approx 95,000$  cubic meters a day. The research findings will be made public at the Washington October 1965 symposium. Great Britain has accumulated a lot of practical experience in the use of desalting plants, and the principal desalinization process will be distillation-flash evaporation. A recently organized Water Resources Service has the duty of coordinating its activities with those of groups interested in water desalinization. Sites suitable for desalting plants are to be selected by 1970.

Israel's desalinization program envisages the construction of dual-purpose reactor desalting plants. A nuclear desalinization plant is scheduled for completion in Israel by 1971, and is scheduled to go on stream in 1972, at full

\*The report will be published in the next issue of "Atomnaya Énergiya."



capacity. Research completed shows that dual-purpose plants may become competitive with fossil-fueled plants, under Israeli conditions, starting at 75MW units of electric power. Calculations of the cost of processed water from dual-purpose nuclear plants generating 125-200 MW electric power run to 10-12 cent per cubic meter.

Greece's desalting program calls for increasing the installed power of electric generating plants from 776 MW in 1964/65 to 2727 MW in 1974/75; the annual water consumption in the Athens region alone will increase from 99 million cubic meters in 1965 to 190 million cubic meters in 1975, going on to 254 million cubic meters in 1984. Power resources will present favorable opportunities for the utilization of dual-purpose nuclear desalting plants.

A communication from the Brazilian representative announced that the projected industrialization of the country will require a formidable back-up of power resources. By 1980, for example, the demand for electric power will be around 160 MW, and the demand for fresh water by that time will reach 300 000 cubic meters daily. Considering 50% of the power demand to be satisfied by petroleum resources, while available coal reserves are remote from the industrial centers, and of poor quality besides, nuclear dual-purpose desalting plants are expected to fill a real need. At the present time, the possibility of constructing a 60 MW(e) dual-purpose nuclear desalination plant is being studied. The cost of electric power generated by this plant would be 1.48 cent per kWh.

The United Arab Republic has been working for 50 or so years on the irrigation problem. But there remains an acute shortage of fresh water in the country. The possibility of siting the first nuclear dual-purpose desalination plant near Alexandria, with a capacity of 20,000 cubic meters processed water daily and an output of 150 MW(e), is being studied. A fossil-fueled desalting plant producing 2400 cubic meters of processed water a day is now being built.

The concluding portion of the conference of desalination experts was devoted to discussion of the IAEA program and of the IAEA role in desalination as a problem of international scope. The IAEA role was formulated in the following terms:

- a) IAEA will become an international center for the solution of problems involving utilization of nuclear power for desalting brine;
- b) aid and advice are to be made available on an organized basis to member nations;
- c) the use of nuclear power for desalination is to be encouraged;
- d) research and planning work by member nations is to be coordinated.

Conferences and engineering seminars are to be scheduled in line with realization of the IAEA program.

We note in concluding that the fifth conference of experts on the use of nuclear reactors for water desalting has made for an extensive exchange of views and experience, and has helped in drawing concrete inferences in one of the most promising trends on the horizon in the utilization of nuclear power for peaceful purposes.

INTERNATIONAL SYMPOSIUM ON CHEMICAL EFFECTS  
CAUSED BY NUCLEAR REACTIONS AND RADIOACTIVE TRANSFORMATIONS

B. G. Dzantiev

Translated from *Atomnaya Énergiya*, Vol. 19, No. 1,  
pp. 94-95, July, 1965

A symposium on the chemical effects associated with nuclear reactions and radioactive transformation was held in Vienna in December 1964, under joint auspices of IAEA and the Joint Commission on Applied Radioactivity. Representatives from 32 countries and international bodies participated in the symposium. The number of delegates totaled around 130. The Vienna international symposium is the second international gathering devoted to discussion of chemical sequelae of nuclear transformations. The first symposium on this topic was held in Prague in 1960.

70-odd reports were presented at the symposium. These can be classified for convenience under the following headings: 1) physics research on recoil atoms produced in gas-phase nuclear processes; 2) reactions of hot atoms, products of nuclear reactions, in the gaseous phase; 3) reactions of hot atoms in condensed organic systems; 4) hot-atom reactions in the solid state; 5) chemical processes in  $\beta$ -decay; 6) new techniques and research trends in chemical effects of nuclear transformations.

Four papers were submitted on the first group of topics. The findings were primarily the result of work with specially designed mass spectrometers. S. Wexler (USA) studied a reaction involving tagged methane recoil atoms ( $\text{THe}^3$ )<sup>+</sup> formed in the  $\beta$ -decay of  $\text{T}_2$ . The purpose of the research is to find an experimental basis for the mechanism of the well-known Wilzbach method (production of hydrogen-labeled organic substances by simple exposure in a tritium-containing mixture). The mechanism suggested earlier by Pratt and Wolfgang includes hypothetical ion-molecular reactions. One of the ions ( $\text{C}_2\text{H}_4\text{T}^+$ ) proposed in the  $\text{T}_2$ - $\text{CH}_4$  system was detected experimentally by Wexler. T. Carlson, and R. White (USA) artificially produced vacancies on the inner electron shells of the atom by exposure to x-radiation of predetermined energy, in order to investigate processes occurring in the wake of some radioactive transformations. The example of  $\text{CH}_3\text{I}$  revealed that an explosion of the original molecule literally occurs in response to the production of a vacancy in the L-envelope of the iodine atom and the charge redistribution between the atoms brought about by coulomb repulsion (subsequent to the Auger cascade). The mass distribution, and energy distribution of fragments of the molecule were investigated: the most probable process is  $\text{CH}_3\text{I} \rightarrow \text{C}^{2+} + 3\text{H}^+ + \text{I}^{5+} + 10\text{e}^-$ . The recoil ions are hot particles: their energies range from 10 to 100 eV. The findings shed some light on the causes of the Szilard-Chalmers effect in such radioactive transformations as K-capture.

N. Steiger (Israel) reported an experimental determination of the charge on the recoil atom resulting from a heavy-ion-initiated nuclear reaction. The object of study was the reaction  $\text{Pr}^{141} (\text{O}^{16}, 8\text{n}) \text{Ho}^{149}$ . M. Dehmer (Belgium) discussed excitation of atomic and molecular levels in nuclear recoil processes, in a theoretical paper.

The second topic was represented by 10 papers. These papers discussed gas-phase reactions of hot hydrogen (tritium) atoms, and of  $\text{C}^{11}$ ,  $\text{N}^{13}$ ,  $\text{F}^{18}$ ,  $\text{S}^{35}$ ,  $\text{Br}^{80}$  hot atoms.

F. Rowland et al. (USA) investigated isotope effects in a study of reactions between hot T atoms and both ordinary and deuterated hydrocarbons. The use of improved gas chromatography techniques enabled them to separate not only HT and DT, but also mixtures of isotope methane molecules  $\text{CH}_3\text{T}$  and  $\text{CD}_3\text{T}$ , and ethylene molecules:  $\text{C}_2\text{H}_3\text{T}$ ,  $\text{C}_2\text{D}_3\text{T}$ ,  $\text{C}_2\text{H}_2\text{DT}$ ,  $\text{C}_2\text{D}_2\text{HT}$ . The substitution  $\text{T} \rightarrow \text{H}$  is more probable than  $\text{T} \rightarrow \text{D}$  (isotope effect 1.33); in the system  $\text{T} + \text{CH}_3\text{CD}_3$ , for example, this can result in the formation of more excited ethane molecules, with HD splitting with greater ease to form labeled ethylene. D. Urch and M. Welch (Great Britain) investigated reactions of hot T atoms with saturated hydrocarbons ( $\text{C}_2$ ,  $\text{C}_4$ ,  $\text{C}_5$ ) and, with Wolfgang's kinetic theory as point of departure, determined numerical values of the I and  $\alpha$  parameters for concrete reactions.

A report by B. G. Dzantiev and A. P. Shvedchikov (USSR) put forth a view of the role of excitation of radicals as active intermediary products in hot-atom reactions. The interaction of hot hydrogen atoms with ethylene was investigated as a model. The kinetic behavior of hot hydrogen atoms of different origin was compared: these origins are in the nuclear reaction  $\text{Li}^6(\text{n}, \alpha)\text{T}$ , in radiolysis of RH, in the photolysis of HI.

The investigation of reactions involving hot carbon atoms revealed a tendency of short-lived  $C^{11}$  to replace  $C^{14}$ . The former is obtained in the nuclear reactions  $C^{12}(n, 2n)C^{11}$ ;  $N^{14}(p, \alpha)C^{11}$ ;  $C^{12}(p, pn)C^{11}$ ;  $O^{16}(p, pn)C^{11}$ , and some others. The projectiles were generated in accelerators. A modification of the method for generating hot carbon atoms resulted in substantial alleviation of radiation effects. A. Wolf et al. (USA) demonstrated that only  $C^{11}H_4$  and  $HC^{11}N$  are formed in the  $N_2-H_2$  system. Carbon-labeled acetylene, ethylene, prussic acid, are formed in excellent yields in  $N_2-RH$  systems (where the RH are saturated hydrocarbons). Hot carbon atoms react effectively with  $O_2$  to form  $C^{11}O$ . Ratios of the formation cross sections of the basic labeled reaction products were reported in the paper. The relative role of  $C^{11}$  atoms and radicals ( $C^{11}H$ ,  $C^{11}H_2$ ,  $C^{11}H_3$ ) in labeling processes are discussed.

As W. Koskie (USA) showed, hot  $N^{13}$  atoms obtained from the nuclear reaction  $C^{12}(d, n)N^{13}$  are stabilized in a hydrocarbon medium in the form of prussic acid and nitriles, but they yield nitrogen-labeled cyanogen halides in interactions with halogen derivatives. The effectiveness of removal of hydrogen atoms or halide atoms by a hot nitrogen atom (with the formation of  $N^{13}H_3$ ,  $N^{13}Cl_3$  resulting) is modest.

A paper submitted by R. Wolfgang et al. (USA) reported reactions of hot  $F^{18}$  atoms with methane. It was shown that the "kinetic theory" developed for hot T atoms is also valid for the heavier  $F^{18}$  atoms. Values of the I and  $\alpha$  parameters were determined. Restrictions of the theory in application to atoms heavier and slower than T were discussed.

K. Panek and K. Mudra (Czechoslovakia) reported on investigations of reactions of  $S^{35}$  with methane and with alkyl chlorides. L. Speiser and A. Gordus (USA) compared the reactivity of hot  $Br^{80}$  atoms obtained in various ways. The role of the kinetic energy of the  $Br^{80}$  recoil atom was noted.

Thirteen papers were contributed on the next topic, six of these by the Soviet delegation. Reactions of the hot atoms T,  $C^{11}$ ,  $C^{14}$ ,  $S^{35}$  in halides were discussed.

Papers by Ac. N. Nesmeyanov et al. (USSR) discussed reactions of the hot atoms T,  $C^{14}$ ,  $Br^{82}$  in binary organic systems. The observed nonlinear relationship between the yields of labeled reaction products and the concentration were interpreted within the frame work of current concepts on energy transfer from excited labeled molecules to molecules of components of a mixture. A. Sokolowska and A. Sijuda (Poland) attempted to give a different interpretation to this phenomenon.

J. Willard (USA) presented a survey paper on concepts offered to account for the reaction mechanism of hot halogen atoms. Experimental results on hot halogen atom reactions in organic media were presented in papers by J. Willard and R. Hahn (USA), S. Kontis et al. (Great Britain), L. Vasaros (Hungary), F. Rowland et al (USA). The last paper discussed transformations of stereoisomers as a result of hot-atom interactions, and the relationship between the stabilization probability and space isomerism. Interesting data on the effect of pressure on stabilization of hot  $Br^{80}$  atoms in liquid bromoethane are found in a paper by P. Shaw (Britain).

A. Voigt et al. (USA) reported on reactions between  $C^{11}$  hot atoms and liquid hydrocarbons incorporating  $C_5$ ,  $C_6$ ,  $C_7$  backbones. The rates of addition reactions are discussed. Two papers by B. G. Dzantiev et al. (USSR) discuss pathways of formation of radioactive polymeric products in the stabilization of  $C^{14}$  and  $S^{35}$  recoil atoms, as well as the principles underlying "hot synthesis" of  $S^{35}$ -labeled complex biologically active molecules.

Many of the papers dealt with the stabilization of radioactive recoil atoms in the solid phase (the fourth heading). The effect of many factors on the chemical fate of the atom appearing in a nuclear reaction was investigated. Such factors include: the type of crystal, lattice imperfections, the chemical form of the compound, the temperature, and the exposure dose. The effect of radiation annealing and thermal annealing was discussed extensively. Some of the more interesting reports were those of A. Maddock et al. (Britain) on the thermal annealing mechanism, G. Schmidt and W. Herr (West Germany) on substitution of ligand groups in  $Br^{80}$  hot-atom reactions, I. Dema and N. G. Zaitseva (USSR) on chemical forms of radioiodine formed by irradiation of CsCl by 660 MeV protons. A paper by H. Müller (West Germany) analyzed retention theory. G. Harbottle and W. Ts'ang (USA) reported on isotope effects in ruthenocene—a "sandwich" compound.

Several papers took up chemical effects accompanying  $\beta$ -decay (the fifth heading). A Gordus (USA) discussed the probability of breaking molecular bonds in labeled molecules in  $\beta$ -decay of  $C^{14}$ , while T. F. Cacacce et al. (Italy) used doubly tagged compounds ( $C_2H_4T_2$ ) in a study of the spectrum of labeled products appearing in  $\alpha$ -decay of one of the tritium atoms. Interesting data are to be found in a paper by F. Baumgärtner (West Germany) on synthesis of labeled molecules with the aid of  $\beta$ -decay and nuclear fission processes. This approach was resorted to in isolating complex compounds of technetium ( $Tc^{99m}$ ), Ru<sup>103</sup> (ruthenocene), and I<sup>131</sup> (iodoferrocene).

The use of new techniques in the investigation of the chemical consequences of nuclear transformations (sixth heading) attracted considerable attention. The use of the Mössbauer effect in studying chemical forms of stabilization of recoil atoms in solids must be viewed as highly encouraging. Reports on this subject were given by Ac. N. Nesmeyanov, A. M. Babeshkin et al. (USSR), R. Gerber, and G. Stekler (USA), G. Perlow and M. Perlow (USA). The first two papers discussed forms of stabilization of Sn recoil atoms. The last paper contained an expanded resume of possible Mössbauer nuclides and reports formation of oxygen compounds of xenon ( $\text{XeO}_3$ ,  $\text{XeO}_4$ ) in the  $\beta$ -decay of  $\text{I}^{129}$  (in molecules containing iodine and oxygen).

A report by V. G. Firsov and V. M. Byakov (USSR) proposed a new method for studying chemical processes involving monatomic hydrogen. The method is based on the simulation of the H atom by a hydrogen-like muonium atom. This makes it possible to investigate high-speed chemical processes by observing the depolarization of  $\mu^+$ -mesons.

## ATOMS FOR PEACE AT THE LEIPZIG FAIR

Yu. Mityaev

Translated from Atomnaya Énergiya, Vol. 19, No. 1,  
pp. 95-96, July, 1963

The regularly scheduled Spring Fair held in Leipzig February 28 through March 9, 1965, marked the 80th anniversary of this institution.

Among the numerous exhibits in the USSR pavilion, which was the largest foreign exhibitor at the fair, much floor space was given over to display stands and working models demonstrating the achievements of our country in the cause of the peaceful uses of atomic energy.

The "Atoms for Peace" exposition, which is the first exhibit seen in the USSR pavilion, consisted of several sections: 1) nuclear power and research reactors; 2) thermonuclear research; 3) the use of radioactive isotopes and radiations in medicine and in various branches of industry; 4) dosimetric instruments and equipment used in nuclear physics work. An automatically operated weather monitoring station employing the radioactive current source BETA-2 was also on display.

Operating models of stationary and portable nuclear power stations (Belyi Yar, Novaya Voronezh, ARBUS, TES-3), mockups of the BN-1000 fast reactor and the ROMASHKA high-temperature breeder reactor, mockups of a series of different research reactors (MIR, SM-2, MR, IR-100, IGR, IBR), and brightly hued dynamic display panels of fast-reactor power plants, of the Belyi Yar power station, and the VK-50, were on display in the first section. Mockups of a fuel assembly and reactor beam holes in the reactors installed at the Novaya Voronezh and Belyi Yar power stations, made life-size and from the same materials as the originals (except for fuel) were also seen.

The fusion research exhibit showed operating models of the OGRA-2, PR-5, TOKAMAK-3, Turbulent heating, Del'ta, and TSIKLON machines, on which Soviet scientists are conducting intensive research in controlled fusion.

The section on applications for radioactive isotopes and radiations displayed many specimens of factory-produced instruments, which can be classed in the following groups:

- 1) instruments for contactless measurement of thickness of materials and coatings (IT-5250, RIT-2, BTP-3, BTP-4);
- 2) instruments for contactless measurement and control of liquid or solid levels in tubes and sealed vessels, and for contactless measurement of the density of fluids (RGE-2V, IUR-2S, URMS-2);
- 3) instruments for geophysical research under laboratory conditions or field conditions (LSU-5, RAP-5, RAP-7, SGS-1, EM-6 AMA-6);
- 4) portable  $\gamma$ -ray facilities for industrial flaw detection in materials and structures (GUP-Ir-52);
- 5) facilities for determining the amount of material conveyed on conveyer belting (GKV-1), for monitoring annunciation of fire alarms (SDPU-1), and miscellaneous radioisotope instrumentation. This section also displayed mockups of the medical  $\gamma$ -therapeutic facilities LUCH, RITS, RAD, and models of two facilities for multifarious research in radiation chemistry.  $\text{Co}^{60}$  is used as radiation source in one of the facilities (the K 60000), and nuclear reactor spent fuel elements are used in the other (UK-1).

In addition to the many stationary and portable dosimetric monitoring instruments on display in the "Atoms for Peace" section, there was also a line of instruments employed in nuclear physics research work: pulse scalers (PP-8, PP-9, PP-12, and ISKRA), a four-channel coincidence and anticoincidence circuit (PS-4), discriminators (ADD 1, PD-2), single-channel and multichannel analyzers (AI-3, AI-128).

An automatically operated weather station with a radioisotope current source was installed at the pavilion entrance, with a panel on which were displayed six criteria on the state of the weather, transmitted once every hour by the radio of the isotope-powered weather station.

Mockups, instruments, and display stands at the "Atoms for Peace" exhibit made a deep impression on both layman visitors to the fair and specialists from various countries.

Even before the fair was opened, the press of the German Democratic Republic made frequent comments on the most interesting USSR exhibits, including the mockups of the self-propelled portable TES-3 nuclear power plant, the ROMASHKA breeder reactor, and the automatic weather station with BETA-2 isotope current source.

The originality and reliability of the design of this radioactive current source, which allows the weather station to operate unattended for 10 years, were awarded with the Leipzig Fair gold medal. Among the best exhibits, it was agreed, were the PP-9 and ISKRA scalars, the AI-3 and AI-128 pulse analyzers, the GKV-1  $\gamma$ -ray conveyor load cells, the deep-hole SGS-1 logging device, a device for continuous monitoring and control of burden fill level in blast furnaces (the URMS-2).

Other models which enjoyed great popularity were those of the Belyi Yar power station, dynamic panels of power reactors, a mockup of the portable ARBUS nuclear power station, models of the thermonuclear machines PR-5, TOKAMAK-3 and DEL'TA, and many dosimetric and radioisotope nucleonic instruments.

The success of the "Atoms for Peace" exhibit at the Leipzig Jubilee Fair owes much of its success to the artistic design by the Chamber of Commerce, the widespread use of automatic display annunciation phones with well formulated texts, and smooth functioning of the entire staff on duty at the exhibit.

The amount of advertising literature was quite insufficient, however,

## THE WARSAW EXHIBIT

Translated from Atomnaya Énergiya, Vol. 19, No. 1,  
pp. 96-97, July, 1965

An exhibit displaying some of the achievements of the COMECON [Council for Mutual Economic Aid] nations in the development of applications for radioactive isotopes in various branches of their national economies and in science was organized in Warsaw in October 1964.

Over 200 displays were shown. The main focus of the exhibit was on instruments with isotope radiation sources for quality control of manufactured goods and for automatic measuring of the thickness of sheet and film materials, thickness of coatings, density of fluids, plus some equipment for geophysical research and for analysis of the composition of materials. The exhibit also displayed a wide variety of radiation detectors, isotope radiation sources for industrial and medical uses, shielding equipment, equipment for isotope applications in medicine, in scientific and industrial research, and also dosimetric, radiometric, and electron physics instruments.

The various exhibits were divided by subject in order to facilitate comparison of the technical characteristics of instruments performing similar functions and made in different countries.

The exhibit opened with stands offering science and engineering literature published in the COMECON nations.

Many facilities, auxiliary equipment, and industrial radiography equipment were presented. It is interesting to note that Polish designers have chosen to design  $\gamma$ -ray radiography equipment with their own novel approach. For example, the ZURAW radioisotope flaw detector is designed for quality control of weldments and castings of complicated geometry. It consists of a lead shielding cask (410 x 433 x 440 mm and weighing 250 kg) carried on a dolly; the cask can accommodate  $\text{Co}^{60}$   $\gamma$ -ray sources of 5 gm-equiv. Ra or  $\text{Ir}^{192}$   $\gamma$ -ray sources of 50 gm-equiv Ra activity. A flexible rubber hose 10 meters or 20 meters in length is attached to the cask, and supplies compressed air from a blower mounted on the dolly handle; an ampule with the source is moved at a travel speed of about 3 meters/sec into operating position. Electric light annunciators provide information on ampule position. The power drain is 400 W.

Other designs of  $\gamma$ -ray flaw detectors utilize hydraulic or electromechanical systems to place the sources in working position.

One distinguishing feature of the Polish designs is the large number of accessory parts (dollies, hose, fasteners, etc.) which greatly ease the work of radiography experts and technicians, thereby heightening the productivity of labor.

Visitors to the exhibit saw various radioisotope relays in 20 distinct types -designed to monitor fill level in containers or to fulfill other functions-which included a GR  $\gamma$ -relay (USSR-manufactured, and a  $\gamma$ -relay device using semiconductors (of Bulgarian manufacture).

The Vakutronik state enterprise (East Germany) demonstrated a general-purpose isotope relay, type VA-T-66, designed to monitor fill level in chlorine tanks, cars, tank cars, hoppers, shaft furnaces; it can be employed to send braking signals on train routes, or for counting the number of cars passing a point. The relay is of explosion-proof design; its sensor head, with two halogen counters, can operate at environmental temperatures from  $-40^{\circ}$  to  $+60^{\circ}\text{C}$ , and up to  $+150^{\circ}\text{C}$  if a water-cooling jacket is added. The relay operates at a radiation dose rate of 0.4 mr/h or over a fourfold variation of intensity. Operating time is no longer than 5 sec.

A mockup of an automatic railroad signal switching system or mine switching system using electrically powered railroad cars attracted much attention. The electric train is provided with a container carrying the  $\gamma$ -ray source (in two positions: operating or neutral), and a probe with a gas-discharge counter is mounted on the tunnel arch at a distance of 50 meters from the railroad switch. When the switch has to be reset, the train engineer pulls the handle to place the container into the operating position, and  $\gamma$ -radiation incident on the counter (and generating an actuating signal in the circuit) energizes the switch positioner. The source activity is about 1 mCi; the system operates excellently at train speeds up to 16 km/h.

The radioisotope level measuring devices include servo level gages fabricated in Rumania, Czechoslovakia, Poland, and the USSR, as well as a variety of level sensors and level controllers of both special design and general-purpose types. A special feature in some designs, e.g. the MN-1S (Czech) instrument, is the use of ionization compensated chambers and wire radiation sources.

The design of an on-off level controller with pneumatic actuator, the IURP-1s, attracted considerable interest. The V-3G level gage has an explosion-proof sensor head; it is capable of operating in an ambient temperature range from  $-40^{\circ}$  to  $+50^{\circ}\text{C}$  and at relative humidities to 90%. Measurement error is  $\pm 20$  mm, and speed of response can be set at 0.5, 1.5, or 5 sec depending on the customer's requirements.

The exhibit also displayed instruments and equipment for isotope applications in medicine, geophysics, scientific and engineering research.

The extensive discussion of the designs and circuits, and comparison of engineering cost factors, enabled participant nations to evaluate the level achieved in the domain of industrial exploitation of radioisotopes, and to adopt recommendations for furtherance of work in this field.



## APPLICATIONS FOR RADIOACTIVE ISOTOPES IN METEOROLOGY

M. T. Dmitriev

Translated from *Atomnaya Énergiya*, Vol. 19, No. 1,  
pp. 97-98, July, 1965

The use of radioisotopes in meteorological instruments is of particular interest for applications under severe and exacting conditions, where high demands are imposed on accuracy in measurements. For example, the atmospheric pressure over an automated hydrometeorological network must be measured to an accuracy of 0.1 mb, the temperature must be measured to within 0.1°, i.e. errors in measurements must be kept within 0.1%. Additional requirements are imposed by the need for contactless sensing and measurement of meteorological variables.

Radioisotope meteorological instruments display high accuracy surpassing that of conventional instruments. At the present time, about 30 of these isotope devices have been developed to measure various meteorological variables [1-8]. For instance, the accuracy of deformation type barometers currently in use is limited by the mechanical properties of the materials which are insensitive to small forces. Radioisotope barometers utilize the ionization of the air by  $\alpha$ -particles; the pressure is determined by the ion current, the number of  $\alpha$ -particles incident on the counter, or the discharge rate of the capacitor under irradiation conditions. Instruments for measuring low pressures have a linear calibration curve for the ionization current vs. pressure, and measurements are to within 0.1% accuracy. When the pressure is measured at sea level, it is more feasible to employ barometers based on the slowing-down of  $\alpha$ -particles at the end of their range, since air pressure varies by only 10% under these conditions. When a  $\text{Po}^{210}$  source of 20 mCi activity is employed as ionizer, and a sodium iodide scintillator with phototube multiplier is used, an accuracy of 0.2 mm Hg can be achieved.

Conventional contacting methods for measuring temperature become inefficient at low pressures because of the reduced rate of heat transfer and the errors caused by sunlight. Isotope thermometers operating on the ionization principle are free of this shortcoming. A radioisotope anemometer comprising an unsealed ionization chamber has an advantage over conventional wind-monitoring instruments in its low inertia and absence of moving parts; it is reliable in service and puts up absolutely no resistance to the stream of air. The measurement range from 1 cm/sec to the maximum possible wind speed and the 2-3% accuracy are advantages. The use of isotopes improves the performance of conventional mechanical wind sensors by allowing for remote-control designs. In a relatively moderate run of pulse counts this sensor can directly report the average wind speed and average wind direction.

An impressive array of meteorological variables can be measured automatically and by remote control only through the use of isotope techniques. Sensors for determining the content of suspended moisture in the air, the intensity of snowfall, rainfall, precipitation in blizzards, dew, or frost, have been developed. Isotope devices measuring rate of evaporation, the amount of precipitation, or for measuring the thickness of ice formation, extent of ice covering, are more reliable and more accurate than non-isotope meteorological instruments.

The use of isotopes has made it possible to design suitable instruments for measuring the characteristics of snow or soils. These devices are based on radiographic penetration of the layer of snow or soil by  $\gamma$ -rays or  $\gamma$ -backscatter or neutron slowing-down techniques. Observers are relieved of backbreaking physical labor (coring of samples, weighing of samples) in measurements taken under field conditions, and results are obtained directly in the measurement process. The same volume of measurements can be completed in one-fifth to one-sixth the time. Remote controlled measurements of the water equivalent and of snow density, soil density and soil moisture could not be carried out by any method other than radioisotope methods in automatic weather patrol stations. The height of the snow and the ground water level are also determined by remote sensing with the aid of isotopes. Accuracy in density and moisture measurements is 2-3%, and accuracy in measurements of the height of snow cover runs 0.5 to 1%.

Radioisotope measurement of the thickness of peat beds is done in similar fashion. The density of floating peat or of peat flooded with water (the natural state of peat bogs) has to be measured to determine the concentration

of vegetation in the bog. When soft  $\gamma$ -rays, say from a  $Tu^{170}$  source, are used in the peat density gage with a scintillation counter, the instrument can double as a peat ash content gage. The thickness of grass land is determined by a horizontal transmission gaging technique.

The natural  $\gamma$ -emitters  $K^{40}$ , RaB, RaC, RaC', ThB, ThC",  $MsTh_2$ , and several others with  $\gamma$ -energies ranging mostly from 0.2 to 2.6 MeV are present in the soil practically in an equilibrium state, and are also utilized in measuring soil moisture, snow water content, and density of vegetation. The  $\gamma$ -emission intensity of soils averages 500 to 700 photons a minute from one square centimeter. In that case a single routine measurement will be the control in the absence of snow cover, or in an area barren of vegetation, or in maximally arid soil (at known moisture), as the case may be. Measurement of the number of pulses counted and then recalculated per unit time, may be carried out either over a specified itinerary traversed by the observer or by means of instruments carried on moving vehicles (tractor, helicopter, airplane). Repeated measurements of pulse count on the same itinerary will provide averages of water content in snow, of vegetation, or of soil humidity over wide areas.

These examples show that applications for radioactive isotopes in meteorology are broad in scope. Moreover, radioisotope electric power supplies will be widely employed in automatic unattended weather patrol stations set up in regions of low and infrequent wind, in zones visited by hurricanes (this applies to practically all of the country east of the Urals and to the littoral sections of European Russia).

The Riga hydrometeorological instrument works has manufactured 1240 radioisotope weather monitoring devices to date. These devices are in use over the entire territory of the Soviet Union and are being exported to many socialist and capitalist countries. The automatic radioisotope meteorological stations are set up in mountainous areas of Central Asia and on the European territories of the nation. There is a continually expanding use of radioisotopes in meteorology.

#### LITERATURE CITED

1. Byulleten' nauchno-techn. informatsii gidrometeor. sluzhby SSSR, No. 12, 54 (1962).
2. Ibid, No. 13, 47 (1963).
3. Ibid, No. 17, 7 (1964).
4. Ibid, No. 18, 47 (1964).
5. Ibid, No. 19, 34 (1964).
6. Ibid, No. 20, 13 (1964).
7. Ibid, No. 21, 3 (1965).
8. Trudy nauchno-issled. inst. gidrometeor. priborostroeniya, No. 11, Moscow, Gidrometeoizdat (1963), p. 49.

## BRIEF COMMUNICATIONS

Translated from Atomnaya Énergiya, Vol. 19, No. 1,  
p. 99, July, 1965

USSR. On May 4, 1965, an agreement was signed in Moscow on collaboration in the use of atomic energy for peaceful purposes. Signatories were the State Committee on the Uses of Atomic Energy of the USSR and the French Commissariat de l'Energie Atomique.

The agreement stipulates in part:

---that there shall be an exchange of delegations of specialists to share knowledge on the scientific and engineering achievements and to discuss scientific research carried out by the two nations in various fields of peaceful uses of atomic energy (nuclear reactor electric power stations, experimental and developmental reactors, processing and disposal of radioactive waste, production and use of radioisotopes and radiation sources, etc.);

---that there shall be an exchange of research specialists in the domain of controlled fusion reactions and plasma physics, as well as in nuclear physics research using accelerators;

---that there shall be an exchange of scientific and technical information, and that bilateral scientific seminars be scheduled on problems studied jointly.

USSR. In late April 1965, the Soviet Union was host to a group of British scientists headed by Dr. J. Adams. The British scientists arrived in the USSR for discussions with Soviet scientists on plasma physics and controlled thermonuclear fusion.

The delegation was staffed by Dr. J. Adams, Director of the laboratory at Cullam, and the staff of that laboratory: Dr. R. Bickerton in charge of experimental section A, Dr. D. Sweetman in charge of experiments on the Phoenix machine, experimental section B; Dr. A. Gibson, leader of the group of experimental section A, and Dr. D. Dukes leader of the theoretical section group.

In the course of their stay, the British scientists paid a visit to the I. V. Kurchatov Institute of Atomic Energy, the A. F. Ioffe Physics and Engineering Institute, the D. V. Efremov Research Institute for Electrophysics Equipment, the Institute of Nuclear Physics of the Siberian Division of the USSR Academy of Sciences, and the P. N. Lebedev Institute of Physics. They held discussions with scientists at these institutes, on various problems in plasma physics and controlled fusion.

USSR. The USSR State Committee on the Uses of Atomic Energy, jointly with official organizations of the Uzbek SSR, and the All-Union Izotop firm, held a seminar in Tashkent in April 1965 on applications of radioisotope techniques and radioisotope devices in industrial process control and monitoring. Prominent engineers in administration capacities in several industries and firms, leading production and power experts, heads of technical sections and of central in-plant laboratories throughout the region, took part in the seminar, where over 40 papers were presented.

Following discussion of the reports and exchanges of views, a decision was adopted to spur the expanded use of radioisotope techniques and instruments at industrial firms throughout the Uzbek SSR. The seminar participants visited an exhibit at which radioisotope techniques used in the national economy were displayed.

IAEA. In April 1965, the International Atomic Energy Agency in collaboration with the UNO Food and Agricultural Organization (FAO) and the World Health Organization, sponsored a conference of experts on methods for determining residual quantities of chemicals employed to protect plants and livestock and found in foodstuffs. The discussion focused on the importance of activation analysis techniques in this work. The recommendations of the conference will be published by the IAEA.

## NEW BOOKS

M. V. Filippov

Translated from *Atomnaya Énergiya*, Vol. 19, No. 1,  
p. 100, July, 1965

"MAGNITNAYA GIDRODINAMIKA" --- A New Journal of Magnetohydrodynamics

Starting 1965, the Academy of Sciences of the Latvian SSR is publishing an all-Union [Russian language] engineering and physics quarterly entitled MAGNITNAYA GIDRODINAMIKA [Magnetohydrodynamics]. The need for this publication is emphasized by the vigorous development of magnetohydrodynamics coupled with the recently established policy of utilizing the achievements of this research in many branches of the national economy and particular in nuclear power industry.

The journal will receive original articles, review articles, and brief correspondence on various magnetohydrodynamical phenomena in plasma and in conducting fluids, as well as on all types of magnetohydrodynamical machines and their uses.

The first issue which appeared opens with an article by a Vice President of the USSR Academy of Sciences, Academician M. D. Millionshchikov, on the aims of the journal.

Next follows an extensive tutorial review paper on research on laminar flow patterns of a conducting fluid in tubes and channels in the presence of a magnetic field. This review takes up exact and approximate solutions and proposes problems requiring further study.

Several original articles appearing in this first issue deal with different aspects of magnetohydrodynamical flow patterns in a conducting fluid. For example, there is a treatment of the flow of mercury around a cylinder and the effect of the relative roughness of the bounding walls on the flow; local turbulent pulsations in the flow speed of a conducting fluid are determined experimentally.

Several papers contain interesting plasma MHD research, with studies of various flow patterns and variables of plasmoids which will be of considerable practical interest.

A good deal of space is reserved in this first issue to designs, optimum operating conditions, and practical use of various MHD machines. One of these reports describes the design of an induction pump operated with basic operating variables held constant for 20 000 h at 350° to 400°C temperature.

The possibility of using MHD techniques in metallurgy is illustrated by articles on experience in the electro-magnetic conveying of molten pig iron and the mixing of a melt of light alloys. The issue ends with some articles on methods for measuring the flow speed of conducting fluids.

The second issue of the quarterly, which appeared recently, also contains quite a bit of fresh material, undoubtedly of great interest to a wide readership of scientists and engineers working not only in the field of magnetohydrodynamics proper, but also in many other fields of science and engineering. Specialists in the study and harnessing of nuclear energy will find a wealth of information in the quarterly which they could put to practical use in their daily work.

The quarterly MAGNITNAYA GIDRODINAMIKA sees as its prime task spreading ideas and providing general information on the potential expansion of the sphere of application of MHD techniques. The solution of this problem will be possible only by drawing from wide areas of the scientific community. We hope that the editorial staff, contributors, and readers together will give this quarterly a worthy place in Soviet scientific and technical periodical literature.

## SOVIET JOURNALS AVAILABLE IN COVER-TO-COVER TRANSLATION

This list includes all Russian journals which—to the publisher's knowledge—were available in cover-to-cover translation on June 30, 1965, or for which definite and immediate plans for cover-to-cover translation had been announced by that date. The list reflects only *current* publication arrangements, but the date and issue listed for first publication refer to translations available from any source. Thus, earlier volumes of a translation journal may have been published by an organization other than that listed as the current publisher, and possibly under a different title (and, for *Doklady Akademii Nauk SSSR*, in a different arrangement of sections).

Five bits of information are furnished, separated by bullets:

1. The abbreviation(s) by which the journals are most frequently referred to in Russian bibliographies (if the name of the journal is customarily spelled out, no abbreviation is given).
2. The transliterated full name of the journal.
3. The full name of the translation journal (in bold type).
4. The year, volume (in parentheses), and issue of first publication of the translation (parentheses are empty if the Russian journal does not use volume numbers).
5. The current publisher of the translation [AGI—American Geological Institute, AGU—American Geophysical Union, AIP—American Institute of Physics, CB—Consultants Bureau, CH—Clearing House for Federal Scientific and Technical Information, CS—The Chemical Society (London), FP—Faraday Press, IEEE—Institute of Electrical and Electronic Engineers, ISA—Instrument Society of America, PP—Pergamon Press].

For convenience in locating bibliographic references the journals are listed in alphabetical order of the *abbreviated* titles.

- AE • Atomnaya énergiya • **Soviet Journal of Atomic Energy** • 1956(1)1 • CB
- Akust. zh. • Akusticheskii zhurnal • **Soviet Physics—Acoustics** • 1955(1)1 • AIP
- Astrofiz. • Astrofizika • **Astrophysics** • 1965(1)1 • FP
- Astr(on). zh(urn). • Astronomicheskii zhurnal • **Soviet Astronomy—AJ** • 1957(34)1 • AIP
- Avtomat. i telemekh. • Avtomatika i telemekhanika • **Automation and Remote Control** • 1956(27)1 • ISA
- Avto(mat). svarka • Avtomaticheskaya svarka • **Automatic Welding** • 1959(12)1 • British Welding Research Association
- Avtometriya • **Autometry** • 1965(1)1 • CB
- Biokhim. • Biokhimiya • **Biochemistry** • 1956(21)1 • CB
- Byul. éksp(erim). biol. (i med.) • Byulleten' éksperimental'noi biologii i meditsiny • **Bulletin of Experimental Biology and Medicine** • 1959(41)1 • CB
- DAN (SSSR) • *see* Doklady AN SSSR
- Defektoskopiya • **Soviet Defectoscopy** • 1965(1)1 • CB
- Diff. urav. • Differentsial'nye uravneniya • **Differential Equations** • 1965(1)1 • FP
- Dokl(ady) AN SSSR; DAN (SSSR) • Doklady Akademii Nauk SSSR • The translation of Doklady is published in various journals, according to subject matter. The sections of Doklady contained in each of the translation journals are listed in parentheses.
- Doklady Biochemistry** (biochemistry) • 1957(112)1 • CB
- Doklady Biological Sciences Sections** (anatomy, cytology, ecology, embryology, endocrinology, evolutionary morphology, parasitology, physiology, zoology) • 1957(112)1 • CB
- Doklady Biophysics** (biophysics) • 1957(112)1 • CB
- Doklady Botany** (botany, phytopathology, plant anatomy, plant ecology, plant embryology, plant physiology, plant morphology) • 1957(112)1 • CB
- Doklady Chemical Technology** (chemical technology) • 1956(106)1 • CB
- Doklady Chemistry** (chemistry) • 1956(106)1 • CB
- Doklady Earth Sciences Sections** (geochemistry, geology, geophysics, hydrogeology, lithology, mineralogy, paleontology, permafrost, petrography) • 1959(124)1 • AGI
- Doklady Physical Chemistry** (physical chemistry) • 1957(112)1 • CB
- Doklady Soil Science** (soil science) • 1964(154)1 • Soil Science Society of America
- Soviet Mathematics—Doklady** (mathematics) • 1960(130)1 • American Mathematical Society
- Soviet Oceanography** (oceanology) • 1959(124)1 • AGU
- Soviet Physics—Doklady** (aerodynamics, astronomy, crystallography, cybernetics and control theory, electrical engineering, energetics, fluid mechanics, heat engineering, hydraulics, mathematical physics, mechanics, physics, technical physics, theory of elasticity) • 1956(106)1 • AIP
- Élektrokhiimiya • **Soviet Electrochemistry** • 1965(1)1 • CB
- Élektrosvyaz' • combined with Radiotekhnika in **Telecommunications and Radio Engineering** • 1957(16)1 • IEEE
- Élektrotekh. • Élektrotekhnika • **Soviet Electrical Engineering** • 1965(36)1 • FP
- Éntom(ol). oboz(r). • Éntomologicheskoe obozrenie • **Entomological Review** • 1958(37)1 • Entomological Society of America
- Fiz. goreniya i vzryva • Fizika goreniya i vzryva • **Combustion, Explosion, and Shock Waves** • 1965(1) • FP
- Fiziol(ogiya) rast. • Fiziologiya rastenii • **Soviet Plant Physiology** • 1957(4)1 • CB
- Fiz.-khim. mekh(anika) mater(ialov); FKHM • Fizikokhimicheskaya mekhanika materialov • **Soviet Materials Science** • 1965(1)1 • FP
- Fiz. met. i metallov.; FMM • Fizika metallov i metallovedenie • **Physics of Metals and Metallography** • 1957(5)1 • Acta Metallurgica
- Fiz.-tekhn. probl. razr. polezn. iskopaem. • Fizikotekhnicheskie problemy razrabotki poleznykh iskopaemykh • **Soviet Mining Science** • 1965(1)1 • CB
- Fiz. tv(erd). tela; FTT • Fizika tverdogo tela • **Soviet Physics—Solid State** • 1959(1)1 • AIP
- FKHM • *see* Fiz.-khim. mekhanika materialov
- FMM • *see* Fiz. met. i metallov.
- FTT • *see* Fiz. tverd. tela
- Geliotekh. • Geliotekhnika • **Applied Solar Energy** • 1965(1)1 • FP
- Geol. nefi i gaza • Geologiya nefi i gaza • **Petroleum Geology** • 1958(2)1 • Petroleum Geology, Box 171, McLean, Va.
- Geomagnet. i aéronom. • Geomagnetizm i aéronomiya • **Geomagnetism and Aeronomy** • 1961(1)1 • AGU
- Inzh.-fiz. zh. • Inzhenerno-fizicheskii zhurnal • **Journal of Engineering Physics** • 1965(8)1 • FP
- Inzh. zh. • Inzhenernyi zhurnal • **Soviet Engineering Journal** • 1965(5)1 • FP
- Iskusstv. sputniki Zemli • Iskusstvennye sputniki Zemli • **Artificial Earth Satellites** • 1958(1)1 • CB [superseded by Kosmich. issled.]
- Izmerit. tekhn(ika) • Izmeritel'naya tekhnika • **Measurement Techniques** • 1958(7)1 • ISA
- Izv. AN SSSR, o(td.) kh(im.) n(auk) (or ser. khim.) • Izvestiya Akademii Nauk SSSR: Otdelenie khimicheskikh nauk (or Seriya khimicheskaya) • **Bulletin of the Academy of Sciences of the USSR: Division of Chemical Science** • 1952(16)1 • CB
- Izv. AN SSSR, ser. fiz(ich). • Izvestiya Akademii Nauk SSSR: Seriya fizicheskaya • **Bulletin of the Academy of Sciences of the USSR: Physical Series** • 1954(18)3 • Columbia Technical Translations
- Izv. AN SSSR, ser. fiz. atm. i okeana • Izvestiya Akademii Nauk SSSR: Seriya fiziki atmosfery i okeana • **Izvestiya, Atmospheric and Oceanic Physics** • 1965( )1 • AGU
- Izv. AN SSSR, ser. fiz. zemli • Izvestiya Akademii Nauk SSSR: Seriya fiziki zemli • **Izvestiya, Physics of the Solid Earth** • 1965( )1 • AGU
- Izv. AN SSSR, ser. geofiz. • Izvestiya Akademii Nauk SSSR: Seriya geofizicheskaya • **Bulletin of the Academy of Sciences of the USSR: Geophysics Series** • 1957(7)1 • AGU [superseded by Izv. AN SSSR, ser. fiz. atm. i okeana and Izv. AN SSSR, ser. fiz. zemli]
- Izv. AN SSSR, ser. geol. • Izvestiya Akademii Nauk SSSR: Seriya geologicheskaya • **Bulletin of the Academy of Sciences of the USSR: Geologic Series** • 1958(23)1 • AGI
- Izv. AN SSSR, ser. neorgan. mat(er). • Izvestiya Akademii Nauk SSSR: Seriya neorganicheskie materialy • **Inorganic Materials** • 1965(1)1 • CB

- Izv. AN SSSR, tekhn. kiber(netika) • Izvestiya Akademii Nauk SSSR: Tekhnicheskaya kibernetika • **Engineering Cybernetics** • 1963(1)1 • IEEE
- Izv. v(yssh.) u(ch.) z(av.) aviats. tekhn. • Izvestiya vysshikh uchebnykh zavedenii. Aviatsonnaya tekhnika • **Aviation Engineering** • 1963(6)1 • CH
- Izv. v(yssh.) u(ch.) z(av.) fiz. • Izvestiya vysshikh uchebnykh zavedenii. Fizika • **Soviet Physics Journal** • 1965(8)1 • FP
- Izv. v(yssh.) u(ch.) z(av.) geodez. i aérofot. • Izvestiya vysshikh uchebnykh zavedenii. Geodeziya i aérofotos'emka • **Geodesy and Aerophotography** • 1959(4)1 • AGU
- Izv. v(yssh.) u(ch.) z(av.) priborostr. • Izvestiya vysshikh uchebnykh zavedenii. Priborostroenie • **Izvestiya VUZOV. Instrument Building** • 1962(5)1 • CH
- Izv. v(yssh.) u(ch.) z(av.) radiofiz. • Izvestiya vysshikh uchebnykh zavedenii. Radiofizika • **Izvestiya VUZOV. Radiophysics** • 1958(1)1 • CH
- Izv. v(yssh.) u(ch.) z(av.) radiotekhn(ika) • Izvestiya vysshikh uchebnykh zavedenii. Radiotekhnika • **Izvestiya VUZOV. Radio Engineering** • 1959(2)1 • CH
- Izv. v(yssh.) u(ch.) z(av.) tekhn. teks. prom. • Izvestiya vysshikh uchebnykh zavedenii. Tekhnologiya tekstilnoi promyshlennosti • **Technology of the Textile Industry, USSR** • 1960(4)1 • The Textile Institute (Manchester)
- Kauch. i rez. • Kauchuk i rezina • **Soviet Rubber Technology** • 1959(18)3 • Maclaren and Sons Ltd.
- Khim. getero(tsik). soed. • Khimiya geterotsiklicheskih soedinenii • **Chemistry of Heterocyclic Compounds** • 1965(1)1 • FP
- Khim. i neft. mash(inostr). • Khimicheskoe i neftyanoe mashinostroenie • **Chemical and Petroleum Engineering** • 1965( )1 • CB
- Khim. i tekhnol. topliv i masel • Khimiya i tekhnologiya topliv i masel • **Chemistry and Technology of Fuels and Oils** • 1965( )1 • CB
- Khim. prirod. soed. • Khimiya prirodnykh soedinenii • **Chemistry of Natural Compounds** • 1965(1)1 • FP
- Kib. • Kibernetika • **Cybernetics** • 1965(1)1 • FP
- Kinet. i katal. • Kinetika i kataliz • **Kinetics and Catalysis** • 1960(1)1 • CB
- Koks i khim. • Koks i khimiya • **Coke and Chemistry, USSR** • 1959( )8 • Coal Tar Research Assn. (Leeds, England)
- Kolloidn. zh(urn). • Kolloidnyi zhurnal • **Colloid Journal** • 1952(14)1 • CB
- Kosmich. issled. • Kosmicheskie issledovaniya • **Cosmic Research** • 1963(1)1 • CB
- Kristallog. • Kristallografiya • **Soviet Physics—Crystallography** • 1957(2)1 • AIP
- Liteinoe proiz(vo). • Liteinoe proizvodstvo • **Russian Castings Production** • 1961(12)1 • British Cast Iron Research Association
- Mag. gidrodin. • Magnitnaya gidrodinamika • **Magnetohydrodynamics** • 1965(1)1 • FP
- Mekh. polim. • Mekhnika polimerov • **Polymer Mechanics** • 1965(1)1 • FP
- Metalloved. i term. obrabotka metal.; MiTOM • Metallovedenie i termicheskaya obrabotka metallov • **Metal Science and Heat Treatment** • 1958(6)1 • CB
- Metallurg • **Metallurgist** • 1957( )1 • CB
- Mikrobiol. • Mikrobiologiya • **Microbiology** • 1957(26)1 • CB
- MiTOM • see Metalloved. i term. obrabotka metal.
- Ogneupory • **Refractories** • 1960(25)1 • CB
- Opt. i spektr.; OS • Optika i spektroskopiya • **Optics and Spectroscopy** • 1959(6)1 • AIP
- Osnovan. fund. i mekh. gruntov • Osnovaniya fundamenty i mekhanika gruntov • **Soil Mechanics and Foundation Engineering** • 1964( )1 • CB
- Paleon. zh(urn). • Paleontologicheskii zhurnal • **Journal of Paleontology** • 1962( )1 • AGI
- Plast. massy • Plasticheskie massy • **Soviet Plastics** • 1960(8)7 • Rubber and Technical Press, Ltd.
- PMM • see Prikl. matem. i mekhàn.
- PMTF • see Zhur. prikl. mekhan. i tekhn. fiz.
- Pochvovedenie • **Soviet Soil Science** • 1958(53)1 • Soil Science Society of America
- Poroshk. met. • Poroshkovaya metallurgiya • **Soviet Powder Metallurgy and Metal Ceramics** • 1962(2)1 • CB
- Priborostroenie • **Instrument Construction** • 1959(4)1 • Taylor and Francis, Ltd.
- Pribory i tekhn. éksp(erimenta); PTE • Pribory i tekhnika éksperimenta • **Instruments and Experimental Techniques** • 1958(3)1 • ISA
- Prikl. biokhim. i mikrobiol. • Prikladnaya biokhimiya i mikrobiologiya • **Applied Biochemistry and Microbiology** • 1965(1)1 • FP
- Prikl. matem. i mekh(an).; PMM • Prikladnaya matematika i mekhanika • **Applied Mathematics and Mechanics** • 1958(22)1 • PP
- Probl. pered. inform. • Problemy peredachi informatsii • **Problems of Information Transmission** • 1965(1)1 • FP
- Probl. severa • Problemy severa • **Problems of the North** • 1958( )1 • National Research Council of Canada
- PTÉ • see Pribory i tekhn. éksperimenta
- Radiokhim. • Radiokhimiya • **Soviet Radiochemistry** • 1962(4)1 • CB
- Radiotekh. • Radiotekhnika • combined with Élektrosvyaz' in **Telecommunications and Radio Engineering** • 1961(16)1 • IEEE
- Radiotekhn. i élektron(ika) • Radiotekhnika i élektronika • **Radio Engineering and Electronic Physics** • 1961(6)1 • IEEE
- Stal' • Stal' in English • 1959(19)1 • The Iron and Steel Institute
- Stanki i instr. • Stanki i instrument • **Machines and Tooling** • 1959(30)1 • Production Engineering Research Association
- Stek. i keram. • Steklo i keramika • **Glass and Ceramics** • 1956(13)1 • CB
- Svaroch. proiz(vo). • Svarochnoe proizvodstvo • **Welding Production** • 1959(5)4 • British Welding Research Association (London)
- Teor. i éksp(erim. khim. • Teoreticheskaya i éksp(erim)ental'naya khimiya • **Theoretical and Experimental Chemistry** • 1965(1)1 • FP
- Teor. veroyat. i prim. • Teoriya veroyatnosti i ee primeneniye • **Theory of Probability and Its Application** • 1956(1)1 • Society for Industrial and Applied Mathematics
- Teploténergetika • **Thermal Engineering** • 1964(11)1 • PP
- Teplotfiz. vys(ok). temp. • Teplofizika vysokikh temperatur • **High Temperature** • 1963(1)1 • CB
- Tsvet. metally • Tsvetnyye metally • **The Soviet Journal of Nonferrous Metals** • 1960(33)1 • Primary Sources
- Usp. fiz. nauk; UFN • Uspekhi fizicheskikh nauk • **Soviet Physics—Uspekhi** • 1958(66)1 • AIP
- Usp. khim.; UKh • Uspekhi khimii • **Russian Chemical Reviews** • 1960(29)1 • CS
- Usp. mat. nauk; UMN • Uspekhi matematicheskaya nauk • **Russian Mathematical Surveys** • 1960(15)1 • Cleaver-Hume Press, Ltd.
- Vest. Akad. med. nauk SSSR • Vestnik Akademii meditsinskikh nauk SSSR • **Vestnik of USSR Academy of Medical Sciences** • 1962(17)1 • CH
- Vest. mashinostroeniya • Vestnik mashinostroeniya • **Russian Engineering Journal** • 1959(39)4 • Production Engineering Research Association
- Vest. svyazi • Vestnik svyazi • **Herald of Communications** • 1954(14)1 • CH
- Vysoko(molek). soed(ineniya) • Vysokomolekulyarnye soedineniya (SSSR) • **Polymer Science (USSR)** • 1959(1)1 • PP
- Yadernaya fizika • **Soviet Journal of Nuclear Physics** • 1965(1)1 • AIP
- Zashch(ita) met(allow) • Zashchita metallov • **Protection of Metals** • 1965(1)1 • CB
- Zav(odsk). lab(oratoriya); ZL • Zavodskaya laboratoriya • **Industrial Laboratory** • 1958(24)1 • ISA
- ZhÉTF pis'ma redaktsiyu • **JETP Letters** • 1965(1)1 • AIP
- Zh(ur). anal(it). khim(ii); ZhAKh • Zhurnal analiticheskoi khimii • **Journal of Analytical Chemistry** • 1952(7)1 • CB
- Zh(ur). éks(perim). i teor. fiz.; ZhÉTF • Zhurnal éksp(erim)ental'noi i teoreticheskoi fiziki • **Soviet Physics—JETP** • 1955(28)1 • AIP
- Zh(ur). fiz. khimii; ZhFKh • Zhurnal fizicheskoi khimii • **Russian Journal of Physical Chemistry** • 1959(33)7 • CS
- Zh(ur). neorg(an). khim.; ZhNKh • Zhurnal neorganicheskoi khimii • **Russian Journal of Inorganic Chemistry** • 1959(4)1 • CS
- Zh(ur). obshch. khim.; ZhOKh • Zhurnal obshchei khimii • **Journal of General Chemistry of the USSR** • 1949(19)1 • CB
- Zh(ur). org. khim.; ZhOrKh(im) • Zhurnal organicheskoi khimii • **Journal of Organic Chemistry of the USSR** • 1965(1)1 • CB
- Zh(ur). prikl. khim.; ZhPKh • Zhurnal prikladnoi khimii • **Journal of Applied Chemistry of the USSR** • 1950(23)1 • CB
- Zh(ur). prikl. mekhan. i tekhn. fiz. • Zhurnal prikladnoi mekhaniki i tekhnicheskoi fiziki • **Journal of Applied Mechanics and Technical Physics** • 1965( )1 • FP
- Zh(ur). prikl. spektr. • Zhurnal prikladnoi spektroskopii • **Journal of Applied Spectroscopy** • 1965(2)1 • FP
- Zh(ur). strukt(urnoi) khim.; ZhSKh • Zhurnal strukturnoi khimii • **Journal of Structural Chemistry** • 1960(1)1 • CB
- Zh(ur). tekhn. fiz.; ZhTF • Zhurnal tekhnicheskoi fiziki • **Soviet Physics—Technical Physics** • 1956(26)1 • AIP
- Zh(ur). vses. khim. ob-va im. Mendeleeva • Zhurnal vsesoyuznogo khimicheskogo obshchestva im. Mendeleeva • **Mendeleev Chemistry Journal** • 1965(10)1 • FP
- Zh(ur). vychis. mat. i mat. fiz. • Zhurnal vychislitel'noi matematika i matematicheskoi fiziki • **USSR Computational Mathematics and Mathematical Physics** • 1962(1)1 • PP
- ZL • see Zavodsk. laboratoriya

SIGNIFICANCE OF ABBREVIATIONS MOST FREQUENTLY  
ENCOUNTERED IN SOVIET PERIODICALS

FIAN	Phys. Inst. Acad. Sci. USSR.
GDI	Water Power Inst.
GITI	State Sci.-Tech. Press
GITTL	State Tech. and Theor. Lit. Press
GONTI	State United Sci.-Tech. Press
Gosenergoizdat	State Power Press
Goskhimizdat	State Chem. Press
GOST	All-Union State Standard
GTTI	State Tech. and Theor. Lit. Press
IL	Foreign Lit. Press
ISN (Izd. Sov. Nauk)	Soviet Science Press
Izd. AN SSSR	Acad. Sci. USSR Press
Izd. MGU	Moscow State Univ. Press
LEIIZhT	Leningrad Power Inst. of Railroad Engineering
LET	Leningrad Elec. Engr. School
LETI	Leningrad Electrotechnical Inst.
LETIIZhT	Leningrad Electrical Engineering Research Inst. of Railroad Engr.
Mashgiz	State Sci.-Tech. Press for Machine Construction Lit.
MEP	Ministry of Electrical Industry
MES	Ministry of Electrical Power Plants
MESEP	Ministry of Electrical Power Plants and the Electrical Industry
MGU	Moscow State Univ.
MKhTI	Moscow Inst. Chem. Tech.
MOPI	Moscow Regional Pedagogical Inst.
MSP	Ministry of Industrial Construction
NI ZVUKSZAPIOI	Scientific Research Inst. of Sound Recording
NIKFI	Sci. Inst. of Modern Motion Picture Photography
ONTI	United Sci.-Tech. Press
OTI	Division of Technical Information
OTN	Div. Tech. Sci.
Stroiizdat	Construction Press
TOE	Association of Power Engineers
TsKTI	Central Research Inst. for Boilers and Turbines
TsNIEL	Central Scientific Research Elec. Engr. Lab.
TsNIEL-MES	Central Scientific Research Elec. Engr. Lab.-Ministry of Electric Power Plants
TsVTI	Central Office of Economic Information
UF	Ural Branch
VIESKh	All-Union Inst. of Rural Elec. Power Stations
VNIIM	All-Union Scientific Research Inst. of Metrology
VNIIZhDT	All-Union Scientific Research Inst. of Railroad Engineering
VTI	All-Union Thermotech. Inst.
VZEI	All-Union Power Correspondence Inst.

Note: Abbreviations not on this list and not explained in the translation have been transliterated, no further information about their significance being available to us. — Publisher.

RUSSIAN TO ENGLISH

# scientist-translators wanted

You can keep abreast of the latest Soviet research in your field while supplementing your **income** by translating **in your own home** on a part-time basis. In the expanding Consultants Bureau publishing program, we **guarantee a continuous flow of translation** in your specialty. If you have a native command of English, a good knowledge of Russian, and experience and academic training in a scientific discipline, you may be qualified for our program. Immediate openings are available in the following fields: physics, chemistry, engineering, biology, geology, and instrumentation. Call or write now for additional information: TRANSLATIONS EDITOR



**CONSULTANTS BUREAU**

227 West 17 Street, New York, N. Y. 10011 • (Area Code: 212) AL-5-0713



**NEW CONSULTANTS BUREAU / PLENUM PRESS TITLES****LEBEDEV PHYSICS SERIES**

Complete English translations of the Proceedings ("Trudy") of the famed Lebedev Physics Institute of the USSR Academy of Sciences published as Consultants Bureau Special Research Reports. Translations begin with Volume 25.

Series edited by D. V. Skobel'tsyn

**OPTICAL METHODS OF INVESTIGATING SOLID BODIES**

"Trudy" Volume 25

Includes papers by N. D. Zhevandrov (on polarized luminescence of crystals), V. P. Chermisimov (on vibrational spectra and structure of oxides in the crystalline and glassy states) and L. A. Vainshtein (on calculation of cross sections for excitation of atoms and ions by electron impact).

194 pages 1965 \$22.50

**COSMIC RAYS**

"Trudy" Volume 26

Deals with experimental investigations into nuclear and electromagnetic interactions at high and ultra-high energies.

262 pages 1965 \$27.50

**RESEARCH IN MOLECULAR SPECTROSCOPY**

"Trudy" Volume 27

Devoted to spectroscopic investigations into matter in various states of aggregation by Raman scattering and infrared absorption.

214 pages 1965 \$22.50

Further volumes in this series will be published approximately 6 months after their appearance in the original Russian.

**MATSCIENCE SYMPOSIA ON THEORETICAL PHYSICS**

Alladi Ramakrishnan, Editor

A new and continuing series emanating from the symposia held at the Institute of Mathematical Sciences, Madras, India

Volume 1: Proceedings of the First Anniversary Symposium

This symposium was arranged in tribute to Prof. R. E. Marshak, who accepted the first Niels-Bohr visiting professorship at the new Institute of Mathematical Sciences. Prof. Marshak contributed the paper "Group Symmetries with R-Invariance" included in this proceedings. The other 10 papers deal mainly with complex problems of particle symmetries and resonances. A Plenum Press book.

Approx. 170 pages 1965 \$9.50

Place your standing order today for books in series. It will ensure the delivery of new volumes *immediately* upon publication; you will be billed later. This arrangement is solely for your convenience and may be cancelled by you at any time.

**NUCLEAR STRUCTURE AND ELECTROMAGNETIC INTERACTIONS**

N. MacDonald, Editor

*Proceedings of the 1964 NATO-Sponsored Scottish Universities' Summer School in Physics*

This collection of review articles by experts in the field of nuclear physics includes discussions on radioactive capture, reactions, photoneuclear reactions, electron scattering, Coulomb excitation and fission, and experimental techniques. Covered are such recent advances in the field as inelastic electron scattering, use of a computer in the experimental setup, analysis of the structure of a fissioning nucleus, use of a lithium-drifted semiconductor counter, and Doppler-shift attenuation method for nuclear lifetimes. A Plenum Press book.

496 pages 1965 \$22.50

**QUANTUM ELECTRON THEORY OF AMORPHOUS CONDUCTORS**

By A. I. Gubanov

This is the first monograph to deal with the physics of amorphous electronic conductors. It includes a critical review of the electrical properties and structure of liquid and glassy semiconductors, a separate chapter on the fundamentals of the quantum electron theory of solids, and a consideration of the similarities and differences between the structures of liquid and crystalline substances. Using one-dimensional models, Gubanov deduces the band structure of the electron theory spectrum and extends the theory for three-dimensional models. A Consultants Bureau book translated from Russian.

277 pages 1965 \$17.50

**SOLAR SYSTEM RADIO ASTRONOMY**

Jules Aarons, Editor

Contains the 18 lectures presented at a 1964 NATO Study Institute on all aspects of the radio and radar exploration of the sun, moon, and planets. Interferometric measurements of the centers of solar activity and flares, the density of the interplanetary medium, the nature of the lunar surface as indicated by radar reflections and apparent temperature at different wavelengths, and planetary radio emission are among the topics discussed. A Plenum Press book.

430 pages 1965 \$17.50

**STELLAR EVOLUTION**

A. G. W. Cameron and R. F. Stein, Editors

This comprehensive collection of 41 authoritative papers on stellar structure and evolution treats such topics as stellar energy balances, radiative absorption, turbulent convection, neutrino generation, pre-main sequence evolution, the dependence of evolution on stellar mass, white dwarfs, novae, and supernovae, Cepheid variables, red giants, T Tauri stars, the photometry of B stars, helium in the galaxy, and composition differences between the galaxy and the Magellanic Clouds. A Plenum Press book.

458 pages 1965 \$19.50

 **CONSULTANTS BUREAU / PLENUM PRESS**

227 West 17th Street, New York, New York 10011